Volume 14, Issue 2, June 2024
pISSN 2158-0510 eISSN - 2158-0529

IJBM

International Journal of BIOMEDICINE

www.ijbm.org

IJBM

INTERNATIONAL JOURNAL OF BIOMEDICINE

Aims and Scope: *International Journal of Biomedicine (IJBM)* publishes peer-reviewed articles on the topics of basic, applied, and translational research on biology and medicine. Original research studies, reviews, hypotheses, editorial commentary, and special reports spanning the spectrum of human and experimental and tissue research will be considered. All research studies involving animals must have been conducted following animal welfare guidelines such as the National Institutes of Health (NIH) Guide for the Care and Use of Laboratory Animals, or equivalent documents. Studies involving human subjects or tissues must adhere to the Declaration of Helsinki and Title 45, US Code of Federal Regulations, Part 46, Protection of Human Subjects, and must have received approval of the appropriate institutional committee charged with oversight of human studies. Informed consent must be obtained.

International Journal of Biomedicine endorses and behaves in accordance with the codes of conduct and international standards established by the Committee on Publication Ethics (COPE).

International Journal of Biomedicine (ISSN 2158-0510) is published four times a year by International Medical Research and Development Corp. (IMRDC), 442 5th Avenue #1196, Manhattan, NY 10018, USA

Customer Service: International Journal of Biomedicine, 442 5th Avenue #1196, Manhattan, NY 10018, USA; Tel: 1-917-740-3053; E-mail: editor@ijbm.org

Photocopying and Permissions: Published papers appear electronically and are freely available from our website. Authors may also use their published .pdf's for any non-commercial use on their personal or non-commercial institution's website. Users are free to read, download, copy, print, search, or link to the full texts of these articles for any non-commercial purpose. Articles from IJBM website may be reproduced, in any media or format, or linked to for any commercial purpose, subject to a selected user license.

Notice: No responsibility is assumed by the Publisher, Corporation or Editors for any injury and/or damage to persons or property as a matter of products liability, negligence, or otherwise, or from any use or operation of any methods, products, instructions, or ideas contained in the material herein. Because of rapid advances in the medical and biological sciences, in particular, independent verification of diagnoses, drug dosages, and devices recommended should be made. Although all advertising material is expected to conform to ethical (medical) standards, inclusion in this publication does not constitute a guarantee or endorsement of the quality or value of such product or of the claims made of it by its manufacturer.

Manuscript Submission: Original works will be accepted with the understanding that they are contributed solely to the Journal, are not under review by another publication, and have not previously been published except in abstract form. Accepted manuscripts become the sole property of the Journal and may not be published elsewhere without the consent of the Journal. A form stating that the authors transfer all copyright ownership to the Journal will be sent from the Publisher when the manuscript is accepted; this form must be signed by all authors of the article. All manuscripts must be submitted through the International Journal of Biomedicine`s online submission and review website. Authors who are unable to provide an electronic version or have other circumstances that prevent online submission must contact the Editorial Office prior to submission to discuss alternate options (editor@ijbm.org).

Copyright © 2024 International Medical Research and Development Corp. All Rights Reserved.

IJBM

INTERNATIONAL JOURNAL OF BIOMEDICINE

Editor-in-Chief
Marietta Eliseyeva
New York, USA

Founding Editor
Simon Edelstein
Detroit, MI, USA

EDITORIAL BOARD

Mary Ann Lila
North Carolina State University
Kannapolis, NC, USA
Ilya Raskin
Rutgers University
New Brunswick, NJ, USA
Yue Wang
National Institute for Viral Disease Control and Prevention, CCDC
Beijing,China
Gulnoz Khamidullaeva
National Center of Cardiology
Tashkent, Uzbekistan
Dmitriy Labunskiy
Lincoln University
Oakland, CA, USA
Randy Lieberman
Detroit Medical Center
Detroit, MI, USA
Seung H. Kim
Hanyang University Medical Center
Seoul, South Korea
Luka Seung H. Kim
Hanyang University Medical Center
Seoul, South Korea
Roy Beran
Griffith University, Queensland
UNSW, Sydney, Australia
Marina Darenskaya
Scientific Centre for Family Health and Human Reproduction Problems
Irkutsk, Russia
Karunakaran Rohini
AIMST University
Bedong, Malaysia
Lev Zhivotovsky
Vavilov Institute of General Genetics
Moscow, Russia
Bhaskar Behera
Agharkar Research Institute
Pune, India
Hesham Abdel-Hady
University of Mansoura
Mansoura, Egypt
Tetsuya Sugiyama
Nakano Eye Clinic
Nakagyo-ku, Kyoto, Japan
Shaoling Wu
Qingdao University, Qingdao
Shandong, China
Biao Xu
Nanjing University, Nanjing, China
Boris Mankovsky
National Medical Academy for Postgraduate Education
Kiev, Ukraine
Bruna Scaggiante
University of Trieste
Trieste, Italy
Alireza Heidari
California South University
Irvine, California, USA
Rupert Fawdry
University Hospitals of Coventry & Warwickshire Coventry, UK
Pulat Sultanov
Republican Research Centre of Emergency Medicine
Tashkent, Uzbekistan
Timur Melkumyan
Tashkent State Dental Institute
Tashkent, Uzbekistan
RUDN University, Moscow, Russia
Luka Tomašević
University of Split Split, Croatia

EDITORIAL STAFF

Paul Edelstein *(Managing Editor)*
Paul Clee *(Copy Editor)*
Dmitriy Eliseyev *(Associate Editor)*
Paul Ogan *(Bilingual Interpreter)*
Nigora Srojidinova *(Editorial Assistant)*
Natalya Kozlova *(Editorial Assistant)*


ECR 2025
EUROPEAN CONGRESS OF RADIOLOGY
PLANET RADIOLOGY
VIENNA / FEBRUARY 26 – MARCH 02
THE ANNUAL MEETING OF
ESR EUROPEAN SOCIETY OF RADIOLOGY
EFRS EUROPEAN FEDERATION OF RADIOGRAPHER SOCIETIES
ESHIMT MOLECULAR TRANSLATIONAL HYBRID IMAGING
MYESR.ORG

IJBM
INTERNATIONAL JOURNAL OF BIOMEDICINE
www.ijbm.org
Volume 14 Issue 2 June 2024

CONTENTS

Congress Program

EBCOG 2025

29th European Congress of Obstetrics and Gynaecology (EBCOG)

5–7 June 2025
Frankfurt am Main, Germany

www.ebcog-congress.de

EUROPE MEETS THE WORLD

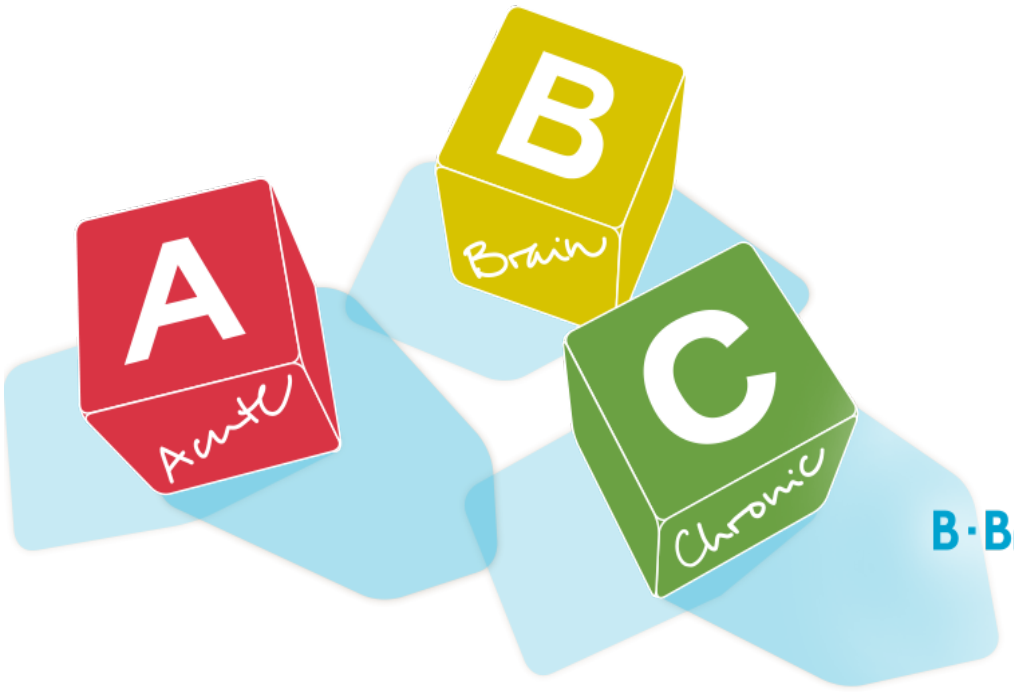

EPNS 2025 munich

8 - 12 July 2025
Germany

A · Acute
B · Brain, Science & Health
C · Chronic

WORLD FEDERATION OF NEUROLOGY

KNA
KOREAN NEUROLOGICAL ASSOCIATION

XXVII WORLD CONGRESS OF NEUROLOGY (WCN 2025)

12-15 OCTOBER 2025
SEOUL, SOUTH KOREA

Seoul

International Journal of Biomedicine 14(2) (2024) 209-216
http://dx.doi.org/10.21103/Article14(2)_RA1

REVIEW ARTICLE

INTERNATIONAL JOURNAL OF BIOMEDICINE

Characteristics and Functions of IL-37

Fang Yang[1,2*], Li Gao[1*], Xinya Wu[1], Xuan Su[1], Weijie Ma[1], Lei Zhong[1], Aihua Liu[1,3**], Fukai Bao[1,3**]

[1]*The Institute for Tropical Medicine, Faculty of Basic Medical Sciences, Kunming Medical University, Kunming 650500, China*
[2]*The First Clinical College, The First Affiliated Hospital, Kunming Medical University, Kunming 650030, China*
[3]*Yunnan Province Key Laboratory of Children's Major Diseases Research, The Affiliated Children Hospital, Kunming Medical University, Kunming 650030, China*

Abstract

Interleukin-37 (IL-37), previously known as IL-1F7, is a member of the IL-1 family of cytokines. There are five basic subtypes of IL-37, including IL-37a, IL-37b, IL-37c, IL-37d, and IL-37e. Like other members of the IL-1 family, IL-37 is initially expressed as an immature precursor protein that needs to be processed enzymatically by caspase-1 to generate the bioactive protein. However, unlike most other members of the IL-1 family, IL-37 induces anti-inflammatory activities in IL-37 receptor-positive target cells. IL-37 functions as an extracellular protein by binding to the IL-18 receptor, IL-18R, and an intracellular protein via its interaction with SMAD family member 3 (SMAD3). This article reviews recent findings regarding the IL-37 protein maturation process and the biological functions mediated by this cytokine.**(International Journal of Biomedicine. 2024;14(2):209-216.)**

Keywords: IL-37 • IL-37 precursor • anti-inflammatory cytokine • IL-18 • Smad3 • IL-1R8 • IL-37 isoforms

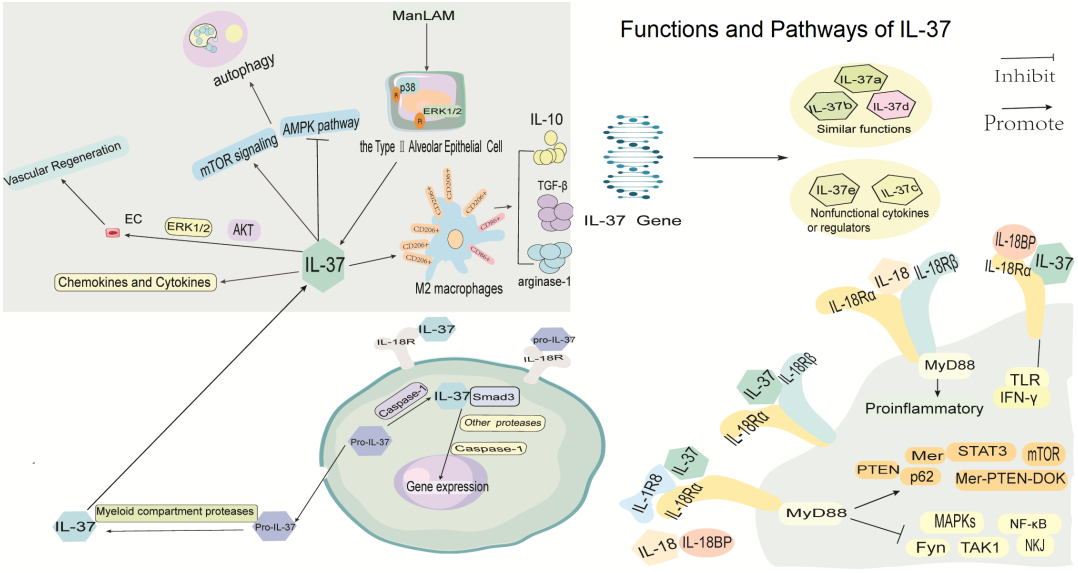

Graphical Abstract

For citation: Yang F, Gao L, Wu X, Su X, Ma W, Zhong L, Liu A, Bao F. Characteristics and Functions of IL-37.. International Journal of Biomedicine. 2024;14(2):209-216. doi:10.21103/Article14(2)_RA1

* Fang Yang and Li Gao contributed equally to the review. ** Corresponding authors: Aihua Liu, Fukai Bao.

Abbreviations

AMPK, AMP-activated kinase; **DC**, dendritic cell; **Dok**, downstream of kinase; **ERK1/2**, extracellular signal-regulated kinase 1/2; **IL-18BP**, IL-18 binding protein; **IL-1F**, IL-1 family; **LPS,** lipopolysaccharide; **Mer**, a receptor tyrosine kinase expressed in **m**onocytes, **e**pithelial, and **r**eproductive tissues; **MAPK**, mitogen-activated protein kinase; **NLRP3**, NOD-, LRR-, and pyrin domain-containing protein 3; **NF-κB**, nuclear factor kappa B; **SIGIRR**, single immunoglobulin IL-1-related receptor; **Tregs**, regulatory T cells; **TGF-β**, transforming growth factor-beta; **TLR**, toll-like receptor; **USP**, ubiquitin specific protease; **VEGF**, vascular endothelial growth factor.

Biological Characteristics of IL-37

Interleukin (IL)-37, commonly known as IL-1F7, was discovered in 1999/2000 by searching human-expressed sequence tag databases and sequencing the IL-1 gene cluster located on human chromosome 2.[1-3] IL-37, a member of the IL-1 family, is a potent anti-inflammatory cytokine with immunomodulatory effects.[4]

The *IL-37* gene, located on chromosome band 2q12.2 between the *IL-1β* and *IL-36γ* genes, with a length of 3.617 kb, contains 6 exons.[5] The *IL-37* gene has a molecular weight of about 17~25 kDa.[6] Alternative splicing of *IL-37* pre-mRNA generates five cytokine isoforms, including IL-37a, IL-37b, IL-37c, IL-37d, and IL-37e.[7] Exons 1-3 encode unique N-terminal sequences of IL-37 that possess a caspase-1 cleavage site and can be processed to its mature form.[8,9] The action of IL-37 is mediated by a β-barrel structural unit in its secondary structure.[10] The 12-β-strand-containing proteins may be formed by amino acid sequences encoded by exons 4, 5, and 6.[11-13] The 12-hypothetical β-strand structural units that constitute the β-trefoil secondary structure of IL-37 are responsible for the protein's function. IL-37a (encoded by exons 3–6), IL-37b (encoded by exons 1, 2, 4–6), and IL-37d (encoded by exons 1, 4–6) contain the encoding sequences of 12 β-strands (exons 4–6) and are speculated to be functional cytokines. IL-37c (encoded by exons 1, 2, 5, and 6) and IL-37e (encoded by exons 1, 5, and 6) are predicted to be nonfunctional because of the lack of exon 4 encoding for *β*-trefoil secondary structure.

The expression of IL-37 isoforms is tissue-specific. For example, the brain, kidney, heart, bone marrow, and testis express IL-37a, IL-37b, IL-37c, IL-37d, and IL-37d, respectively.[11]

IL-37b, encoded by five of six IL-37 exons (exons 1, 2, 4–6), is the longest and the best characterized IL-37 isoform, and is known to possess the strongest anti-inflammatory effects.[11,14] IL-37b is detected in lymph nodes, placenta, colon, lung, kidney, testis, thymus, and uterus[15,16] and acts as an anti-inflammatory cytokine. IL-37b inhibits the expression of multiple pro-inflammatory cytokines, such as IL-1α, IL-1β, IL-6, and TNF-α. [6,17-20]

Isoform IL-37a, encoded by exons 3, 4, 5, and 6, does not contain exon 1, but it is the only variant that contains exon 3, which encodes a unique N-terminus.[10,11,21] Some studies indicate that IL-37a is protective against hepatic ischemia–reperfusion injury.[9] However, further investigations are needed to better understand IL-37a functions.

IL-37c and IL-37e probably could not represent a functional form of a cytokine. IL-37e, encoded by exons 1, 5, and 6, cannot bind to IL-18R because it lacks exon 4.[21,22]

IL-37d, encoded by exons 1, 4, 5, and 6, inhibits the activation of TNF-α-induced NF-κB in T cells. It is a positive feedback loop. The downregulation of the NF-κB pathway reduced the production of TNF-α, which lately abolished its stimulation to NF-κB activation.[23] Besides, IL-37d relies on the IL-1R8 receptor-mediated pathway to inhibit NLRP3[9,23] (Figure 1). The mature IL-37d could translocate into the nucleus, interacting with Smad3 and impacting its nuclear translocation to inhibit pro-inflammation, which is similar to IL-37b.[9]

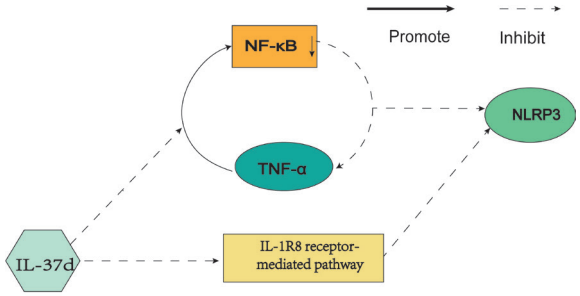

***Fig. 1**. IL-37d pathways for the inhibition of NLRP3 transcription.*

IL-37d inhibits NLRP3 transcription by suppressing the NF-κB signaling pathway. IL-37d inhibits the TNF-α-induced NF-κB activation via a positive feedback loop. The suppression of NF-κB signaling reduces TNF-α levels, thereby inhibiting its stimulation of NF-κB activation.[23] IL-37d inhibits NLRP3 via the IL-1R8 receptor-mediated pathway.[9,23]

Balanced selection keeps several human IL37 gene variations in the human evolution process. There have been 14 IL-37 protein variants found in various human populations. "Var1," "Var2," and "Ref" are three major variants occupying over 97% of those IL-37 protein variants.[24] Var2 induces a stronger, shorter-lived immune response due to preferential proteasome degradation compared to Var1 and Ref.[25]

Biological Activities of IL-37

IL-37 maturation process

Upon interaction with Smad3, IL-37 translocates into the nucleus, resulting in biological activity and the generation of its mature form via caspase-1 activity, although the mechanism requires further investigation.[26] Pan-caspase inhibition does not completely inhibit IL-37 processing, suggesting other proteases may be involved[26] (Figure 2).

The caspase-1 cleavage site maps between amino acid residues D20 and E21 on exon 1.[22,26] IL-37D20A-mutant cells have less mature IL-37 and lower rates of IL-37 nuclear translocation. However, the mutation does not completely inhibit IL-37 processing, indicating that other caspase-1 cleavage sites or other proteases may mediate IL-37 maturation.[27]

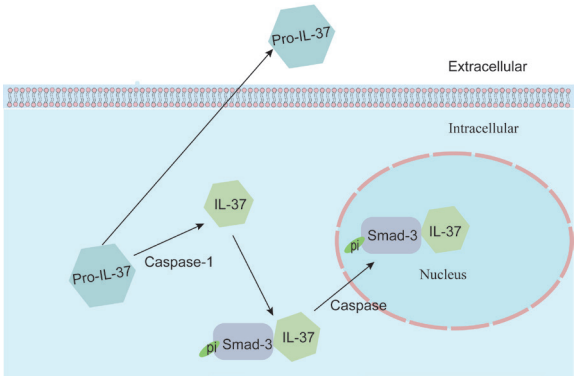

Fig. 2. *The maturation process of IL-37.*

The carboxyl domain of IL-37 binds to Smad3, leading to Smad3 phosphorylation and the translocation of the IL-37/Smad3 complex into the nucleus, where IL-37 matures and exerts biological activity.[1] Caspase-1 is required for this process.[22,27] The intracellular IL-37 precursor exits the cell through loss of membrane integrity or frank cell death.[8]

IL-37 precursor molecules localize in the cytoplasm. Some studies show that human blood monocytes stimulated with LPS and exogenous ATP mostly secrete precursor IL-37.[8] To mature, extracellular precursor IL-37 may need the activity of myeloid compartment proteases.[8] Moreover, the extracellular secretion of the IL-37 precursor does not require caspase-1 activity, and it can be secreted upon loss of membrane integrity or during cell death. However, the mature IL-37 is processed by caspase-1.[8,26] IL-37 is released via the classical ER-Golgi protein secretion pathway in response to LPS stimulation of TLR-4 on human monocytes.[28,29]

Both the IL-37 precursor and its mature form have biological activity, but the mature form binds more stably to receptors.[7,30] The caspase-1 cleavage site located on exon 1 between residues D20 and E21 generates an N terminus exactly nine amino acids upstream from the IL-1 family consensus sequence (A-X-D) to optimal folding of the beta-fold barrel structure for receptor binding of IL-1 family cytokines.[26] For example, IL-37b with the N-terminus at valine 46 is more active than the IL-37b precursor.[31,32]

Spontaneous dimerization and levels of IL-37 in normal serum

IL-37 mRNA has a ten-nucleotide A-rich homology box located at the 3'-end of exon 4 and may cause IL-37 instability.[28] However, IL-37b or IL-37c mutants that lack exon 5 exhibits significantly higher steady-state mRNA levels compared with the slight increase associated with exon 4-lacking IL-37c mutations. Thus, exon 5 may be more critical in limiting IL-37 mRNA stability. Exon instability causes IL-37 instability.[28]

IL-37 acts via a structural shift from dimeric to monomeric form.[33] Studies indicate that the symmetrical head-to-head IL-37b homodimer is created by subunits, including the β3–β4 loops and the β-trefoil sheet (β2-β3-β11).[10] IL-37 dimers can form the mature protein or from the precursor.[27] However, spontaneous IL-37 dimerization may cause a loss of biological function. When IL-37 levels are low, IL-37 dimers can dissociate into monomers. Thus, IL-37 homodimerization may be a mechanism for regulating IL-37 function.[27] Additionally, the function of IL-37 monomers increases with rising IL-37 levels.

The reference range for circulating IL-37 levels in healthy individuals has not been determined.[34] Its serum levels have not been found to vary significantly with gender and age.[35,36] However, the serum levels of IL-37 are higher in systemic lupus erythematosus patients of Asian ancestry when compared with patients of other ethnicities, and IL-37 levels (mean of weighted means) are also higher in the Chinese population than in non-Chinese populations.[36,37]

Functional and Regulatory Pathways of IL-37

IL-37 regulates inflammation by inhibiting IL-18 functions

IL-37 has two conserved amino acid residues (Glu-35 and Lys-124) that are structurally similar to the two conserved residues of IL-18 (Glu-35 and Lys-89),[38,39] indicating that IL-37 and IL-18 may have the same receptors (IL-18BP or IL-18Rα). IL-18 can play the proinflammatory activity by binding the complex IL-18Rα/IL-18Rβ, myeloid differentiation factor 88 (MyD88) combines with the TIR domain of the IL-18R chain to activate the proinflammatory signal.[8,38] The Tightness of binding between IL-37 and IL-18Rα is one-fiftieth as close as that of IL-18 and IL-18Rα.[27] Thus, IL-37 cannot affect IL-18 by combining with IL-18Rα. However, IL-37 can bind to IL-18Rα to form a complex with IL-18BP, a natural antagonist of IL-18. IL-37b can bind to IL-18BP to form a complex with IL-18Rβ, which can reduce the formation of IL-18Rα/β complex and thus inhibit the signal transduction pathway of IL-18.[14]

On the surface of peripheral blood mononuclear cells (PBMCs), the IL-37/IL-18Rα/IL-1R8 complex binds to MyD88 to block inflammation, which triggers multiple switches, including inhibiting the MAPKs, JNK, and NF-κB signaling pathways, activating the Mer-PTEN-DOK pathway and the pseudo-starvation effects of the mTOR pathway, inhibiting TAK1 and Fyn pathways, activating STAT3, Mer, and PTEN, and inducing p62 (dok) expression[8,40] (Figure 3). IL-1R8, also known as TIR8 or SIGIRR, acts as a negative regulator dampening ILR and TLR signaling and as a co-receptor for human IL-37. Inactivated IL-1R8 prevents MyD88 recruitment and then impacts the effect of IL-37, suggesting that IL-1R8 is the key for the IL-18Rα /IL-37 complex to play biological effects.[41] Being an orphan receptor, IL-1R8 also inhibits IL-1 and toll-like receptor (TLR)-dependent inflammation. IL-37 diminishes various inflammatory responses through ligation to its receptor IL-1R8/Sigirr. IL-37 induces Sigirr degradation in the ubiquitin-proteasome system through site-specific ubiquitination, which can be reversed by a deubiquitinase, USP13.[42] IL-37 activates glycogen synthesis kinase 3β (GSK3β), which plays a role in feedback control of IL-1R8/Sigirr abundance.[43] Besides, the activation of GSK3b promotes Sigirr phosphorylation, ubiquitination, internalization, and degradation by disrupting Sigirr association with USP13.[43] Thereby, IL-37 downregulates IL-1R8 expression by disturbing the internation USP13 with IL-1R8 and by promoting IL-1R8 phosphorylation (Figure 4).

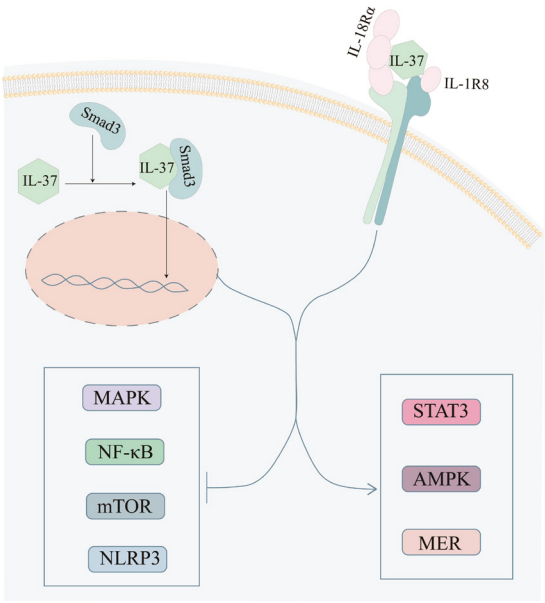

Fig. 3. *IL-37 pathways.*

Smad3 is a transcriptional regulator of the TGF-β pathway and plays an important role in IL-37 activity, which translocates into the nucleus. Upon caspase-1-mediated cleavage, IL-37 suppresses the expression of proinflammatory cytokines and the recruitment of neutrophils into the lungs by inhibiting the activity of the NLRP3 inflammasome.[5] IL-37 also inhibits kinases in the MAPK and NF-KB pathways and activates the anti-inflammatory factors, STAT3, and Mer. IL-37 also inhibits mTOR and activates AMPK.[41] On the surface of peripheral blood mononuclear cells (PBMCs), the IL-37/IL-18Rα/IL-1R8 complex binds to MyD88 to block inflammation, which triggers multiple switches, including inhibiting the MAPKs, JNK, and NF-κB signaling pathways, activating the Mer-PTEN-DOK pathway and the pseudo-starvation effects of the mTOR pathway, inhibiting TAK1 and Fyn pathways, activating STAT3, Mer, and PTEN, and inducing p62 (dok) expression.[8,40]

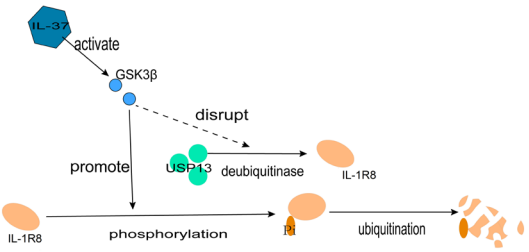

Fig. 4. *IL-37-mediated IL-1R8/Sigirr degradation.*

IL-37 induces IL-1R8/Sigirr degradation in the ubiquitin-proteasome system through site-specific ubiquitination, which can be reversed by a deubiquitinase, USP13.[42] IL-37 activates glycogen synthesis kinase 3β (GSK3β), which plays a role in feedback control of IL-1R8/Sigirr abundance.[43] The activation of GSK3b promotes Sigirr phosphorylation, ubiquitination, internalization, and degradation by disrupting Sigirr association with USP13.

Under physiological conditions, the concentration of plasma IL-18BP is ~20 times higher than that of IL-18, which prevents IL-18 from binding to its cellular receptor.[44,45] This effect also inhibits IL-18-induced IFNγ expression, indicating that IL-18BP has an anti-inflammatory function.[8] However, the anti-inflammatory properties of IL-18BP are lost at high IL-18BP concentrations, but the mechanism involved needs further investigation. The ternary complex, IL-37/IL-18Rβ/IL-18BP competes with IL-18 for IL-18Rβ, which inhibits IL-18 function. This complex also competes with IL-18 for IL-18BP.[21] It has been shown that IL-37 enhances the ability of IL-18BP to inhibit IL-18, but this requires further investigation.[28] Moreover, the IL-37/IL-18Rα/IL-18BP ternary complex inhibits immune responses and exerts anti-inflammatory effects by repressing the expression of IFN-γ and TLR signaling extracellularly.[21]

IL-18 mediates IFN-γ-induced Th1 responses and activates NK cell cytotoxic activity, the production of adhesion molecules, the synthesis of nitric oxide synthase, and the production of chemokines. IL-18 also drives Th2 responses and the expression of IL-13 and IL-4 [46,47] (Figures 5 and 6). IL-18 promotes the synthesis of pro-inflammatory Th1 cytokines, including IFN-γ and GM-CSF, and concurrently suppresses the production of the anti-inflammatory cytokine IL-10. Thus, IL-37 impacts IL-18 and then influences the above processes.

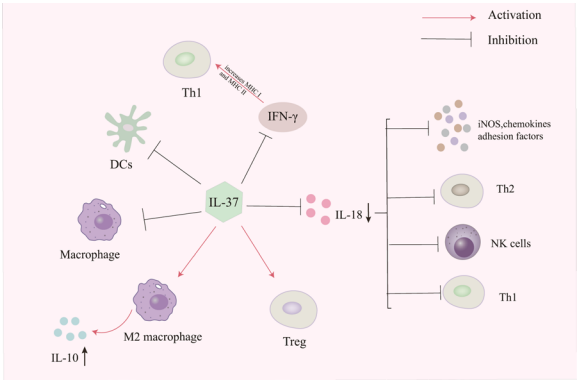

Fig. 5. *Functional and Regulatory Pathways of IL-37.*

IL-37 inhibits IL-18 activity and downregulates IL-18-mediated expression of pro-inflammatory factors, the development of IFN-γ-associated Th1 responses, the activation of NK cell cytotoxic activity, the production of adhesion molecules, the synthesis of nitric oxide synthase, chemokine production, as well as Th2 responses and the expression of IL-13 and IL-4.[47,48] Possible role of IL-37 in modulating the immune response of Tregs and function of DCs.[7] IL-37 promotes macrophage polarization toward the M2 subtype and inhibits macrophage transmigration, apoptosis, and proliferation.[56]

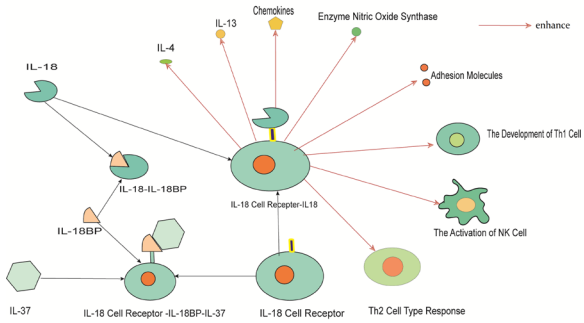

Fig. 6. IL-37 signaling via IL-18.

Excessive IL-18 levels are reduced by IL-18BP,[45] which blocks the binding of IL-18 to its cell receptor.[44,46] The IL-37/IL-18BP/IL-18Rβ complex may compete with IL-18Rβ, thereby inhibiting the function of IL-18. IL-18 triggers IFN-γ-associated Th1 response, the activation of NK cell cytotoxic activity, the production of adhesion molecules, the synthesis of nitric oxide synthase, chemokine production, as well as Th2 responses and the expression of IL-13 and IL-4.[47,48]

IL-37 interacts with Smad3 to influence gene expression

The binding of IL-37 to Smad3 is mediated by IL-37's carboxyl domain. The resulting complex then translocates to the nucleus upon Smad3 phosphorylation (Figure 2), where it regulates gene expression. IL-37 interacts with phosphorylated and non-phosphorylated Smads to regulate some key enzymes and signaling pathways, including focal adhesion kinase, proline-rich tyrosine kinase (Pyk2), MAP kinase p38α, signal transducer and activator of transcription (STAT), p53, and mTOR signaling[48] (Figure 3).

IL-37/Smad3 complexes also compete with Smad2/3/4 complexes. Smad2 and Smad4 may function in the nucleus by competing with IL-37 and reducing the phosphorylation of the IL-37/Smad3 complex, although the mechanism is unclear.[9]

Sources of IL-37 and ManLAM-induced IL-37 production

IL-37 is mainly secreted by macrophages. IL-37 can also be expressed in monocytes, activated B cells, plasma cells, CD4+Treg, dendritic cells, keratinocytes, renal tubular epithelial cells, synovial cells, tonsil B cells, gastrointestinal epithelial cells, carcinoma cells, testis, thymus, uterus, both in the nucleus and the cytoplasm.[7,49] Besides, some cells can secrete the IL-37 during the stimulation by LPS. Dendritic cells (DCs) can also secrete the IL-37 under no stimulated conditions.[8]

Mannose-capped lipoarabinomannan (ManLAM), the virulence factor of *Mycobacterium tuberculosis* (Mtb),[50] elevates IL-10 production by DCs while suppressing their production of IL-12. It also stimulates the phosphorylation of extracellular signal-regulated kinase 1/2 (ERK1/2) and p38 in A549 cells and cell surface TLR2 expression. The phosphorylation of ERK1/2 and p38MAPK in the type II alveolar epithelial cell line, A549, induces IL-37 expression.[26] Several TLR2 and TLR4 ligands also induce IL-37 expression.[51] Impairing TLR2 expression markedly suppresses the phosphorylation of ERK1/2 and p38, and ManLAM-induced IL-37 expression. However, impairing TLR4 function did not affect IL-37 expression.[51] The interaction of LPS-activated TLR4 and its intracellular adaptor on the cell surface induces NF-κB-mediated transcriptional expression of proinflammatory genes. TLRs and proinflammatory factors also enhance IL-37 expression[22] (Figure 7).

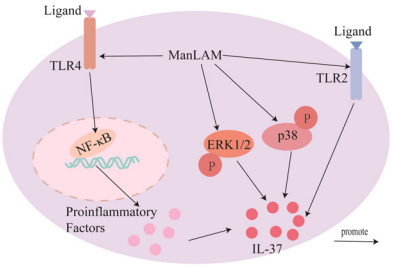

Fig. 7. *ManLAM and TLR4 enhance the expression of IL-37.*
Mannose-capped lipoarabinomannan (ManLAM) stimulates the phosphorylation of ERK1/2 and p38 (A549 cells) and induces TLR2 expression, which can induce IL-37 expression. Several toll-like receptor (TLR) ligands also induce IL-37 expression. The LPS-activated TLR4 stimulates NF-κB signaling, thereby driving the expression of pro-inflammatory genes. TLRs and proinflammatory factors enhance IL-37 production.[5]

Moreover, IL-37 levels are reported to rise upon treatment of relapsed TB, severe TB, and drug-resistant TB. In sputum smear (Mtb)+ patients, IL-37 levels fall after short-term anti-TB chemotherapy.[52] In vitro, TB-sensitive monocytes continuously produce IL-37b without antigen stimulation.[52]

IL-37 and Vascular Regeneration

Granuloma-associated angiogenesis may influence the occurrence, progression, and prognosis of diseases. IL-37 is a novel proangiogenic factor that promotes endothelial cell (EC) proliferation, migration, and capillary formation in vitro, as well as vessel sprouting from aortic rings ex vivo.[53] Hypoxia, which influences vascular regeneration, upregulates IL-37 expression; the IL-37 upregulation is suppressed by HIF-1α downregulation.[53] IL-37 also stimulates the activation of ERK1/2 and protein kinase B (AKT), which is critical for endothelial activation and viability.[54] Additionally, IL-37 promotes angiogenesis by modulating inflammatory responses[53] (Figure 8).

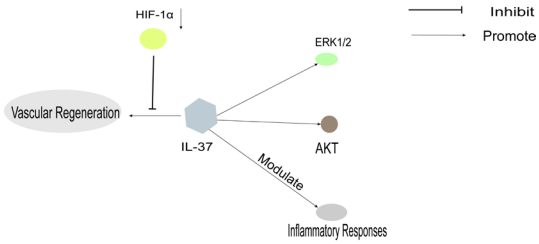

Fig. 8. *IL-37 and vascular regeneration.*
IL-37 upregulates vascular regeneration, but its effects can be inhibited by the downregulation of HIF-1α expression. IL-37 stimulates the activation of ERK1/2 and AKT, which are critical for endothelial activation and viability.[53] In addition, IL-37 promotes angiogenesis by modulating inflammatory responses.

However, other studies have suggested that the effect of IL-37 on blood vessels is dose-dependent. The dose-dependent proangiogenic effect of IL-37 might be because the impact of many angiogenic factors is biphasic. For example, at optimal concentration, PAI-1 has proangiogenic functions, but at high concentration, it has antiangiogenic activity. At low concentrations, IL-8 enhances the chemotaxis and proliferation of ECs, but its effects are diminished at high concentrations. IL-18Rα and IL-1R8 play a reserve role in angiogenesis in different concentrations.[53] IP-10 and thrombospondin suppress angiogenesis at low concentrations but at high concentrations, they induce EC chemotaxis.[53]

IL-37 and macrophage polarization

IL-37 is reported to inhibit macrophage transmigration, apoptosis, and proliferation. It enhances the expression of THP1-derived macrophages with a higher CD206+ and lower CD86+, which are markers of M2 macrophages. IL-37 also upregulates the mRNA levels of arginase-1, TGF-β, and IL-10. Besides, IL-37 suppresses the expression of CD 86, IL-1β, iNOs, and IL-12, which are markers of M1 macrophages. Because M2 macrophages enhance phagocytosis, IL-37-induced macrophage polarization drives phagocytosis.[55]

The inactive Mtb strain, H37Rv (iH37Rv), polarizes macrophages into the M1 subtype and increases the expression of CD86, iNOs, IL-12, and IL-1β, while reducing the levels of CD206, TGF-β, and IL-10. SiRNA-mediated IL-37 silencing enhanced this polarizing phenomenon. However, exogenous IL-37 has the opposite effect of polarizing macrophages toward the M2 subtype.[55] Although some studies have shown that endogenous lL-37 increases nitric oxide levels, exogenous IL-37 has the opposite effect.[55]

The role of IL-37 in the regulation of autophagy

IL-37 inhibits mTOR signaling and activates the AMPK pathway (Figure 3), triggering pseudo-starvation, the main autophagy regulation mechanism. Autophagy is thought to be critical for the delivery of bacteria to the lysosome for degradation, which limits the survival of intracellular bacteria. Other autophagy functions include promoting antigen presentation and reducing inflammation by sequestering and processing microbial components.[56,57] IL-37 influences antifibrotic activity associated with autophagy activation in fibrotic lungs.[58]

IL-37 modulates the expression of chemokines and cytokines

Some proinflammatory cytokines may promote the expression of IL 37, which may inhibit the overproduction of proinflammatory cytokines through negative feedback. In addition, IL-12, IL-32, and granulocyte-macrophage colony-stimulating factor (GM-CSF) suppress IL-37 production,[7] probably because GM-CSF and IL-4 stimulate the differentiation of monocytes to dendritic cells. In human immune cells, monocytes, DCs, and T cells may account for 81%–91%, 1%–2%, and 6%–8% of secreted IL-37.[8] So, GM-CSF and IL-4 suppresses monocyte-induced IL-37 levels.[22]

IL-37 inhibits the production of inflammatory factors, including IL-1α, IL-1β, IL-1Rα, IL-6, IL-17, IL-8, IL-23, TNF-α, IFN-γ, IL 4, IL-13, IL-3, IL-14, as well as cytokines IL-13, IL-10, and I-309, and the chemokines CXCL-2, CCL12, CXCL13, M-GSF, GM-CSF, IACM-1, NLRP3, MIP-2/CXCLE, MCP-5/CCL12, and BDCA-1/CXCL13, but elevates TNF-β and NO levels.[7,8,21,59,60]

IL-37 and various signal pathway

IL-37 suppresses immune responses by regulating the MertK-dependent pathway in monosodium urate crystals-stimulated THP-1 cells. IL-37 stimulates the AMPK pathway to counterbalance inflammation in THP-1 cells. Eosinophils, smooth muscle cells, and epithelial cells secrete VEGF, which is inhibited by IL-37.[61] IL-37 can also inhibit the Warburg effect by activating MAPK signaling and inhibiting the mTOR pathway.[8]

IL-37 exerts immunosuppressive effects by inhibiting the activation of the NOD-like receptor family pyrin domain-containing 3 (NLRP3) inflammasome, which is a critical factor in various inflammatory signaling pathways.[62] By inhibiting the activity of the NLRP3 inflammasome, IL-37 suppresses the production of proinflammatory cytokines and the recruitment of neutrophils into the lungs.[63]

IL-37 affects T-cell balance. DCs from IL-37 transgenic mice exhibit a reduced ability to activate native T cells and antigen-specific T cells and an enhanced ability to cause Treg cell polarization. Thus, IL-37 affects T-cell balance and, therefore, attenuates T-cell-mediated inflammation.[7,64]

Conclusion

IL-37, through interaction with various receptors, inhibits the production of proinflammatory cytokines, promotes the proliferation and differentiation of macrophages, and regulates autophagy and vascular regeneration. A better understanding of the functions of IL-37 may uncover intervention strategies for various diseases.

Funding

National Natural Science Foundation of China (No. 81860644, 32060180, 82160304, 81860644) and Joint Foundation of Yunnan Province Department of Science, Technology-Kunming Medical University [No. 2019FE001 (-002) and 2017FE467 (-001)].

Acknowledgments

This work was supported by grants from the National Natural Science Foundation of China and Yunnan Province Department of Science and Technology-Kunming Medical University Joint Fund Projects. The funding institutions were not involved in the design of the study or the review of the manuscript.

Disclosure and Competing Interests

The authors declare that they have no competing interests. The views presented in this paper are the views of the authors and not the official position of the institution or funder.

References

1. Kumar S, McDonnell PC, Lehr R, Tierney L, Tzimas MN, Griswold DE, et al. Identification and initial characterization of four novel members of the interleukin-1 family. J Biol Chem. 2000 Apr 7;275(14):10308-14. doi: 10.1074/jbc.275.14.10308.
2. Mulero JJ, Pace AM, Nelken ST, Loeb DB, Correa TR, Drmanac R, Ford JE. IL1HY1: A novel interleukin-1 receptor antagonist gene. Biochem Biophys Res Commun. 1999 Oct 5;263(3):702-6. doi: 10.1006/bbrc.1999.1440.
3. Dunn E, Sims JE, Nicklin MJ, O'Neill LA. Annotating genes with potential roles in the immune system: six new members of the IL-1 family. Trends Immunol. 2001 Oct;22(10):533-6. doi: 10.1016/s1471-4906(01)02034-8.
4. Wang L, Quan Y, Yue Y, Heng X, Che F. Interleukin-37: A crucial cytokine with multiple roles in disease and potentially clinical therapy. Oncol Lett. 2018 Apr;15(4):4711-4719. doi: 10.3892/ol.2018.7982.
5. Liu H, Ge B. Interleukin-37: a new molecular target for host-directed therapy of tuberculosis. Future Microbiol. 2017 May;12:465-468. doi: 10.2217/fmb-2017-0030.
6. Tete S, Tripodi D, Rosati M, Conti F, Maccauro G, Saggini A, et al. IL-37 (IL-1F7) the newest anti-inflammatory cytokine which suppresses immune responses and inflammation. Int

J Immunopathol Pharmacol. 2012 Jan-Mar;25(1):31-8. doi: 10.1177/039463201202500105.
7. Nold MF, Nold-Petry CA, Zepp JA, Palmer BE, Bufler P, Dinarello CA. IL-37 is a fundamental inhibitor of innate immunity. Nat Immunol. 2010 Nov;11(11):1014-22. doi: 10.1038/ni.1944.
8. Cavalli G, Dinarello CA. Suppression of inflammation and acquired immunity by IL-37. Immunol Rev. 2018 Jan;281(1):179-190. doi: 10.1111/imr.12605.
9. Zhao M, Li Y, Guo C, Wang L, Chu H, Zhu F, et al. IL-37 isoform D downregulates pro-inflammatory cytokines expression in a Smad3-dependent manner. Cell Death Dis. 2018 May 22;9(6):582. doi: 10.1038/s41419-018-0664-0.
10. Zeng H, Zhou K, Ye Z. Biology of interleukin-37 and its role in autoimmune diseases (Review). Exp Ther Med. 2022 Jun 7;24(2):495. doi: 10.3892/etm.2022.11422.
11. Wang L, Quan Y, Yue Y, Heng X, Che F. Interleukin-37: A crucial cytokine with multiple roles in disease and potentially clinical therapy. Oncol Lett. 2018 Apr;15(4):4711-4719. doi: 10.3892/ol.2018.7982.
12. Quirk S, Agrawal DK. Immunobiology of IL-37: mechanism of action and clinical perspectives. Expert Rev Clin Immunol. 2014 Dec;10(12):1703-9. doi: 10.1586/1744666X.2014.971014.
13. Cavalli G, Dinarello CA. Suppression of inflammation and acquired immunity by IL-37. Immunol Rev. 2018 Jan;281(1):179-190. doi: 10.1111/imr.12605.
14. Sakai N, Van Sweringen HL, Belizaire RM, Quillin RC, Schuster R, Blanchard J, et al. Interleukin-37 reduces liver inflammatory injury via effects on hepatocytes and non-parenchymal cells. J Gastroenterol Hepatol. 2012 Oct;27(10):1609-16. doi: 10.1111/j.1440-1746.2012.07187.x.
15. Taylor SL, Renshaw BR, Garka KE, Smith DE, Sims JE. Genomic organization of the interleukin-1 locus. Genomics. 2002 May;79(5):726-33. doi: 10.1006/geno.2002.6752.
16. Dinarello CA, Bufler P. Interleukin-37. Semin Immunol. 2013 Dec 15;25(6):466-8. doi: 10.1016/j.smim.2013.10.004.
17. Banchereau J, Pascual V, O'Garra A. From IL-2 to IL-37: the expanding spectrum of anti-inflammatory cytokines. Nat Immunol. 2012 Oct;13(10):925-31. doi: 10.1038/ni.2406.
18. Chen HM, Fujita M. IL-37: a new player in immune tolerance. Cytokine. 2015 Mar;72(1):113-4. doi: 10.1016/j.cyto.2014.11.025.
19. Xie Y, Li Y, Cai X, Wang X, Li J. Interleukin-37 suppresses ICAM-1 expression in parallel with NF-κB down-regulation following TLR2 activation of human coronary artery endothelial cells. Int Immunopharmacol. 2016 Sep;38:26-30. doi: 10.1016/j.intimp.2016.05.003.
20. Zeng M, Dang W, Chen B, Qing Y, Xie W, Zhao M, Zhou J. IL-37 inhibits the production of pro-inflammatory cytokines in MSU crystal-induced inflammatory response. Clin Rheumatol. 2016 Sep;35(9):2251-8. doi: 10.1007/s10067-015-3109-5.
21. Jia H, Liu J, Han B. Reviews of Interleukin-37: Functions, Receptors, and Roles in Diseases. Biomed Res Int. 2018 Apr 1;2018:3058640. doi: 10.1155/2018/3058640.
22. Boraschi D, Lucchesi D, Hainzl S, Leitner M, Maier E, Mangelberger D, et al. IL-37: a new anti-inflammatory cytokine of the IL-1 family. Eur Cytokine Netw. 2011 Sep;22(3):127-47. doi: 10.1684/ecn.2011.0288.
23. Li Y, Chu H, Zhao M, Li C, Guan Y, Guo C, et al. IL-37d Negatively Regulates NLRP3 Transcription via Receptor-mediated Pathway and Alleviates DSS-induced Colitis. Inflamm Bowel Dis. 2021 Jan 1;27(1):84-93. doi: 10.1093/ibd/izaa124.
24. Kang B, Cheng S, Peng J, Yan J, Zhang S. Interleukin-37 gene variants segregated anciently coexist during hominid evolution. Eur J Hum Genet. 2015 Oct;23(10):1392-8. doi: 10.1038/ejhg.2014.302.
25. Yan J, Zhang Y, Cheng S, Kang B, Peng J, Zhang X, et al. Common genetic heterogeneity of human interleukin-37 leads to functional variance. Cell Mol Immunol. 2017 Sep;14(9):783-791. doi: 10.1038/cmi.2016.48.
26. Bulau AM, Nold MF, Li S, Nold-Petry CA, Fink M, Mansell A, et al. Role of caspase-1 in nuclear translocation of IL-37, release of the cytokine, and IL-37 inhibition of innate immune responses. Proc Natl Acad Sci U S A. 2014 Feb 18;111(7):2650-5. doi: 10.1073/pnas.1324140111.
27. Ellisdon AM, Nold-Petry CA, D'Andrea L, Cho SX, Lao JC, Rudloff I, et al. Homodimerization attenuates the anti-inflammatory activity of interleukin-37. Sci Immunol. 2017 Feb 10;2(8):eaaj1548. doi: 10.1126/sciimmunol.aaj1548.
28. Bufler P, Gamboni-Robertson F, Azam T, Kim SH, Dinarello CA. Interleukin-1 homologues IL-1F7b and IL-18 contain functional mRNA instability elements within the coding region responsive to lipopolysaccharide. Biochem J. 2004 Jul 15;381(Pt 2):503-10. doi: 10.1042/BJ20040217.
29. Rudloff I, Cho SX, Lao JC, Ngo D, McKenzie M, Nold-Petry CA, Nold MF. Monocytes and dendritic cells are the primary sources of interleukin 37 in human immune cells. J Leukoc Biol. 2017 Apr;101(4):901-911. doi: 10.1189/jlb.3MA0616-287R.
30. Shi Y, Massagué J. Mechanisms of TGF-beta signaling from cell membrane to the nucleus. Cell. 2003 Jun 13;113(6):685-700. doi: 10.1016/s0092-8674(03)00432-x.
31. Pan G, Risser P, Mao W, Baldwin DT, Zhong AW, Filvaroff E, et al. IL-1H, an interleukin 1-related protein that binds IL-18 receptor/IL-1Rrp. Cytokine. 2001 Jan 7;13(1):1-7. doi: 10.1006/cyto.2000.0799.
32. Li S, Neff CP, Barber K, Hong J, Luo Y, Azam T, et al. Extracellular forms of IL-37 inhibit innate inflammation in vitro and in vivo but require the IL-1 family decoy receptor IL-1R8. Proc Natl Acad Sci U S A. 2015 Feb 24;112(8):2497-502. doi: 10.1073/pnas.1424626112.
33. Bello RO, Chin VK, Abd Rachman Isnadi MF, Abd Majid R, Atmadini Abdullah M, Lee TY, et al. The Role, Involvement and Function(s) of Interleukin-35 and Interleukin-37 in Disease Pathogenesis. Int J Mol Sci. 2018 Apr 11;19(4):1149. doi: 10.3390/ijms19041149.
34. Jiang J, Jiang Z, Xue M. Serum and peritoneal fluid levels of interleukin-6 and interleukin-37 as biomarkers for endometriosis. Gynecol Endocrinol. 2019 Jul;35(7):571-575. doi: 10.1080/09513590.2018.1554034.
35. Farrokhi M, Rezaei A, Amani-Beni A, Etemadifar M, Kouchaki E, Zahedi A. Increased serum level of IL-37 in patients with multiple sclerosis and neuromyelitis optica. Acta Neurol Belg. 2015 Dec;115(4):609-14. doi: 10.1007/s13760-015-0491-3.
36. Santarelli DM, Vincent FB, Rudloff I, Nold-Petry CA, Nold MF, Russo MA. Circulating Interleukin-37 Levels in Healthy Adult Humans - Establishing a Reference Range. Front Immunol. 2021 Jul 23;12:708425. doi: 10.3389/fimmu.2021.708425.
37. Godsell J, Rudloff I, Kandane-Rathnayake R, Hoi A, Nold MF, Morand EF, Harris J. Clinical associations of IL-10 and IL-37 in systemic lupus erythematosus. Sci Rep. 2016 Oct 6;6:34604. doi: 10.1038/srep34604.
38. Bufler P, Azam T, Gamboni-Robertson F, Reznikov LL,

Kumar S, Dinarello CA, Kim SH. A complex of the IL-1 homologue IL-1F7b and IL-18-binding protein reduces IL-18 activity. Proc Natl Acad Sci U S A. 2002 Oct 15;99(21):13723-8. doi: 10.1073/pnas.212519099.
39. Kim SH, Azam T, Novick D, Yoon DY, Reznikov LL, Bufler P, et al. Identification of amino acid residues critical for biological activity in human interleukin-18. J Biol Chem. 2002 Mar 29;277(13):10998-1003. doi: 10.1074/jbc.M108311200.
40. Nold-Petry CA, Lo CY, Rudloff I, Elgass KD, Li S, Gantier MP, et al. IL-37 requires the receptors IL-18Rα and IL-1R8 (SIGIRR) to carry out its multifaceted anti-inflammatory program upon innate signal transduction. Nat Immunol. 2015 Apr;16(4):354-65. doi: 10.1038/ni.3103.
41. Garlanda C, Anders HJ, Mantovani A. TIR8/SIGIRR: an IL-1R/TLR family member with regulatory functions in inflammation and T cell polarization. Trends Immunol. 2009 Sep;30(9):439-46. doi: 10.1016/j.it.2009.06.001.
42. Li L, Wei J, Li S, Jacko AM, Weathington NM, Mallampalli RK, et al. The deubiquitinase USP13 stabilizes the anti-inflammatory receptor IL-1R8/Sigirr to suppress lung inflammation. EBioMedicine. 2019 Jul;45:553-562. doi: 10.1016/j.ebiom.2019.06.011.
43. Li L, Wei J, Suber TL, Ye Q, Miao J, Li S, et al. IL-37-induced activation of glycogen synthase kinase 3β promotes IL-1R8/Sigirr phosphorylation, internalization, and degradation in lung epithelial cells. J Cell Physiol. 2021 Aug;236(8):5676-5685. doi: 10.1002/jcp.30253.
44. Dinarello CA, Novick D, Kim S, Kaplanski G. Interleukin-18 and IL-18 binding protein. Front Immunol. 2013 Oct 8;4:289. doi: 10.3389/fimmu.2013.00289.
45. Novick D, Kim S, Kaplanski G, Dinarello CA. Interleukin-18, more than a Th1 cytokine. Semin Immunol. 2013 Dec 15;25(6):439-48. doi: 10.1016/j.smim.2013.10.014.
46. Wawrocki S, Druszczynska M, Kowalewicz-Kulbat M, Rudnicka W. Interleukin 18 (IL-18) as a target for immune intervention. Acta Biochim Pol. 2016;63(1):59-63. doi: 10.18388/abp.2015_1153.
47. Wawrocki S, Kielnierowski G, Rudnicka W, Seweryn M, Druszczynska M. Interleukin-18, Functional IL-18 Receptor and IL-18 Binding Protein Expression in Active and Latent Tuberculosis. Pathogens. 2020 Jun 8;9(6):451. doi: 10.3390/pathogens9060451.
48. Chen YH, Zhou BY, Wu XJ, Xu JF, Zhang JA, Chen YH, Liang SS. CCL22 and IL-37 inhibit the proliferation and epithelial-mesenchymal transition process of NSCLC A549 cells. Oncol Rep. 2016 Oct;36(4):2017-24. doi: 10.3892/or.2016.4995. Epub 2016 Aug 2. Erratum in: Oncol Rep. 2021 Feb;45(2):786.
49. Dinarello CA, Nold-Petry C, Nold M, Fujita M, Li S, Kim S, Bufler P. Suppression of innate inflammation and immunity by interleukin-37. Eur J Immunol. 2016 May;46(5):1067-81. doi: 10.1002/eji.201545828.
50. Józefowski S, Sobota A, Pawłowski A, Kwiatkowska K. Mycobacterium tuberculosis lipoarabinomannan enhances LPS-induced TNF-α production and inhibits NO secretion by engaging scavenger receptors. Microb Pathog. 2011 Jun;50(6):350-9. doi: 10.1016/j.micpath.2011.03.001.
51. Huang Z, Zhao GW, Gao CH, Chi XW, Zeng T, Hu YW, Zheng L, Wang Q. Mannose-capped Lipoarabinomannan from Mycobacterium tuberculosis induces IL-37 production via upregulating ERK1/2 and p38 in human type II alveolar epithelial cells. Int J Clin Exp Med. 2015 May 15;8(5):7279-87. Erratum in: Int J Clin Exp Med. 2015;8(10):19791.
52. Zhang JA, Liu GB, Zheng BY, Lu YB, Gao YC, Cai XZ, et al. Tuberculosis-sensitized monocytes sustain immune response of interleukin-37. Mol Immunol. 2016 Nov;79:14-21. doi: 10.1016/j.molimm.2016.09.018.
53. Yang T, Lin Q, Zhao M, Hu Y, Yu Y, Jin J, et al. IL-37 Is a Novel Proangiogenic Factor of Developmental and Pathological Angiogenesis. Arterioscler Thromb Vasc Biol. 2015 Dec;35(12):2638-46. doi: 10.1161/ATVBAHA.115.306543.
54. Shiojima I, Walsh K. Role of Akt signaling in vascular homeostasis and angiogenesis. Circ Res. 2002 Jun 28;90(12):1243-50. doi: 10.1161/01.res.0000022200.71892.9f.
55. Huang Z, Gao C, Chi X, Hu YW, Zheng L, Zeng T, Wang Q. IL-37 Expression is Upregulated in Patients with Tuberculosis and Induces Macrophages Towards an M2-like Phenotype. Scand J Immunol. 2015 Oct;82(4):370-9. doi: 10.1111/sji.12326.
56. Liang M, Habib Z, Sakamoto K, Chen X, Cao G. Mycobacteria and Autophagy: Many Questions and Few Answers. Curr Issues Mol Biol. 2017;21:63-72.
57. Pan Y, Wen X, Hao D, Wang Y, Wang L, He G, Jiang X. The role of IL-37 in skin and connective tissue diseases. Biomed Pharmacother. 2020 Feb;122:109705. doi: 10.1016/j.biopha.2019.109705.
58. Kim MS, Baek AR, Lee JH, Jang AS, Kim DJ, Chin SS, Park SW. IL-37 Attenuates Lung Fibrosis by Inducing Autophagy and Regulating TGF-β1 Production in Mice. J Immunol. 2019 Oct 15;203(8):2265-2275. doi: 10.4049/jimmunol.1801515.
59. Lei H, Sun Y, Quan S. IL-37 relieves allergic inflammation by inhibiting the CCL11 signaling pathway in a mouse model of allergic rhinitis. Exp Ther Med. 2020 Oct;20(4):3114-3121. doi: 10.3892/etm.2020.9078.
60. Shen Y, Ke X, Yun L, Hu GH, Kang HY, Hong SL. Decreased expression of interleukin37 and its antiinflammatory effect in allergic rhinitis. Mol Med Rep. 2018 Jan;17(1):1333-1339. doi: 10.3892/mmr.2017.7988.
61. Meyer N, Akdis CA. Vascular endothelial growth factor as a key inducer of angiogenesis in the asthmatic airways. Curr Allergy Asthma Rep. 2013 Feb;13(1):1-9. doi: 10.1007/s11882-012-0317-9.
62. Moretti S, Bozza S, Oikonomou V, Renga G, Casagrande A, Iannitti RG, et al. IL-37 inhibits inflammasome activation and disease severity in murine aspergillosis. PLoS Pathog. 2014 Nov 6;10(11):e1004462. doi: 10.1371/journal.ppat.1004462.
63. Cavalli G, Justice JN, Boyle KE, D'Alessandro A, Eisenmesser EZ, Herrera JJ, et al. Interleukin 37 reverses the metabolic cost of inflammation, increases oxidative respiration, and improves exercise tolerance. Proc Natl Acad Sci U S A. 2017 Feb 28;114(9):2313-2318. doi: 10.1073/pnas.1619011114.
64. Liu H, Zheng R, Wang P, Yang H, He X, Ji Q, et al. IL-37 Confers Protection against Mycobacterial Infection Involving Suppressing Inflammation and Modulating T Cell Activation. PLoS One. 2017 Jan 11;12(1):e0169922. doi: 10.1371/journal.pone.0169922.

Corresponding authors:

Prof. Aihua Liu, PhD, The Institute for Tropical Medicine, Faculty of Basic Medical Sciences, Kunming Medical University, Kunming 650500, China, E-mail: liuaihua@kmmu.edu.cn

Prof. Fukai Bao, MD, The Institute for Tropical Medicine, Faculty of Basic Medical Sciences, Kunming Medical University, Kunming 650500, China, E-mail: baofukai@kmmu.edu.cn

International Journal of Biomedicine 14(2) (2024) 217-226
http://dx.doi.org/10.21103/Article14(2)_RA2

REVIEW ARTICLE

INTERNATIONAL JOURNAL OF BIOMEDICINE

A Narrative Review of the Impacts of Obesity on Pulmonary Function and Muscle Strength

Ahad Fahad Alzahrani[1], Wessam Ezzat[2,3], Walid Kamal Abdelbasset[1*]

[1]*Department of Physical therapy, College of Health Sciences, University of Sharjah, Sharjah, United Arab Emirates*
[2]*Department of Physiology, Faculty of Medicine, Ain-Shams University, Cairo, Egypt*
[3]*Department of Physiology, Armed Forces college of Medicine, Cairo, Egypt*

Abstract

Obesity has reached alarming proportions worldwide, requiring close attention and comprehensive knowledge about its health consequences. Obesity today affects people of all ages and socioeconomic levels. This narrative review is devoted to the multifaceted impacts of obesity on pulmonary function and muscle strength. Obesity, characterized by excessive fat accumulation, induces complex physiological changes, transforming adipose tissue into a metabolically dynamic organ. The multifarious nature of obesity causes complicated physiological alterations that affect the whole body. Besides its well-known impacts on metabolic health, obesity, particularly abdominal obesity, challenges the respiratory system mechanically. This review navigates through the mechanical challenges that obesity poses to pulmonary function, elucidating how excess adipose tissue in the abdominal region compromises lung expansion and increases the workload on respiratory muscles. Simultaneously, the review explores the dynamic interplay between obesity and muscle strength. Obesity and muscle strength are linked by metabolic dysfunction, muscle composition changes, and lifestyle variables. Clinical implications of obesity extend beyond metabolic consequences, emphasizing impaired pulmonary function and diminished muscle strength as crucial determinants of clinical outcomes. A multidisciplinary approach involving collaboration among healthcare professionals is advocated, addressing the physiological and psychological factors contributing to obesity.**(International Journal of Biomedicine. 2024;14(2):217-226.)**

Keywords: adipose tissue • obesity • pulmonary function • muscle strength

For citation: Alzahrani AF, Ezzat W, Abdelbasset WK. A Narrative Review of the Impacts of Obesity on Pulmonary Function and Muscle Strength. International Journal of Biomedicine. 2024;14(2):217-226. doi:10.21103/Article14(2)_RA2

Abbreviations

AT, adipose tissue; **BMI**, body mass index; **CBT**, cognitive behavioral therapy; **COPD**, chronic obstructive pulmonary disease; **ERV**, expiratory reserve volume; **FEV1**, forced expiratory volume in 1 second**; FVC**, forced vital capacity; **FRC**, functional residual capacity; **MIP**, maximal inspiratory pressure; **MEP**, maximal expiratory pressure; **OSA**, obstructive sleep apnea; **OHS**, obesity-hypoventilation syndrome; **WHO,** World Health Organization.

Introduction

Obesity is a metabolic state generated by the expansion of adipose tissue resulting from a complex interaction of hereditary, environmental, and behavioral variables.(1) The primary cause of obesity is an imbalance between energy intake and expenditure, disrupting energy homeostasis and resulting in initial fat accumulation in adipose tissue and subsequent accumulation in other tissues.

Obesity has reached worrisome proportions globally due to lifestyle and nutritional changes, requiring careful attention and a comprehensive knowledge of its health effects. Around 800 million people worldwide are living with obesity, according to statistics from 2016. WHO (2) estimates that by 2025, approximately 167 million more people will become less healthy because they are overweight or obese. This frequency crosses socioeconomic borders, impacting people in industrialized and underdeveloped countries.

The obesogenic environment, with the easy availability of high-calorie meals and a sedentary lifestyle, leads to rising obesity rates. Obesity contributes to the development of type 2 diabetes, cardiovascular disease, liver dysfunction, and cancer, which collectively account for over 70% of premature deaths worldwide.[3-7] This highlights the critical need for comprehensive initiatives that address lifestyle choices and social and environmental variables affecting obesity.

Body mass index (BMI) is one of the ways to measure obesity in the population.[8-10] Obesity is linked not only to an increased BMI and body weight but also affects multiple physiological systems, causing complex alterations beyond adipose tissue.[11] Obesity involves a complex interaction of metabolic, hormonal, and inflammatory variables that disrupt the body beyond outward indicators of obesity and cause a variety of health issues.[12] Global obesity is a major public health issue. Obesity today affects people of all ages and socioeconomic levels. The WHO considers obesity a major risk factor for a variety of chronic illnesses, including cardiovascular disease, metabolic disorders, and cancer.[13] This change in viewpoint emphasizes the need for a comprehensive strategy to treat obesity's complex health concerns beyond its evident physical effects.[8,11]

This review aims to assess the complex interactions in obesity and, in particular, the impact of obesity on pulmonary function and muscle strength.

Some Physiological Changes in Obesity

Adipose tissue is an endocrine organ that not only stores lipids but also secretes various biologically active substances, such as cytokines, adipokines, chemokines, and hormonal factors, that regulate metabolic processes in the organism and affect inflammation and endocrine functions.[14,15] Adipokines are involved in many functions and processes, including modulation of energy and appetite, lipid and glucose metabolism, insulin sensitivity, endothelial cell function, inflammation, blood pressure, the development of metabolic syndrome, and atherosclerosis.[16,17] Visfatin, a recently discovered adipokine, has been positively correlated with the accumulation of adipose tissue. Visfatin has pro-oxidant and pro-inflammatory activity and is elevated in obese individuals. Chemerin, highly expressed in white adipose, is involved in inflammation, angiogenesis, adipogenesis, energy metabolism, and oxidative stress.[16] Chemerin is best characterized as a chemoattractant for dendritic cells and macrophages. Most studies report increased chemerin levels with increased body weight.

Obesity is associated with the activation of pro-inflammatory adipokines and the development of chronic low-grade inflammation.[18,19] One of the best-known pro-inflammatory adipokines is leptin. Leptin, a hormone synthesized mainly in adipocytes, provides central weight control and appetite regulation. Obesity-induced hyperleptinemia stimulates the production of pro-inflammatory cytokines such as TNF-α, IL-6, IL-2, IL-1β, and IFN-γ by monocytes and T-helper 1 and also inhibits the production of the anti-inflammatory cytokine IL-4.[20,21] Studies have also shown that leptin increases serum levels of C-reactive protein. The abnormal expression of TNF-α in adipose tissue plays a critical role in peripheral insulin resistance in obesity. It has been demonstrated as a marker of insulin resistance.[22]

Inflammation contributes to the development of leptin resistance. Leptin resistance reduces leptin's ability to send satiety signals to the brain, causing overeating and weight gain.[23] In contrast to leptin, adiponectin, which is secreted by differentiated adipocytes, has anti-inflammatory and anti-atherogenic effects. In obesity, adiponectin, a key adipokine for insulin sensitivity and glucose control, paradoxically decreases,[24,25] causing metabolic events such as impaired glucose absorption and a higher risk of type 2 diabetes.[24] The complex hormonal and inflammatory environment of obesity's adipose tissue shows its dynamic character.[24,25]

Various biologically active substances secreted by adipose tissue, including adipokines, cytokines, chemokines, excess lipids, and toxic lipid metabolites, promote insulin resistance, an impaired biologic response of target tissues to insulin stimulation. Abdominal obesity and insulin resistance, along with hypertension and dyslipidemia, are key components of metabolic syndrome,[26] which contributes to endothelial dysfunction, platelet hyperactivity, oxidative stress, and low-grade inflammation, resulting in the development of cardiovascular disease.

Dyslipidemia (elevated levels of triglycerides and low-density lipoprotein cholesterol), low-grade inflammation, and metabolic dysregulation associated with obesity contribute to the development of atherosclerosis and cardiovascular complications.[27,28]

In obesity, the total blood volume increases due to adipose tissue excess, leading to increased stroke volume and cardiac output.[29] Increasing cardiac output in obese patients is intended to meet the metabolic demands of excess adipose tissue. The left ventricle (LV) dilates to accommodate the increased venous return and becomes hypertrophied. The left atrium also dilates due to increased circulating blood volume and elevated LV diastolic filling pressure. A dilated left atrium and increased LV filling pressure increase the risk of heart failure and atrial fibrillation. Changes in myocardial structure due to infiltration of adipose tissue predispose to conduction abnormalities and ventricular arrhythmias,[30,31] worsening heart failure. The long-term cardiovascular effects of metabolic dysfunction in obesity necessitate a comprehensive strategy.

Obesity and Pulmonary Function

Besides its well-known impacts on metabolic health, obesity, particularly abdominal obesity, challenges the respiratory system mechanically. Excess body fat, or obesity, affects pulmonary function via several routes.[32] Obesity limits lung expansion mechanically. Excess chest and abdominal fat restrict the diaphragm's fall during inhalation, reducing lung expansion. Obesity alters the breathing pattern, resulting in a substantial reduction in both the expiratory reserve volume and the resting volume of the lung, known as the functional residual capacity (FRC).[33] The reduction in FRC is proportional to the

severity of obesity – overweight, mildly obese and severely obese subjects without asthma demonstrate reductions in FRC of up to 10%, 22% and 33%, respectively.[34]

The lowering in FVC and FEV1 impedes gas exchange. Weight also strains respiratory muscles, making them work harder to overcome resistance.[35] This increased effort may cause tiredness and respiratory muscle weakness. Obesity is linked to chronic inflammation beyond mechanical consequences.[25,36] Inflammatory mediators released by adipose tissue in obesity may affect airway anatomy and function.[37] This inflammatory milieu may cause respiratory disorders, including asthma and chronic obstructive pulmonary disease (COPD). Leptin resistance and other hormonal variables significantly influence the complex interaction between obesity and pulmonary function. Adipose tissue produces leptin, which regulates hunger and energy. Obesity may cause leptin resistance.[38] Leptin resistance may upregulate the generation of reactive oxygen species, increasing oxidative stress and promoting inflammation in airways and lung parenchyma.[39]

Obstructive sleep apnea (OSA), strongly associated with obesity, especially central obesity, complicates matters. Obesity, especially around the neck and throat, narrows or collapses the upper airway, obstructing sleep. Obstructive sleep apnea causes disrupted sleep patterns, periodic hypoxia and hypercapnia, straining the respiratory system. The cyclical nature of OSA, with periods of slowed or stopped breathing followed by sudden awakenings, makes it harder for obese people to maintain adequate respiratory function. Disrupted sleep habits may increase weight gain, affecting hormone balance and hunger, causing daily weariness and impairment of cognitive performance.[40]

Obesity-related neuromuscular, mechanical, and metabolic factors may cause obesity hypoventilation syndrome (OHS), [41,42] also known as Pickwickian syndrome. Obesity hypoventilation syndrome is defined as the presence of awake alveolar hypoventilation characterized by daytime hypercapnia, which is thought to be a consequence of diminished ventilatory drive and capacity related to obesity. Obesity hypoventilation syndrome results from the mechanical load on the respiratory pump, leading to low tidal volumes and blunting of the chemoreflex to CO_2, leading to inappropriate central respiratory effort in individuals with obesity. The hypercapnia of OHS may be augmented by leptin resistance. Individuals with OHS have a greater degree of central obesity reflected by larger neck circumferences and higher waist-to-hip ratios than those with eucapnic obesity or OSA, which explains the lower lung volumes seen in such individuals.[43] Individuals with OHS are exposed to prolonged periods of daytime and nocturnal hypoxia and are consequently at higher risk for pulmonary hypertension and cor pulmonale.[44-47] Obesity hypoventilation syndrome is more common in women than men and postmenopausal women with OSA have a higher prevalence of OHS due to hormonal influences.

Due to lower lung function, obese people may also be more susceptible to respiratory infections. Obesity's impaired mucus clearance and immune response promote respiratory diseases, including pneumonia and bronchitis. Airway hyperresponsiveness, a hallmark of asthma, is linked to obesity. Due to airway sensitivity, obese people may acquire or worsen asthma. Asthma is one of the best-characterized diseases related to obesity. A meta-analysis involving over 300,000 adults found obesity and asthma were related, and the risk of asthma increased with increasing BMI.[48] Excess weight weakens the respiratory muscles, reducing airflow, especially when the respiratory load is high.

Thus, respiratory dysfunctions observed in patients with obesity are characterized by impaired breathing mechanics, decreased respiratory system compliance, increased small airway resistance, and alterations in both breathing patterns and respiratory drive. [49-52]

Pulmonary Function Assessment

The multimodal evaluation of pulmonary function in obese people provides useful insights into the complex relationship between obesity and respiratory health. FVC and FEV1 readings in pulmonary function tests frequently suggest a restrictive pattern, indicating decreased lung capacity. Body fat distribution patterns have a stronger relationship with lung function than weight or BMI.[53,54] A large population-based study of 121,965 people found that abdominal obesity predicted FEV1 and FVC independent of BMI.[53] Changing pulmonary function due to obesity is not limited to volume changes. Respiratory mechanics are also impacted, with greater breathing effort and decreased respiratory muscle efficiency. This is essential because it shows that obesity and respiratory health are dynamic beyond volume measures.[35]

Some studies showed that measuring respiratory system impedance may be a more sensitive measure of lung dysfunction related to obesity than spirometry.[55-57] Whole-body plethysmography, impulse oscillometry, or the forced oscillation technique can also be used to assess the mechanical properties of the airways in obese individuals. Respiratory muscle strength can be assessed by measuring maximal inspiratory pressure (MIP) and maximal expiratory pressure (MEP). In obese individuals, both MIP and MEP may be reduced.

Obesity also affects gas exchange. Ventilation-perfusion mismatch and poor diffusion capacity are common, stressing the necessity for a complete respiratory examination. Comprehensive examinations are important for identifying obesity's increased risk of respiratory disorders, such as hypoventilation syndromes and OSA.[58]

Obesity-related changes in pulmonary function vary by person. Body fat distribution, obesity duration, and comorbidities affect pulmonary function measures. Thus, obesity-related pulmonary function testing must be nuanced and customized for correct diagnosis, risk classification, and focused therapy.[59] A complete study of pulmonary function in obese persons gives a full understanding of the complicated link between excess body weight and respiratory health, enabling informed clinical decision-making and individualized therapy methods.

Obesity and Muscle Strength

Obesity and muscle strength are interconnected health factors. Body mass index, which incorporates weight and height, measures obesity as excessive body fat. In contrast, muscle strength encompasses muscle size, composition, and neuromuscular efficiency, determining force production.[60]

Obesity affects muscle mass, which is vital to body composition and health. Sarcopenia and excessive body fat commonly occur with obesity. The rise in body fat and decrease in lean muscle mass are combined issues. Strength depends on muscle mass. In obesity, extra body fat may hide muscle atrophy, making it harder to diagnose and treat. The role of adipose tissue in maintaining muscle mass and function has been well studied. Adipose tissue is an active endocrine organ that produces signaling chemicals that may cause inflammation. This inflammatory milieu may further catabolize muscle tissue, disrupting muscle protein production and breakdown.[61] Chronic, low-grade inflammation, often found in obesity, reduces muscle strength, impairs physical function, and can cause sarcopenia. Insulin resistance in obesity can affect the ability of muscle cells to use glucose for energy, affecting strength and function. Obesity-related inflammation can affect neuromuscular connections, leading to decreased coordinated contractility.[61,62]

The relationship between fat and muscle strength grows increasingly complex with age. Muscle mass and muscle strength naturally drop with age. Marcus et al. reported that intramuscular adipose tissue was inversely related to physical performance in older adults.[63] Moreover, aging results in a shift towards a higher proportion of type I muscle fibers, muscle fiber atrophy, especially in type II fibers,[64] and changes in muscle structure (i.e., pennation angle, and fascicle length).[65]

Sarcopenia, age-related muscle loss and function, is aggravated by hormonal changes, reduced physical activity, and nutrition metabolism changes. Obesity rises with age. Obesity and age together threaten muscular health. Sarcopenic obesity, when muscle loss and body fat increase with age, exacerbates this.[61] Chronic inflammation accelerates muscle deterioration in obese older adults. Aging and fat cause inflammation, which might make muscle tissue more vulnerable. Chronic inflammation increases muscle atrophy and age-related illnesses, including arthritis and cardiovascular disease, reducing mobility and functioning. The reduction in muscle mass and muscle strength caused by aging and obesity affects older persons' functional independence and quality of life. Muscle weakness may cause falls, fragility, and difficulty with regular tasks.

Obesity affects the musculoskeletal system beyond muscle strength. The skeletal system, including joints, carries the body's weight, and excessive load may damage joint function and health, especially knees and hips.[66] This increased strain may accelerate joint cartilage wear and tear, contributing to degenerative disorders and osteoarthritis.[67,68] The production of several pro-inflammatory cytokines during obesity contributes to joint tissue destruction.

Maintaining older physical strength is essential for mobility, independence, and well-being. To address the difficulties of aging and obesity, a personalized strategy is necessary. Interventions should include lifestyle changes, physical exercise, and nutritional choices to address the relationship between obesity and muscle strength. A balanced diet is essential for weight control. Regular aerobic and resistance training are needed to maintain muscle mass and muscle strength. Resistance exercise reduces age-related muscle loss and boosts strength.[69,70] Weight reduction should be gradual and sustained to minimize muscle loss.[71,72]

Muscle Strength Assessment

Examining muscle strength in obesity reveals a complex picture beyond weight control. Excess weight severely impacts musculoskeletal health, affecting muscle function and performance. Understanding the complex relationship between obesity and musculoskeletal function requires comprehensive muscle strength evaluation in obese people. Research consistently links obesity to decreased muscle strength in both proximal and distal muscle groups. Increased mechanical strain on weight-bearing joints, changed muscle composition, and extra adipose tissue-related inflammation contribute to this strength loss. These variables reduce muscular force production and endurance, affecting everyday functioning and quality of life.[61,62]

Isometric and isokinetic tests measure obesity-related muscular strength. Detailed strength analysis across joint motions reveals damaged muscle areas using these data. The assessment of arms, shoulders, and lower extremity strength is particularly relevant.

In two British cohort studies, grip strength was positively associated with BMI, while it was negatively associated with central obesity measured using waist circumference.[73,74] Some studies reported a relationship between muscle/grip strength with blood lipid profile.[75,76,77]

Systematically testing muscle strength helps uncover weakening patterns and comprehend functional consequences for everyday life and mobility.[59] Sedentary behavior worsens muscular weakness, fat and musculoskeletal health are linked. A complete health plan must include measures to preserve and improve muscle strength in obese people.

Interaction between Pulmonary Function and Muscle Strength

The relationship between pulmonary function and muscle strength is complicated, especially in obesity. Multiple factors, including mechanical, inflammatory, metabolic, and lifestyle variables, may affect this relationship in obesity. [35,66] As obesity increases, the function of the respiratory muscles may be impaired due to stress on the diaphragm. Respiratory muscle dysfunction may be partially explained by increased resistance caused by the presence of excess fatty tissue on the chest and abdomen, which leads to mechanical damage to these muscles.[78,79]

This increased breathing effort may cause dyspnea and weariness, especially during oxygen-intensive tasks.

Ventilatory muscle weakness reduces respiratory functions, vital capacity, and lung function. Inspiratory and expiratory flows may be impeded, affecting lung gas exchange. Reduced carbon dioxide clearance may cause respiratory issues and low oxygen saturation.

In addition to mechanical restrictions, obesity causes persistent low-grade inflammation that affects the respiratory system. This inflammation may damage airways and lung tissues, worsening asthma and chronic obstructive pulmonary disease. The inflammatory milieu in obesity may make the respiratory system more susceptible to malfunction, affecting pulmonary function.[37,80]

Obesity-related metabolic changes impair pulmonary function. The body's metabolic and respiratory systems are interconnected, highlighting obesity's systemic effects. Obesity contributes to difficulty breathing and decreased respiratory efficiency due to mechanical, immunological, and metabolic effects. Obesity-related muscle strength and respiratory alterations impair exercise tolerance. Obesity weakens respiratory muscles and muscle strength, making prolonged physical activity difficult. A positive feedback loop exists between exercise ability and musculoskeletal health.[81] Weak muscles and joint tension hinder physical activity, deconditioning muscles and reducing exercise capacity. Evaluating metabolic variables and their systemic effects on obesity is vital for comprehending the connection between the pulmonary and musculoskeletal systems.[82] Insulin resistance and persistent low-grade inflammation impair the respiratory and musculoskeletal systems. Insulin resistance, as a characteristic of obesity, is crucial to metabolic variables and musculoskeletal health. With insulin resistance, skeletal muscles absorb glucose less, and energy production by muscle cells decreases, leading to muscle weakness and fatigue. Muscle dysfunction may influence musculoskeletal health, mobility, and exercise performance.[83]

Understanding these pulmonary problems and functional muscle damage in the setting of obesity is essential for creating tailored therapies to improve respiratory health and avoid respiratory consequences in obese people.[35]

Non-Pharmacological Therapeutic Modalities for Obesity

Comprehensive obesity treatment emphasizes non-pharmacological therapies. Obesity control relies on lifestyle changes, especially nutrition. A balanced, calorie-controlled diet rich in nutritious foods, fruits, vegetables, and lean meats promotes healthy eating habits. Structured exercise regimens, which include aerobic and resistance training, help lose weight, maintain muscle mass, and improve metabolic health.[84] Thus, lifestyle modification, which generally consists of a combination of nutrition, physical activity, and behavioral modification, is an oft-used strategy to help patients achieve weight loss and maintenance.[85,86]

Several studies have investigated the effects of weight loss on airway reactivity.[56, 87, 88] Aaron et al.[87] found a trend towards reduced airway hyperresponsiveness with weight loss following an intense diet-induced weight reduction program in obese asthmatics and controls. Several studies have shown that ERV increases after weight loss, adopting a calorie-restricted diet, or bariatric surgery. Hakala et al. [89] found a considerable increase in the ERV of patients whose BMI decreased from 45 to 39 kg/m^2 after adopting a calorie-restricted diet. Weight loss also causes changes in other parameters, including functional residual capacity, total lung capacity, and gas exchange, resulting in increased blood oxygenation.[89] Babb et al. showed that even modest reductions in weight, i.e., a decrease in BMI from 35 to 33 kg/m^2, induce an increase in end-expiratory lung volume during submaximal exercise.[90]

Addressing obesity's complex psychosocial implications requires behavioral therapies. Cognitive behavioral therapy (CBT) for obesity is a treatment modality that combines the traditional procedures of standard behavioral therapy for obesity with a set of specific cognitive strategies and procedures. It is aimed at not only losing weight but also preventing weight regain, thereby avoiding the dissatisfactory long-term results of earlier behavioral treatments.[91,92] These behavioral techniques are enhanced by goal setting, self-monitoring, and stress- and emotion-management strategies.[93,94]

Regarding the appropriate threshold, previous behavioral weight-loss studies often reported 5% weight loss as a clinically significant threshold.[95-98] In a study by Dalle Grave,[99] 67 adult patients with obesity (BMI $\geq$ 30 kg/m^2) were recruited from consecutive referrals to an Italian National Health Service obesity clinic. Each patient was offered 22 group cognitive behavioral therapy sessions (14 in the 6-month weight-loss phase and 8 in the subsequent 12-month weight-maintenance phase). Weight loss of 11.5% after 6 months and 9.9% after 18 months of CBT was associated with a significant reduction in cardiovascular risk factors, anxiety, depression, eating disorder psychopathology, and an improvement in obesity-related quality of life.

Technological advances have extended non-pharmacological obesity treatments. Self-monitoring, goal setting, and progress tracking are possible via mobile apps, wearables, and internet platforms. This tech-driven strategy improves responsibility, gives real-time feedback, and empowers diet and exercise choices.[100]

Non-pharmacological therapies need long-term maintenance. Long-term success goes beyond weight reduction. Relapse prevention, behavioral support, and frequent evaluation and revisions of the intervention plan are essential for enduring improvements and decreasing obesity-related comorbidities.[101,102]

Conclusion

This narrative review illuminates the complex links between obesity, pulmonary function, and muscle strength. The multifarious nature of obesity causes complicated physiological alterations that affect the whole body. Excess belly fat tissue hinders lung expansion and strains respiratory muscles. Obesity and muscle strength are linked by metabolic dysfunction, muscle composition changes, and lifestyle variables. Obesity has far-reaching health effects, including

reduced respiratory functioning and muscle strength. Obesity's loss in pulmonary function and muscle strength highlights the necessity for multimodal intervention and therapy. This strategy should include doctors, nutritionists, physical therapists, and psychologists working together to address the behavioral and psychological causes of obesity.

Competing Interests

The authors declare that they have no competing interests.

References

1. Horwitz A, Birk R. Adipose Tissue Hyperplasia and Hypertrophy in Common and Syndromic Obesity-The Case of BBS Obesity. Nutrients. 2023 Aug 4;15(15):3445. doi: 10.3390/nu15153445. PMID: 37571382; PMCID: PMC10421039.
2. WHO. World Obesity Day 2022 – Accelerating action to stop obesity. March 2022. Available from: https://www.who.int/news/item/04-03-2022-world-obesity-day-2022-accelerating-action-to-stop-obesity
3. Apovian CM. Obesity: definition, comorbidities, causes, and burden. Am J Manag Care. 2016 Jun;22(7 Suppl):s176-85. PMID: 27356115.
4. Cnop M, Foufelle F, Velloso LA. Endoplasmic reticulum stress, obesity and diabetes. Trends Mol Med. 2012 Jan;18(1):59-68. doi: 10.1016/j.molmed.2011.07.010. Epub 2011 Aug 31. PMID: 21889406.
5. Jung UJ, Choi MS. Obesity and its metabolic complications: the role of adipokines and the relationship between obesity, inflammation, insulin resistance, dyslipidemia and nonalcoholic fatty liver disease. Int J Mol Sci. 2014 Apr 11;15(4):6184-223. doi: 10.3390/ijms15046184. PMID: 24733068; PMCID: PMC4013623.
6. Haczeyni F, Wang H, Barn V, Mridha AR, Yeh MM, Haigh WG, Ioannou GN, Choi YJ, McWherter CA, Teoh NC, Farrell GC. The selective peroxisome proliferator-activated receptor-delta agonist seladelpar reverses nonalcoholic steatohepatitis pathology by abrogating lipotoxicity in diabetic obese mice. Hepatol Commun. 2017 Jul 31;1(7):663-674. doi: 10.1002/hep4.1072. PMID: 29404484; PMCID: PMC5721439.
7. Bhaskaran K, Douglas I, Forbes H, dos-Santos-Silva I, Leon DA, Smeeth L. Body-mass index and risk of 22 specific cancers: a population-based cohort study of 5·24 million UK adults. Lancet. 2014 Aug 30;384(9945):755-65. doi: 10.1016/S0140-6736(14)60892-8. Epub 2014 Aug 13. PMID: 25129328; PMCID: PMC4151483.
8. Panuganti KK, Nguyen M, Kshirsagar RK. Obesity. 2023 Aug 8. In: StatPearls [Internet]. Treasure Island (FL): StatPearls Publishing; 2024 Jan–. PMID: 29083734.
9. Nuttall FQ. Body Mass Index: Obesity, BMI, and Health: A Critical Review. Nutr Today. 2015 May;50(3):117-128. doi: 10.1097/NT.0000000000000092. Epub 2015 Apr 7. PMID: 27340299; PMCID: PMC4890841.
10. Alqarni AM, Aljabr AS, Abdelwahab MM, Alhallafi AH, Alessa MT, Alreedy AH, Elmaki SA, Alamer NA, Darwish MA. Accuracy of body mass index compared to whole-body dual energy X-ray absorptiometry in diagnosing obesity in adults in the Eastern Province of Saudi Arabia: A cross-sectional study. J Family Community Med. 2023 Oct-Dec;30(4):259-266. doi: 10.4103/jfcm.jfcm_85_23. Epub 2023 Oct 13. PMID: 38044973; PMCID: PMC10688584.
11. Washington TB, Johnson VR, Kendrick K, Ibrahim AA, Tu L, Sun K, Stanford FC. Disparities in Access and Quality of Obesity Care. Gastroenterol Clin North Am. 2023 Jun;52(2):429-441. doi: 10.1016/j.gtc.2023.02.003. Epub 2023 Apr 7. PMID: 37197884; PMCID: PMC10198472.
12. Uranga RM, Keller JN. The Complex Interactions Between Obesity, Metabolism and the Brain. Front Neurosci. 2019 May 24;13:513. doi: 10.3389/fnins.2019.00513. PMID: 31178685; PMCID: PMC6542999.
13. Sørensen TIA, Martinez AR, Jørgensen TSH. Epidemiology of Obesity. Handb Exp Pharmacol. 2022;274:3-27. doi: 10.1007/164_2022_581. PMID: 35419622.
14. Liu L, Shi Z, Ji X, Zhang W, Luan J, Zahr T, Qiang L. Adipokines, adiposity, and atherosclerosis. Cell Mol Life Sci. 2022 May 3;79(5):272. doi: 10.1007/s00018-022-04286-2. PMID: 35503385.
15. Kwon H, Pessin JE. Adipokines mediate inflammation and insulin resistance. Front Endocrinol (Lausanne). 2013 Jun 12;4:71. doi: 10.3389/fendo.2013.00071. PMID: 23781214; PMCID: PMC3679475.
16. Metz S, Huang LO, Kilpeläinen TO. Genetic variation, adipokines, and cardiometabolic disease. Curr Opin Pharmacol. 2020 Jun;52:33-39. doi: 10.1016/j.coph.2020.04.006. Epub 2020 May 29. PMID: 32480034.
17. Farkhondeh T, Llorens S, Pourbagher-Shahri AM, Ashrafizadeh M, Talebi M, Shakibaei M, Samarghandian S. An Overview of the Role of Adipokines in Cardiometabolic Diseases. Molecules. 2020 Nov 9;25(21):5218. doi: 10.3390/molecules25215218. PMID: 33182462; PMCID: PMC7665135.
18. Unamuno X, Gómez-Ambrosi J, Rodríguez A, Becerril S, Frühbeck G, Catalán V. Adipokine dysregulation and adipose tissue inflammation in human obesity. Eur J Clin Invest. 2018 Sep;48(9):e12997. doi: 10.1111/eci.12997. Epub 2018 Aug 3. PMID: 29995306.
19. Wei Z, Chen Y, Upender RP. Sleep Disturbance and Metabolic Dysfunction: The Roles of Adipokines. Int J Mol Sci. 2022 Feb 1;23(3):1706. doi: 10.3390/ijms23031706. PMID: 35163627; PMCID: PMC8835888.
20. Rajesh Y, Sarkar D. Association of Adipose Tissue and Adipokines with Development of Obesity-Induced Liver Cancer. Int J Mol Sci. 2021 Feb 22;22(4):2163. doi: 10.3390/ijms22042163. PMID: 33671547; PMCID: PMC7926723.
21. Para I, Albu A, Porojan MD. Adipokines and Arterial Stiffness in Obesity. Medicina (Kaunas). 2021 Jun 25;57(7):653. doi: 10.3390/medicina57070653. PMID: 34202323; PMCID: PMC8305474.
22. Hofmann C, Lorenz K, Braithwaite SS, Colca JR, Palazuk BJ, Hotamisligil GS, Spiegelman BM. Altered gene expression for tumor necrosis factor-alpha and its receptors during drug and dietary modulation of insulin resistance. Endocrinology. 1994 Jan;134(1):264-70. doi: 10.1210/endo.134.1.8275942. PMID: 8275942.

23. Zammit C, Liddicoat H, Moonsie I, Makker H. Obesity and respiratory diseases. Int J Gen Med. 2010 Oct 20;3:335-43. doi: 10.2147/IJGM.S11926. PMID: 21116339; PMCID: PMC2990395.
24. Chait A, den Hartigh LJ. Adipose Tissue Distribution, Inflammation and Its Metabolic Consequences, Including Diabetes and Cardiovascular Disease. Front Cardiovasc Med. 2020 Feb 25;7:22. doi: 10.3389/fcvm.2020.00022. PMID: 32158768; PMCID: PMC7052117.
25. Arner P, Rydén M. Human white adipose tissue: A highly dynamic metabolic organ. J Intern Med. 2022 May;291(5):611-621. doi: 10.1111/joim.13435. Epub 2022 Jan 16. PMID: 34914848.
26. Rochlani Y, Pothineni NV, Kovelamudi S, Mehta JL. Metabolic syndrome: pathophysiology, management, and modulation by natural compounds. Ther Adv Cardiovasc Dis. 2017 Aug;11(8):215-225. doi: 10.1177/1753944717711379. Epub 2017 Jun 22. PMID: 28639538; PMCID: PMC5933580.
27. Bonora E. The metabolic syndrome and cardiovascular disease. Ann Med. 2006;38(1):64-80. doi: 10.1080/07853890500401234. PMID: 16448990.
28. Henning RJ. Obesity and obesity-induced inflammatory disease contribute to atherosclerosis: a review of the pathophysiology and treatment of obesity. Am J Cardiovasc Dis. 2021 Aug 15;11(4):504-529. PMID: 34548951; PMCID: PMC8449192.
29. Ashraf MJ, Baweja P. Obesity: the 'huge' problem in cardiovascular diseases. Mo Med. 2013 Nov-Dec;110(6):499-504. PMID: 24564002; PMCID: PMC6179812.
30. Messerli FH, Nunez BD, Ventura HO, Snyder DW. Overweight and sudden death. Increased ventricular ectopy in cardiopathy of obesity. Arch Intern Med. 1987 Oct;147(10):1725-8. doi: 10.1001/archinte.147.10.1725. PMID: 2444173.
31. Balsaver AM, Morales AR, Whitehouse FW. Fat infiltration of myocardium as a cause of cardiac conduction defect. Am J Cardiol. 1967 Feb;19(2):261-5. doi: 10.1016/0002-9149(67)90543-7. PMID: 6016426.
32. Hegewald MJ. Impact of obesity on pulmonary function: current understanding and knowledge gaps. Curr Opin Pulm Med. 2021 Mar 1;27(2):132-140. doi: 10.1097/MCP.0000000000000754. PMID: 33394747.
33. Dixon AE, Peters U. The effect of obesity on lung function. Expert Rev Respir Med. 2018 Sep;12(9):755-767. doi: 10.1080/17476348.2018.1506331. Epub 2018 Aug 14. PMID: 30056777; PMCID: PMC6311385.
34. Jones RL, Nzekwu MM. The effects of body mass index on lung volumes. Chest. 2006 Sep;130(3):827-33. doi: 10.1378/chest.130.3.827. PMID: 16963682.
35. Zammit C, Liddicoat H, Moonsie I, Makker H. Obesity and respiratory diseases. Int J Gen Med. 2010 Oct 20;3:335-43. doi: 10.2147/IJGM.S11926. PMID: 21116339; PMCID: PMC2990395.
36. Westphal SA. Obesity, abdominal obesity, and insulin resistance. Clin Cornerstone. 2008;9(1):23-29; discussion 30-1. doi: 10.1016/s1098-3597(08)60025-3. PMID: 19046737.
37. Hornung F, Rogal J, Loskill P, Löffler B, Deinhardt-Emmer S. The Inflammatory Profile of Obesity and the Role on Pulmonary Bacterial and Viral Infections. Int J Mol Sci. 2021 Mar 26;22(7):3456. doi: 10.3390/ijms22073456. PMID: 33810619; PMCID: PMC8037155.
38. Peters U, Suratt BT, Bates JHT, Dixon AE. Beyond BMI: Obesity and Lung Disease. Chest. 2018 Mar;153(3):702-709. doi: 10.1016/j.chest.2017.07.010. Epub 2017 Jul 17. PMID: 28728934; PMCID: PMC5989645.
39. Malli F, Papaioannou AI, Gourgoulianis KI, Daniil Z. The role of leptin in the respiratory system: an overview. Respir Res. 2010 Oct 31;11(1):152. doi: 10.1186/1465-9921-11-152. PMID: 21040518; PMCID: PMC2988727.
40. Ho ML, Brass SD. Obstructive sleep apnea. Neurol Int. 2011 Nov 29;3(3):e15. doi: 10.4081/ni.2011.e15. Epub 2011 Dec 2. PMID: 22368774; PMCID: PMC3286155.
41. Tomlinson DJ, Erskine RM, Morse CI, Winwood K, Onambélé-Pearson G. The impact of obesity on skeletal muscle strength and structure through adolescence to old age. Biogerontology. 2016 Jun;17(3):467-83. doi: 10.1007/s10522-015-9626-4. Epub 2015 Dec 14. PMID: 26667010; PMCID: PMC4889641.
42. Ellulu MS, Patimah I, Khaza'ai H, Rahmat A, Abed Y. Obesity and inflammation: the linking mechanism and the complications. Arch Med Sci. 2017 Jun;13(4):851-863. doi: 10.5114/aoms.2016.58928. Epub 2016 Mar 31. PMID: 28721154; PMCID: PMC5507106.
43. Resta O, Foschino-Barbaro MP, Bonfitto P, Talamo S, Legari G, De Pergola G, Minenna A, Giorgino R. Prevalence and mechanisms of diurnal hypercapnia in a sample of morbidly obese subjects with obstructive sleep apnoea. Respir Med. 2000 Mar;94(3):240-6. doi: 10.1053/rmed.1999.0732. PMID: 10783935.
44. Kessler R, Chaouat A, Schinkewitch P, Faller M, Casel S, Krieger J, Weitzenblum E. The obesity-hypoventilation syndrome revisited: a prospective study of 34 consecutive cases. Chest. 2001 Aug;120(2):369-76. doi: 10.1378/chest.120.2.369. PMID: 11502631.
45. Berg G, Delaive K, Manfreda J, Walld R, Kryger MH. The use of health-care resources in obesity-hypoventilation syndrome. Chest. 2001 Aug;120(2):377-83. doi: 10.1378/chest.120.2.377. PMID: 11502632.
46. Borel JC, Roux-Lombard P, Tamisier R, Arnaud C, Monneret D, Arnol N, Baguet JP, Levy P, Pepin JL. Endothelial dysfunction and specific inflammation in obesity hypoventilation syndrome. PLoS One. 2009 Aug 24;4(8):e6733. doi: 10.1371/journal.pone.0006733. PMID: 19701463; PMCID: PMC2726948.
47. Masa JF, Pépin JL, Borel JC, Mokhlesi B, Murphy PB, Sánchez-Quiroga MÁ. Obesity hypoventilation syndrome. Eur Respir Rev. 2019 Mar 14;28(151):180097. doi: 10.1183/16000617.0097-2018. PMID: 30872398; PMCID: PMC9491327.
48. Beuther DA, Sutherland ER. Overweight, obesity, and incident asthma: a meta-analysis of prospective epidemiologic studies. American journal of respiratory and critical care medicine 2007. April 1;175(7):661–6. doi: 10.1164/rccm.200611-1717OC.
49. Babb TG. Obesity: challenges to ventilatory control during exercise--a brief review. Respir Physiol Neurobiol.

2013 Nov 1;189(2):364-70. doi: 10.1016/j.resp.2013.05.019. Epub 2013 May 21. PMID: 23707540; PMCID: PMC3797147.
50. Chlif M, Keochkerian D, Choquet D, Vaidie A, Ahmaidi S. Effects of obesity on breathing pattern, ventilatory neural drive and mechanics. Respir Physiol Neurobiol. 2009 Sep 30;168(3):198-202. doi: 10.1016/j.resp.2009.06.012. Epub 2009 Jun 24. PMID: 19559105.
51. Lin CK, Lin CC. Work of breathing and respiratory drive in obesity. Respirology. 2012 Apr;17(3):402-11. doi: 10.1111/j.1440-1843.2011.02124.x. PMID: 22212441.
52. Sood A. Altered resting and exercise respiratory physiology in obesity. Clin Chest Med. 2009 Sep;30(3):445-54, vii. doi: 10.1016/j.ccm.2009.05.003. PMID: 19700043; PMCID: PMC2765111.
53. Leone N, Courbon D, Thomas F, Bean K, Jégo B, Leynaert B, Guize L, Zureik M. Lung function impairment and metabolic syndrome: the critical role of abdominal obesity. Am J Respir Crit Care Med. 2009 Mar 15;179(6):509-16. doi: 10.1164/rccm.200807-1195OC. Epub 2009 Jan 8. PMID: 19136371.
54. Ochs-Balcom HM, Grant BJ, Muti P, Sempos CT, Freudenheim JL, Trevisan M, Cassano PA, Iacoviello L, Schünemann HJ. Pulmonary function and abdominal adiposity in the general population. Chest. 2006 Apr;129(4):853-62. doi: 10.1378/chest.129.4.853. PMID: 16608930.
55. Salome CM, Munoz PA, Berend N, Thorpe CW, Schachter LM, King GG. Effect of obesity on breathlessness and airway responsiveness to methacholine in non-asthmatic subjects. Int J Obes (Lond). 2008 Mar;32(3):502-9. doi: 10.1038/sj.ijo.0803752. Epub 2007 Oct 23. PMID: 17955030.
56. Chapman DG, Irvin CG, Kaminsky DA, Forgione PM, Bates JH, Dixon AE. Influence of distinct asthma phenotypes on lung function following weight loss in the obese. Respirology. 2014 Nov;19(8):1170-7. doi: 10.1111/resp.12368. Epub 2014 Aug 19. PMID: 25138203; PMCID: PMC4194162.
57. Al-Alwan A, Bates JH, Chapman DG, Kaminsky DA, DeSarno MJ, Irvin CG, Dixon AE. The nonallergic asthma of obesity. A matter of distal lung compliance. Am J Respir Crit Care Med. 2014 Jun 15;189(12):1494-502. doi: 10.1164/rccm.201401-0178OC. PMID: 24821412; PMCID: PMC4226017.
58. Zadek F, Rubin J, Grassi L, Van Den Kroonenberg D, Larson G, Capriles M, De Santis Santiago R, Florio G, Imber DA, Bittner EA, Hibbert KA, Legassey A, LaRocque J, Cudemus-Deseda G, Bagchi A, Crowley J, Shelton K, Kacmarek R, Berra L. Individualized Multimodal Physiologic Approach to Mechanical Ventilation in Patients With Obesity and Severe Acute Respiratory Distress Syndrome Reduced Venovenous Extracorporeal Membrane Oxygenation Utilization. Crit Care Explor. 2021 Jun 29;3(7):e0461. doi: 10.1097/CCE.0000000000000461. PMID: 34235455; PMCID: PMC8245114.
59. Sizoo D, de Heide LJM, Emous M, van Zutphen T, Navis G, van Beek AP. Measuring Muscle Mass and Strength in Obesity: a Review of Various Methods. Obes Surg. 2021 Jan;31(1):384-393. doi: 10.1007/s11695-020-05082-2. Epub 2020 Nov 6. PMID: 33159294; PMCID: PMC7808984.
60. Kuschel LB, Sonnenburg D, Engel T. Factors of Muscle Quality and Determinants of Muscle Strength: A Systematic Literature Review. Healthcare (Basel). 2022 Oct 3;10(10):1937. doi: 10.3390/healthcare10101937. PMID: 36292384; PMCID: PMC9601777.
61. Tomlinson DJ, Erskine RM, Morse CI, Winwood K, Onambélé-Pearson G. The impact of obesity on skeletal muscle strength and structure through adolescence to old age. Biogerontology. 2016 Jun;17(3):467-83. doi: 10.1007/s10522-015-9626-4. Epub 2015 Dec 14. PMID: 26667010; PMCID: PMC4889641.
62. Stenholm S, Mehta NK, Elo IT, Heliövaara M, Koskinen S, Aromaa A. Obesity and muscle strength as long-term determinants of all-cause mortality--a 33-year follow-up of the Mini-Finland Health Examination Survey. Int J Obes (Lond). 2014 Aug;38(8):1126-32. doi: 10.1038/ijo.2013.214. Epub 2013 Nov 15. PMID: 24232499; PMCID: PMC4022712.
63. Marcus RL, Addison O, Dibble LE, Foreman KB, Morrell G, Lastayo P. Intramuscular adipose tissue, sarcopenia, and mobility function in older individuals. J Aging Res. 2012;2012:629637. doi: 10.1155/2012/629637. Epub 2012 Feb 6. PMID: 22500231; PMCID: PMC3303569.
64. Nilwik R, Snijders T, Leenders M, Groen BB, van Kranenburg J, Verdijk LB, van Loon LJ. The decline in skeletal muscle mass with aging is mainly attributed to a reduction in type II muscle fiber size. Exp Gerontol. 2013 May;48(5):492-8. doi: 10.1016/j.exger.2013.02.012. Epub 2013 Feb 17. PMID: 23425621.
65. Narici MV, Maganaris CN, Reeves ND, Capodaglio P. Effect of aging on human muscle architecture. J Appl Physiol (1985). 2003 Dec;95(6):2229-34. doi: 10.1152/japplphysiol.00433.2003. Epub 2003 Jul 3. PMID: 12844499.
66. Anandacoomarasamy A, Fransen M, March L. Obesity and the musculoskeletal system. Curr Opin Rheumatol. 2009 Jan;21(1):71-7. doi: 10.1097/bor.0b013e32831bc0d7. PMID: 19093327.
67. King LK, March L, Anandacoomarasamy A. Obesity & osteoarthritis. Indian J Med Res. 2013;138(2):185-93. PMID: 24056594; PMCID: PMC3788203.
68. Griffin TM, Guilak F. Why is obesity associated with osteoarthritis? Insights from mouse models of obesity. Biorheology. 2008;45(3-4):387-98. PMID: 18836239; PMCID: PMC2748656.
69. Billot M, Calvani R, Urtamo A, Sánchez-Sánchez JL, Ciccolari-Micaldi C, Chang M, Roller-Wirnsberger R, Wirnsberger G, Sinclair A, Vaquero-Pinto N, Jyväkorpi S, Öhman H, Strandberg T, Schols JMGA, Schols AMWJ, Smeets N, Topinkova E, Michalkova H, Bonfigli AR, Lattanzio F, Rodríguez-Mañas L, Coelho-Júnior H, Broccatelli M, D'Elia ME, Biscotti D, Marzetti E, Freiberger E. Preserving Mobility in Older Adults with Physical Frailty and Sarcopenia: Opportunities, Challenges, and Recommendations for Physical Activity Interventions. Clin Interv Aging. 2020 Sep 16;15:1675-1690. doi: 10.2147/CIA.S253535. PMID: 32982201; PMCID: PMC7508031.
70. Macaluso A, De Vito G. Muscle strength, power and adaptations to resistance training in older people. Eur J Appl

Physiol. 2004 Apr;91(4):450-72. doi: 10.1007/s00421-003-0991-3. Epub 2003 Nov 25. PMID: 14639481.
71. Flego A, Dowsey MM, Choong PF, Moodie M. Addressing obesity in the management of knee and hip osteoarthritis - weighing in from an economic perspective. BMC Musculoskelet Disord. 2016 May 26;17:233. doi: 10.1186/s12891-016-1087-7. PMID: 27229924; PMCID: PMC4882789.
72. Magni NE, McNair PJ, Rice DA. The effects of resistance training on muscle strength, joint pain, and hand function in individuals with hand osteoarthritis: a systematic review and meta-analysis. Arthritis Res Ther. 2017 Jun 13;19(1):131. doi: 10.1186/s13075-017-1348-3. PMID: 28610637; PMCID: PMC5470180.
73. Keevil VL, Luben R, Dalzell N, Hayat S, Sayer AA, Wareham NJ, Khaw KT. Cross-sectional associations between different measures of obesity and muscle strength in men and women in a British cohort study. J Nutr Health Aging. 2015 Jan;19(1):3-11. doi: 10.1007/s12603-014-0492-6. PMID: 25560810; PMCID: PMC6284799.
74. Sayer AA, Syddall HE, Dennison EM, Martin HJ, Phillips DI, Cooper C, Byrne CD; Hertfordshire Cohort. Grip strength and the metabolic syndrome: findings from the Hertfordshire Cohort Study. QJM. 2007 Nov;100(11):707-13. doi: 10.1093/qjmed/hcm095. Epub 2007 Oct 19. PMID: 17951315; PMCID: PMC2292249.
75. Gubelmann C, Vollenweider P, Marques-Vidal P. Association of grip strength with cardiovascular risk markers. Eur J Prev Cardiol. 2017 Mar;24(5):514-521. doi: 10.1177/2047487316680695. Epub 2016 Nov 25. PMID: 27885059.
76. García-Artero E, Ortega FB, Ruiz JR, Mesa JL, Delgado M, González-Gross M, García-Fuentes M, Vicente-Rodríguez G, Gutiérrez A, Castillo MJ. El perfil lipídico-metabólico en los adolescentes está más influido por la condición física que por la actividad física (estudio AVENA) [Lipid and metabolic profiles in adolescents are affected more by physical fitness than physical activity (AVENA study)]. Rev Esp Cardiol. 2007 Jun;60(6):581-8. Spanish. doi: 10.1157/13107114. PMID: 17580046.
77. Peterson MD, Duchowny K, Meng Q, Wang Y, Chen X, Zhao Y. Low Normalized Grip Strength is a Biomarker for Cardiometabolic Disease and Physical Disabilities Among U.S. and Chinese Adults. J Gerontol A Biol Sci Med Sci. 2017 Oct 12;72(11):1525-1531. doi: 10.1093/gerona/glx031. PMID: 28329157; PMCID: PMC5861974.
78. Mafort TT, Rufino R, Costa CH, Lopes AJ. Obesity: systemic and pulmonary complications, biochemical abnormalities, and impairment of lung function. Multidiscip Respir Med. 2016 Jul 12;11:28. doi: 10.1186/s40248-016-0066-z. PMID: 27408717; PMCID: PMC4940831.
79. Manuel AR, Hart N, Stradling JR. Correlates of obesity-related chronic ventilatory failure. BMJ Open Respir Res. 2016 Feb 18;3(1):e000110. doi: 10.1136/bmjresp-2015-000110. PMID: 26918192; PMCID: PMC4762144.
80. Ellulu MS, Patimah I, Khaza'ai H, Rahmat A, Abed Y. Obesity and inflammation: the linking mechanism and the complications. Arch Med Sci. 2017 Jun;13(4):851-863. doi: 10.5114/aoms.2016.58928. Epub 2016 Mar 31. PMID: 28721154; PMCID: PMC5507106.
81. Cannon CP. Obesity-related cardiometabolic complications. Clin Cornerstone. 2008;9(1):11-9; discussion 20-2. doi: 10.1016/s1098-3597(08)60024-1. PMID: 19046736.
82. Singla P, Bardoloi A, Parkash AA. Metabolic effects of obesity: A review. World J Diabetes. 2010 Jul 15;1(3):76-88. doi: 10.4239/wjd.v1.i3.76. PMID: 21537431; PMCID: PMC3083889.
83. Wells CE, Polkey MI, Baker EH. Insulin resistance is associated with skeletal muscle weakness in COPD. Respirology. 2016 May;21(4):689-96. doi: 10.1111/resp.12716. Epub 2015 Dec 18. PMID: 26678022.
84. Higuera-Hernández MF, Reyes-Cuapio E, Gutiérrez-Mendoza M, Rocha NB, Veras AB, Budde H, Jesse J, Zaldívar-Rae J, Blanco-Centurión C, Machado S, Murillo-Rodríguez E. Fighting obesity: Non-pharmacological interventions. Clin Nutr ESPEN. 2018 Jun;25:50-55. doi: 10.1016/j.clnesp.2018.04.005. Epub 2018 Apr 18. PMID: 29779818.
85. Berkel LA, Poston WS, Reeves RS, Foreyt JP. Behavioral interventions for obesity. J Am Diet Assoc. 2005 May;105(5 Suppl 1):S35-43. doi: 10.1016/j.jada.2005.02.031. PMID: 15867894.
86. Lang A, Froelicher ES. Management of overweight and obesity in adults: behavioral intervention for long-term weight loss and maintenance. Eur J Cardiovasc Nurs. 2006 Jun;5(2):102-14. doi: 10.1016/j.ejcnurse.2005.11.002. Epub 2006 Jan 10. PMID: 16406709.
87. Aaron SD, Fergusson D, Dent R, Chen Y, Vandemheen KL, Dales RE. Effect of weight reduction on respiratory function and airway reactivity in obese women. Chest. 2004 Jun;125(6):2046-52. doi: 10.1378/chest.125.6.2046. PMID: 15189920.
88. Dixon AE, Pratley RE, Forgione PM, Kaminsky DA, Whittaker-Leclair LA, Griffes LA, Garudathri J, Raymond D, Poynter ME, Bunn JY, Irvin CG. Effects of obesity and bariatric surgery on airway hyperresponsiveness, asthma control, and inflammation. J Allergy Clin Immunol. 2011 Sep;128(3):508-15.e1-2. doi: 10.1016/j.jaci.2011.06.009. Epub 2011 Jul 23. PMID: 21782230; PMCID: PMC3164923.
89. Hakala K, Mustajoki P, Aittomäki J, Sovijärvi AR. Effect of weight loss and body position on pulmonary function and gas exchange abnormalities in morbid obesity. Int J Obes Relat Metab Disord. 1995 May;19(5):343-6. PMID: 7647827.
90. Babb TG, Wyrick BL, Chase PJ, DeLorey DS, Rodder SG, Feng MY, Ranasinghe KG. Weight loss via diet and exercise improves exercise breathing mechanics in obese men. Chest. 2011 Aug;140(2):454-460. doi: 10.1378/chest.10-1088. Epub 2011 Jan 27. PMID: 21273293.
91. Dalle Grave R, Sartirana M, Calugi S. Personalized cognitive-behavioural therapy for obesity (CBT-OB): theory, strategies and procedures. Biopsychosoc Med. 2020 Mar 9;14:5. doi: 10.1186/s13030-020-00177-9. PMID: 32175002; PMCID: PMC7063798.
92. Kim M, Kim Y, Go Y, Lee S, Na M, Lee Y, Choi S, Choi HJ. Multidimensional Cognitive Behavioral Therapy for

Obesity Applied by Psychologists Using a Digital Platform: Open-Label Randomized Controlled Trial. JMIR Mhealth Uhealth. 2020 Apr 30;8(4):e14817. doi: 10.2196/14817. PMID: 32352391; PMCID: PMC7226050.
93. Swancutt D, Tarrant M, Pinkney J. How Group-Based Interventions Can Improve Services for People with Severe Obesity. Curr Obes Rep. 2019 Sep;8(3):333-339. doi: 10.1007/s13679-019-00348-y. PMID: 31062202; PMCID: PMC6661023.
94. Imanaka M, Ando M, Kitamura T, Kawamura T. Impact of Registered Dietitian Expertise in Health Guidance for Weight Loss. PLoS One. 2016 Mar 22;11(3):e0151456. doi: 10.1371/journal.pone.0151456. PMID: 27003943; PMCID: PMC4803206.
95. Cooper Z, Doll HA, Hawker DM, Byrne S, Bonner G, Eeley E, O'Connor ME, Fairburn CG. Testing a new cognitive behavioural treatment for obesity: A randomized controlled trial with three-year follow-up. Behav Res Ther. 2010 Aug;48(8):706-13. doi: 10.1016/j.brat.2010.03.008. PMID: 20691328; PMCID: PMC2923743.
96. Carter MC, Burley VJ, Nykjaer C, Cade JE. Adherence to a smartphone application for weight loss compared to website and paper diary: pilot randomized controlled trial. J Med Internet Res. 2013 Apr 15;15(4):e32. doi: 10.2196/jmir.2283. PMID: 23587561; PMCID: PMC3636323.
97. Michaelides A, Raby C, Wood M, Farr K, Toro-Ramos T. Weight loss efficacy of a novel mobile Diabetes Prevention Program delivery platform with human coaching. BMJ Open Diabetes Res Care. 2016 Sep 5;4(1):e000264. doi: 10.1136/bmjdrc-2016-000264. PMID: 27651911; PMCID: PMC5020857.
98. Spring B, Pellegrini CA, Pfammatter A, Duncan JM, Pictor A, McFadden HG, Siddique J, Hedeker D. Effects of an abbreviated obesity intervention supported by mobile technology: The ENGAGED randomized clinical trial. Obesity (Silver Spring). 2017 Jul;25(7):1191-1198. doi: 10.1002/oby.21842. Epub 2017 May 11. PMID: 28494136; PMCID: PMC5487285.
99. Dalle Grave R, Calugi S, Bosco G, Valerio L, Valenti C, El Ghoch M, Zini D. Personalized group cognitive behavioural therapy for obesity: a longitudinal study in a real-world clinical setting. Eat Weight Disord. 2020 Apr;25(2):337-346. doi: 10.1007/s40519-018-0593-z. Epub 2018 Oct 10. PMID: 30306498.
100. Rumbo-Rodríguez L, Sánchez-SanSegundo M, Ruiz-Robledillo N, Albaladejo-Blázquez N, Ferrer-Cascales R, Zaragoza-Martí A. Use of Technology-Based Interventions in the Treatment of Patients with Overweight and Obesity: A Systematic Review. Nutrients. 2020 Nov 26;12(12):3634. doi: 10.3390/nu12123634. PMID: 33255982; PMCID: PMC7760174.
101. Perri MG, Nezu AM, McKelvey WF, Shermer RL, Renjilian DA, Viegener BJ. Relapse prevention training and problem-solving therapy in the long-term management of obesity. J Consult Clin Psychol. 2001 Aug;69(4):722-6. PMID: 11550740.
102. Van Dorsten B, Lindley EM. Cognitive and behavioral approaches in the treatment of obesity. Med Clin North Am. 2011 Sep;95(5):971-88. doi: 10.1016/j.mcna.2011.06.008.

***Corresponding author**: Prof. Walid Kamal Abdelbasset, Department of Physical therapy, College of Health Sciences, University of Sharjah, Sharjah 27272, United Arab Emirates. E-mail: wkamal@sharjah.ac.ae*

International Journal of Biomedicine 14(2) (2024) 227-230
http://dx.doi.org/10.21103/Article14(2)_RA3

REVIEW ARTICLE

INTERNATIONAL JOURNAL OF BIOMEDICINE

Prognostic Value of Melatonin in Patients with Chronic Obstructive Pulmonary Disease

Andrey V. Budnevsky[1], Sergey N. Avdeev[2], Evgeniy S. Ovsyannikov[1], Karina V. Vostrikova[1], Sofiya A. Budnevskaya[1], Avag G. Kitoyan[1]

[1]*Voronezh State Medical University named after N.N. Burdenko, Voronezh, Russia*
[2]*I. M. Sechenov First Moscow State Medical University (Sechenov University), Moscow, Russia*

Abstract

The article outlines a detailed examination of multiple scientific studies investigating how melatonin affects COPD's advancement and growth. The severity of oxidative stress in COPD, a complex disease with multiple factors, is significantly reduced by melatonin by activating intracellular antioxidants, as suggested by the data acquired. Considering the available data, we can conclude that melatonin has a protective role against oxidative stress in COPD patients in addition to regulating the circadian rhythm.**(International Journal of Biomedicine. 2024;14(2):227-230.)**

Keywords: COPD • oxidative stress • reactive oxygen species • melatonin

For citation: Budnevsky AV, Avdeev SN, Ovsyannikov ES, Vostrikova KV, Budnevskaya SA, Kitoyan AG. Prognostic Value of Melatonin in Patients with Chronic Obstructive Pulmonary Disease. International Journal of Biomedicine. 2024;14(2):227-230. doi:10.21103/Article14(2)_RA3

Abbreviations

COPD, chronic obstructive pulmonary disease; **CAT,** catalase; **GLT**, glutathione; **MDA**, malondialdehyde; **ROS**, reactive oxygen species; **SOD**, superoxide dismutase.

Introduction

Chronic obstructive pulmonary disease (COPD) is recognized by the WHO as a leading cause of death worldwide, with an estimated 3 million people falling victim to it annually. According to Rosstat, COPD accounts for 14.1% of the morbidity structure and 26% of the mortality structure. [1-4] By the year 2060, it is projected that there will be a staggering 5.4 million deaths annually from COPD and related illnesses due to the rise in smoking rates in low- and middle-income countries and to the growing number of elderly patients in high-income nations.

In the pathogenesis of COPD, oxidative stress plays a crucial role as it disrupts the delicate equilibrium between antioxidants and oxidants. Reactive oxygen species (ROS) are generated by electron leakage from the electron transport chain within mitochondria, which is a natural occurrence. However, a myriad internal and external factors intensify this phenomenon.[5]

Mitochondria are key regulators of metabolism, redox homeostasis, and cell proliferation. An imbalance in COPD has been determined at the level of various tissues: alveolar cells, epithelial cells of lung tissue, smooth myocytes of the respiratory tract, alveolar macrophages, striated muscles, mesenchymal stromal cells, and progenitor cells.[6]

External factors such as smoking and air pollution, and internal factors (ROS released by inflammatory cells, especially neutrophils and macrophages), can lead to oxidative stress in the lung tissues.[7] Oxidative stress damages all structural components of the lungs and leads to irreversible changes in the pulmonary parenchyma, respiratory tract, and pulmonary vessels.[8]

***Corresponding author**: Karina V. Vostrikova. Department of Faculty Therapy of the Voronezh State Medical University named after N.N. Burdenko. Voronezh, Russia. E-mail: prudnikova.2012@inbox.ru*

The most studied mechanisms of oxidative stress's influence on the body of patients with COPD are excessive formation of ROS and reactive nitrogen species and a decrease in the activity of enzymes in the antioxidant system. Oxidative stress in COPD is one of the factors that support chronic inflammation and cellular aging and disrupt autophagy by ROS, which leads to decreased DNA repair, increased autoimmune reactions, increased mucus production, and a weakened anti-inflammatory response.[9]

Patients with COPD showed a significant rise in oxidative stress markers, with a notable increase in MAD, a decrease in SOD, and a substantial elevation in ROS content. This contrasted sharply with the control group, indicating a clear imbalance in the antioxidant defense system of individuals with this respiratory condition.[10] The development of endothelial dysfunction and thromboembolic complications is directly linked to the level of fibrinogen in the blood, as has been illustrated by the correlation of ROS values.

Activation of autophagy by ROS promotes cell adaptation, reducing the circulation of damaged macromolecules and dysfunctional cellular organelles. Oxidative stress causes changes in signaling pathways, which ultimately regulate autophagy. The important role of autophagy in the pathogenesis of COPD as a response to oxidative stress has been highlighted. Exploring the mechanisms of oxidative stress and autophagy in COPD is crucial to pave the way for innovative treatment options tailored to combat this illness. The focus should be on uncovering novel insights that can guide future research in this field.[11]

Autophagy is an important process in which cells break down parts of themselves inside. This process supports cell survival and homeostasis by removing molecules, mainly proteins, damaged organelles, and cytoplasmic macromolecules, as well as processing product decay. One of the special forms of autophagy is the selective removal or degradation of mitochondria. Various forms of cellular stress, such as oxidative stress, hypoxia, and pathogenic infections, can affect autophagy, causing the formation of free radicals and reactive oxygen species, which, in turn, stimulate the antioxidant response.[12]

Mast cells are known to play a crucial role in shaping the microenvironment of tissues, impacting diverse physiological and pathological functions within the organism. By releasing tryptase and/or chymase, mast cells actively modulate inflammatory processes, promote the formation of new blood vessels, cause allergic reactions, and influence cancer-related activities. Research using laboratory cell cultures and living organisms has highlighted the vital role of reactive oxygen intermediates in controlling the release of mast cell granules.[13]

It was found that hospitalized patients with COPD showed increased levels of MDA, protein products of increased oxidation, and total oxidative status. At the same time, SOD activity was significantly lower both during hospitalization and at discharge.[14]

As the condition of patients suffering from COPD worsened, a decrease in the level of catalase (CAT) and glutathione (GLT) activity and an increase in the level of MDA was noted.[15] The Tiffeneau index (FEV1/FVC) in patients is positively correlated with the activity of CAT and SOD and negatively with the level of MAD, which confirms the presence of an oxidant-antioxidant imbalance in COPD patients and emphasizes the importance of glutathione peroxidase in maintaining lung function.

During the various stages of COPD progression, a notable variance in the indicators of oxidative stress has been was observed. In patients with mild to moderate COPD, the levels of CAT, SOD, and glutathione peroxidase were found to be significantly decreased, compared to those with the most severe form of the disease. The study's findings suggest a correlation between the extent of oxidative stress and COPD severity.[16]

Sotgia et al.[17] assessed the blood concentration of the total and reduced forms of the low-molecular-weight thiol antioxidant glutathione in COPD patients, compared with healthy people. The control group showed a markedly higher level of glutathione thiol, compared to the patients, as indicated by recent findings.

Initially, the release of ROS from mitochondria triggers a stress response in the respiratory tract's epithelial cells, causing oxidative damage to membranes and organelles. Furthermore, damage occurs to DNA and proteases. Mitochondrial antioxidants and DNA are involved in activating the NLRP3 inflammasome, along with the DNA sensors cyclic GMP-AMP synthase and a stimulator of interferon genes (STING). These activations accelerate cell death pathways, including caspase activation, leading to inflammation and increased alveolar septa destruction, remodeling, and fibrosis.[18]

Systemic inflammation, which develops during long-term COPD, is also a pathogenetic mechanism for the development of coronary artery disease. A high concentration of systemic inflammation markers is associated with worsening atherosclerosis, the development of its complications, and the progression of coronary artery disease.[19]

Over the past 15 years, attention has been focused on the intimate link between COPD and cardiovascular disease as a key component of the broad range of effects COPD has on the body. The enduring presence of a mild, chronic inflammatory response throughout the body in COPD patients is the primary factor behind the elevated occurrence of cardiovascular disease in this group.[20]

Chronic heart failure (CHF) and COPD are characterized by widespread prevalence and high mortality, especially when combined. Diagnosing comorbidity of CHF and COPD can pose challenges due to the overlap in risk factors, shared disease pathways, and similar symptomatology. Nevertheless, enhancing diagnostic accuracy and optimizing outcomes for these individuals is achievable.[21]

It is known that melatonin can restore the structural and functional organization of damaged lung tissue through several mechanisms, including the regulation of signaling molecules, oxidative status, lipid homeostasis, and support of optimal mitochondrial membrane potential. The role of melatonin in various lung diseases is believed to be linked to its interaction with the alpha-7 nicotinic receptor and the aryl hydrocarbon receptor, which together regulate mitochondrial function and integrate the effects of this hormone.[22] The mechanism of the

antioxidant action of this hormone is its ability to bind free radicals and exogenous carcinogens.[23] At the same time, by activating several enzymes, melatonin is able to enhance the formation of glutathione as well as increase the activity of SOD and CAT. Due to this, the balance between antioxidant and prooxidant enzymes ultimately shifts towards antioxidants.[22]

A study by Morvaridzadeh et al.[24] confirmed the relationship between melatonin consumption and a significant increase in the body's total antioxidant capacity. COPD patients experienced a notable rise in the levels of glutathione, SOD, glutathione peroxidase, and glutathione reductase, alongside a reduction in MDA. In addition to the fact that exogenous melatonin helps reduce the intensity of oxidative stress and the severity of shortness of breath in COPD, it also inhibits phosphorylation of ERK kinase and Sp1 expression and reduces the level of 8-isoprostane by 1.6 times.[25]

In vivo and in vitro, the observed protective effect of melatonin on damaged lung tissue is clearly evident.[26] The melatonin effect is to weaken the inflammatory process in the lungs. It activates intracellular Trx1, inhibits TXNIP/NLRP1, and inhibits impaired mitophagy mediated by inflammasome activation. PINK-1, a protein that regulates autophagy and is linked to microtubules (LC3B-II), demonstrates a rising expression level. Melatonin also improves the overall antioxidant status of the lungs in COPD by restoring the transcription factor NRF-2-HO-1.

A new target of melatonin is the NLRP3 inflammasome, which promotes increased IL-1β levels, activation of caspase-1, and stimulation of pyroptosis. By inhibiting NLRP3, melatonin reduces inflammation and affects various molecular pathways, such as SIRT1, microRNA, long non-coding RNA, and Wnt/β-catenin.[27]

In a study conducted on rats,[28] the influence of melatonin on the progression of COPD was confirmed, showing its ability to reduce the functioning of the NLRP3 and IL-1β inflammasomes. Additionally, an increase in SIRT1 levels was noticed in the lung tissues of rats with COPD, indicating a decrease in the protective effects of melatonin against COPD when SIRT1 activity was suppressed.

In addition to the antioxidant effects of melatonin, there is evidence of the potential benefit of melatonin in reducing the severity of COPD symptoms by improving sleep quality. Melatonin significantly improved Pittsburgh Quality of Life Index (PSQI) scores, especially sleep quality, duration, and efficiency. During the daytime, there was no observable discrepancy in levels of drowsiness, lung capacity, or oxygen saturation.[29]

Correction of sleep disturbances with the use of melatonin in elderly patients with COPD increased the effectiveness of its treatment and reduced the frequency and duration of exacerbations, as well as the number of outpatient visits and hospitalizations.[30] In addition, several studies have assessed the effectiveness of integrating patient education, smoking cessation, exercise training, and nutritional interventions into standard COPD therapy. Results showed significant reductions in COPD exacerbations, hospitalizations, and symptom severity, as well as improvements in quality of life and exercise capacity.[31]

Considering the available data, we can conclude that melatonin has a protective role against oxidative stress in COPD patients in addition to regulating the circadian rhythm.

Competing Interests

The authors declare that they have no competing interests.

Disclaimer

We state that the views expressed in the submitted article are ours and not an official position of the institution or funder.

References

1. Federal clinical guidelines: Chronic obstructive pulmonary disease. Revision:2023. Available from: https://spulmo.ru/upload/kr/HOBL_2023_draft.pdf?ysclid=lrq75428cz630397288. (In Russian).
2. Morbidity of the population of the Russian Federation by main classes of diseases. Federal State Statistics Service, Official statistics, Healthcare. Available from: https://rosstat.gov.ru/folder/13721. (In Russian).
3. World Health Organization. Available from: https://www.who.int/ru/news-room/fact-sheets/detail/chronic-obstructive-pulmonary-disease-(copd).
4. Global Initiative for Chronic Obstructive Lung Disease (GOLD). Global strategy for the diagnosis, management, and prevention of COPD. Available from: https://goldcopd.org/wp-content/uploads/2024/01/GOLD-2024_v1.2-11Jan24_WMV-1.pdf
5. Białas AJ, Sitarek P, Miłkowska-Dymanowska J, Piotrowski WJ, Górski P. The Role of Mitochondria and Oxidative/Antioxidative Imbalance in Pathobiology of Chronic Obstructive Pulmonary Disease. Oxid Med Cell Longev. 2016;2016:7808576. doi: 10.1155/2016/7808576. Epub 2016 Dec 26. PMID: 28105251; PMCID: PMC5220474.
6. Sundar IK, Yao H, Rahman I. Oxidative stress and chromatin remodeling in chronic obstructive pulmonary disease and smoking-related diseases. Antioxid Redox Signal. 2013 May 20;18(15):1956-71. doi: 10.1089/ars.2012.4863. Epub 2012 Nov 6. PMID: 22978694; PMCID: PMC3624634.
7. Barnes PJ. Inflammatory mechanisms in patients with chronic obstructive pulmonary disease. J Allergy Clin Immunol. 2016 Jul;138(1):16-27. doi: 10.1016/j.jaci.2016.05.011. Epub 2016 May 27. PMID: 27373322.
8. Polverino F, Celli BR, Owen CA. COPD as an endothelial disorder: endothelial injury linking lesions in the lungs and other organs? (2017 Grover Conference Series). Pulm Circ. 2018 Jan-Mar;8(1):2045894018758528. doi: 10.1177/2045894018758528. PMID: 29468936; PMCID: PMC5826015.
9. Bernardo I, Bozinovski S, Vlahos R. Targeting oxidant-dependent mechanisms for the treatment of COPD and its comorbidities. Pharmacol Ther. 2015 Nov;155:60-79. doi: 10.1016/j.pharmthera.2015.08.005. Epub 2015 Aug 19. PMID: 26297673.
10. Saburova AM, Nasyrdzhonova HR, Sharipova HE, Kurbanova MB. Features of free radical oxidation and

metabolic activity of vascular endothelium in patients with chronic obstructive pulmonary disease. Avicenna's Bulletin. 2019; 21(1): 38-42. doi: 10.25005/2074-0581-2019-21-1-38-42. (In Russian).
11. Zhao X, Zhang Q, Zheng R. The interplay between oxidative stress and autophagy in chronic obstructive pulmonary disease. Front Physiol. 2022 Sep 26;13:1004275. doi: 10.3389/fphys.2022.1004275. PMID: 36225291; PMCID: PMC9548529.
12. Albano GD, Montalbano AM, Gagliardo R, Profita M. Autophagy/Mitophagy in Airway Diseases: Impact of Oxidative Stress on Epithelial Cells. Biomolecules. 2023 Aug 4;13(8):1217. doi: 10.3390/biom13081217. PMID: 37627282; PMCID: PMC10452925.
13. Atiakshin DA, Shishkina VV, Esaulenko DI, Ovsyannikov ES. Mast Cells as the Target of the Biological Effects of Molecular Hydrogen in the Specific Tissue Microenvironment. International Journal of Biomedicine. 2022; 12(2):183-187. doi: 10.21103/Article12(2)_RA2
14. Stanojkovic I, Kotur-Stevuljevic J, Milenkovic B, Spasic S, Vujic T, Stefanovic A, Llic A, Ivanisevic J. Pulmonary function, oxidative stress and inflammatory markers in severe COPD exacerbation. Respir Med. 2011 Oct;105 Suppl 1:S31-7. doi: 10.1016/S0954-6111(11)70008-7. PMID: 22015083.
15. Arja C, Surapaneni KM, Raya P, Adimoolam C, Balisetty B, Kanala KR. Oxidative stress and antioxidant enzyme activity in South Indian male smokers with chronic obstructive pulmonary disease. Respirology. 2013 Oct;18(7):1069-75. doi: 10.1111/resp.12118. PMID: 23683270.
16. Singh S, Verma SK, Kumar S, Ahmad MK, Nischal A, Singh SK, Dixit RK. Evaluation of Oxidative Stress and Antioxidant Status in Chronic Obstructive Pulmonary Disease. Scand J Immunol. 2017 Feb;85(2):130-137. doi: 10.1111/sji.12498. PMID: 28256060.
17. Sotgia S, Paliogiannis P, Sotgiu E, Mellino S, Zinellu E, Fois AG, Pirina P, Carru C, Mangoni AA, Zinellu A. Systematic Review and Meta-Analysis of the Blood Glutathione Redox State in Chronic Obstructive Pulmonary Disease. Antioxidants (Basel). 2020 Nov 18;9(11):1146. doi: 10.3390/antiox9111146. PMID: 33218130; PMCID: PMC7698942.
18. Wiegman CH, Li F, Ryffel B, Togbe D, Chung KF. Oxidative Stress in Ozone-Induced Chronic Lung Inflammation and Emphysema: A Facet of Chronic Obstructive Pulmonary Disease. Front Immunol. 2020 Sep 2;11:1957. doi: 10.3389/fimmu.2020.01957. PMID: 32983127; PMCID: PMC7492639.
19. Provotorov VM, Budnevskiĭ AV, Semenkova GG, Shishkina ES. [PROINFLAMMATORY CYTOKINES IN COMBINATION OF CORONARY HEART DISEASE AND CHRONIC OBSTRUCTIVE PULMONARY DISEASE]. Klin Med (Mosk). 2015;93(2):5-9. Russian. PMID: 26117912.
20. Budnevsky AV, Malysh EY. [Clinico-Pathogenetic Relationship of Cardiovascular Diseases and Chronic Obstructive Pulmonary Disease]. Kardiologiia. 2017 Apr;57(4):89-93. Russian. PMID: 28762911.
21. Tokmachev RE, Mukhortova MS, Budnevsky AV, Tokmachev E.V., Ovsyannikov ES. Comorbidity of chronic heart failure and chronic obstructive pulmonary disease: features of pathogenesis, clinical and diagnosis. Cardiovascular Therapy and Prevention. 2018; 17 (6): 62-68. Doi: 10.15829/1728-8800-2018-6-62-68. (In Russian).
22. Mazzoccoli G, Kvetnoy I, Mironova E, Yablonskiy P, Sokolovich E, Krylova J, Carbone A, Anderson G, Polyakova V. The melatonergic pathway and its interactions in modulating respiratory system disorders. Biomed Pharmacother. 2021 May;137:111397. doi: 10.1016/j.biopha.2021.111397. Epub 2021 Feb 19. PMID: 33761613.
23. Arushanyan EB. The protective role of melatonin in disorders of cerebral circulation. RMJ. 2010; 18(8): 495-499. (In Russian).
24. Morvaridzadeh M, Nachvak SM, Agah S, Sepidarkish M, Dehghani F, Rahimlou M, Pizarro AB, Heshmati J. Effect of soy products and isoflavones on oxidative stress parameters: A systematic review and meta-analysis of randomized controlled trials. Food Res Int. 2020 Nov;137:109578. doi: 10.1016/j.foodres.2020.109578. Epub 2020 Jul 21. PMID: 33233189.
25. Budnevsky AV, Tsvetikova LN, Ovsyannikov ES, Goncharenko OV. Melatonin: role in the development of chronic obstructive pulmonary disease. Pulmonology. 2016;26(3):372-378. doi: 10.18093/0869-0189-2016-26-3-372-378. (In Russian).
26. Mahalanobish S, Dutta S, Saha S, Sil PC. Melatonin induced suppression of ER stress and mitochondrial dysfunction inhibited NLRP3 inflammasome activation in COPD mice. Food Chem Toxicol. 2020 Oct;144:111588. doi: 10.1016/j.fct.2020.111588. Epub 2020 Jul 30. Erratum in: Food Chem Toxicol. 2024 Feb;184:114408. PMID: 32738376.
27. Ashrafizadeh M, Najafi M, Kavyiani N, Mohammadinejad R, Farkhondeh T, Samarghandian S. Anti-Inflammatory Activity of Melatonin: a Focus on the Role of NLRP3 Inflammasome. Inflammation. 2021 Aug;44(4):1207-1222. doi: 10.1007/s10753-021-01428-9. Epub 2021 Mar 2. PMID: 33651308.
28. Peng Z, Zhang W, Qiao J, He B. Melatonin attenuates airway inflammation via SIRT1 dependent inhibition of NLRP3 inflammasome and IL-1β in rats with COPD. Int Immunopharmacol. 2018 Sep;62:23-28. doi: 10.1016/j.intimp.2018.06.033. Epub 2018 Jun 30. PMID: 29990691.
29. Halvani A, Mohsenpour F, Abadi EEF. Effect of melatonin on sleep quality of chronic obstructive pulmonary disease (COPD) patients. Eur Respir J 2012; 40: Suppl. 56, 3477
30. Tsvetikova LN, Goncharenko OV, Budnevsky AV, Ovsyannikov ES, Belov VN, Kudashova EA, Shkatova YS. Melatonin in treatment of sleep disorders in elderly patients with chronic obstructive pulmonary disease. International Journal of Biomedicine. 2017;7(2):108-110. doi: 10.21103/Article7(2)_OA4
31. Budnevsky AV, Isaeva YV, Malysh EY, Kozhevnikova SA. [Pulmonary rehabilitation as an effective method for optimizing therapeutic and preventive measures in patients with chronic obstructive pulmonary disease concurrent with metabolic syndrome]. Ter Arkh. 2016;88(8):25-29. Russian. doi: 10.17116/terarkh201688825-29. PMID: 27636923.

International Journal of Biomedicine 14(2) (2024) 231-234
http://dx.doi.org/10.21103/Article14(2)_RA4

REVIEW ARTICLE

INTERNATIONAL JOURNAL OF BIOMEDICINE

Thyroid Hormones and Their Role in Male Infertility: A Comprehensive Review

Ramadan S. Hussein*

Department of Dermatology, College of Medicine, Prince Sattam Bin Abdulaziz University Al-Kharj, Saudi Arabia

Abstract

Thyroid hormones are pivotal regulators of various physiological processes, including reproductive function. While the impact of thyroid dysfunction on female fertility has been extensively studied, its association with male infertility has gained increasing recognition. This comprehensive review explores the role of thyroid hormones in male infertility, focusing on their effects on spermatogenesis, sperm quality, and reproductive outcomes. The review delves into the physiology of thyroid hormones, the presence of thyroid hormone receptors in the male reproductive system, and the influence of thyroid dysfunction on spermatogenesis and semen parameters. Additionally, it examines the molecular mechanisms underlying thyroid hormone action in the male reproductive system and discusses potential therapeutic strategies targeting thyroid hormone pathways to improve male fertility. Understanding the intricate relationship between thyroid hormones and male infertility is crucial for advancing diagnostic and therapeutic approaches in the management of male infertility associated with thyroid dysfunction.**(International Journal of Biomedicine. 2024;14(2):231-234.)**

Keywords: thyroid hormones • testes • spermatogenesis • male infertility

For citation: Hussein RS. Thyroid Hormones and Their Role in Male Infertility: A Comprehensive Review. International Journal of Biomedicine. 2024;14(2):231-234. doi:10.21103/Article14(2)_RA4

Abbreviations

TSH, thyroid-stimulating hormone; **T4**, thyroxine; **T3**, triiodothyronine; **FT3**, free triiodothyronine; **FT4**, free thyroxine.

Introduction

Thyroid hormones, predominantly thyroxine (T4) and triiodothyronine (T3), serve as pivotal modulators of metabolic processes, growth, and developmental pathways. Beyond their well-established roles in maintaining metabolic homeostasis, thyroid hormones exert profound effects on various physiological processes, including reproduction.[1] Within the repertoire of thyroid gland-secreted hormones, T4 stands as the predominant form, undergoing conversion into the bioactive hormone T3 facilitated by deiodinase enzymes.[2]

In clinical contexts, hyperthyroidism manifests with elevated levels of thyroid hormones, augmenting basal metabolic rate and oxygen consumption. Left untreated, hyperthyroidism fosters heightened production of reactive oxygen species, inducing oxidative damage and lipid peroxidation in biomembranes, while also triggering free radical generation within mitochondria.[3,4]

Furthermore, hyperthyroidism is recognized to instigate pro-oxidant mechanisms within tissues, including heightened nitric oxide synthase activity and pro-inflammatory reactions. In individuals with hyperthyroidism, T3 prompts a significant elevation—up to 80-fold—in serum levels of TNF-α, IL-10, and NF-κB activation. These effects are notably observed subsequent to the mobilization and activation of testicular interstitial macrophages.[1,5,6]

Changes in thyroid function are linked to disruptions in sexual functions and compromised fertility in both humans and rats. The testes, characterized by high levels of polyunsaturated fatty acids and limited antioxidant defenses, are particularly susceptible to peroxidative damage, compared

***Corresponding author**: Ramadan S. Hussein, MD. Department of Dermatology, College of Medicine, Prince Sattam Bin Abdulaziz University, Al-Kharj, Saudi Arabia. E-mail: rs.mohamed@psau.edu.sa*

to other organs.[4,5] In their study, Dahmani-Said et al.[2] observed that rats administered thyroxine exhibited symptoms of hyperthyroidism, including alterations in the seminiferous tubules and the testicular interstitium.

Notably, the observed disturbance in the testicular oxidant-antioxidant equilibrium caused by hyperthyroidism could lead to substantial DNA damage and apoptosis within the testes, potentially exacerbating testicular complications. A notable inverse relationship has been documented between the extent of oxidative DNA damage in sperm and the overall sperm count. Additionally, caspase-3, B-cell lymphoma 2 (Bcl-2), and Bcl-2-associated X protein (BAX) have been identified as potential regulators of germ cell apoptosis in the rat testis.[7] Caspases are a family of cysteine proteases pivotal in the regulation of apoptosis and inflammation. Upon receiving pro-apoptotic signals, they become activated, initiating a cascade of proteolytic cleavage of cellular proteins, ultimately culminating in cell death. Caspase-3, in particular, serves as a critical mediator in apoptosis, with its activation occurring through both extrinsic and intrinsic signaling pathways during the execution phase of programmed cell death.[8] Furthermore, the Bcl-2 family comprises numerous members, encompassing both pro-apoptotic (*Bax*, *Bak*) and anti-apoptotic (*Bcl-2*, *Bcl-XL*, *Mcl-1*) genes. Primarily, the Bcl-2 protein is involved in the mitochondrial apoptosis pathway, known as the Bcl-2-regulated pathway.[9]

Antithyroid medications persist as the primary therapeutic approach for managing hyperthyroidism and regulating thyroid function preoperatively. The antithyroid thioamide medication carbimazole stands as a cornerstone treatment for Graves' disease globally and is applicable in the management of other etiologies of hyperthyroidism, such as toxic nodular goiter.[10]

While the impact of thyroid dysfunction on female fertility has been extensively studied, its influence on male reproductive health has garnered increasing attention in recent years. This introduction sets the stage for a comprehensive review aimed at elucidating the role of thyroid hormones in male infertility. It highlights the importance of understanding the interplay between thyroid function and male reproductive physiology, emphasizing the need for a deeper exploration of this relationship to improve diagnostic and therapeutic strategies for male infertility associated with thyroid dysfunction.

Thyroid Hormones and Spermatogenesis

Thyroid Hormone Physiology

Thyroid hormones, namely T4 and T3, are produced and released by the thyroid gland under the influence of thyroid-stimulating hormone (TSH) secreted by the pituitary gland. T4 represents the primary hormone discharged by the thyroid gland, while T3, possessing greater biological activity, is derived from T4 via enzymatic conversion in peripheral tissues.[11] The synthesis and release of thyroid hormones are tightly regulated by feedback mechanisms involving the hypothalamus, pituitary gland, and thyroid gland. TSH from the pituitary gland prompts the thyroid gland to generate and release T4 and T3 in response to fluctuating levels of circulating thyroid hormones. These hormones exert widespread effects on various tissues and organs throughout the body, regulating metabolic rate, energy expenditure, heart rate, and body temperature.[11,12]

Thyroid Hormone Receptors in the Male Reproductive System

Thyroid hormone receptors are protein entities present in the cellular milieu of the male reproductive system, comprising Sertoli cells, Leydig cells, and germ cells within the testes.[13] These receptors hold pivotal significance in orchestrating the impact of thyroid hormones on spermatogenesis and male fertility. Upon interaction with thyroid hormones, thyroid hormone receptors undergo translocation to the nucleus, where they modulate the expression of target genes implicated in cellular proliferation, differentiation, and apoptosis.[14] Within the testes, thyroid hormone receptors exert influence over a spectrum of processes crucial for spermatogenesis. These include the development and maturation of germ cells, the synthesis of androgen-binding protein within Sertoli cells, and the production of testosterone by Leydig cells. The presence of thyroid hormone receptors underscores the pivotal role of thyroid hormones in coordinating the complex mechanisms governing male reproductive function.[13,14] The hormones T3 and T4 modulate testicular function via genomic and nongenomic pathways. Genomic effects occur upon T3 binding to thyroid hormone receptor within the nuclei of Sertoli and Leydig cells, triggering gene transcription and protein synthesis.[15] Thyroid hormone receptor isoforms, particularly TRα1, play a significant role in regulating germ cell development and Sertoli cell proliferation. T3 also acts on Leydig cells, stimulating steroidogenesis acutely but inhibiting it chronically, and stops Sertoli cell proliferation.[16] Nongenomic effects involve T3 and T4 binding to nonnuclear receptors on the spermatozoon, stimulating cyclic adenosine monophosphate (cAMP) synthesis and, thereby, sperm motility. Recent studies demonstrate that T4 rapidly increases sperm motility and improves the recovery of motile sperm for insemination.[17,18] Other iodothyronines, such as rT3 and T2, may also act through nongenomic mechanisms. Thyroid hormones regulate the redox status of the testis through antioxidant systems such as glutathione peroxidase, which is crucial for sperm motility and antiapoptotic action.[1] Selenium, an essential micronutrient incorporated into glutathione peroxidase and iodothyronine deiodinases, plays a vital role in thyroid homeostasis and sperm motility. Additionally, thyroid hormones modulate the expression of antioxidant systems in the testis. Alterations in thyroid function can affect spermatogenesis and semen quality.[19]

Effects of Thyroid Dysfunction on Spermatogenesis

Thyroid dysfunction, characterized by hypo- or hyperthyroidism, can disrupt normal spermatogenesis and impair male fertility. Hypothyroidism, characterized by insufficient thyroid hormone levels, may lead to reduced sperm production, impaired sperm motility, and altered sperm morphology. In rats administered antithyroid drugs, there is a decrease in seminal volume, arrest of spermatogenesis, and a reduction in the number and diameter of seminal tubules, accompanied by diminished weight of the testes and accessory glands compared

to euthyroid controls.[20] Progressive sperm motility, along with sperm transit time through the epididymis and epididymal secretory activity, are likewise impacted. Additionally, persistent hypothyroidism in rats leads to decreased testicular germ cells and live sperm count, potentially due to increased oxidative stress and reduced antioxidant systems.[21] In newborn mice treated with propylthiouracil, oxidative stress reduces the expression of glucose transporter proteins in Sertoli and Leydig cells, leading to diminished testicular glucose levels and increased apoptosis of germ cells. Additionally, oxidative stress diminishes the expression of connexin 43, a protein involved in regulating germ cell proliferation and apoptosis within the seminiferous epithelium.[22] In humans, teratozoospermia is the most prevalent semen abnormality observed in individuals with hypothyroidism, showing a negative correlation with serum T4 levels. Furthermore, altered sperm motility, reduced accessory gland secretory activity, and decreased ejaculate volume are also documented. Notably, semen abnormalities associated with hypothyroidism are reversible upon restoration of euthyroid status.[23] Conversely, hyperthyroidism, marked by excessive thyroid hormone levels, can also negatively impact spermatogenesis, resulting in decreased sperm quality and fertility. Hyperthyroidism in rodents leads to delayed spermatogenesis, maturation arrest, decreased seminiferous tubule diameters, impaired mitochondrial activity, and reduced lipid concentration.[21] It also affects antioxidant systems, with upregulated catalase and downregulated glutathione peroxidase.[20] In individuals with thyrotoxicosis, more than half experience asthenozoospermia, while approximately 40% manifest oligozoospermia and teratozoospermia, often accompanied by decreased semen volume.[24] Research indicates that hyperthyroid patients typically have lower sperm motility than euthyroid counterparts; however, semen parameters tend to normalize following treatment for hyperthyroidism.[25] A recent study observed significant differences in seminal vesicle volume changes before and after ejaculation between hyperthyroid and hypothyroid patients. Seminal vesicle volume, emptying, and fructose concentration positively correlated with serum FT3 levels. Moreover, there was a positive association between FT3, FT4, and ejaculate volume.[26] Thyroid dysfunction may disrupt germ cell development, impair sperm maturation processes, and induce changes in testicular morphology, contributing to male infertility.[20,26]

Future Directions: An overview of the research gaps is shown in Table 1.

Limitations

The literature presents three main limitations in the existing studies. First, the criteria for diagnosing semen abnormalities varied across studies. Second, many studies included cohorts from infertile couples, complicating the interpretation of results as these men may have had low semen quality due to factors unrelated to thyroid dysfunction. Third, the studies conducted so far often had small cohorts, which reduced their statistical power.

Conclusion

This review highlights the intricate interplay between thyroid hormones and male infertility, emphasizing the importance of thyroid function in spermatogenesis, sperm quality, and reproductive outcomes. Understanding the role of thyroid hormones in male fertility may pave the way for novel diagnostic and therapeutic approaches to address male infertility associated with thyroid dysfunction.

Table 1.

Overview of the research gaps and proposed future research directions in the field of thyroid dysfunction and reproduction. [1, 20, 26]

Research focus	Existing gaps	Proposed research directions
Thyroid dysfunction and male infertility	Lack of comprehensive understanding of causal mechanisms underlying the association between thyroid dysfunction and male infertility	Conduct prospective studies elucidating causal mechanisms between thyroid dysfunction and male infertility.
	Limited longitudinal investigations examining the long-term impact of thyroid hormone levels on reproductive outcomes	Undertake longitudinal investigations examining the impact of thyroid hormone levels on spermatogenesis, sperm quality, and fertility.
	Insufficient clinical trials evaluating the efficacy of thyroid hormone modulation in improving fertility outcomes in men	Design well-controlled clinical trials assessing the efficacy of thyroid hormone modulation in improving fertility outcomes.
	Limited evidence on the effects of thyroid hormone replacement therapy on sperm parameters and reproductive hormone levels	Evaluate the effects of thyroid hormone replacement therapy on sperm parameters, reproductive hormone levels, and pregnancy rates.
	Scarcity of research exploring the potential role of novel therapeutic targets in male fertility	Explore the potential role of novel therapeutic targets targeting thyroid hormone pathways in male fertility.
	Inadequate assessment of the safety and efficacy of thyroid hormone analogs and receptor modulators	Investigate the safety and efficacy of thyroid hormone analogs, receptor modulators, or pharmacological agents in improving fertility.
	Lack of optimized diagnostic and therapeutic strategies for improving reproductive outcomes in affected individuals	Foster research endeavors to optimize diagnostic and therapeutic strategies for improving reproductive outcomes in affected individuals.

Additional investigation is necessary to explore the impact of hyperthyroidism or hypothyroidism on nontraditional sperm parameters and the potential influence of subclinical thyroid dysfunction on male fertility.

Acknowledgments

This study was funded by Prince Sattam bin Abdulaziz University project number (PSAU/2023/R/1444).

Competing Interests

The authors declare that they have no competing interests.

References

1. La Vignera S, Vita R, Condorelli RA, Mongioì LM, Presti S, Benvenga S, Calogero AE. Impact of thyroid disease on testicular function. Endocrine. 2017 Dec;58(3):397-407. doi: 10.1007/s12020-017-1303-8.
2. Souhila DS, Zohra HS, Kamel A, Hadj-Bekkouche F. Effects of thyroxine treatment during lactation on the testicular function of rats across different ages. Folia Histochem Cytobiol. 2013;51(2):107-14. doi: 10.5603/FHC.2013.0017.
3. Mogulkoc R, Baltaci AK, Oztekin E, Aydin L, Tuncer I. Hyperthyroidism causes lipid peroxidation in kidney and testis tissues of rats: protective role of melatonin. Neuro Endocrinol Lett. 2005 Dec;26(6):806-10. PMID: 16380687.
4. Mohamed H, Bushra R. Effects of Simultaneous Melatonin Administration on the Testis of the Experimentally Induced Hyper- and Hypothyroidism in the Adult Male Albino Rat. Egypt J Histol. 2017;40:52–67. doi:10.21608/EJH.2017.3701.
5. Sahoo DK, Roy A, Bhanja S, Chainy GB. Hypothyroidism impairs antioxidant defence system and testicular physiology during development and maturation. Gen Comp Endocrinol. 2008 Mar 1;156(1):63-70. doi: 10.1016/j.ygcen.2007.11.007.
6. La Vignera S, Vita R. Thyroid dysfunction and semen quality. Int J Immunopathol Pharmacol. 2018 Jan-Dec;32:2058738418775241. doi: 10.1177/2058738418775241.
7. El-Kashlan AM, Nooh MM, Hassan WA, Rizk SM. Therapeutic Potential of Date Palm Pollen for Testicular Dysfunction Induced by Thyroid Disorders in Male Rats. PLoS One. 2015 Oct 1;10(10):e0139493. doi: 10.1371/journal.pone.0139493.
8. Mosadegh M, Hasanzadeh S, Razi M. Nicotine-induced damages in testicular tissue of rats; evidences for bcl-2, p53 and caspase-3 expression. Iran J Basic Med Sci. 2017 Feb;20(2):199-208. doi: 10.22038/ijbms.2017.8249.
9. Shukla KK, Mahdi AA, Rajender S. Apoptosis, spermatogenesis and male infertility. Front Biosci (Elite Ed). 2012 Jan 1;4(2):746-54. doi: 10.2741/415. PMID: 22201910.
10. Sakr SA-R, Hassab ELnaby SE, Okdah YA, El-Shabka AM. Impact of ginger aqueous extract on carbimazole induced testicular degenerative alterations and oxidative stress in albino rats. J. Coast. Life Med. 2017;5:167–173. doi: 10.12980/jclm.5.2017J6-219.
11. Cicatiello AG, Di Girolamo D, Dentice M. Metabolic Effects of the Intracellular Regulation of Thyroid Hormone: Old Players, New Concepts. Front Endocrinol (Lausanne). 2018 Sep 11;9:474. doi: 10.3389/fendo.2018.00474.
12. Brent GA. Mechanisms of thyroid hormone action. J Clin Invest. 2012 Sep;122(9):3035-43. doi: 10.1172/JCI60047.
13. Holsberger DR, Cooke PS. Understanding the role of thyroid hormone in Sertoli cell development: a mechanistic hypothesis. Cell Tissue Res. 2005 Oct;322(1):133-40. doi: 10.1007/s00441-005-1082-z.
14. Mendeluk GR, Rosales M. Thyroxin Is Useful to Improve Sperm Motility. Int J Fertil Steril. 2016 Jul-Sep;10(2):208-14. doi: 10.22074/ijfs.2016.4911.
15. Wagner MS, Wajner SM, Maia AL. The role of thyroid hormone in testicular development and function. J Endocrinol. 2008 Dec;199(3):351-65. doi: 10.1677/JOE-08-0218.
16. Wajner SM, Wagner MS, Maia AL. Clinical implications of altered thyroid status in male testicular function. Arq Bras Endocrinol Metabol. 2009 Nov;53(8):976-82. doi: 10.1590/s0004-27302009000800011.
17. Davis PJ, Goglia F, Leonard JL. Nongenomic actions of thyroid hormone. Nat Rev Endocrinol. 2016 Feb;12(2):111-21. doi: 10.1038/nrendo.2015.205.
18. Mendeluk GR, Rosales M. Thyroxin Is Useful to Improve Sperm Motility. Int J Fertil Steril. 2016 Jul-Sep;10(2):208-14. doi: 10.22074/ijfs.2016.4911.
19. Duntas LH, Benvenga S. Selenium: an element for life. Endocrine. 2015 Apr;48(3):756-75. doi: 10.1007/s12020-014-0477-6.
20. Choudhury S, Chainy GB, Mishro MM. Experimentally induced hypo- and hyper-thyroidism influence on the antioxidant defence system in adult rat testis. Andrologia. 2003 Jun;35(3):131-40. doi: 10.1046/j.1439-0272.2003.00548.x.
21. Romano RM, Gomes SN, Cardoso NC, Schiessl L, Romano MA, Oliveira CA. New insights for male infertility revealed by alterations in spermatic function and differential testicular expression of thyroid-related genes. Endocrine. 2017 Feb;55(2):607-617. doi: 10.1007/s12020-016-0952-3.
22. Sahoo DK, Roy A, Bhanja S, Chainy GB. Hypothyroidism impairs antioxidant defence system and testicular physiology during development and maturation. Gen Comp Endocrinol. 2008 Mar 1;156(1):63-70. doi: 10.1016/j.ygcen.2007.11.007.
23. Krassas GE, Poppe K, Glinoer D. Thyroid function and human reproductive health. Endocr Rev. 2010 Oct;31(5):702-55. doi: 10.1210/er.2009-0041.
24. Abalovich M, Levalle O, Hermes R, Scaglia H, Aranda C, Zylbersztein C, Oneto A, Aquilano D, Gutierrez S. Hypothalamic-pituitary-testicular axis and seminal parameters in hyperthyroid males. Thyroid. 1999 Sep;9(9):857-63. doi: 10.1089/thy.1999.9.857.
25. Krassas GE, Pontikides N, Deligianni V, Miras K. A prospective controlled study of the impact of hyperthyroidism on reproductive function in males. J Clin Endocrinol Metab. 2002 Aug;87(8):3667-71. doi: 10.1210/jcem.87.8.8714.
26. Lotti F, Maseroli E, Fralassi N, Degl'Innocenti S, Boni L, Baldi E, Maggi M. Is thyroid hormones evaluation of clinical value in the work-up of males of infertile couples? Hum Reprod. 2016 Mar;31(3):518-29. doi: 10.1093/humrep/dev338.

International Journal of Biomedicine 14(2) (2024) 235-239
http://dx.doi.org/10.21103/Article14(2)_RA5

REVIEW ARTICLE

INTERNATIONAL JOURNAL OF BIOMEDICINE

How Much Radiation Are Women in Saudi Arabia Receiving from Mammography? A Review

Sarah K. Albahiti[1,2*]

[1]*Department of Radiology, King Abdulaziz University Hospital, King Abdulaziz University, Jeddah, Saudi Arabia*
[2]*Department of Radiology, Faculty of Medicine, King Abdulaziz University, Jeddah, Saudi Arabia*

Abstract

This review compiles and assesses data from recent studies on mammographic radiation doses in Saudi Arabia, aiming to evaluate mean glandular dose (MGD) exposure during mammography and its implications in breast cancer risk. The reviewed studies spanned from 2019 to 2023 and included a range of sample sizes and institutional settings, with patients' ages from 27 to 85 years. Considerations such as the number of mammographic views and compressed breast thickness were examined. The studies reported average MGDs below the National Diagnostic Reference Level set by the Saudi Food and Drug Authority. However, limitations were noted regarding sample size selection and incomplete data on all mammographic projections. Despite these limitations, the findings highlight the need for continued assessment of patient doses to optimize mammography practices and address the absence of quality standardization acts in Saudi Arabia. These insights are critical for governing authorities to ensure that effective patient dose monitoring occurs regularly and that the establishment of minimum quality standards for breast cancer screening is intact.**(International Journal of Biomedicine. 2024;14(2):235-239.)**

Keywords: mammography • breast cancer • patient dose • diagnostic reference level

For citation: Albahiti SK. How Much Radiation Are Women in Saudi Arabia Receiving from Mammography? A Review. International Journal of Biomedicine. 2024;14(2):235-239. doi:10.21103/Article14(2)_RA5

Abbreviations

BC, breast cancer; **CR**, cancer risk; **CC**, cranio-caudal; **CBT**, compressed breast thickness; **DRLs**, Diagnostic Reference Levels; **ESAK**, entrance surface air kerma; **ICRP**, International Commission on Radiological Protection; **MGD**, mean glandular dose; **MLO**, mediolateral oblique; **MQSA**, Mammography Quality Standards Act; **NDRLs**, National Diagnostic Reference Levels; **QAP**, quality assurance program.

Introduction

Breast cancer (BC) is a significant health concern and the main cause of cancer death in women globally, with an estimated 2.3 million new cancer cases and 685,000 cancer deaths in 2020, as per the Global Cancer Observatory (GLOBOCAN) database from 185 countries.[1] The incidence of BC among women in Saudi Arabia is higher than the global average, accounting for 28% of all cancers in the country.[2] It is a major health concern, especially among women, and its prevalence is expected to rise in the coming years.[3] The precise detection and prediction of BC are critical for better patient outcomes. Machine learning techniques, such as Explainable Artificial Intelligence, have been used to predict benign and malignant BC based on clinical and pathological characteristics.[4] Furthermore, BC survivors in Saudi Arabia have poor health-related quality of life, which is influenced by a variety of factors, such as age, type of therapy, and comorbidities.[5]

Different imaging modalities, including mammography, are used for accurate diagnosis and screening of breast tissue. Although it remains the gold standard for screening to date, mammography still has its limitations due to small differences in contrast between normal and malignant tissues. On the other hand, mammography has provided evidence that it is beneficial in detecting BC at an early stage, when changes in the breast are often too small to detect by self-examination.[6]

***Correspondence**: Sarah K. Albahiti, King Abdulaziz University, Jeddah, Saudi Arabia. E-mail: sarahalbahiti@gmail.com*

Efforts to improve the current situation must address several factors, including patient, public, and medical team awareness levels, to further improve outcomes.

Al-Wassia et al.[7] conducted a cross-sectional study of 3,245 women aged 40 and older in five geographic regions of Saudi Arabia to assess mammography utilization, knowledge, and barriers. They discovered that mammography utilization and knowledge were poor, and they concluded that raising awareness through educational initiatives could assist in overcoming current barriers and misconceptions.

In addition, medical students in Saudi Arabia were found to have low awareness of BC, but there is a willingness to participate in BC prevention activities.[8] Text mining algorithms and natural language processing models have been used to analyze clinical data and extract valuable insights from medical notes of BC patients in Saudi Arabia.[9]

Nevertheless, the radiation dose involved in mammography imaging is of concern because glandular tissue is sensitive to radiation, and the procedure itself could add to the risk of BC development.[10] Mammographic procedures typically involve two views for each side, with reported average doses ranging from 1.1 to 2.2 mGy per view and 2.0 to 5.4 mGy per breast.[11] This is highly dependent on several factors like compressed breast thickness, technique used, positioning, qualifications of staff, and the frequent need for more projections or views for full assessment. Assessing patient doses during mammography is necessary to ensure compliance with guidelines for radiation protection safety and to minimize unnecessary exposure.

Despite the potential risk of radiation-induced malignancy, the benefits of mammographic imaging, such as early detection and reduced mortality risk, outweigh the associated risks. The benefit can reduce the mortality rate up to 25% of the screened female population and avoid aggressive treatment.[12] This is on the condition that centers providing screening and diagnostic mammography services are aware of every patient dose and undergo a comprehensive quality assurance program (QAP). Implementation of a QAP in every mammography facility is crucial. Such programs include protocol evaluation, quality control tests, radiographer and radiologist qualifications, sample image quality assessment, and peer-reviewed reports.

The US Congress passed the Mammography Quality Standards Act (MQSA) to govern the quality of care provided by mammography service providers.[13] The Act was implemented in 1994. In 1995, the US FDA began inspecting mammography facilities to ensure their compliance. This Act aimed to create basic requirements for ensuring that all women have access to quality mammography treatments.[13] The MQSA requires that an FDA-approved accreditation body accredit facilities. Currently, the American College of Radiology is the only nationally approved body.[14]

In addition, the International Commission on Radiological Protection (ICRP) has emphasized the need for QAPs in mammography to ensure high-quality images and accurate BC diagnosis.[15] QAPs are systematic actions, including quality control checks, that provide high-quality images while limiting radiation exposure.[16] Implementation and continuous evaluation of QAPs have a direct impact on improving mammography image quality and reducing patient dose, resulting in enhanced BC diagnosis and management.[17]

Continuous attempts to improve mammography quality and safety in Saudi Arabia started in 2020.[18] Currently, MQSA and similar local accreditation programs for mammography facilities are non-existent. In addition, there is a lack of comprehensive data on the radiation doses received by women undergoing mammograms in Saudi Arabia. Patient radiation doses from diagnostic imaging procedures in many healthcare centers are unknown and not documented in their medical records. The Saudi Food and Drug Authority published National Diagnostic Reference Levels (NDRLs) in early 2023 for mammography and issued a higher decree to force healthcare providers to compare their patient doses to the National Diagnostic Reference Levels (NDRLs) and establish their own Diagnostic Reference Levels (DRL).[19]

The International Atomic Energy Agency has set Diagnostic Reference Levels for diagnostic examinations, such as mammography, to enhance patient safeguarding by minimizing unnecessary radiation exposure. DRLs are used as reference points but are not intended to be dose restrictions but rather as benchmarks to ensure that doses are maintained at the lowest possible level while still obtaining the necessary diagnostic information.[20]

In mammography, DRLs are usually established based on the average glandular dosage to the breast. They vary across countries and are often established using nationwide surveys of patient dose data, considering the specific equipment, procedures, and practices employed in each country. Healthcare providers should regularly assess their doses and compare them with NDRLs. If consistently exceeding the DRLs, providers should evaluate their practices and make necessary adjustments to reduce doses without compromising image quality. Maintaining image quality is crucial for the accurate detection of BC.[21]

The existing literature on radiation doses from mammograms predominantly focuses on Western populations, with limited information available specifically for practices in Saudi Arabia. Comparable studies from neighboring regions provide some insights into the radiation doses received during mammography, but we still need more national studies to document and optimize the doses the Saudi population is receiving. Therefore, this study reviews all articles that document radiation doses from mammography in Saudi Arabia.

Radiation Exposure in Mammography

The MGD, which refers to the average amount of radiation absorbed by breast glandular tissues, is the preferred dosimetry quantity for evaluating potential risks, as recommended by the ICRP.[22] The MGD is indirectly approximated using the entrance surface air kerma (ESAK) and half-value layer. It is determined using established breast parameters. Thus, MGD is estimated by utilizing the ESAK and conversion coefficients by Dance et al.[23]

The number of views for a mammography imaging procedure varies depending on the specific case and the diagnostic requirements, but it typically involves four views, with two views for each breast in different projections: cranio-

caudal (CC) and mediolateral oblique (MLO).[24] Sometimes, a mediolateral (ML) projection is added to both CC and MLO.

However, additional views may be necessary to cover all breast tissue, with 12% of screen-film mammography cases and 21% of full-field digital mammography cases requiring more than the normal four views to achieve comprehensive coverage.[25] Additionally, spot compression, magnification, extended views, and additional views, may be necessary to characterize and localize abnormalities.[26]

The NDRL for mammography, published by the SFDA in 2023, is 1.5 mGy for CC view. The SFDA has still to publish the full range of projections in 2024.[19]

Estimation of CR during mammography procedures

The ICRP has assessed and measured the probability of developing cancer, namely malignant tumors, to be 5.5%. The radiation-induced risk coefficient for BC is 116×10^{4} Sv^{-1}. This coefficient was used to calculate the possibility of developing cancer per medical exposure.[22]

Estimating CRs during mammography procedures is a critical consideration in BC screening. The cumulative risk of an invasive procedure with a benign outcome from mammographic screening has been reported to range from 1.8% to 6.3%.[27] Additionally, factors such as double mammogram reading, number of views, digital mammography, menopausal status, hormone replacement therapy, previous invasive procedures, and familial history can increase the risk or lead to false positives.[28]

Methods

A literature search was conducted using Scopus, PubMed, and Google Scholar databases for studies reported on mammography patient doses conducted in Saudi Arabia between 2013 and 2023. The search terms used were "mammography in Saudi Arabia," "patient dose," "radiation dose," and "diagnostic reference levels." Abstracts of all results were reviewed to assess suitability for the review's purpose of identifying women's radiation exposure from mammography in the Saudi population. In addition, references in each paper were tracked down to find more relevant publications. Studies in languages other than English conducted on men or phantoms were excluded. Data measured in Saudi hospitals were included in this review, represented in five original articles.

Results

Since radiation dose from mammograms may increase the risk of developing cancer, this study intended to quantify radiation doses and estimate the cancer risks. Sixty patients (an average age of 44) were evaluated using a digital mammography unit at King Khaled Hospital in Alkharj (Saudi Arabia).[10]

The average ESAK was 4.4±1.1 mGy, with a range of 1.7-7.9 mGy. The average MGD per procedure was 1.1±0.26 mGy, with range from 0.4 to 1.9 mGy. The third quartile values for ESAK and MGD were 5 and 1.2 mGy, respectively.[10]

The total number of views for each patient was 6, 3 on each side. The average MGD per projection (view) was reported for CC, MLO, and LM as follows: 1.02±0.2 mGy for CC view and 1.1±0.3 mGy for MLO and LM. In addition, the study concluded that 80% of the procedures had normal findings, but precise justification is required for young patients. Also, CR was calculated using mean organ equivalent dose and radiation risk factors product. Suleiman et al. estimated CR per projection was 177 per million procedures. The study's main limitation is the small sample size (60) and the fact that no mention was made of how the patients were chosen nor the institution's daily mammography load.

Local DRL based on patient radiation exposure during digital mammography was established at Riyadh Care Hospital (Riyadh Saudi Arabia).[29] The authors included 1055 participants with mammography procedures using a direct digital mammography system. Patient age ranged from 28 to 75 (mean of 51.65±9.3), and compressed breast thickness ranged from 19 to 125 mm (mean of 55.1±13.9). The study reports exposure parameters but does not report the total number of views patients received during a mammography exam. The average ESAK was 5.19±3.18 mGy, with a range of 0.33-29.9 mGy. The average MGD per procedure was 1.3±1.0 mGy. The third quartile values for ESAK and MGD were 6 and 1.5mGy, respectively. This study also does not report the total number of views patients received but the total procedure dose. Furthermore, the authors have not reported individual projection average doses within their center to compare them to the NDRL.

A study conducted at Najran University Hospital (Najan, Saudi Arabia) included 85 patients who underwent mammography studies.[30] Their protocol for suspicious cases exposes patients to three projections (CC, MLO and ML) for each side, like Suleiman et al.;[10] therefore, a total of 510 mammograms were assessed. Patient age ranged from 27 to 71 and most of the patients (71%) were between the ages of 30 to 50. The author stated that since they are young, "They are more vulnerable to risk than older patients."[30] Compressed breast thickness for the study population ranged from 24 to 76 mm. The average MGD and ESKD was 1.1 and 4.3 mGy respectively. The study reported the average MGD for each of the three projections and their associated exposure parameters. In addition, they correlated the patient doses with compressed breast thickness (CBT) (Table 1). Finally, the study estimated two cancer cases per 10,000 patients per breast as the CR due to mammography.[30]

Table 1.

Compressed breast thickness in millimeters and average mean glandular dose for the three projections.[30]

Parameter	Projection		
	CC*	MLO*	ML*
CBT, mm	43.5 ± 5.0 (24.0 to 63.0)	53.4 ± 11.0 (29.0 to 76.0)	50.2 ± 7.4 (27.0 to 69.0)
MGD, mGy	1.01 ± 0.3 (0.3 to 1.7)	1.09 ± 0.2 (0.4 to 1.8)	1.09 ± 0.2 (0.4 to 1.9)

**Mean ± SD (range)*

Alahmad et al.[31] studied the radiation dose exposure of 167 patients, representing a randomly chosen small sample from King Fahad Medical City (Riyadh, Saudi Arabia), where

over 3436 patients had bilateral mammograms from January 2020 to July 2023. Patient age ranged from 30 to 85 and compressed breast thickness from 20 to 86mm. The average MGD and ESAK was 1.17 and 5.87 mGy, respectively, for the single reported projection. In addition, patients were grouped according to their age: under 40, from 40 to 49, from 50 to 64, and above 64 to report the same projection data for the individual groups. The highest average MGD was 1.3 mGy in the 40-49 age group. Patients were also grouped depending on compressed breast thickness, where 29 mm and less received an average MGD of 0.71 mGy, from 30 to 49 mm received 0.8 mGy, and those 50 mm and above received 1.49 mGy. The main study limitation was that no MLO data was retrievable, and the researchers only reported CC view data, while a full mammogram procedure will always include at least 2 CC and 2 MLO for each patient. The authors have not specified how the small number of patients were selected from the larger pool of patients they scanned during the study period.

A group of researchers at King Fahd Hospital at Imam Abdulrahman Bin Faisal University (Al-Khobar City, Saudi Arabia) conducted a study between May 25 and November 4, 2021, to document patient radiation doses in diagnostic imaging.[32] Data management software was used to extract dose information from mammography and radiography patients. The study evaluated the impact of this software on radiation dose, developed DRLs, and documented achievable doses in mammography and radiography. Still, for the sake of the review, only their mammography data was evaluated. The study population included 2897 mammographs from 795 patients (average of 3.6 images per patient) using a combo-mode technique (two-dimensional and tomosynthesis) for screening and diagnostic protocols. Also, the authors have categorized the results of this paper in terms of two phases: pre and post-implementation of software.[32] There was no valid explanation why the average accumulated MGD had increased significantly in the post-implementation phase compared to the pre-implementation phase, from 5.65 to15.6 mGy. Also, the average ESAKs were 8.67 mGy and 9.20 mGy in the pre- and post-implementation phases, respectively. The limitation of this study is that it included data from seven men, but when reporting the MGD and ESAK the data was grouped together, which might have shifted the results and DRLs slightly. Similarly, the authors reported average MGD and ESKD per side (right and left breast) and not per projection; therefore, the results couldn't be compared to NDRL or the other four studies in this review (Table 2).

Table 2.

The average MGD reported in the reviewed studies in comparison with the NDRL published by the SFDA.

Author	MGD (mGy)	Projection
Suleiman et al, 2019 [10]	1.1	Per view (CC)
Tamam et al, 2021 [29]	1.3	Per procedure*
Saeed et al, 2021 [30]	1.01	Per view (CC)
Alahmad et al, 2023 [31]	1.17	Per view (CC)
SFDA NDRL [19]	1.5	Per view (CC)

** No specific view projection was described, and no number of views was reported for each procedure.*

Conclusion

Although there is limited data on the topic, these studies may offer valuable reference points for assessing the situation in Saudi Arabia and guiding further research endeavors. The current situation requires answers to a different question: Is it only about how much women are receiving from mammography procedures or also who is measuring? The percentage of mammography service providers who do not measure and patient doses that remain unknown is large. With the lack of licensing and monitoring of mammography facilities comes low quality images that result in unnecessary exposure. Therefore, the reviewed studies provide a comprehensive overview of the present measured patient doses and the need for continuous assessment to ensure the current practice is optimized under the prevailing lack of quality standardization acts for mammography within the country. All the research represented here demonstrates the crucial need for the governing authorities to enforce patient dose monitoring in mammography and set quality standards, especially for screening purposes.

Competing Interests

The authors declare that they have no competing interests.

References

1. Sedeta ET, Jobre B, Avezbakiyev B. Breast cancer: Global patterns of incidence, mortality, and trends. Journal of Clinical Oncology. 2023;41(16_suppl).
2. Bazarbashi S, Al Eid H, Minguet J. Cancer Incidence in Saudi Arabia: 2012 Data from the Saudi Cancer Registry. Asian Pac J Cancer Prev. 2017 Sep 27;18(9):2437-2444. doi: 10.22034/APJCP.2017.18.9.2437.
3. Abusanad AM, Iskanderani O, Al-hajeili MR, Ujaimi R, Alwassia R. Survival in patients with brain metastasis secondary to breast cancer from Saudi Arabia. Journal of Clinical Oncology. 2023;41(16_suppl).
4. Amaaao AT. Explainable Artificial Intelligence in Quantifying Breast Cancer Factors: Saudi Arabia Context. JMIR Preprints. 2023;49615.
5. Omar MTA, Al Dhwayan N, Al-Karni MAT, Ajarim D, Idreess MJN, Gwada RFM. Factors Associated with Health-Related Quality of Life Among Breast Cancer Survivors in the Saudi Arabia: Cross Sectional Study. Research Square. 2023; April.
6. Glechner A, Wagner G, Mitus JW, Teufer B, Klerings I, Böck N, Grillich L, Berzaczy D, Helbich TH, Gartlehner G. Mammography in combination with breast ultrasonography versus mammography for breast cancer screening in women at average risk. Cochrane Database Syst Rev. 2023 Mar 31;3(3):CD009632. doi: 10.1002/14651858.CD009632.pub3.
7. Al-Wassia RK, Farsi NJ, Merdad LA, Hagi SK. Patterns, knowledge, and barriers of mammography use among women in Saudi Arabia. Saudi Med J. 2017 Sep;38(9):913-921. doi: 10.15537/smj.2017.9.20842. PMID: 28889149; PMCID:
8. Miskeen E, Al-Shahrani AM. Breast Cancer Awareness Among Medical Students, University of Bisha, Saudi Arabia.

Breast Cancer (Dove Med Press). 2023 Apr 17;15:271-279. doi: 10.2147/BCTT.S403803. PMID: 37091353; PMCID: PMC10120833.
9. Gollapalli M, Alqusser M, Althobaiti A, Alzaid L, Alorefan R, Alnajim S, et al. Text Mining to Analyze Mammogram Screening Results for Breast Cancer Patients in Saudi Arabia. In: Proceedings - 2023 6th International Conference of Women in Data Science at Prince Sultan University, WiDS-PSU, 2023. doi: 10.1109/wids-psu57071.2023.00016
10. Sulieman A, Serhan O, Al-Mohammed HI, Mahmoud MZ, Alkhorayef M, Alonazi B, Manssor E, Yousef A. Estimation of cancer risks during mammography procedure in Saudi Arabia. Saudi J Biol Sci. 2019 Sep;26(6):1107-1111. doi: 10.1016/j.sjbs.2018.10.005. Epub 2018 Oct 4. PMID: 31516336; PMCID: PMC6733693.
11. Kabir NA, Okoh FO, Mohd Yusof MF. Radiological and physical properties of tissue equivalent mammography phantom: Characterization and analysis methods. Radiation Physics and Chemistry. 2021;180, 109271.
12. Duffy SW, Yen AM, Tabar L, Lin AT, Chen SL, Hsu CY, Dean PB, Smith RA, Chen TH. Beneficial effect of repeated participation in breast cancer screening upon survival. J Med Screen. 2024 Mar;31(1):3-7. doi: 10.1177/09691413231186686. Epub 2023 Jul 12. PMID: 37437178; PMCID: PMC10878004.
13. Sippo DA, Nagy P. Quality improvement projects for value-based care in breast imaging. J Am Coll Radiol. 2014 Dec;11(12 Pt A):1189-90. doi: 10.1016/j.jacr.2014.08.019. Epub 2014 Oct 11. PMID: 25307675.
14. Lillé S, Marshall W. EQUIP: Enhancing Quality Using the Inspection Program. Radiol Technol. 2017 May;88(5):556-561. PMID: 28500100.
15. Gonzalez-Ruiz A, Sánchez Mendoza HI, Santos Cuevas CL, Isidro-Ortega FJ, Estrada JF, Domínguez-García MV, Flores-Merino MV. An evaluation of the present status of quality assurance program implementation in digital mammography facilities in a developing country. J Radiol Prot. 2022 Nov 28;42(4). doi: 10.1088/1361-6498/aca0fe. PMID: 36347024.
16. Hejduk P, Sexauer R, Ruppert C, Borkowski K, Unkelbach J, Schmidt N. Automatic and standardized quality assurance of digital mammography and tomosynthesis with deep convolutional neural networks. Insights Imaging. 2023 May 18;14(1):90. doi: 10.1186/s13244-023-01396-8. PMID: 37199794; PMCID: PMC10195933.
17. Selvan CS, Sureka CS. Quality Assurance and Average Glandular dose Measurement in Mammography Units. J Med Phys. 2017 Jul-Sep;42(3):181-190. doi: 10.4103/jmp.JMP_69_16. PMID: 28974865; PMCID: PMC5618466.
18. Alrehily F. DIAGNOSTIC REFERENCE LEVELS OF RADIOGRAPHIC AND CT EXAMINATIONS IN SAUDI ARABIA: A SYSTEMATIC REVIEW. Radiat Prot Dosimetry. 2022 Oct 16;198(19):1451-1461. doi: 10.1093/rpd/ncac183.
19. SFDA. Saudi Food & Drug Authority National Diagnostic Reference Levels. https://www.sfda.gov.sa/sites/default/files/2023-02/NDRL-En.pdf. 2023.
20. Radiatioin Protection of Patients. IAEA Diagnostic Reference Levels (DRLs) in Medical Imaging . https://www.iaea.org/resources/rpop/health-professionals/nuclear-medicine/diagnostic-nuclear-medicine/diagnostic-reference-levels-in-medical-imaging.
21. Yaffe MJ. Developing a quality control program for digital mammography: Achievements so far and challenges to come. Imaging in Medicine. 2011; 3(1).
22. The 2007 Recommendations of the International Commission on Radiological Protection. ICRP publication 103. Ann ICRP. 2007;37(2-4):1-332. doi: 10.1016/j.icrp.2007.10.003. PMID: 18082557.
23. Dance DR, Sechopoulos I. Dosimetry in x-ray-based breast imaging. Phys Med Biol. 2016 Oct 7;61(19):R271-R304. doi: 10.1088/0031-9155/61/19/R271. Epub 2016 Sep 12. PMID: 27617767; PMCID: PMC5061150.
24. Sardanelli F, Helbich TH; European Society of Breast Imaging (EUSOBI). Mammography: EUSOBI recommendations for women's information. Insights Imaging. 2012 Feb;3(1):7-10. doi: 10.1007/s13244-011-0127-y. Epub 2011 Oct 28. PMID: 22695994; PMCID: PMC3292646.
25. Hendrick RE, Pisano ED, Averbukh A, Moran C, Berns EA, Yaffe MJ, Herman B, Acharyya S, Gatsonis C. Comparison of acquisition parameters and breast dose in digital mammography and screen-film mammography in the American College of Radiology Imaging Network digital mammographic imaging screening trial. AJR Am J Roentgenol. 2010 Feb;194(2):362-9. doi: 10.2214/AJR.08.2114.
26. Gilbert FJ, Pinker-Domenig K. Diagnosis and Staging of Breast Cancer: When and How to Use Mammography, Tomosynthesis, Ultrasound, Contrast-Enhanced Mammography, and Magnetic Resonance Imaging. 2019 Feb 20. In: Hodler J, Kubik-Huch RA, von Schulthess GK, editors. Diseases of the Chest, Breast, Heart and Vessels 2019-2022: Diagnostic and Interventional Imaging [Internet]. Cham (CH): Springer; 2019. Chapter 13. PMID: 32096932.
27. Hofvind S, Ponti A, Patnick J, Ascunce N, Njor S, Broeders M, et al. False-positive results in mammographic screening for breast cancer in Europe: a literature review and survey of service screening programmes. J Med Screen. 2012;19 Suppl 1:57-66. doi: 10.1258/jms.2012.012083. PMID: 22972811.
28. Román R, Sala M, Salas D, Ascunce N, Zubizarreta R, Castells X. Effect of protocol-related variables and women's characteristics on the cumulative false-positive risk in breast cancer screening. Ann Oncol. 2012 Jan;23(1):104-111. doi: 10.1093/annonc/mdr032. Epub 2011 Mar 23. PMID: 21430183; PMCID: PMC3276323.
29. Tamam N, Salah H, Rabbaa M, Abuljoud M, Sulieman A, Alkhorayef M, et al. Evaluation of patients radiation dose during mammography imaging procedure. Radiation Physics and Chemistry. 2021;188, 109680.
30. Saeed MK. Radiation doses and potential cancer risks during mammography procedures at southern Saudi Arabia. International Journal of Radiation Research. 2021;19(4):929-936.
31. Alahmad H, AlEnazi K, Alshahrani A, Albariqi S, Alnafea M. Evaluation of mean glandular dose from mammography screening: A single-center study. Journal of Radiation Research and Applied Sciences. 2023-11-08 , doi:10.1016/j.jrras.2023.100749
32. Hegazi TM, AlSharydah AM, Alfawaz I, Al-Muhanna AF, Faisal SY. The Impact of Data Management on the Achievable Dose and Efficiency of Mammography and Radiography During the COVID-19 Era: A Facility-Based Cohort Study. Risk Manag Healthc Policy. 2023 Mar 14;16:401-414. doi: 10.2147/RMHP.S389960.

International Journal of Biomedicine 14(2) (2024) 240-245
http://dx.doi.org/10.21103/Article14(2)_RA6

REVIEW ARTICLE

INTERNATIONAL JOURNAL OF BIOMEDICINE

Silver in Wound and Trophic Ulcer Treatment: A Modern View of the Problem

Serhiy H. Hryvenko[1*], Aleksander A. Golomidov[1], Sydyk A. Sidikov[2], Manvel S. Margarian[2], Madina R. Bostanova[2], Zaineb I. Salpagarova[2]

[1]*Medical Institute named after S.I. Georgievsky of Vernadsky CFU, Simferopol, Crimea*
[2]*Rostov State Medical University, Rostov-on-Don, Russian Federation*

Abstract

This review presents published data on the history of use, mechanism of action, and effectiveness of silver and silver-based drugs in surgical practice. A literature search was carried out using PubMed, EMBASE, Google Scholar, and E-Library databases. Analysis of available literature data convincingly demonstrates the effectiveness of silver nanocomposites as antibacterial and anti-inflammatory agents. The demonstrated antimicrobial property of silver nanoparticles (AgNPs) against various antibiotic-resistant bacteria is especially significant for clinical use. Silver nanoparticles have clinically proven effective in treating wounds and trophic ulcers.**(International Journal of Biomedicine. 2024;14(2):240-245.)**

Keywords*:* silver • silver nanoparticles • wound • trophic ulcer

For citation: Hryvenko SH, Golomidov AA, Sidikov SA, Margarian MS, Bostanova MR, Salpagarova ZI. Silver in Wound and Trophic Ulcer Treatment: A Modern View of the Problem. International Journal of Biomedicine. 2024;14(2):240-245. doi:10.21103/Article14(2)_RA6

Abbreviations

Ag, silver; **AgNPs**, silver nanoparticles; **DNA**, deoxyribonucleic acid; **GSH**, reduced glutathione; **ROS**, reactive oxygen species.

Introduction

Silver (Ag) is one of the metals most intensively used by humanity for medical purposes since ancient civilizations. The use of silver in medicine is based primarily on its disinfectant properties since silver has the most potent bactericidal effect among metals.[1] The bactericidal effect of Ag-based compounds is 1750 times more powerful than the effect of the same concentration of carbolic acid, 1500 times higher than the effect of the same concentration of phenol, and 3.5 times stronger than the effect of sublimate. Silver, having a powerful antimicrobial effect, is detrimental to antibiotic-resistant strains of more than 500 species of bacteria.[2] It has been established that Ag has the most powerful bactericidal effect among heavy metals.[3]

Hippocrates, the father of modern medicine, believed that silver powder has healing properties and is recommended for treating trophic ulcers.[1,4] One of the first silver compounds used in medical practice was silver nitrate. It was originally used in a solid form known as lapis, or hellstone.[1] In the 19th century, lapis became widespread for cauterizing excessive granulations in wounds and treating burns, and Ag-based compounds became one of the main means for the treatment and prevention of wound infections before the invention of antibiotics.[5] It was in the 19th century that active scientific study of silver and its compounds began, which led to the discovery of its antiviral, antibacterial, and immunomodulatory activities.[6] From the end of the 19th to the beginning of the 20th century, several Ag-based compounds and drugs were developed: collargol, protargol, elargol, silargel, argosulfan, and others. Some of them are still successfully used today.[1]

After the discovery of penicillin, the first antibiotic, in 1941, interest in silver as an antimicrobial drug disappeared for almost 40 years. Some experts believe that before the discovery of antibiotics, silver salts were one of the most widely used agents with antimicrobial activity.[7] However, the emergence of antibiotic-resistant strains of microorganisms has led to the search for new silver-based antibacterial drugs. In 1968, silver

[*]***Corresponding author****: Serhiy H. Hryvenko, MD, PhD, ScD. Medical Academy named after S.I. Georgievsky of Vernadsky CFU, Simferopol, Crimea. E-mail: hryva@mail.ru*

sulfadiazine was introduced into clinical practice and began one of the most successful silver-containing antimicrobials. Since that time, topical silver sulfadiazine ointment has been the standard antibacterial treatment for major burns and is widely used in their therapy.[8] The therapeutic effect of silver sulfadiazine in the local treatment of wounds and wound infections is associated with its anti-inflammatory and antiseptic effects, as well as stimulation of the proliferation and differentiation of keratinocytes.[9]

Currently, one of the most effective topical Ag-based drugs for the local treatment of wounds and wound infections is silver sulfathiazole. According to immunohistochemical analysis, when using silver sulfathiazole for local therapy in the complex treatment of complicated diabetic foot syndrome, there is a decreased expression of CD68+ macrophages in the studied tissues of trophic ulcers and wounds. In a study by Kalinichenko et al.,[10] a gradual increase in the coefficient of macrophage activity in biopsy specimens, with the systematic achievement of a threshold level of 1.0, was a reliable sign of a better regenerative response and indicated the optimal nature of the course of the wound process. The use of silver sulfathiazole in the complex treatment of patients with diabetic foot syndrome reduced the intensity of inflammatory reactions and the content of C-reactive protein and neopterin,[11] and it had a protective effect on the vascular endothelium.[12]

In recent years, various silver-based dressings have been proposed for treating wounds (Silversel, Silverlon, Silvasorb, Contreet-H, Arglaes, Aquacel-Ag, Acticoat, Nucryst, and others). Such dressings have a more practical application than metallic silver or silver salts.[13] Several studies have noted a significant reduction in the time of wound cleansing and healing, in elimination of systemic manifestations of the infectious process, in duration of required antibacterial therapy, and in hospitalization in patients using silver-based dressings. Using silver-based dressings in a moist microenvironment creates optimal conditions for epithelization during the wound process.[14]

It is now generally accepted that silver is a broad-spectrum antimicrobial agent. Because of the broad spectrum of antibacterial action, from bacteriostatic to bactericidal, Ag-based compounds have found wide applications in medicine.[15,16] In 2009, approximately 15 tons of silver were included in medical products worldwide.[17]

New prospects for the medical use of silver are opening in connection with the production of its most unique form—silver nanoparticles (AgNPs), which have more outstanding physiochemical and biological properties beyond bulk silver.[18] AgNPs can destroy multiple drug-resistant strains and prevent biofilm formation, indicating significant potential in antibacterial application.[19]

The antibacterial mechanisms of AgNPs have been discussed extensively, but the exact effect of AgNPs on bacteria is still undefined.[20] However, two mechanisms attract attention, namely contact killing and ion-mediated killing.

Ionized silver can "attack" at least three cellular components: cell membranes, cytoplasmic organelles, and DNA.[21] Silver ions interact with membrane proteins and further block the respiratory chain.[22] It has been reported that AgNPs can anchor to the bacterial cell wall, causing physical changes in the bacterial membrane followed by its damage, which can lead to leakage of cellular contents and bacterial death.[23-25] After adhesion to the bacterial wall, AgNPs can also penetrate the bacteria through the membrane. Small nanoparticles, which have a larger surface area in contact with bacterial cells, can reach the cytoplasm more often than larger nanoparticles.[24] Once inside the microbial cell, AgNPs can interact with cellular structures and biomolecules such as proteins, lipids, and DNA, thereby leading to bacterial dysfunction and, ultimately, death.[26-29] It is also speculated that AgNPs interact effectively with the carboxyl and thiol groups of β-galactosidase and inhibit intracellular biological functions, leading to cell death.[30]

In addition, the antibacterial mechanism of AgNPs is also due to their ability to produce high levels of reactive oxygen species (ROS) and free radicals,[31-33] while suppressing the expression of antioxidant enzymes (glutathione [GSH], superoxide dismutase and catalase), thereby accelerating ROS accumulation.[34,35] The released Ag^+ from AgNPs can interact with respiratory chain proteins on the membrane, interrupt intracellular O_2 reduction, and induce ROS production.[36] In turn, the accumulation of ROS leads to an apoptosis-like response, lipid peroxidation, GSH depletion, and DNA damage.[37-39]

Silver nanoparticles' unique properties make them suitable catalysts in various chemical reactions. The enhanced antimicrobial and virucidal effects of AgNPs are explained by their increased reactivity. In the range of 1–100 nm, AgNPs are tens and hundreds of times more active than other known biocidal and antibiotic drugs and are considered more promising agents as an alternative to antibiotics.[40] In the available literature, we have not found data on the formation of resistance of microorganisms to AgNPs, which, according to several authors, opens the way to overcoming resistance to antibiotics.[40,41]

At the same time, some studies have reported bacterial resistance to AgNPs. In a study by Kaweeteerawat et al.,[42] it was found that AgNPs enhanced bacterial resistance to antibiotics by promoting stress tolerance by inducing intracellular ROS. In addition, the gram-negative bacteria *Escherichia coli* 013 and *Pseudomonas aeruginosa* CCM 3955, and *E. coli* CCM 3954 can develop resistance to AgNPs after repeated exposure. This resistance was due to the production of flagellin, an adhesive protein of the bacterial flagellum, which caused the aggregation of AgNPs and thereby eliminated their antibacterial effect.[43] Genes encoding silver resistance were detected most frequently in *Enterobacter* spp. (48%), followed by *Klebsiella* spp.(41%) and *Escherichia coli* (4%).[44]

It was initially believed that AgNPs exert their activity only by releasing ions, acting as a depot. Modern research indicates that both ions and nanoparticles themselves exhibit activity.[45,46] Their pharmacological activity is based on the ability of silver to be an electron pair acceptor.[47,48] It has been demonstrated that the cellular membrane of bacteria has a negative charge due to the presence of carboxyl, phosphate, and amino groups.[49] The bactericidal efficiency of various positively and negatively charged silver nanoparticles has been extensively evaluated in the literature. The positively

charged silver nanoparticles showed the highest bactericidal activity against all microorganisms tested.[50]

Thus, the interaction of Ag^+ with a bacterial cell is complex and multifactorial.[51] Since the mechanism of action of AgNPs is not specific, AgNPs act almost equally on both gram-positive and gram-negative microflora.[1] Due to the multi-component mechanism of action, microorganisms' resistance to Ag preparations rarely develops. The antifungal activity of silver preparations has also been described, with a predominantly positive mechanism of action in the form of cell membrane destruction.

In addition to antimicrobial and antifungal effects, Ag-based drugs are characterized by local anti-inflammatory activity.[52] In contrast to the antimicrobial effect, the anti-inflammatory effect of silver at the molecular level has not been sufficiently studied.[51] The acceleration of the transition of a wound from inflammation to regeneration in experiments on animal models is associated with an increase in the concentration of epithelial growth factor after the application of silver dressing to the wound.[8] Studies on human cells have found that application of silver at concentrations of 10–20 μg/ml causes a decrease in TNF-α, IL, and IL-6.[53]

Despite significant clinical experience with the use of Ag-based compounds in medical practice, the results of scientific studies of their effectiveness and safety have been regularly subjected to critical evaluation.[54] One potential adverse reaction of using silver preparations with local exposure to wounds is the risk of developing argyria.[55] It should also be noted that there may be a deposition of silver in the cutaneous scar tissue and a change in skin color with prolonged use of the silver dressing.[56] In vitro studies have shown that there is a difference between the number of fibroblasts and the amount of collagen they produce when exposed to silver and non-silver dressings. Silver dressings reduce the number of fibroblasts by 54%–70% and collagen by 48%–68%.[57]

The study of the effectiveness of Ag^+ in antimicrobial agents has resumed. Published results of randomized clinical trials about the topical use of Ag-based preparations in the treatment of pressure ulcers,[58] microbially contaminated wounds with a high risk of infection,[59,60] acute wounds during vacuum therapy,[61] and colorectal[62-64] and plastic surgery[65,66] indicate their safety and clinical effectiveness.

A wide range of studies have focused on the use of AgNPs for wound healing. The use of AgNPs in ointments and dressings[67-70] for the purpose of preventing wound infection[71] and treating infected wounds[72] is said to be mandatory in many works. Many authors note the effectiveness of AgNPs as antibacterial agents,[73,74] as well as nanocomposites, which include silver in nanosized form[75,76] and nanofibers.[77,78] Some researchers have been able to combine the antibacterial and proliferative effects of Ag-nanocomposites. In burn wounds, they have been shown to induce the proliferation and migration of keratinocytes and fibroblasts, promoting accelerated wound healing in diabetic mice.[79,80] It was found that AgNPs stabilized with chitosan and polyvinyl alcohol not only inhibit the growth of bacteria but also can accelerate wound repair.[81,82]

In addition, AgNP targets mesenchymal stem cell proliferation and osteogenic differentiation in vitro.[83] Mouse models of burn wounds have demonstrated pronounced anti-inflammatory properties of polyamidoamine dendrimer-stabilized AgNPs.[84]

One of the most important problems is the synthesis of sufficiently stable AgNPs of a given size that retain high chemical or biological activity for a long time. In this regard, when developing methods for synthesizing AgNPs, much attention is paid to the choice of stabilizers, which determine the. stability level of AgNPs.[85] One of the possible solutions to this problem was using sodium alginate, a biopolymer of plant origin.[86] It has been shown that sodium alginate macromolecules reduce Ag^+ into small nanoparticles and simultaneously stabilize them. It has been observed that one composition not only combines the properties of two biologically active substances but also their synergy.[86]

The data analysis demonstrates the effectiveness of AgNPs as antibacterial and anti-inflammatory agents. Silver compounds have been shown to inhibit the growth and formation of bacterial biofilms.[87] In addition, it has been shown that the use of silver compounds in the treatment of wounds is also characterized by an improvement in the quality of life of patients and good cost-effectiveness. From this perspective, the development and introduction into clinical practice of new AgNP-based drugs for treating wounds and trophic ulcers, and the search for enhancing their bactericidal effect, is extremely relevant.

Competing Interests

The authors declare that they have no competing interests.

References

1. Rzheussky SE. Silver nanoparticles in medicine. Vestnik VGMU. 2022;21(2):15-24. doi: 10.22263/2312-4156.2022.2.15. (In Russ.)
2. Rzheussky SE, Kuhach VV, Valueva MA. Economic aspects of application and antimicrobial activity of silver-containing drugs. Vestnik Farmacii. 2013;2(60):25-30. (In Russ.)
3. Shrestha R, Joshi DR, Gopali J, Piya S. Oligodynamic fraction of silver, copper and brass on enteric bacteria isolated from water of Kathmandu Valley. Nepal Journal of Science and Technology. 2009;10:189-193. doi:10.3126/njst.v10i0.2959
4. Melaiye A, Youngs WJ. Silver and its application as an antimicrobial agent. Expert Opin Ther Pat. 2005;15(2):125-30. doi: 10.1517/13543776.15.2.125
5. Sattori I, Mahmudov KB, Rajabov U, Rajabali M, Nazarov F. Historical aspects of the application of silver compounds. Report of the TAAS. 2018;1:62-65. (In Russ.)
6. Marx DE, Barillo DJ. Silver in medicine: the basic science. Burns. 2014 Dec;40 Suppl 1:S9-S18. doi: 10.1016/j.burns.2014.09.010.
7. Mijnendonckx K, Leys N, Mahillon J, Silver S, Van Houdt R. Antimicrobial silver: uses, toxicity and potential for resistance. Biometals. 2013 Aug;26(4):609-21. doi: 10.1007/s10534-013-9645-z.
8. Nadworny PL, Wang J, Tredget EE, Burrell RE. Anti-inflammatory activity of nanocrystalline silver-derived solutions in porcine contact dermatitis. J Inflamm (Lond). 2010

Feb 19;7:13. doi: 10.1186/1476-9255-7-13.
9. Elliott C. The effects of silver dressings on chronic and burns wound healing. Br J Nurs. 2010 Aug 12-Sep 8;19(15):S32-6. doi: 10.12968/bjon.2010.19.Sup5.77707.
10. Kalinichenko AP, Hryvenko SH, Umerov EE, Uzbekova LD, Usmanova TE, Izosimov VV. The Morphological Rationality for the Expediency of Topical Application of Silver Sulfathiazole in Patients with Diabetic Foot Syndrome. International Journal of Biomedicine. 2022;12(3):404-408. doi:10.21103/Article12(3)_OA10
11. Kalinichenko A, Grivenko S, Umerov E. Features of the dynamics of inflammatory markers during local treatment of complicated forms of diabetic foot syndrome. MIA Medical Bulletin. 2022;121(6):11-14. doi:10.52341/20738080_2022_121_6_11. (In Russ.)
12. Kalinichenko AP, Grivenko SG, Umerov EE. Monitoring of molecular mechanisms of a complicated reparative process during local treatment of the diabetic foot syndrome. Tavricheskiy mediko-biologicheskiy vestnik. 2022;25(4):22-28. doi: 10.29039/2070-8092-2022-25-4-22-28. (In Russ.)
13. Lansdown AB, Sampson B, Rowe A. Sequential changes in trace metal, metallothionein and calmodulin concentrations in healing skin wounds. J Anat. 1999 Oct;195(Pt 3):375-86. doi: 10.1046/j.1469-7580.1999.19530375.x.
14. Helary C, Bataille I, Abed A, Illoul C, Anglo A, Louedec L, Letourneur D, Meddahi-Pellé A, Giraud-Guille MM. Concentrated collagen hydrogels as dermal substitutes. Biomaterials. 2010 Jan;31(3):481-90. doi: 10.1016/j.biomaterials.2009.09.073.
15. Lansdown AB. Silver in health care: antimicrobial effects and safety in use. Curr Probl Dermatol. 2006;33:17-34. doi: 10.1159/000093928.
16. Privolnev VV, Zabrosaev VS, Danilenkov NV. Silver in topical treatment of infected wounds. Vestnik of the SSMA. 2015;14(3):85-91. (In Russ.)
17. Randall CP, Oyama LB, Bostock JM, Chopra I, O'Neill AJ. The silver cation (Ag+): antistaphylococcal activity, mode of action and resistance studies. J Antimicrob Chemother. 2013 Jan;68(1):131-8. doi: 10.1093/jac/dks372.
18. Beyene HD, Werkneh AA, Bezabh HK, Ambaye TG. Synthesis paradigm and applications of silver nanoparticles (AgNPs), a review. Sustainable Materials and Technologies. 2017;13:18-23. doi:10.1016/j.susmat.2017.08.001
19. Yuan YG, Peng QL, Gurunathan S. Effects of Silver Nanoparticles on Multiple Drug-Resistant Strains of Staphylococcus aureus and Pseudomonas aeruginosa from Mastitis-Infected Goats: An Alternative Approach for Antimicrobial Therapy. Int J Mol Sci. 2017 Mar 6;18(3):569. doi: 10.3390/ijms18030569.
20. Dovnar RI, Smotrin SM. Application of silver in medicine: historical aspects and modern view on the problem. Problemy zdorov′â i èkologii. 2011;3:149-153. doi:10.51523/2708-6011.2011-8-3-30. (In Russ.)
21. Rodin AV, Golub AV, Privolnev VV. Topical administration of sulfathiazole silver in the treatment of chronic wounds. RMJ. Medical Review. 2018;12:19-23. (In Russ.)
22. Konop M, Damps T, Misicka A, Rudnicka L. Certain Aspects of Silver and Silver Nanoparticles in Wound Care: A Minireview. Journal of Nanomaterials. 2016;7614753:47. doi: 10.1155/2016/7614753
23. Seong M, Lee DG. Silver Nanoparticles Against Salmonella enterica Serotype Typhimurium: Role of Inner Membrane Dysfunction. Curr Microbiol. 2017 Jun;74(6):661-670. doi: 10.1007/s00284-017-1235-9.
24. Khalandi B, Asadi N, Milani M, Davaran S, Abadi AJ, Abasi E, Akbarzadeh A. A Review on Potential Role of Silver Nanoparticles and Possible Mechanisms of their Actions on Bacteria. Drug Res (Stuttg). 2017 Feb;67(2):70-76. doi: 10.1055/s-0042-113383.
25. Rajesha S, Dharanishanthiband V, Kanna AV. Antibacterial mechanism of biogenic silver nanoparticles of Lactobacillus acidophilus. Journal of Experimental Nanoscience. 2015;10(15):1143-1152. doi:10.1080/17458080.2014.985750
26. Qing Y, Cheng L, Li R, Liu G, Zhang Y, Tang X, Wang J, Liu H, Qin Y. Potential antibacterial mechanism of silver nanoparticles and the optimization of orthopedic implants by advanced modification technologies. Int J Nanomedicine. 2018 Jun 5;13:3311-3327. doi: 10.2147/IJN.S165125.
27. Liao C, Li Y, Tjong SC. Bactericidal and Cytotoxic Properties of Silver Nanoparticles. Int J Mol Sci. 2019 Jan 21;20(2):449. doi: 10.3390/ijms20020449.
28. Rinna A, Magdolenova Z, Hudecova A, Kruszewski M, Refsnes M, Dusinska M. Effect of silver nanoparticles on mitogen-activated protein kinases activation: role of reactive oxygen species and implication in DNA damage. Mutagenesis. 2015 Jan;30(1):59-66. doi: 10.1093/mutage/geu057.
29. López-Carballo G, Higueras L, Gavara R, Hernández-Muñoz P. Silver ions release from antibacterial chitosan films containing in situ generated silver nanoparticles. J Agric Food Chem. 2013 Jan 9;61(1):260-7. doi: 10.1021/jf304006y.
30. You C, Han C, Wang X, Zheng Y, Li Q, Hu X, Sun H. The progress of silver nanoparticles in the antibacterial mechanism, clinical application and cytotoxicity. Mol Biol Rep. 2012 Sep;39(9):9193-201. doi: 10.1007/s11033-012-1792-8.
31. Zhao R, Lv M, Li Y, Sun M, Kong W, Wang L, Song S, Fan C, Jia L, Qiu S, Sun Y, Song H, Hao R. Stable Nanocomposite Based on PEGylated and Silver Nanoparticles Loaded Graphene Oxide for Long-Term Antibacterial Activity. ACS Appl Mater Interfaces. 2017 May 10;9(18):15328-15341. doi: 10.1021/acsami.7b03987.
32. Gomaa EZ. Silver nanoparticles as an antimicrobial agent: A case study on Staphylococcus aureus and Escherichia coli as models for Gram-positive and Gram-negative bacteria. J Gen Appl Microbiol. 2017 Mar 17;63(1):36-43. doi: 10.2323/jgam.2016.07.004.
33. Siritongsuk P, Hongsing N, Thammawithan S, Daduang S, Klaynongsruang S, Tuanyok A, Patramanon R. Two-Phase Bactericidal Mechanism of Silver Nanoparticles against Burkholderia pseudomallei. PLoS One. 2016 Dec 15;11(12):e0168098. doi: 10.1371/journal.pone.0168098.
34. Yuan YG, Peng QL, Gurunathan S. Effects of Silver Nanoparticles on Multiple Drug-Resistant Strains of Staphylococcus aureus and Pseudomonas aeruginosa from Mastitis-Infected Goats: An Alternative Approach for Antimicrobial Therapy. Int J Mol Sci. 2017 Mar 6;18(3):569. doi: 10.3390/ijms18030569.
35. Ramkumar VS, Pugazhendhi A, Gopalakrishnan K, Sivagurunathan P, Saratale GD, Dung TNB, Kannapiran E. Biofabrication and characterization of silver nanoparticles using aqueous extract of seaweed *Enteromorpha compressa* and its biomedical properties. Biotechnol Rep (Amst). 2017 Feb 10;14:1-7. doi: 10.1016/j.btre.2017.02.001.
36. Long YM, Hu LG, Yan XT, Zhao XC, Zhou QF, Cai Y, Jiang GB. Surface ligand controls silver ion release of

nanosilver and its antibacterial activity against *Escherichia coli*. Int J Nanomedicine. 2017 Apr 18;12:3193-3206. doi: 10.2147/IJN.S132327.
37. Korshed P, Li L, Liu Z, Wang T. The Molecular Mechanisms of the Antibacterial Effect of Picosecond Laser Generated Silver Nanoparticles and Their Toxicity to Human Cells. PLoS One. 2016 Aug 30;11(8):e0160078. doi: 10.1371/journal.pone.0160078. Erratum in: PLoS One. 2018 Aug 30;13(8):e0203636.
38. Lee W, Kim KJ, Lee DG. A novel mechanism for the antibacterial effect of silver nanoparticles on Escherichia coli. Biometals. 2014 Dec;27(6):1191-201. doi: 10.1007/s10534-014-9782-z.
39. Tang S, Zheng J. Antibacterial Activity of Silver Nanoparticles: Structural Effects. Adv Healthc Mater. 2018 Jul;7(13):e1701503. doi: 10.1002/adhm.201701503.
40. Gladkih PG. Effect of silver nanoparticles on biofilms of microorganisms (Review). Journal of New Medical Technologies, eEdition. 2015;1. doi:10.12737/8117. (In Russ.)
41. Gladkih PG. Effect of silver nanoparticles in combination with methyluracil on the biofilms in an experimental model of peritonitis in rats. Journal of New Medical Technologies, eEdition. 2016;2. doi: 10.12737/20408. (In Russ.)
42. Kaweeteerawat C, Na Ubol P, Sangmuang S, Aueviriyavit S, Maniratanachote R. Mechanisms of antibiotic resistance in bacteria mediated by silver nanoparticles. J Toxicol Environ Health A. 2017;80(23-24):1276-1289. doi: 10.1080/15287394.2017.1376727.
43. Panáček A, Kvítek L, Smékalová M, Večeřová R, Kolář M, Röderová M, Dyčka F, Šebela M, Prucek R, Tomanec O, Zbořil R. Bacterial resistance to silver nanoparticles and how to overcome it. Nat Nanotechnol. 2018 Jan;13(1):65-71. doi: 10.1038/s41565-017-0013-y.
44. Sütterlin S, Dahlö M, Tellgren-Roth C, Schaal W, Melhus Å. High frequency of silver resistance genes in invasive isolates of Enterobacter and Klebsiella species. J Hosp Infect. 2017 Jul;96(3):256-261. doi: 10.1016/j.jhin.2017.04.017.
45. Reidy B, Haase A, Luch A, Dawson KA, Lynch I. Mechanisms of Silver Nanoparticle Release, Transformation and Toxicity: A Critical Review of Current Knowledge and Recommendations for Future Studies and Applications. Materials (Basel). 2013 Jun 5;6(6):2295-2350. doi: 10.3390/ma6062295.
46. Liao C, Li Y, Tjong SC. Bactericidal and Cytotoxic Properties of Silver Nanoparticles. Int J Mol Sci. 2019 Jan 21;20(2):449. doi: 10.3390/ijms20020449.
47. Dakal TC, Kumar A, Majumdar RS, Yadav V. Mechanistic Basis of Antimicrobial Actions of Silver Nanoparticles. Front Microbiol. 2016 Nov 16;7:1831. doi: 10.3389/fmicb.2016.01831.
48. Ansari MA, Khan HM, Khan AA, Ahmad MK, Mahdi AA, Pal R, Cameotra SS. Interaction of silver nanoparticles with Escherichia coli and their cell envelope biomolecules. J Basic Microbiol. 2014 Sep;54(9):905-15. doi: 10.1002/jobm.201300457.
49. Van Der Wal A, Norde W, Zehnder AJB, Lyklema J. Determination of the total charge in the cell walls of Gram-positive bacteria. Colloids Surf B Biointerfaces. 1997;**9**(1–2):81–100.
50. You C, Han C, Wang X, Zheng Y, Li Q, Hu X, Sun H. The progress of silver nanoparticles in the antibacterial mechanism, clinical application and cytotoxicity. Mol Biol Rep. 2012 Sep;39(9):9193-201. doi: 10.1007/s11033-012-1792-8.
51. Rodin AV, Privolnev VV, Barsukov AN. Therapeutic potential of sulfathiazole silver for topical treatment of wound infection. Ambulatory Surgery. 2018;1–2:69-70. (In Russ.)
52. Khansa I, Schoenbrunner AR, Kraft CT, Janis JE. Silver in Wound Care-Friend or Foe?: A Comprehensive Review. Plast Reconstr Surg Glob Open. 2019 Aug 12;7(8):e2390. doi: 10.1097/GOX.0000000000002390.
53. Aparna Mani KM, Seethalakshmi S, Gopal V. Evaluation of in-vitro anti-inflammatory activity of silver nanoparticles synthesised using piper nigrum extract. Journal of Nanomedicine & Nanotechnology. 2015;6:2. doi:10.4172/2157-7439.1000268
54. Dissemond J, Böttrich JG, Braunwarth H, Hilt J, Wilken P, Münter KC. Evidence for silver in wound care - meta-analysis of clinical studies from 2000-2015. J Dtsch Dermatol Ges. 2017 May;15(5):524-535. doi: 10.1111/ddg.13233.
55. McCague A, Joe VC. A Case of Argyria and Acute Leukopenia Associated with the Use of an Antimicrobial Soft Silicone Foam Dressing. J Burn Care Res. 2016 Sep-Oct;37(5):e493-6. doi: 10.1097/BCR.0000000000000275.
56. Wang XQ, Chang HE, Francis R, Olszowy H, Liu PY, Kempf M, Cuttle L, Kravchuk O, Phillips GE, Kimble RM. Silver deposits in cutaneous burn scar tissue is a common phenomenon following application of a silver dressing. J Cutan Pathol. 2009 Jul;36(7):788-92. doi: 10.1111/j.1600-0560.2008.01141.x.
57. Zou SB, Yoon WY, Han SK, Jeong SH, Cui ZJ, Kim WK. Cytotoxicity of silver dressings on diabetic fibroblasts. Int Wound J. 2013 Jun;10(3):306-12. doi: 10.1111/j.1742-481X.2012.00977.x.
58. Chuangsuwanich A, Charnsanti O, Lohsiriwat V, Kangwanpoom C, Thong-In N. The efficacy of silver mesh dressing compared with silver sulfadiazine cream for the treatment of pressure ulcers. J Med Assoc Thai. 2011 May;94(5):559-65.
59. Beele H, Meuleneire F, Nahuys M, Percival SL. A prospective randomised open label study to evaluate the potential of a new silver alginate/carboxymethylcellulose antimicrobial wound dressing to promote wound healing. Int Wound J. 2010 Aug;7(4):262-70. doi: 10.1111/j.1742-481X.2010.00669.x.
60. Eberlein T, Haemmerle G, Signer M, Gruber Moesenbacher U, Traber J, Mittlboeck M, Abel M, Strohal R. Comparison of PHMB-containing dressing and silver dressings in patients with critically colonised or locally infected wounds. J Wound Care. 2012 Jan;21(1):12, 14-6, 18-20. doi: 10.12968/jowc.2012.21.1.12.
61. Siegel HJ, Herrera DF, Gay J. Silver negative pressure dressing with vacuum-assisted closure of massive pelvic and extremity wounds. Clin Orthop Relat Res. 2014 Mar;472(3):830-5. doi: 10.1007/s11999-013-3123-3.
62. Krieger BR, Davis DM, Sanchez JE, Mateka JJ, Nfonsam VN, Frattini JC, Marcet JE. The use of silver nylon in preventing surgical site infections following colon and rectal surgery. Dis Colon Rectum. 2011 Aug;54(8):1014-9. doi: 10.1097/DCR.0b013e31821c495d.
63. Siah CJ, Yatim J. Efficacy of a total occlusive ionic silver-containing dressing combination in decreasing risk of surgical site infection: an RCT. J Wound Care. 2011 Dec;20(12):561-8. doi: 10.12968/jowc.2011.20.12.561.
64. Tomasello G, Bellavia M, Damiani F, Damiano G, Palumbo VD, Fiorentini T, Puleio R, Spinelli G, Damiani P, Ficarella S, Bruno A, Lo Monte AI. Argentum-quarz solution in the treatment of anorectal fistulas: is it possible a conservative

approach? Med Hypotheses. 2012 Oct;79(4):542-3. doi: 10.1016/j.mehy.2012.07.015.
65. Bailey S, Carmean M, Cinat M, Burton K, Lane C, Malinoski D. A randomized comparison study of Aquacel Ag and Glucan II as donor site dressings with regard to healing time, cosmesis, infection rate, and patient's perceived pain: a pilot study. J Burn Care Res. 2011 Nov-Dec;32(6):627-32. doi: 10.1097/BCR.0b013e31822dc409.
66. Lohsiriwat V, Chuangsuwanich A. Comparison of the ionic silver-containing hydrofiber and paraffin gauze dressing on split-thickness skin graft donor sites. Ann Plast Surg. 2009 Apr;62(4):421-2. doi: 10.1097/SAP.0b013e31818a65e9.
67. Pei Z, Sun Q, Sun X, Wang Y, Zhao P. Preparation and characterization of silver nanoparticles on silk fibroin/carboxymethylchitosan composite sponge as anti-bacterial wound dressing. Biomed Mater Eng. 2015;26 Suppl 1:S111-8. doi: 10.3233/BME-151296.
68. Fries CA, Ayalew Y, Penn-Barwell JG, Porter K, Jeffery SL, Midwinter MJ. Prospective randomised controlled trial of nanocrystalline silver dressing versus plain gauze as the initial post-debridement management of military wounds on wound microbiology and healing. Injury. 2014 Jul;45(7):1111-6. doi: 10.1016/j.injury.2013.12.005.
69. Jenwitheesuk K, Surakunprapha P, Chowchuen B. The use of nanocrystalline silver for the treatment of massive soft tissue defects with exposed bone. J Med Assoc Thai. 2013 Sep;96 Suppl 4:S177-84.
70. Guthrie KM, Agarwal A, Tackes DS, Johnson KW, Abbott NL, Murphy CJ, Czuprynski CJ, Kierski PR, Schurr MJ, McAnulty JF. Antibacterial efficacy of silver-impregnated polyelectrolyte multilayers immobilized on a biological dressing in a murine wound infection model. Ann Surg. 2012 Aug;256(2):371-7. doi: 10.1097/SLA.0b013e318256ff99.
71. Keen JS, Desai PP, Smith CS, Suk M. Efficacy of hydrosurgical debridement and nanocrystalline silver dressings for infection prevention in type II and III open injuries. Int Wound J. 2012 Feb;9(1):7-13. doi: 10.1111/j.1742-481X.2011.00822.x.
72. Asz J, Asz D, Moushey R, Seigel J, Mallory SB, Foglia RP. Treatment of toxic epidermal necrolysis in a pediatric patient with a nanocrystalline silver dressing. J Pediatr Surg. 2006 Dec;41(12):e9-12. doi: 10.1016/j.jpedsurg.2006.08.043.
73. Dhapte V, Kadam S, Moghe A, Pokharkar V. Probing the wound healing potential of biogenic silver nanoparticles. J Wound Care. 2014 Sep;23(9):431-2, 434, 436 passim. doi: 10.12968/jowc.2014.23.9.431.
74. Hebeish A, El-Rafie MH, El-Sheikh MA, Seleem AA, El-Naggar ME. Antimicrobial wound dressing and anti-inflammatory efficacy of silver nanoparticles. Int J Biol Macromol. 2014 Apr;65:509-15. doi: 10.1016/j.ijbiomac.2014.01.071.
75. Singh D, Singh A, Singh R. Polyvinyl pyrrolidone/carrageenan blend hydrogels with nanosilver prepared by gamma radiation for use as an antimicrobial wound dressing. J Biomater Sci Polym Ed. 2015;26(17):1269-85. doi: 10.1080/09205063.2015.1087366.
76. Im AR, Kim JY, Kim HS, Cho S, Park Y, Kim YS. Wound healing and antibacterial activities of chondroitin sulfate- and acharan sulfate-reduced silver nanoparticles. Nanotechnology. 2013 Oct 4;24(39):395102. doi: 10.1088/0957-4484/24/39/395102.
77. GhavamiNejad A, Rajan Unnithan A, Ramachandra Kurup Sasikala A, Samarikhalaj M, Thomas RG, Jeong YY, Nasseri S, Murugesan P, Wu D, Hee Park C, Kim CS. Mussel-Inspired Electrospun Nanofibers Functionalized with Size-Controlled Silver Nanoparticles for Wound Dressing Application. ACS Appl Mater Interfaces. 2015 Jun 10;7(22):12176-83. doi: 10.1021/acsami.5b02542.
78. Wu J, Zheng Y, Wen X, Lin Q, Chen X, Wu Z. Silver nanoparticle/bacterial cellulose gel membranes for antibacterial wound dressing: investigation in vitro and in vivo. Biomed Mater. 2014 Jun;9(3):035005. doi: 10.1088/1748-6041/9/3/035005.
79. Rangasamy S, Tak YK, Kim S, Paul A, Song JM. Bifunctional Therapeutic High-Valence Silver-Pyridoxine Nanoparticles with Proliferative and Antibacterial Wound-Healing Activities. J Biomed Nanotechnol. 2016 Jan;12(1):182-96. doi: 10.1166/jbn.2016.2179.
80. Abdel-Mohsen AM, Jancar J, Abdel-Rahman RM, Vojtek L, Hyršl P, Dušková M, Nejezchlebová H. A novel in situ silver/hyaluronan bio-nanocomposite fabrics for wound and chronic ulcer dressing: In vitro and in vivo evaluations. Int J Pharm. 2017 Mar 30;520(1-2):241-253. doi: 10.1016/j.ijpharm.2017.02.003.
81. Li C, Fu R, Yu C, Li Z, Guan H, Hu D, Zhao D, Lu L. Silver nanoparticle/chitosan oligosaccharide/poly(vinyl alcohol) nanofibers as wound dressings: a preclinical study. Int J Nanomedicine. 2013;8:4131-45. doi: 10.2147/IJN.S51679.
82. Li CW, Wang Q, Li J, Hu M, Shi SJ, Li ZW, Wu GL, Cui HH, Li YY, Zhang Q, Yu XH, Lu LC. Silver nanoparticles/chitosan oligosaccharide/poly(vinyl alcohol) nanofiber promotes wound healing by activating TGFβ1/Smad signaling pathway. Int J Nanomedicine. 2016 Jan 21;11:373-86. doi: 10.2147/IJN.S91975.
83. Zhang R, Lee P, Lui VC, Chen Y, Liu X, Lok CN, To M, Yeung KW, Wong KK. Silver nanoparticles promote osteogenesis of mesenchymal stem cells and improve bone fracture healing in osteogenesis mechanism mouse model. Nanomedicine. 2015 Nov;11(8):1949-59. doi: 10.1016/j.nano.2015.07.016.
84. Liu X, Hao W, Lok CN, Wang YC, Zhang R, Wong KK. Dendrimer encapsulation enhances anti-inflammatory efficacy of silver nanoparticles. J Pediatr Surg. 2014 Dec;49(12):1846-51. doi: 10.1016/j.jpedsurg.2014.09.033.
85. Shulgina TA, Nechaeva OV, Glinskaya EV, Daryin NI, Torgashova AS, Teslyuk DA, Babailova AV, Panfilova EA. Antimycotic Activity of Silver Nanoparticles Depending on the Stabilizer Used. Izv. Saratov Univ. (N.S.), Ser. Chemistry. Biology. Ecology. 2017;17(4):465-468. doi: 10.18500/1816-9775-2017-17-4-465-468. (In Russ.)
86. Riabushko VI, Yurkova IM, Riabushko LI, Estrela-Lopys VR, inventors; Riabushko VI, Yurkova IM, Riabushko LI, Estrela-Lopys VR, assignees. The method of obtaining a water-soluble bactericidal composition containing silver nanoparticles. Ukraine patent UA 10539. 2005 November 15. (In Ukrainian).
87. Mohanta YK, Biswas K, Jena SK, Hashem A, Abd Allah EF, Mohanta TK. Anti-biofilm and Antibacterial Activities of Silver Nanoparticles Synthesized by the Reducing Activity of Phytoconstituents Present in the Indian Medicinal Plants. Front Microbiol. 2020 Jun 23;11:1143. doi: 10.3389/fmicb.2020.01143. Erratum in: Front Microbiol. 2020 Sep 11;11:1784.

International Journal of Biomedicine 14(2) (2024) 246-252
http://dx.doi.org/10.21103/Article14(2)_OA1

ORIGINAL ARTICLE

Cardiology

INTERNATIONAL JOURNAL OF BIOMEDICINE

10-Year Cardiovascular Risk in Hypertensive Patients: Insights from Central Vietnam Using WHO 2019 Chart

Ho Anh Hien[1,2], Nguyen Minh Tam[1], Dirk Devroey[2], Stefan Heytens[3], Vo Tam[4], Tran Binh Thang[5], Hoang Thi Bach Yen[5], Doan Pham Phuoc Long[4], Huynh Van Minh[4], Hoang Anh Tien[4*]

[1]*Department of Family Medicine, University of Medicine and Pharmacy, Hue University, Hue, Vietnam*
[2]*Department of Family Medicine and Chronic Care, Faculty of Medicine and Pharmacy, Vrije Universiteit Brussel, Brussels, Belgium*
[3]*Department of Public Health and Primary Care, Faculty of Medicine and Health Sciences, Ghent University, Ghent, Belgium*
[4]*Department of Internal Medicine, University of Medicine and Pharmacy, Hue University, Hue, Vietnam*
[5]*Faculty of Public Health, University of Medicine and Pharmacy, Hue University, Hue, Vietnam*

Abstract

Background: Assessing the 10-year cardiovascular disease (CVD) risk is crucial for effective prevention and management. Despite its significance, information is limited on CVD risk among hypertensive patients in primary care in Central Vietnam. We conducted this study to estimate 10-year CVD risk in primary care settings and explore its associated risk factors, using the 2019 WHO CVD risk chart.

Methods and Results: This cross-sectional study collected socio-demographic and clinical data through a standardized questionnaire. Cardiovascular risk was estimated using the WHO CVD risk charts for Southeast Asia. The prevalence of low, moderate, and high CVD risk was 52.1%, 38.9%, and 9.0%, respectively. Notably, men had significantly higher rates of moderate (48.6%) and high (17.6%) CVD risk than women (31.4 and 2.4%, respectively) (P<0.001). Age was a significant factor, with an increasing prevalence of moderate and high CVD risk as age advanced. Specifically, the 50-59 age group had a moderate risk of 18.6%, rising to 69.9% in the 70-74 age group. High CVD risk increased from 0.6% to 27.6% in the same age groups. Lower educational levels were associated with a higher proportion of moderate CVD risk. Smoking and excessive alcohol consumption were linked to elevated CVD risks (25.0% and 30.0%, respectively), surpassing those without these behaviors. Similar trends were observed for individuals with diabetes, high total cholesterol, and high blood pressure.

Conclusion: Approximately one-tenth of hypertensive patients face a high risk of developing CVDs within the next 10 years. A comprehensive approach, encompassing behavioral changes and the management of metabolic risk factors, is essential to reduce CVD risk effectively.**(International Journal of Biomedicine. 2024;14(2):246-252.)**

Keywords: blood pressure • hypertension • cardiovascular risk • risk chart

For citation: Hien HA, Tam NM, Devroey D, Heytens S, Tam V, Thang TB, Yen HTB, Long DPP, Minh HV, Tien HA. 10-Year Cardiovascular Risk in Hypertensive Patients: Insights from Central Vietnam Using WHO 2019 Chart. International Journal of Biomedicine. 2024;14(2):246-252. doi:10.21103/Article14(2)_OA1

Abbreviations

BP, blood pressure; **CVR**, cardiovascular risk; **CVD**, cardiovascular disease; **CV**, Central Vietnam; **TC**, total cholesterol.

Introduction

In 2019, CVDs accounted for 32% of global deaths, with more than 75% occurring in developing nations.[1] In Vietnam, the growing burden of heart-related issues stands out as a significant public health problem, reflecting the country's rapid economic growth and lifestyle changes. Over the past 10 years, CVDs have consistently been the leading cause of both death and disability in the country, with conditions like heart attacks and strokes contributing significantly. The prevalence of CVDs, including coronary artery disease and stroke, has consistently increased in recent years, making up 31% of all deaths in 2016, exceeding 170,000 fatalities.[2] Ischemic heart disease and stroke consistently ranked as leading causes of death in Vietnam.[3]

Predictable risk factors, such as age, gender, and lifestyle choices, significantly contribute to CVD development.[4-6] Among these, age is a non-modifiable factor, as the risk of CVD increases with advancing age. Age increases the risk of CVD, while gender differences tend to equalize post-menopause. Unhealthy dietary habits, tobacco use, family history, and physiological factors like hypertension, diabetes, and obesity further elevate cardiovascular risk (CVR). Awareness and management of these factors are vital for effective prevention.[4-6]

Calculating the 10-year CVD risk through risk prediction models proves to be a valuable tool for prevention and management.[7-9] This approach enables early identification of high-risk individuals, facilitating targeted interventions. Utilizing established charts assists healthcare providers in creating personalized treatment plans, optimizing resource allocation, and enhancing patient awareness. Given limited information on cardiovascular risk among hypertensive patients in CV's community health centers, we conducted this study to estimate 10-year CVD risk in primary care settings and explore its associated risk factors, using the 2019 WHO CVD risk chart.[8]

Materials and Methods

Study Design and Population

This analysis draws on data from an ongoing cross-sectional study, currently under peer review, aimed at evaluating medication adherence and hypertension knowledge among hypertensive patients in primary care settings across Central Vietnam. The dataset was obtained from community health centers in three provinces: Thua Thien Hue, Khanh Hoa, and Lam Dong, all situated in Central Vietnam. Within each province, one urban and one rural area were designated for inclusion in the study. Two to four community health centers in these areas were randomly selected to ensure a diverse participant pool. Recruitment followed a random process, selecting individuals at intervals of 5 from hypertensive patient lists at these community health centers, targeting 50 to 70 participants. Eligibility criteria encompassed individuals aged 40 to 74 diagnosed with primary hypertension, with exclusion criteria applied to those receiving treatment for less than six months or experiencing secondary hypertension or hypertension related to pregnancy.

Sample Size and Data Collection

To achieve a 5% margin of error and a study power of 99%, considering a reported medication adherence prevalence of 49.8% from a previous study, we calculated a sample size of 660 eligible subjects. To address potential non-response, we initially invited 792 patients, ultimately collecting data from 761 participants. Subsequently, we excluded 107 participants with a known history of cardiovascular events (e.g., stroke, coronary heart diseases), resulting in a sample size of 654 participants for CVD risk assessment using the WHO chart.[8]

Selected participants were asked to visit local community health centers on weekend mornings after refraining from eating or drinking. They were also requested to bring accurate blood pressure and cholesterol readings. A semi-structured, interviewer-administered questionnaire adapted from the WHO STEPS instrument was employed for data collection on CVD risk factors.[11] Information encompassed basic details, anthropometric measurements, personal behaviors, medication adherence, hypertension knowledge, and health metrics, including blood pressure (BP) and cholesterol levels. All team members underwent training to ensure a clear understanding of the study objectives and proper data collection procedures. The survey was conducted from March to June in the year 2023.

Variables

The study utilized the updated WHO CVD 2019 risk charts for Southeast Asia to estimate the ten-year risk of fatal or non-fatal cardiovascular events among hypertensive patients.[8] These laboratory-based charts incorporated parameters such as diabetes status, sex, age groups, smoking habits, blood cholesterol levels, and systolic BP, offering precise risk scores for individuals aged 40 to 74 without established CVDs, categorized into five groups. In our study, participants were further grouped into risk categories: low [very low and low] (<10%), moderate (10%–<20%), and high [high and very high] (≥20%). Current smokers were defined as those currently using or having quit smoking within the last 12 months, while diabetes was diagnosed by medical professionals or by the use of insulin or oral hypoglycemic drugs at the time of our survey. Hypercholesterolemia was identified as a blood TC value of ≥5.1 mmol/L. Blood pressure was measured using automatic sphygmomanometers, and controlled hypertension was defined as systolic BP <140 mmHg and diastolic BP <90 mmHg.[12]

Demographic information, personal medical history, and CVR factors were collected from participants. Education levels were stratified into three categories, depending on years of formal schooling: low (<6 years), middle (6-9 years), and high (>9 years). Occupations were grouped as manual workers (farmers, traders, housekeepers, and production roles), government staff, or other occupations (retirees, elderly, and unemployed). Most respondents belonged to the ethnic majority in Vietnam known as "Kinh." Urban and rural residences were determined based on administrative divisions within each province. Physical activity was assessed using metabolically equivalent tasks per minute per week (MET/min/week), with physical inactivity defined as having fewer than

600 MET/min/week of physical activity. Excessive alcohol consumption was categorized as more than 2 standard units per day or 14 standard units per week for men and more than 1 standard unit per day or 7 standard units per week for women.[11] Body mass index (BMI) was calculated as weight (kg) per height squared (m^2), with overweight defined as BMI from 23 to 24.9 kg/m^2 and obesity as BMI ≥25 kg/m^2.[13] Medication adherence was determined using the 5-item version of the self-report Medication Adherence Report Scale (MARS-5), where scores from 5 to 23 indicated non-adherence and scores of 24 to 25 were classified as adherent.[14]

Statistical analyses

We used EpiData Entry 3.1 to ensure precision in the data collection process. For descriptive and analytical purposes, we used SPSS 27.0. Inter-group comparisons were performed using the chi-square test. All analyses followed a two-sided approach; a probability value of $P<0.05$ was considered statistically significant.

Results

Table 1 outlines the socio-demographic characteristics of the 654 research participants. Among them, 370 were women, constituting 56.6% of the sample. Notably, individuals aged 60-69 represented half of the participants, with a higher proportion of women in this age group (53.0% vs. 44.4%). In the 70-74 age group, nearly one-fifth of the participants were men, showing a higher proportion than women (22.2% vs. 16.2%). Ethnic minorities constituted 7.3% of the participants. In terms of educational attainment, 40% of participants had a high level of education, with a higher prevalence among men than women. Manual workers comprised three-quarters of the participants, with a higher proportion of women in this category. Conversely, among employed or retired individuals, men outnumbered women.

The prevalence of smoking was 23.3%, with a significantly higher prevalence in men (45,8%) than in women (5.9%) ($P<0.001$).

Table 1.

Socio-demographic and clinical characteristics of the study population by gender.

Characteristics		Men n (%)	Women n (%)	Total n (%)	*P*-value
Overall (n)		284	370	654	
Age group	40-49	30 (10.6)	23 (6.2)	53 (8.1)	0.024
	50-59	65 (22.9)	91 (24.6)	156 (23.9)	
	60-69	126 (44.4)	196 (53.0)	322 (49.2)	
	70-74	63 (22.2)	60 (16.2)	123 (18.8)	
Residence	Urban	141 (49.6)	173 (46.8)	314 (48.0)	0.46
	Rural	143 (50.4)	197 (53.2)	340 (52.0)	
Ethnicity	Ethnic majority	263 (92.6)	343 (92.7)	606 (92.7)	0.95
	Ethnic minorities	21 (7.4)	27 (7.3)	48 (7.3)	
Educational level	Low	49 (17.3)	151 (40.8)	200 (30.6)	<0.001
	Medium	95 (33.5)	103 (27.8)	198 (30.3)	
	High	140 (49.3)	116 (31.4)	256 (39.1)	
Occupation	Manual worker	166 (58.5)	274 (74.1)	440 (67.3)	<0.001
	Governmental staff	28 (9.9)	17 (4.6)	45 (6.9)	
	Retired, Unemployed	90 (31.7)	79 (21.4)	169 (25.8)	
Health insurance	Yes	275 (96.8)	350 (94.6)	625 (95.6)	0.169
	No	9 (3.2)	20 (5.4)	29 (4.4)	
Smoking	Yes	130 (45.8)	22 (5.9)	152 (23.2)	<0.001
	No	154 (54.2)	348 (94.1)	502 (76.8)	
Excessive alcohol consumption	Yes	19 (6.7)	1 (0.3)	20 (3.1)	<0.001
	No	265 (93.3)	369 (99.7)	634 (96.9)	
Physical inactivity	Yes	156 (54.9)	237 (64.1)	393 (60.1)	0.018
	No	128 (45.1)	133 (35.9)	261 (39.9)	
Fruits & Vegetables	≥5 servings/day	176 (62.0)	236 (63.8)	412 (63.0)	0.634
	<5 servings/day	108 (38.0)	134 (36.2)	242 (37.0)	
BMI	Underweight	158 (55.6)	189 (51.1)	29 (4.4)	0.402
	Normal weight	13 (4.6)	16 (4.3)	347 (53.1)	
	Overweight,	52 (18.3)	88 (23.8)	140 (21.4)	
	Obesity	61 (21.5)	77 (20.8)	138 (21.1)	
Diabetes	Yes	37 (13.0)	48 (13.0)	85 (13.0)	1.00
	No	204 (71.8)	265 (71.6)	469 (71.7)	
	Unknown	43 (15.2)	57 (15.4)	100 (15.3)	
High TC	Yes	157 (55.3)	214 (57.8)	371 (56.7)	0.513
	No	127 (44.7)	156 (42.2)	283 (43.3)	
Hypertension control	Yes	220 (77.5)	319 (86.2)	539 (82.4)	0.004
	No	64 (22.5)	51 (13.8)	115 (17.6)	
Medication adherence	High	153 (53.9)	172 (46.5)	325 (49.7)	0.061
	Low	131 (46.1)	198 (53.5)	329 (50.3)	

Excessive alcohol consumption was found in 3.1% of the population, predominantly in men (6.7%), with a statistically significant difference (P<0.001). The prevalence of physical inactivity and overweight was higher in women than in men (64.1% vs. 54.9% and 23.8% vs. 18.3%, respectively). The prevalence of diabetes and high cholesterol stood at 13% and 56.7%, respectively, with no significant gender difference. Hypertension control was achieved in 82.4% of cases, with a higher proportion observed in women than in men (86.2% vs. 77.5%, P=0.004) (Table 1).

Table 2 displays the distribution of 10-year CVD risk across demographic factors. The prevalence of low, moderate, and high CVD risk was 52.1%, 38.9%, and 9.0%, respectively. Notably, men had significantly higher rates of moderate (48.6%) and high (17.6%) CVD risk than women (31.4 and 2.4%, respectively) (P<0.001). Age was a significant factor, with an increasing prevalence of moderate and high CVD risk as age advanced. Specifically, the 50-59 age group had a moderate risk of 18.6%, rising to 69.9% in the 70-74 age group. High CVD risk increased from 0.6% to 27.6% in the same age groups.

Table 2.

Distribution of 10-year risk for fatal or non-fatal cardiovascular events based on background characteristics.

Characteristics		CVD risk			*P*-value
		Low (<10%), n (%)	Moderate (10-20%), n (%)	High (>20%), n (%)	
Overall		341 (52.1)	254 (38.9)	59 (9.0)	
Gender	Men	96 (33.8)	138 (48.6)	50 (17.6)	<0.001
	Women	245 (66.2)	116 (31.4)	9 (2.4)	
Age group	40-49	51 (96.2)	2 (3.8)	0 (0.0)	<0.001
	50-59	126 (80.8)	29 (18.6)	1 (0.6)	
	60-69	161 (50.0)	137 (42.5)	24 (7.5)	
	70-74	3 (2.4)	86 (69.9)	34 (27.6)	
Residence	Urban	160 (51.0)	116 (36.9)	38 (12.1)	0.029
	Rural	181 (53.2)	138 (40.6)	21 (6.2)	
Ethnicity	Ethnic majority	310 (51.2)	240 (39.6)	56 (9.2)	0.188
	Ethnic minorities	31 (64.6)	14 (29.2)	3 (6.3)	
Educational level	Low	86 (43.0)	96 (48.0)	18 (9.0)	0.016
	Medium	117 (59.1)	65 (32.8)	16 (8.1)	
	High	138 (53.9)	93 (36.3)	25 (9.8)	
Occupation	Manual worker	251 (57.0)	162 (36.8)	27 (6.1)	<0.001
	Governmental staff	31 (68.9)	12 (26.7)	2 (4.4)	
	Retired, Unemployed	59 (34.9)	80 (47.3)	30 (17.8)	
Health Insurance	Yes	324 (51.8)	245 (39.2)	56 (9.0)	0.677
	No	17 (58.6)	9 (31.0)	3 (10.3)	
Home BP monitoring	Yes	137 (50.2)	107 (39.2)	29 (10.6)	0.429
	No	204 (53.5)	147 (38.6)	30 (7.9)	
Smoking	Yes	29 (19.1)	85 (55.9)	38 (25.0)	<0.001
	No	312 (62.2)	169 (33.7)	21 (4.2)	
Excessive alcohol consumption	Yes	7 (35.0)	7 (35.0)	6 (30.0)	0.004
	No	334 (52.7)	247 (39.0)	53 (8.4)	
Physical inactivity	Yes	196 (49.9)	157 (39.9)	40 (10.2)	0.253
	No	145 (55.6)	97 (37.2)	19 (7.3)	
Fruits & Vegetables	≥5 servings/day	223 (54.1)	152 (36.9)	37 (9.0)	0.380
	<5 servings/day	118 (48.8)	102 (42.1)	22 (9.1)	
BMI	Underweight	10 (34.5)	17 (58.6)	2 (6.9)	0.131
	Normal weight	173 (49.9)	137 (39.5)	37 (10.7)	
	Overweight	76 (54.3)	54 (38.6)	10 (7.1)	
	Obesity	82 (59.4)	46 (33.3)	10 (7.2)	
Diabetes	Yes	18 (21.2)	48 (56.5)	19 (22.4)	<0.001
	No	272 (58.0)	165 (35.2)	32 (6.8)	
	Unknown	51 (51.0)	41 (41.0)	8 (8.0)	
High TC	Yes	175 (47.2)	154 (41.5)	42 (11.3)	0.005
	No	166 (58.7)	100 (35.3)	17 (6.0)	
Hypertension control	Yes	309 (57.3)	196 (36.4)	34 (6.3)	<0.001
	No	32 (27.8)	58 (50.4)	25 (21.7)	
Medication adherence	High	164 (50.5)	127 (39.1)	34 (10.5)	0.398
	Low	177 (53.8)	127 (38.6)	25 (7.6)	

Urban areas exhibited a higher prevalence of high CVD risk (12.1%) than rural areas (6.2%). Lower educational levels were associated with a higher proportion of moderate CVD risk. Smoking and excessive alcohol consumption were linked to elevated CVD risks (25.0% and 30.0%, respectively), surpassing those without these behaviors. Similar trends were observed for individuals with diabetes, high TC, and high BP. However, no significant differences were found in terms of physical inactivity, fruit and vegetable consumption, BMI, hypertension knowledge, or hypertension medication adherence.

Distinct patterns in the prevalence of elevated CVD risk emerged across age groups stratified by gender. Among men, the prevalence of high CVD risk increased notably, escalating from 1.5% in the 50-59 age group to 17.5% in the 60-69 age group and 42.9% in the 70-74 age group. In contrast, this increase was more gradual among women, starting at 1% in the 60-69 age group and reaching 11.7% in the 70-74 age group. The proportion of moderate CVD risk in the 50-59 and 60-69 age groups was significantly higher in men than in women (36.9% and 60.3% vs. 5.5% and 31.1%, respectively). However, in the 70-74 age group, this proportion was higher in women (83.3% vs. 57.1%). Additionally, the proportion of low CVR in women exceeded that in men across all age groups (Table 3).

Table 3.

Variation in CVD risk levels across age and gender of participants.

Gender	Age group	CVD risk		
		Low (<10%) n (%)	Moderate (10-20%) n (%)	High (>20%) n (%)
Men	40-49	28 (93.3)	2 (6.7)	0 (0.0)
	50-59	40 (61.5)	24 (36.9)	1 (1.5)
	60-69	28 (22.2)	76 (60.3)	22 (17.5)
	70-74	0 (0.0)	36 (57.1)	27 (42.9)
Women	40-49	23 (100.0)	0 (0.0)	0 (0.0)
	50-59	86 (94.5)	5 (5.5)	0 (0.0)
	60-69	133 (67.9)	61 (31.1)	2 (1.0)
	70-74	3 (5.0)	50 (83.3)	7 (11.7)

Discussion

Using a 10-year CVR chart is crucial in both clinical practice and community health for prevention. Firstly, it provides a standardized and evidence-based tool to assess an individual's risk of developing CVDs over a specific timeframe. This allows healthcare professionals to stratify patients based on risk levels, facilitating targeted interventions and personalized preventive strategies. Secondly, risk charts, such as the WHO CVD risk chart for Southeast Asia, integrate various risk factors, including age, gender, smoking, diabetes, TC, and hypertension, providing a comprehensive evaluation. In hypertensive patients, the CVD risk could be much higher than in the general community. In resource-limited areas like community health centers in Central Vietnam, employing such a tool enables primary healthcare practitioners to make informed decisions, optimize resource allocation, and improve CVD prevention and management outcomes. Our study provides information on the 10-year CVD risk in hypertensive patients in primary care settings in Central Vietnam.

In the present study, the overall prevalence of low, moderate, and high CVD risk was 52.1%, 38.9%, and 9.0%, respectively. It is crucial to note that the distribution of CVD risk varies across different countries in Asia.[15-18] Mongolia, Malaysia, and Cambodia exhibit notably low CVD risk, ranging from 89.6% in Mongolia to 94.4% in Malaysia and 97% in Cambodia.[17] Notably, the percentage of the population at high CVD risk is highest in Mongolia at 6%, compared to 2.3% in Malaysia and 1.3% in Cambodia. Bangladesh and Oman show an increase in the proportion of high CVD risk. In Bangladesh,[16] the prevalence of low, moderate, and high CVD risk was 69.5%, 25.9%, and 1.7%, respectively, while in Oman,[19] these proportions were 68.0%, 19.1%, and 12.9%, respectively. These differences could be attributed to distinct participant characteristics in each country. It is worth highlighting that the moderate and high CVD risk observed in our study is comparatively higher, given that we focused on estimating the 10-year CVD risk in hypertensive patients.

In our study, the prevalence of moderate and high CVD risk was significantly higher in men than in women. Moreover, these proportions increased with age, although the trends varied between genders. Among men, the prevalence of high CVD risk exhibited a notable rise, escalating from 0% in the 40-49 age group to 17.5% in the 60-69 age group and 42.9% in the 70-74 age group. In contrast, the increase was more gradual among women, starting at 0% in the 40-59 age group, rising to 1% in the 60-69 age group, and reaching 11.7% in the 70-74 age group. Similar patterns were observed in other Asian countries.[16-18] For instance, in Bangladesh,[16] the proportion of persons with high CVD risk increased from 0% in the 40–49 age group to 12.3% in those aged 70+, with a higher prevalence in men (17.6%) than in women (2.4%). In Cambodia,[17] high CVD risk among men increased from 0.6% in the 40-49 age group to 6.8% in the 60-64 age group, while among women, it increased from 0.2% to 3.4% in the same age groups. The observed gender differences in CVD risk can be attributed to the interplay of biological, hormonal, and lifestyle factors. Lifestyle choices such as higher rates of smoking and excessive alcohol consumption are more common in men, contributing to an elevated risk of cardiovascular events. Estrogen, the predominant hormone in women, is believed to have protective effects on the cardiovascular system. Therefore, considering male patients in CVD prevention and management is crucial to reduce the overall burden on the community.

The association between CVD risk and educational levels was evident in our study, aligning with findings from prior research in Nepal [18] and Oman.[19] For example, 52.3% of participants with no formal education exhibited elevated CVD risk compared to 16.0% among those with higher education in Oman. Educational levels have a discernible impact on patient knowledge and health behavior, a significance underscored by the prevalence of high-risk CVD cases among elderly

individuals with lower educational attainment in our study. Enhancing knowledge and awareness of risk factors is crucial for preventing and mitigating CVD risk, as emphasized by the study conducted by Kubota.[20] Risk factors such as smoking, diabetes, high BP, and high TC were identified as significant contributors to increased CVD risk, aligning with key elements in various risk charts predicting CVD and corroborating findings from previous studies.[4,5,7,9]

Strengths and Limitations

This study represents the pioneering effort to estimate the total 10-year CVD risk among hypertensive patients in primary care settings in Central Vietnam. Our research adopts a novel approach, employing the updated WHO CVD 2019 risk chart. This chart, rooted in extensive research and epidemiological data, establishes a robust foundation for accuracy and reliability. Its simplicity and user-friendly design enhance accessibility for a diverse range of healthcare professionals, allowing for a swift assessment of CVR without the need for intricate calculations. The evidence generated from our study holds significance for healthcare planners and researchers, offering valuable insights for the development of effective interventions.

Despite these strengths, our study has certain limitations. The risk charts are primarily designed based on data from specific populations in Southeast Asia, lacking specificity for the Vietnamese population. While these charts encompass common risk factors like age, gender, smoking status, BP, and cholesterol levels, they may not fully consider emerging risk factors or individual variations that could influence cardiovascular risk. Consequently, there is a potential for underestimating CVD risk, a general limitation inherent in almost all CVD risk charts. Recognizing these limitations is crucial for interpreting the findings and underscores the need for ongoing research to refine risk assessments for specific populations.

Conclusion

The 10-year CVR among hypertensive patients in primary care settings in Central Vietnam emerged as notably high. The distribution revealed that 52.1% had low risk, 38.9% moderate risk, and 9.0% high risk. Moreover, the incidence of high CVD risk was significantly higher in men than in women, rising with advancing age. Educational level, occupation, smoking, excessive alcohol consumption, diabetes, high TC, and high BP emerged as robust indicators strongly associated with CVD risk. These findings highlighted the imperative of formulating and implementing targeted interventions for hypertensive patients in primary care settings, aiming to reduce the burden of CVDs. Recognizing the multifactorial nature of CVD risk and addressing these modifiable risk factors through tailored interventions is paramount for enhancing preventive strategies and overall cardiovascular health in this population.

Ethical Approval

The research obtained ethical approval from the University of Medicine and Pharmacy, Hue University, with the reference number H2023/027. Additional approvals were secured from the health departments of the three respective provinces. Adhering strictly to ethical standards, detailed explanations of the study's objectives and procedures were provided to all potential participants, and written informed consent was obtained before participating in the research.

Acknowledgments

We are grateful to Prof. Anselme Derese (Ghent University) for dedicated support. We would also like to express our thanks to the University of Medicine and Pharmacy, Hue University, for their wonderful support. Finally, we extend our gratitude to the study participants, investigators, and the provincial health departments in Thua-Thien Hue, Lam Dong, and Khanh Hoa.

Sources of Funding

This work was supported by the Vietnam Ministry of Education and Training with grant number 2190/QĐ-BGDĐT, June 30, 2021. The funders had no role in the study design, data collection and analysis, decision to publish, or manuscript preparation.

Disclosure and Competing Interests

The authors declare that they have no competing interests. The views presented in this paper are the views of the authors and not of the organizations present.

Data Availability

The data set is owned by the University of Medicine and Pharmacy, Hue University, and the research partners. The data set underlying the study's findings is available on request to Hoang Anh Tien, the corresponding author of this study.

References

1. World Health Organization. Fact sheets: cardiovascular diseases (CVDs). Available from: https://www. who.int/news-room/fact-sheets/detail/cardiovascular-diseases-(cvds) (accessed 25 Dec 2023).
2. Hillary Ta BS BL and LP. Vietnamese and Vietnamese-American Health Statistics, 2003–2019: Stanford medicine; 2020 [updated March 2020. Available from: https://med.stanford.edu/content/dam/sm/care/VNDataBrief.pdf.
3. Nguyen TT, Trevisan M. Vietnam a country in transition: health challenges. BMJ Nutr Prev Health. 2020 May 6;3(1):60-66. doi: 10.1136/bmjnph-2020-000069. PMID: 33235972; PMCID: PMC7664505.
4. Visseren FLJ, Mach F, Smulders YM, Carballo D, Koskinas KC, Bäck M, et al.; ESC National Cardiac Societies;

***Corresponding author**: Assoc. Prof. Hoang Anh Tien, MD, PhD. Department of Internal Medicine, Hue University of Medicine and Pharmacy, Hue University, 06 Ngo Quyen, Hue City, Vietnam. E-mail: hatien@hueuni.edu.vn*

ESC Scientific Document Group. 2021 ESC Guidelines on cardiovascular disease prevention in clinical practice. Eur Heart J. 2021 Sep 7;42(34):3227-3337. doi: 10.1093/eurheartj/ehab484. Erratum in: Eur Heart J. 2022 Nov 7;43(42):4468. PMID: 34458905.

5. Arnett DK, Blumenthal RS, Albert MA, Buroker AB, Goldberger ZD, Hahn EJ, et al. 2019 ACC/AHA Guideline on the Primary Prevention of Cardiovascular Disease: A Report of the American College of Cardiology/American Heart Association Task Force on Clinical Practice Guidelines. Circulation. 2019 Sep 10;140(11):e596-e646. doi: 10.1161/CIR.0000000000000678. Epub 2019 Mar 17. Erratum in: Circulation. 2019 Sep 10;140(11):e649-e650. Erratum in: Circulation. 2020 Jan 28;141(4):e60. Erratum in: Circulation. 2020 Apr 21;141(16):e774. PMID: 30879355; PMCID: PMC7734661.

6. Hajar R. Risk Factors for Coronary Artery Disease: Historical Perspectives. Heart Views. 2017 Jul-Sep;18(3):109-114. doi: 10.4103/HEARTVIEWS.HEARTVIEWS_106_17. PMID: 29184622; PMCID: PMC5686931.

7. D'Agostino RB Sr, Vasan RS, Pencina MJ, Wolf PA, Cobain M, Massaro JM, Kannel WB. General cardiovascular risk profile for use in primary care: the Framingham Heart Study. Circulation. 2008 Feb 12;117(6):743-53. doi: 10.1161/CIRCULATIONAHA.107.699579. Epub 2008 Jan 22. PMID: 18212285.

8. WHO CVD Risk Chart Working Group. World Health Organization cardiovascular disease risk charts: revised models to estimate risk in 21 global regions. Lancet Glob Health. 2019 Oct;7(10):e1332-e1345. doi: 10.1016/S2214-109X(19)30318-3. Epub 2019 Sep 2. Erratum in: Lancet Glob Health. 2023 Feb;11(2):e196. PMID: 31488387; PMCID: PMC7025029.

9. Piepoli MF, Hoes AW, Agewall S, Albus C, Brotons C, Catapano AL, et al.; ESC Scientific Document Group. 2016 European Guidelines on cardiovascular disease prevention in clinical practice: The Sixth Joint Task Force of the European Society of Cardiology and Other Societies on Cardiovascular Disease Prevention in Clinical Practice (constituted by representatives of 10 societies and by invited experts) Developed with the special contribution of the European Association for Cardiovascular Prevention & Rehabilitation (EACPR). Eur Heart J. 2016 Aug 1;37(29):2315-2381. doi: 10.1093/eurheartj/ehw106. Epub 2016 May 23. PMID: 27222591; PMCID: PMC4986030.

10. Nguyen TP, Schuiling-Veninga CC, Nguyen TB, Vu TH, Wright EP, Postma MJ. Adherence to hypertension medication: Quantitative and qualitative investigations in a rural Northern Vietnamese community. PLoS One. 2017 Feb 1;12(2):e0171203. doi: 10.1371/journal.pone.0171203. PMID: 28146584; PMCID: PMC5287477.

11. World Health Organization (WHO). WHO STEPS Surveillance Manual: The WHO STEP-wise Approach to Chronic Disease Risk Factors Surveillance, World Health Organization: Non-communicable Diseases and Mental health, Geneva, World Health Organization. 2005;

12. Van Minh H, Van Huy T, Long DPP, Tien HA. Highlights of the 2022 Vietnamese Society of Hypertension guidelines for the diagnosis and treatment of arterial hypertension: The collaboration of the Vietnamese Society of Hypertension (VSH) task force with the contribution of the Vietnam National Heart Association (VNHA): The collaboration of the Vietnamese Society of Hypertension (VSH) task force with the contribution of the Vietnam National Heart Association (VNHA). J Clin Hypertens (Greenwich). 2022 Sep;24(9):1121-1138. doi: 10.1111/jch.14580. PMID: 36196473; PMCID: PMC9532930.

13. International Diabetes Institute/ Western Pacific World Health Organization/ International, Force A for the study of OIOT. The Asia-Pacific perspective: redefining obesity and its treatment. Geneva, Switzerland: World Health Organization. 2000. p. 56.

14. Chan AHY, Horne R, Hankins M, Chisari C. The Medication Adherence Report Scale: A measurement tool for eliciting patients' reports of nonadherence. Br J Clin Pharmacol. 2020 Jul;86(7):1281-1288. doi: 10.1111/bcp.14193. Epub 2020 May 18. PMID: 31823381; PMCID: PMC7319010.

15. Jaiswal A, Selva Das PA, Singh G, Sathiyamoorthy R, Deori TJ, Dwarakanathan V, Malhotra S, Verma M, Goel S. Assessment of cardiovascular risk using WHO CVD risk prediction chart with respect to hypertension status among Indian population: A secondary analysis of National Family Health Survey (2015-16). J Family Med Prim Care. 2022 Sep;11(9):5757-5765. doi: 10.4103/jfmpc.jfmpc_158_22. Epub 2022 Oct 14. PMID: 36505633; PMCID: PMC9731046.

16. Hanif AAM, Hasan M, Khan MSA, Hossain MM, Shamim AA, Hossaine M, et al. Ten-years cardiovascular risk among Bangladeshi population using non-laboratory-based risk chart of the World Health Organization: Findings from a nationally representative survey. PLoS One. 2021 May 26;16(5):e0251967. doi: 10.1371/journal.pone.0251967. PMID: 34038457; PMCID: PMC8153482.

17. Otgontuya D, Oum S, Buckley BS, Bonita R. Assessment of total cardiovascular risk using WHO/ISH risk prediction charts in three low and middle income countries in Asia. BMC Public Health. 2013 Jun 5;13:539. doi: 10.1186/1471-2458-13-539. PMID: 23734670; PMCID: PMC3679976.

18. Khanal MK, Ahmed MS, Moniruzzaman M, Banik PC, Dhungana RR, Bhandari P, Devkota S, Shayami A. Total cardiovascular risk for next 10 years among rural population of Nepal using WHO/ISH risk prediction chart. BMC Res Notes. 2017 Mar 7;10(1):120. doi: 10.1186/s13104-017-2436-9. PMID: 28270186; PMCID: PMC5341399.

19. Al-Mawali A, Al-Harrasi A, Pinto AD, Jayapal SK, Morsi M, Al-Shekaili W, et al. Assessment of Total Cardiovascular Risk Using WHO/ISH Risk Prediction Chart Among Adults in Oman: A Nationally Representative Survey. Oman Med J. 2023 May 31;38(3):e501. doi: 10.5001/omj.2023.70. PMID: 37496864; PMCID: PMC10366652.

20. Kubota Y, Heiss G, MacLehose RF, Roetker NS, Folsom AR. Association of Educational Attainment With Lifetime Risk of Cardiovascular Disease: The Atherosclerosis Risk in Communities Study. JAMA Intern Med. 2017 Aug 1;177(8):1165-1172. doi: 10.1001/jamainternmed.2017.1877. PMID: 28604921; PMCID: PMC5710437.

International Journal of Biomedicine 14(2) (2024) 253-259
http://dx.doi.org/10.21103/Article14(2)_OA2

ORIGINAL ARTICLE

Cardiology

INTERNATIONAL JOURNAL OF BIOMEDICINE

Clinical Effectiveness of the Fixed-Dose vs Free-Dose Triple Combinations in Patients with Uncontrolled Arterial Hypertension

D. Yu. Shukurova, G. A. Khamidullaeva*, G. Zh. Abdullaeva, Kh. F. Yusupova, A. D. Yuldasheva, Sh. Fayzullaeva, Zh. B. Safarov, Sh. M. Masharipov

Republican Specialized Center of Cardiology
Tashkent, Uzbekistan

Abstract

Background: The purpose of our study was a comparative assessment of the antihypertensive effectiveness of 2 triple combination antihypertensive therapy (AHT) regimens in a free-dose and fixed-dose combination of perindopril, indapamide, and amlodipine in hypertensive patients with high cardiovascular risk and a poor response to the 2-drug combinations in the clinic practice.

Methods and Results: Our study included 143 patients (79 men and 88 women) with arterial hypertension (AH) Grades 1-3 (ESC/ESH, 2018) and high cardiovascular risk who did not achieve the target blood pressure on dual combination AHT. The mean age of patients was 55.76±9.35 years; the average duration of AH was 10.69±6.61 years. All patients underwent the examinations according to the 2018 ESC/ESH Guidelines for the management of arterial hypertension.

Patients included in the study were divided into 2 groups using the envelope method: Group 1 (n=84) received a fixed-dose, triple combination of perindopril, indapamide, and amlodipine; Group 2 (n=83) received a free-dose combination of these drugs. In both groups, treatment began after discontinuation of previous therapy, with a low dose of a triple combination of antihypertensive drugs (perindopril [5 mg/day], indapamide [1.25 mg/day], amlodipine [5 mg/day]) in the form of a fixed or free combination. The initial doses of perindopril/indapamide/amlodipine in both groups were not statistically different: 6.9±2.4/1.74±0.6/7.1±2.4 mg/day in Group 1 and 6.9±2.7/1.95±0.6/7.1±2.5 mg/day in Group 2. After 4 weeks of therapy, if necessary, the doses of drugs were increased, starting with perindopril; the next adjustment of drug doses was carried out after 12 weeks of therapy. The final treatment results were determined after 24 weeks of AHT.

Target blood pressure of <140/90 mmHg was reached by 94.4% of patients in Group 1 and 83.3% in Group 2 (χ^2=7.471, *P*=0.006). Target blood pressure of <130/80 mmHg was reached by 70% of patients in Group 1 and 42% in Group 2 (χ^2=11.61, *P*=0.0001). A significant improvement in the diurnal BP profile was also revealed during treatment. According to 24-hour ambulatory blood pressure monitoring data, both groups achieved target blood pressure in terms of the average 24-h and average daytime systolic blood pressure (SBP) and diastolic blood pressure (DBP). Regarding average nighttime SBP and DBP and normalization of average nighttime diastolic blood pressure variability, target values were achieved only in Group 1 (*P*=0.028). In both groups, 24-week triple-combination therapy led to a significant decrease in central SBP, central DBP, and pulse wave velocity. At the same time, the positive dynamics of central SBP were more pronounced in Group 1 than in Group 2, and pulse wave velocity in Group 1 reached standard values.

Conclusion: The results of our study showed that in the treatment of uncontrolled hypertension on previous therapy in AH patients with high cardiovascular risk, a single-pill triple combination of the ACEI perindopril, the CCB amlodipine, and the thiazide-like diuretic indapamide contributed to the effective daily blood pressure control, the improvement of diurnal blood pressure profile, and a positive effect on central blood pressure and pulse wave velocity, thereby having a positive impact on the prognosis and quality of life of AH patients with high cardiovascular risk.**(International Journal of Biomedicine. 2024;14(2):253-259.)**

Keywords: arterial hypertension • antihypertensive therapy • target blood pressure • single-pill triple combination

For citation: Shukurova DYu, Khamidullaeva GA, Abdullaeva GZh, Yusupova KhF, Yuldasheva AD, Fayzullaeva Sh, Safarov ZhB, Masharipov ShM. Clinical Effectiveness of the Fixed-Dose vs Free-Dose Triple Combinations in Patients with Uncontrolled Arterial Hypertension. International Journal of Biomedicine. 2024;14(2):253-259. doi:10.21103/Article14(2)_OA2

Abbreviations

ABPM, 24-hour ambulatory blood pressure monitoring; **AH**, arterial hypertension; **AHD**, antihypertensive drug; **AHT**, antihypertensive therapy; **ACEI**, angiotensin-converting enzyme inhibitor; **ARB**, angiotensin receptor blocker; **BP**, blood pressure; **BPV**, BP variability; **CCB**, calcium channel blocker; **CHD**, coronary heart disease; **CIMT**, carotid intima-media thickness; **CHF**, chronic heart failure; **DBP**, diastolic BP; **DBPc**, central DBP; **DBPV**, diastolic BPV; **eGFR**, estimated glomerular filtration rate; **FBG**, fasting blood glucose; **HR**, heart rate; **HDL-C**, high-density lipoprotein cholesterol; **LVDD**, left ventricular diastolic dysfunction; **LVH**, left ventricular hypertrophy; **LVMI**, left ventricular mass index; **LDL-C**, low-density lipoprotein cholesterol; **MAU**, microalbuminuria; **MBP**, mean BP; **PP**, pulse pressure; **PPc**, central PP; **PWV**, pulse wave velocity; **RAAS**, renin-angiotensin-aldosterone system; **SBP**, systolic BP; **SBPc**, central SBP; **SBPV**, systolic BPV; **SPTC**, single-pill triple combination; **TBP**, target BP; **T2DM**, type 2 diabetes mellitus; **TC**, total cholesterol; **TG**, triglycerides.

Introduction

The combined antihypertensive therapy (AHT) is the regimen of choice in patients with arterial hypertension (AH) Grades 1-3 (ESC/ESH, 2018)[1] and high cardiovascular risk. In ESH/ESC-2018 and ESH-2023 recommendations,[1,2] a double combination of antihypertensive drugs is the starting step in the treatment of AH patients with high cardiovascular risk, which accounts for 70%-80% of hypertensive patients. It is recommended to start combining AHT with a dual-combination of antihypertensive drugs, one of which is an RAAS blocker and the other - a calcium channel blocker (CCB) or a diuretic, preferably in a single pill. Often, AH patients with high cardiovascular risk are resistant to the dual-combination and require switching to a triple combination AHT, consisting of ACEI/ARB, CCB, and diuretics, also preferably in a single-pill triple combination (SPTC), to increase patient adherence to therapy.[1] According to multicenter studies, about 30% of AH patients with high cardiovascular risk need a triple antihypertensive combination.[3]

High adherence to AHT is the main requirement for achieving the target blood pressure (TBP). According to the 2018 ESH/ESH Guidelines for the management of AH,[1] the primary target SBP and DBP are <140 mmHg and <90 mmHg, respectively. At the same time, for hypertensive patients aged 18-64 years without serious renal pathology, the recommended target SBP and DBP is ≤130/80 mmHg but not lower than 120/70 mmHg.

A SPRINT study recruited 9,361 adults ≥50 years of age who were at increased risk for cardiovascular disease and had an average SBP of 130–180 mmHg. They were randomized to the SPB treatment goal of either <120 mmHg (Intensive) or <140 mmHg (Standard). In the 2015 SPRINT main results report, the primary outcome and all-cause mortality were 25% (P<0.001) and 27% (P=0.003) lower in the Intensive than in the Standard group.[4] This included a 43% reduction (P=0.005) in cardiovascular death and a 38% reduction (P=0.002) in acute decompensated heart failure. The SPRINT findings indicated that more intensive blood pressure (BP) reduction yields substantial health benefits that outweigh the risks of adverse events (hypotension, syncope, electrolyte imbalance, and acute kidney injury).[5]

The purpose of our study was a comparative assessment of the antihypertensive effectiveness of 2 triple combination AHT regimens in a free-dose and fixed-dose combination of perindopril, indapamide, and amlodipine in AH patients with high cardiovascular risk and a poor response to the 2-drug combinations in the clinic practice.

Materials and Methods

Our study included 143 patients (79 men and 88 women) with AH Grades 1-3 (ESC/ESH, 2018) and high cardiovascular risk who did not achieve the TBP on dual combination AHT. The mean age of patients was 55.76±9.35 years; the average duration of AH was 10.69±6.61 years.

Based on the anamnestic data and examination results, some associated stable clinical conditions were diagnosed (CHD [angina pectoris FC I-II], T2DM, CHF [NYHA FC I-II]), which were included in the study.

Exclusion criteria were symptomatic hypertension, acute coronary syndrome, CHF (NYHA FC>III), cardiac arrhythmia, history of myocardial infarction, renal impairment, severe co-morbidities.

Patients included in the study were divided into 2 groups using the envelope method: Group 1 (n=84) received a fixed-dose, triple combination of perindopril, indapamide, and amlodipine; Group 2 (n=83) received a free-dose combination of these drugs. In both groups, treatment began after discontinuation of previous therapy, with a low dose of a triple combination of antihypertensive drugs (perindopril [5 mg/day], indapamide [1.25 mg/day], amlodipine [5 mg/day]) in the form of a fixed or free combination. The initial doses of perindopril/indapamide/amlodipine in both groups were not statistically different: 6.9±2.4/1.74±0.6/7.1±2.4 mg/day in Group 1 and 6.9±2.7/1.95±0.6/7.1±2.5 mg/day in Group 2. After 4 weeks of therapy, if necessary, the doses of drugs were increased, starting with perindopril; the next adjustment of drug doses was carried out after 12 weeks of therapy. The final treatment results were determined after 24 weeks of AHT.

All patients underwent the following examinations: assessment of traditional risk factors, physical examination, clinical and biochemical laboratory methods, 12-lead ECG, echocardiography, and 24-hour ABPM. Office BP was measured using a mercury sphygmomanometer, according to Korotkov's method. Blood pressure was measured 3 times, and the means of these measurements were used in the analyses. The 24-hour ABPM was performed using a BR-102 plus (SCHILLER, Switzerland). BP was measured during the daytime (07:00–23:00) every 30 min and at night (23:00–07:00) every 60 min.

The pulse contour analysis was carried out using the SphygmoCor device (AtCor Medical, Australia), which obtains peripheral arterial pressure waveforms by applying an arterial applanation tonometer to the wrist. Such indicators

as the central SBP (SBPc), central DBP (DBPc), central PP (PPc), and pulse wave velocity (PWV) were analyzed.

All patients underwent echocardiography with the determination of the left ventricular mass index (LVMI), left ventricular hypertrophy[1] and left ventricular diastolic dysfunction (LVDD); ultrasound examination of the carotid intima-media thickness (CIMT), as well as the determination of the level of microalbuminuria (MAU), blood creatinine, and glomerular filtration rate (GFR) calculation according to the CKD-EPI equation.

Blood levels of TC, TG, HDL-C, LDL-C, and VLDL-C were determined in the venous blood using automatic biochemical analyzer Daytona (RANDOX, United Kingdom) and RANDOX test systems by the enzymatic colorimetric method.

Statistical analysis was performed using the statistical software «Statistica» (v10.0, StatSoft, USA). The normality of distribution of continuous variables was tested by the Kolmogorov-Smirnov test with the Lilliefors correction and Shapiro-Wilk test. Baseline characteristics were summarized as frequencies and percentages for categorical variables and as median (Me) and interquartile range (IQR [Q1; Q3]), mean±standard deviation (SD) for continuous variables. For data with normal distribution, inter-group comparisons were performed using Student's t-test. The Mann-Whitney U Test was used to compare the differences between the two independent groups (for nonparametric data). Group comparisons with respect to categorical variables were performed using chi-square test. A probability value of $P<0.05$ was considered statistically significant.

Results

At the initial stage of the study, patients in both groups did not differ in gender and age, risk factors, markers of target organ damage, biochemical parameters, and associated clinical conditions (Table 1).

Table 1.

Clinical characteristics of AH patients.

Characteristics	General group (n=167)	Group 1 (n=84)	Group 2 (n=83)
Women, n (%)	88 (52.7%)	34 (40.5%)	54 (65%)
Men, n (%)	79 (47.3%)	43 (51.2%)	36 (43.4%)
Current smoker, n (%)	30 (18.0%)	12 (14.3%)	18 (21.7%)
CHD (FC I-II)	91 (54.5%)	42 (50%)	49 (59%)
T2DM, n (%)	26 (15.6%)	12 (14.3%)	14 (16.9%)
History of stroke, n (%)	5 (3.0%)	3 (3.57%)	2 (2.4%)
CHF (NYHA FC I-II), n (%)	55 (33.0%)	28 (33.3%)	27 (32.5%)
BMI >30 kg/m^2, (n / %)	100 (60%)	50 (59,5%)	50 (60,2%)
LVH, (n / %)	138 (82.6%)	68 (81%)	70 (84.3%)
LVDD, (n / %)	38 (22.7%)	20 (25.8%)	18 (21.7%)
CIMT ≥0.9 mm, (n / %)	140 (83.8%)	68 (81%)	72 (86.7%)
MAU, n (%)	60 (36%)	33 (39.3%)	27 (32.5%)
PWV >10 m/sec, (n / %)	80 (48%)	42 (50%)	38 (45.8%)

.

According to the average values of SBP (171.06±17.7 mmHg) and DBP (100.06±8.7 mmHg), the patients were characterized by AH Grade 2 (Table 2).

Table 2.

Indicators of clinical, functional, and laboratory data in the study groups at the initial examination stage and after 24 weeks of AHT.

Variable	General group (n=167)	Group 1 (n=84)	Group 2 (n=83)
	M±SD Me [Q1; Q3]	M±SD Me [Q1; Q3]	M±SD Me [Q1; Q3]
Age, years	55.68±9.8 49 [58;73]	54.9±10.3 31 [54;72]	56.3±9.3 26[59;73]
AH duration, years	10.7±6.6 5 [10;44]	11.2±7.9 1 [10;44]	10.28±5.2 1 [10;26]
BMI (kg/m^2)	32.3±5.07 22.8 [32;46]	32.9±5.2 22.1 [32.7;44.2]	31.7±4.9 16.7 [31.3;46.8]
SBP, mmHg	171.06±17.7 160 [170;240]	171.3±17.2 140 [170;240]	170.7±18.2 140 [170;240]
DBP, mmHg	100.06±8.7 100 [100;140]	100.8±8.2 80 [100;140]	99.38±9.2 65 [100;140]
MBP, mmHg	122.9±9.9 120 [123;173]	122.6±8.6 106.6 [123.3;150]	123.2±11 98.3 [123.3;73.3]
PWV, m/sec	10.9±2.4 9.4 [10.8;22.8]	10.8±2.4 6.4 [10.5;19.2]	11±2.4 7 [11;22.8]
LVMI, g/m^2	139.9±32.8 136.8 [117.2;237.6]	139.19±32.7 136.6 [116,8;208.6]	140.8±32.9 137.9 [121;237.6]
CIMT, mm	1.027±0.19 1 [0.9;1.5]	1.02±0.19 1 [0.7;1.5]	1.03±0.19 1 [0.5;1.5]
FBG, mmol/L	6.14±2.29 5 [5.4;16.5]	6.28±2.5 4.1 [5.4;15.6]	6.01±2.06 4.2 [5.4;16.5]
Creatinine, µmol/L	94.5±22.2 79 [92;207]	93.79±23.6 51 [91;207]	95.2±21.02 51 [95;144]
eGFR mL/min/1.73m^2	70.25±17.1 57.15 [67.4;120.68]	73.1±17.58 28 [70;112.35]	67.66±16.4 34.8 [64;120.68]
MAU, mg/24-h	43.6±42.06 29.8 [15.1;218.8]	45.7±41.5 32.5 [16.2;212.8]	41.4±42.4 25.4 [14.7;200.0]
Uric acid, mg/dL	6.25±1.65 5.1 [6.2;11.2]	6.15±1.4 3.1 [6.2;9.4]	6.35±1.8 2.6 [6.2;11.2]
TC, mg/dL	205±47.8 169 [205;364]	202.96±47.9 97 [207;321]	202.96±47.9 102 [203;364]
TG, mg/dL	166.8±83.2 105.25 [151;407]	164.87±82.6 60 [143.5;402]	168.2±83.8 6.7 [157;407]
LDL-C, mg/dL	122.02±43.6 100 [123;274]	122.13±46.4 5 [124;246]	121.7±41.2 29 [122;274]
HDL-C, mg/dL	44.26±11.1 37 [43;97]	44.35±11.9 24 [43;97]	44.16±10.3 24 [43;80]
Atherogenic index	3.64±1.16 3 [3.4;7.1]	3.67±1.25 2 [3.4;7.1]	3.60±1.08 2 [3.4;6.9]

Against a background of 24-week treatment, the obtained indicators in 2 modes of triple combined AHT were analyzed comparatively. A highly significant reduction in BP using different types of measurements was obtained in both groups (Table 3).

Table 3.

BP parameters after 24 weeks of AHT in the study groups.

Variable	Group	Initial data	After 24-week AHT	P_1	P_2	P_3
SBP, mmHg	1	171.3±17.2	121.95±6.7	0.0001	NS	0.0001
	2	170.7±18.2	128.38±8.5	0.0001		
DBP, mmHg	1	100.8±8.2	77.23±5.59	0.0001	NS	0.0001
	2	99.38±9.2	80.89±6.38	0.0001		
MBP, mmHg	1	122.64±8.92	92.23±5.47	0.0001	NS	0.0001
	2	123.53±10.59	96.72±6.18	0.0001		
Average 24-h SBP, mmHg	1	147.23±15.37	124.53±9.64	0.0001	NS	NS
	2	145.98±20.24	127.2±13.03	0.0001		
Average 24-h DBP, mmHg	1	89.01±11.34	75.77±6.11	0.0001	NS	NS
	2	88.86±14.26	77.74±11.13	0.0001		
Average daytime SBP, mmHg	1	149.24±15.26	126.89±10.2	0.0001	NS	NS
	2	147.38±20.33	129.22±13.65	0.0001		
Average daytime DBP, mmHg	1	90.49±11.45	77.61±6.84	0.0001	NS	NS
	2	89.98±14.08	79.86±11.89	0.0001		
Average nighttime SBP, mmHg	1	141.03±20.32	118.28±10.24	0.0001	NS	0.017
	2	141.76±23.53	123.12±15.32	0.0001		
Average nighttime DBP, mmHg.	1	84.49±13.66	70.01±7.86	0.0001	NS	NS
	2	85.4±16.81	73.12±11.63	0.0001		
Average 24-h SBPV, mmHg	1	17.66±4.36	14.46±3.7	0.0001	NS	NS
	2	18.32±5.37	15.34±3.45	0.0001		
Average 24-h DBPV, mmHg	1	13.66±3.74	12.32±3.69	0.032	NS	NS
	2	13.27±3.69	12.78±3.43	NS		
Average daytime SBPV, mmHg	1	16.88±4.86	13.81±3.84	0.0001	NS	NS
	2	17.27±6.1	14.83±4.06	0.0001		
Average daytime DBPV, mmHg	1	13.28±4.18	11.73±3.93	0.023	NS	NS
	2	12.83±4.11	12.34±3.64	NS		
Average nighttime SBPV, mmHg	1	15.9±4.93	13.27±4.67	0.044	NS	NS
	2	16.06±5.52	13.22±4.06	0.006		
Average nighttime DBPV, mmHg	1	11.1±3.66	11.12±4.74	NS	NS	NS
	2	12.18±7.4	10.84±4.46	NS		
Daytime SBP load, %	1	64.87±27.2	20.06±23.31	0.0001	NS	0.021
	2	56.18±27.61	30.16±28.28	0.0001		
Daytime DBP load, %	1	49.86±29.6	15.56±16.09	0.0001	NS	0.005
	2	47.04±31.83	26.0±26.65	0.0001		
Nighttime SBP load, %	1	79.34±25.74	25.69±17.38	0.0001	NS	0.0001
	2	77.54±26.14	57.45±34.36	0.0001		
Nighttime DBP load, %	1	59.16±31.64	23.49±20.17	0.0001	NS	0.015
	2	59.64±34.54	34.96±33.69	0.0001		
Nocturnal SBP fall, %	1	5.53±9.65	6.64±7.28	NS	NS	NS
	2	3.41±8.68	4.89±8.89	NS		
HR, bpm	1	82.8±10.59	70.47±8.85	0.0001	NS	NS
	2	78.96±9.07	69.19±6.6	0.0001		

P_1 – between initial data and data after 24-week AHT; P_2 – between Groups 1 and 2 for initial data; P_3 – between Groups 1 and 2 for data after 24-week AHT

However, the reduction percentage in SBP and DBP was significantly more pronounced in Group 1 than in Group 2 (ΔSBP: -27.76±5.95% versus -24.46±9.85% (*P*=0.024); ΔDBP%: -22.61±6.87% versus -18.1±10.17% (*P*=0.004); Δ MAD: -24.47±5.27% versus -21.23±8.52% (*P*=0.011)). TBP of <140/90 mmHg was reached by 94.4% of patients in Group 1 and 83.3% in Group 2 (χ^2=7.471, *P*=0.006). TBP of <130/80 mmHg was reached by 70% of patients in Group 1 and 42% in Group 2 (χ^2=11.61, *P*=0.0001).

A significant improvement in the diurnal BP profile was also revealed during treatment. According to ABPM data, both groups achieved TBP in terms of the average 24-h and average daytime SBP and DBP. Regarding average nighttime SBP and DBP and normalization of average nighttime diastolic BP variability, target values were achieved only in Group 1 (*P*=0.028).

A significant decrease in daytime/nighttime SBP load and DBP load was noted in both groups, but it was more pronounced in Group 1 (Table 3) with the achievement of standard values, which is associated with the possibility of protecting target organs.

One of the important markers of vascular damage in hypertension is indicators of central BP (SBPc, DBPc, and PPc) and PWV. In both groups, 24-week triple-combination therapy led to a significant decrease in SBPc, DBPc, and PWV. At the same time, the positive dynamics of SBPc were more pronounced in Group 1 than in Group 2 (Table 4), and PWV in Group 1 reached standard values.

Table 4.

Indicators of central BP and PWV after 24 weeks of AHT in the study groups.

Variable	Group	Initial data	After 24-week AHT	P_1	P_2	P_3
SBPc, mmHg	1	161.85±21.55	134.27±12.84	0.0001	NS	0.027
	2	156.77±18.75	139.66±17.98	0.0001		
DBPc, mmHg	1	91.78±12.32	80.9±8.11	0.0001	NS	NS
	2	88.16±12.5	82.54±10.5	0.0001		
PPc, mmHg	1	72.36±20.67	54.29±13.21	0.0001	NS	NS
	2	70.77±18.7	56.24±16.43	0.0001		
PWV, m/sec	1	10.86±2.53	8.49±2.02	0.0001	NS	0.028
	2	10.9±2.56	9.2±2.12	0.0001		

P_1 – between initial data and data after 24-week AHT; P_2 – between Groups 1 and 2 for initial data; P_3 – between Groups 1 and 2 for data after 24-week AHT

In general, the 2-treatment regimens were well tolerated; only 1 patient from Group 2 reported swelling of the ankles after 12 weeks of therapy.

Discussion

Despite the widespread availability of effective antihypertensive drugs, most AH patients remain uncontrolled and do not reach the TBP. Non-compliance with pharmacotherapy is an important reason for poor BP control. According to the results of studies conducted in recent years, only ~40% of AH patients receive AHT, of which only ~10%-35% achieve the TBP of <140/90 mmHg, which is clear evidence of unsatisfactory control of hypertension.[6] Uncontrolled hypertension increases the risk of all-cause and cardiovascular mortality. A review of 28 studies in 15 countries found that 45.2% of AH patients were not taking medications, and 83.7% had uncontrolled hypertension.[7] Achieving TBP in the short term is the goal of therapy and may lead to improved cardiovascular outcomes. Clinical studies have shown that BP can be adequately controlled with a combination of up to 4 antihypertensive drugs.[8] In AH persons with high cardiovascular risk, it is recommended that combined AHT be initiated and doses titrated rapidly.[9] In cases of resistance to the dual combination of AHT, the most appropriate is a triple combination of AHT.

Studies have shown that, compared with dual-component therapy, triple AHT provides better BP control and significantly reduces cardiovascular complications.[10,11] At the same time, a fixed combination allows one to achieve goals faster and improve treatment adherence than a free combination of drugs.[10-13] Triple combinations, namely an ACEI, a CCB, and a diuretic, optimally control hypertension with fewer dose-related side effects.[9-13] In addition, when combined, each component can reduce the adverse effects of other components.[14] A recent meta-analysis of 44 studies compared a fixed combination of AHT with a free combination of AHT.[14,15] In this study, patients receiving fixed-dose combination therapy had significant reductions in SBP and DBP after 12 weeks of follow-up, as well as positive effects on PP and improved adherence to treatment, resulting in better BP control.

The PETRA study (n=11209) showed that a 3-month fixed antihypertensive combination of perindopril/indapamide/amlodipine was sufficient to achieve TBP at the lowest doses in almost half of all enrolled patients.[16] In addition, the fixed combination has a good effect on vascular stiffness parameters, which leads to improved microcirculation and a reduction in cardiovascular complications. The combination of perindopril/indapamide/amlodipine reduces the glomerular filtration rate and MAU in AH patients, promoting nephroprotection.[13,16,17] The high antihypertensive and organ-protective effectiveness of the fixed triple combinations (perindopril/indapamide/amlodipine) was shown in the PETRA, TRIO, PIONIST, TRICOLOR, and PAINT studies.[16-20]

Our previous study[21] demonstrated the achievement of a TBP <140/90 mmHg in more than 92% of patients with uncontrolled hypertension on 24-week therapy with SPTC (perindopril/indapamide/amlodipine and telmisartan/hydrochlorothiazide/amlodipine); TBP <130/80 mmHg was achieved in more than 82% of patients. In the present study, the primary TBP was achieved in 94.4% of patients in the SPTC group. The recommended TBP <130/80mmHg was achieved in 70% of patients treated with an SPTC and 42% of patients receiving a separate combination of perindopril/indapamide/amlodipine. Such different percentages of patients achieving

TBP are explained by differences in AH patient samples. The present study included patients with a longer duration of hypertension, higher SBP values, and a higher incidence of coronary artery disease than in the previous work.

A recent population-based retrospective cohort study found that the primary outcome (death or hospitalization for acute myocardial infarction or stroke) was lower in patients receiving SPTC.[7] SPTC (perindopril/indapamide/amlodipine) is more economical than the free-dose combination of perindopril/indapamide/amlodipine.[22] Although several studies have been conducted on combination AHT, comparing fixed-dose and free-dose combination therapy still requires more research.[23]

AH patients often have comorbidities that require multiple medications, so SPTC therapy may help overcome this problem, reduce dosing complexity, and improve treatment efficacy.[14] According to the WHO Quality-of-Life Scale (WHOQOL-BREF), patients receiving the perindopril/indapamide/amlodipine in SPTC significantly improved their quality of life compared to patients receiving the free-dose combination.[13] In another study, SPTC showed significant control of depression and effective control of BP.[13,24]

Thus, studies have shown that one-third of AH patients require 3 AHDs to control BP. Inadequate doses of drugs, irrational combinations, complex treatment regimens, and many pills reduce treatment adherence, leading to poor BP control. Reducing the burden of taking pills using SPTC and subsequently switching to polypill, with the addition of a statin and/or acetylsalicylic acid, will allow achieving the TBP and reducing cardiovascular risk.[2]

The results of our study showed that in the treatment of uncontrolled hypertension on previous therapy in AH patients with high cardiovascular risk, an SPTC of the ACEI perindopril, the CCB amlodipine, and the thiazide-like diuretic indapamide contributed to the effective daily BP control, the improvement of diurnal BP profile, and a positive effect on central BP and PWV, thereby having a positive impact on the prognosis and quality of life of AH patients with high cardiovascular risk.

Ethical Considerations

The study protocol was reviewed and approved by the Ethics Committee of the Republican Specialized Centre of Cardiology. All participants provided written informed consent.

Competing Interests

The authors declare that they have no competing interests.

References

1. Williams B, Mancia G, Spiering W, Agabiti Rosei E, Azizi M, Burnier M, Clement DL, Coca A, de Simone G, Dominiczak A, Kahan T, Mahfoud F, Redon J, Ruilope L, Zanchetti A, Kerins M, Kjeldsen SE, Kreutz R, Laurent S, Lip GYH, McManus R, Narkiewicz K, Ruschitzka F, Schmieder RE, Shlyakhto E, Tsioufis C, Aboyans V, Desormais I; ESC Scientific Document Group. 2018 ESC/ESH Guidelines for the management of arterial hypertension. Eur Heart J. 2018 Sep 1;39(33):3021-3104. doi: 10.1093/eurheartj/ehy339. Erratum in: Eur Heart J. 2019 Feb 1;40(5):475. PMID: 30165516.

2. Mancia G, Kreutz R, Brunström M, Burnier M, Grassi G, Januszewicz A, et al. SE. 2023 ESH Guidelines for the management of arterial hypertension The Task Force for the management of arterial hypertension of the European Society of Hypertension: Endorsed by the International Society of Hypertension (ISH) and the European Renal Association (ERA). J Hypertens. 2023 Dec 1;41(12):1874-2071. doi: 10.1097/HJH.0000000000003480. Epub 2023 Sep 26. Erratum in: J Hypertens. 2024 Jan 1;42(1):194.

3. Thoenes M, Neuberger HR, Volpe M, Khan BV, Kirch W, Böhm M. Antihypertensive drug therapy and blood pressure control in men and women: an international perspective. J Hum Hypertens. 2010 May;24(5):336-44. doi: 10.1038/jhh.2009.76. Epub 2009 Oct 1. PMID: 19798089.

4. Berlowitz DR, Foy CG, Kazis LE, Bolin LP, Conroy MB, Fitzpatrick P, Gure TR, Kimmel PL, Kirchner K, Morisky DE, Newman J, Olney C, Oparil S, Pajewski NM, Powell J, Ramsey T, Simmons DL, Snyder J, Supiano MA, Weiner DE, Whittle J; SPRINT Research Group. Effect of Intensive Blood-Pressure Treatment on Patient-Reported Outcomes. N Engl J Med. 2017 Aug 24;377(8):733-744. doi: 10.1056/NEJMoa1611179. PMID: 28834483; PMCID: PMC5706112.

5. Wright JT Jr, Whelton PK, Johnson KC, Snyder JK, Reboussin DM, Cushman WC, Williamson JD, Pajewski NM, Cheung AK, Lewis CE, Oparil S, Rocco MV, Beddhu S, Fine LJ, Cutler JA, Ambrosius WT, Rahman M, Still CH, Chen Z, Tatsuoka C; SPRINT Research Group. SPRINT Revisited: Updated Results and Implications. Hypertension. 2021 Dec;78(6):1701-1710. doi: 10.1161/HYPERTENSIONAHA.121.17682. Epub 2021 Nov 10. PMID: 34757768; PMCID: PMC8824314.

6. Chow CK, Teo KK, Rangarajan S, Islam S, Gupta R, Avezum A, Bahonar A, Chifamba J, Dagenais G, Diaz R, Kazmi K, Lanas F, Wei L, Lopez-Jaramillo P, Fanghong L, Ismail NH, Puoane T, Rosengren A, Szuba A, Temizhan A, Wielgosz A, Yusuf R, Yusufali A, McKee M, Liu L, Mony P, Yusuf S; PURE (Prospective Urban Rural Epidemiology) Study investigators. Prevalence, awareness, treatment, and control of hypertension in rural and urban communities in high-, middle-, and low-income countries. JAMA. 2013 Sep 4;310(9):959-68. doi: 10.1001/jama.2013.184182.

7. Abegaz TM, Shehab A, Gebreyohannes EA, Bhagavathula AS, Elnour AA. Nonadherence to antihypertensive drugs: A systematic review and meta-analysis. Medicine (Baltimore). 2017 Jan;96(4):e5641. doi: 10.1097/MD.0000000000005641. PMID: 28121920; PMCID: PMC5287944.

8. Bramlage P, Böhm M, Volpe M, Khan BV, Paar WD, Tebbe U, Thoenes M. A global perspective on blood pressure treatment and control in a referred cohort of hypertensive patients. J Clin Hypertens (Greenwich). 2010 Sep;12(9):666-77. doi: 10.1111/j.1751-7176.2010.00322.x. PMID: 20883226.

***Corresponding author**: Prof. Gulnoz A. Khamidullaeva, PhD, ScD. The Republican Specialized Center of Cardiology, Tashkent, Uzbekistan. E-mail: gulnoz0566@mail.ru*

9. Stafylas P, Kourlaba G, Hatzikou M, Georgiopoulos D, Sarafidis P, Maniadakis N. Economic evaluation of a single-pill triple antihypertensive therapy with valsartan, amlodipine, and hydrochlorothiazide against its dual components. Cost Eff Resour Alloc. 2015 Jun 9;13:10. doi: 10.1186/s12962-015-0036-x. PMID: 26097434; PMCID: PMC4474457.
10. Chalmers J, Arima H, Woodward M, Mancia G, Poulter N, Hirakawa Y, Zoungas S, Patel A, Williams B, Harrap S. Effects of combination of perindopril, indapamide, and calcium channel blockers in patients with type 2 diabetes mellitus: results from the Action In Diabetes and Vascular Disease: Preterax and Diamicron Controlled Evaluation (ADVANCE) trial. Hypertension. 2014 Feb;63(2):259-64. doi: 10.1161/HYPERTENSIONAHA.113.02252. Epub 2013 Dec 9. Erratum in: Hypertension. 2015 Jul;66(1):e2. PMID: 24324048.
11. Yamout H, Bakris GL. Evidence-based triple antihypertensive therapy yields lower mortality in older patients with diabetes mellitus. Hypertension. 2014 Feb;63(2):220-1. doi: 10.1161/HYPERTENSIONAHA.113.02659. Epub 2013 Dec 9. PMID: 24324049.
12. Mahfoud F, Kieble M, Enners S, Kintscher U, Laufs U, Böhm M, Schulz M. Use of fixed-dose combination antihypertensives in Germany between 2016 and 2020: an example of guideline inertia. Clin Res Cardiol. 2023 Feb;112(2):197-202. doi: 10.1007/s00392-022-01993-5. Epub 2022 Feb 27. PMID: 35220445; PMCID: PMC9898344.
13. Syed YY. Perindopril/Indapamide/Amlodipine in Hypertension: A Profile of Its Use. Am J Cardiovasc Drugs. 2022 Mar;22(2):219-230. doi: 10.1007/s40256-022-00521-0. Epub 2022 Mar 8. Erratum in: Am J Cardiovasc Drugs. 2022 May;22(3):355. PMID: 35257306; PMCID: PMC8964631.
14. Nedogoda SV, Stojanov VJ. Single-Pill Combination of Perindopril/Indapamide/Amlodipine in Patients with Uncontrolled Hypertension: A Randomized Controlled Trial. Cardiol Ther. 2017 Jun;6(1):91-104. doi: 10.1007/s40119-017-0085-7. Epub 2017 Feb 8. PMID: 28181192.
15. Burnier M, Redon J, Volpe M. Single-Pill Combination with Three Antihypertensive Agents to Improve Blood Pressure Control in Hypertension: Focus on Olmesartan-Based Combinations. High Blood Press Cardiovasc Prev. 2023 Mar;30(2):109-121. doi: 10.1007/s40292-023-00563-8. Epub 2023 Jan 25. PMID: 36696054; PMCID: PMC10090015.
16. Ábrahám G, Dézsi CA. The Antihypertensive Efficacy of the Triple Fixed Combination of Perindopril, Indapamide, and Amlodipine: The Results of the PETRA Study. Adv Ther. 2017 Jul;34(7):1753-1763. doi: 10.1007/s12325-017-0572-1. Epub 2017 Jun 23. PMID: 28646394.
17. Mareev VY, Minina YV, Begrambekova YL, Levin AM. [Therapeutic approaches to the Rational Use of triple combination therapy with a fixed combination of amlodipine, indapamide and perindopril arginine (TRIPLE COMBINATION) in patients with hypertension who do not control blood pressure on conventional treatment. (Description and main results of the TRIO program)]. Kardiologiia. 2020 Jun 3;60(5):1149. Russian. doi: 10.18087/cardio.2020.5.n1149.
18. Tóth K; PIANIST Investigators. Antihypertensive efficacy of triple combination perindopril/indapamide plus amlodipine in high-risk hypertensives: results of the PIANIST study (Perindopril-Indapamide plus AmlodipiNe in high rISk hyperTensive patients). Am J Cardiovasc Drugs. 2014 Apr;14(2):137-45. doi: 10.1007/s40256-014-0067-2. Erratum in: Am J Cardiovasc Drugs. 2014 Jun;14(3):239. PMID: 24590580.
19. Logunova N, Khomitskaya Y, Karpov Y, et al. Antihypertensive efectiveness and tolerability of perindopril/indapamide/amlodipine triple single-pill combination in the treatment of patients with arterial hypertension (TRICOLOR). J Hypertens. 2021;39(Suppl 1): e373.
20. Páll D, Szántó I, Szabó Z. Triple combination therapy in hypertension: the antihypertensive efficacy of treatment with perindopril, amlodipine, and indapamide SR. Clin Drug Investig. 2014 Oct;34(10):701-8. doi: 10.1007/s40261-014-0223-0. PMID: 25212574.
21. Masharipov Sh, Ataniyazov Kh, Shukurova D, Khamidullaeva G, Abdullaeva G, Kurbanov R. The Effectiveness of the Triple Fixed-Dose Combination Therapy in the Management of Uncontrolled Arterial Hypertension. International Journal of Biomedicine. 2020;10(4):334-341. doi: 10.21103/Article10(4)_OA1
22. Mbanya A, Ackbarkhan A, Mittoo MY, Ramamonjisoa HA, Ramilitiana B, Ranivoharisoa EM, Ratsimbazafy SJN, Mbanya JC. Use of Perindopril Arginine/Indapamide/Amlodipine in the Management of Hypertension in Two Sub-Saharan African Island Countries of Madagascar and Mauritius. Adv Ther. 2022 Jun;39(6):2850-2861. doi: 10.1007/s12325-022-02134-0. Epub 2022 Apr 18. PMID: 35438448;
23. Mazza A, Lenti S, Schiavon L, Sacco AP, Dell'Avvocata F, Rigatelli G, Ramazzina E. Fixed-Dose Triple Combination of Antihypertensive Drugs Improves Blood Pressure Control: From Clinical Trials to Clinical Practice. Adv Ther. 2017 Apr;34(4):975-985. doi: 10.1007/s12325-017-0511-1. Epub 2017 Mar 15. PMID: 28299716.
24. Larina V, Orlov D, Litvin A. Efectiveness of a fxed combination of three antihypertensive drugs in outpatients with hypertension. J Hypertens. 2019;37(Suppl 1): e250.

International Journal of Biomedicine 14(2) (2024) 260-264
http://dx.doi.org/10.21103/Article14(2)_OA3

ORIGINAL ARTICLE

Neurology

INTERNATIONAL JOURNAL OF BIOMEDICINE

Investigating the Role of Serum Hepcidin and Interleukin-6 in Non-Anemic Women with Acute Ischemic Stroke

Zahir Hussain*

Department of Physiology, Faculty of Medicine, Umm Al-Qura University
Makkah, Saudi Arabia

Abstract

Background: Hepcidin (HP) is an important regulator of iron homeostasis. Iron status and IL-6 have been shown to regulate the expression of HP. Serum iron (SI), HP, and IL-6 have a highly significant role in inflammation since inflammation elevates the levels of HP for expressing the ischemic condition. The present study was carried out to investigate the impact of an interactive association between HP, SI, and IL-6 in non-anemic women with acute ischemic stroke (AIS).

Methods and Results: The present case-control, descriptive study comprised 25 non-anemic women with AIS and 25 healthy non-anemic women controls. The age range of AIS and control subjects was 50 to 54 years. Non-anemic AIS women within 8 hours after AIS onset (AIS<8 hrs) and 72 hours after onset of AIS (AIS-72 hours) were examined. The patients underwent assessment of traditional risk factors, physical examination, CBC, blood biochemistry test, 12-lead ECG, CT scans, MRI, CT or MR angiogram, carotid ultrasound of the arteries, transcranial doppler ultrasound, and EEG. Office blood pressure was measured using a mercury sphygmomanometer. Significantly increased values were obtained for systolic blood pressure and diastolic blood pressure in AIS women, compared to the control subjects: 137.44±12.35 vs. 130.88±7.30 mmHg (P=0.0267) and 86.72± 8.48 vs. 81.80± 5.42 mmHg (P=0.0183), respectively. Serum C-reactive protein and low-density lipoprotein cholesterol levels in AIS were significantly higher than in healthy control women (P<0.0001).

A significant increase in serum HP, SI, and IL-6 for AIS<8 hrs was found, compared to AIS-72 hrs (P<0.001 in all cases). Comparison for AIS<8 hrs vs. controls showed a highly significant increase in serum HP, SI, and IL-6 for AIS<8 hrs (P<0.001 in all cases). On the other hand, AIS-72 hrs vs. controls indicated a significant increase in SI (P=0.0028) and IL-6 (P=0.0065) but a non-significant increase in serum HP (P>0.05) in AIS-72 hrs. Linear regression expressed a high strength of the relationship between serum HP and SI for AIS<8 hrs (R^2=0.82, P<0.0001) and AIS-72 hrs (R^2=0.73, P<0.0001), but a negligible linear association for controls (R^2=0.01, P=0.5990). There was a high relationship between HP and IL-6 for AIS<8 hrs (R^2=0.67, P<0.0001) and AIS-72 hrs (R^2=0.67, P<0.0001), but a small linear association for controls (R^2=0.28, P=0.0063). The R^2 value of 0.47 (P<0.0002) and 0.42 (P<0.0004) was found between SI and IL-6 for AIS<8 hrs and AIS-72 hrs, and a negligible linear association (R^2=0.006, P=0.7250) for controls.

Conclusion: The present study provides evidence of the association of AIS in non-anemic women with increased hepcidin. The interactive pathophysiological role of HP, IL-6, and SI in non-anemic women with AIS has also been shown.**(International Journal of Biomedicine. 2024;14(2):260-264.)**

Keywords: acute ischemic stroke • non-anemic women • hepcidin • serum iron • interleukin-6

For citation: Hussain Z. Investigating the Role of Serum Hepcidin and Interleukin-6 in Non-Anemic Women with Acute Ischemic Stroke. International Journal of Biomedicine. 2024;14(2):260-264. doi:10.21103/Article14(2)_OA3

Abbreviations

AIS, acute ischemic stroke; **BMI**, body mass index; **BP**, blood pressure; **CBC**, complete blood count; **CKD**, chronic kidney disease; **CRP**, C-reactive protein; **CT**, computed tomography; **DBP**, diastolic blood pressure; **ELISA**, enzyme-linked immunosorbent assay **Hb**, hemoglobin; **HDL-C**, high density lipoprotein cholesterol; **HP**, hepcidin; **IL-6**, interleukin-6 **IS**, ischemic stroke; **LDL-C**, low-density lipoprotein cholesterol; **MRI**, magnetic resonance imaging; **SBP**, systolic blood pressure; **SI**, serum iron.

Introduction

Stroke is one of the leading causes of disability and death in adults[1] suffering from diabetes, heart disease, hypertension, and chronic kidney disease.[2,3] Despite enormous research that has been conducted, an incomplete understanding of the pathophysiology of stroke is the one main barrier limiting the research progress.

The majority of stroke cases (about 90%) are ischemic.[4] Several conditions or risk factors[5] predisposing to ischemic stroke (IS) include high blood pressure (BP), high cholesterol levels, and cardiovascular diseases, among other causes. Patients with acute ischemic stroke (AIS) present with the most common symptoms of the sudden occurrences of abnormal functions and deficits in the nervous system, making it harder to diagnose during the initial 24 hours properly. The AIS is caused by sudden obstruction or blockage of arteries by a thrombus or embolus and leads to almost immediate loss of oxygen and glucose supply to the brain. It causes irreparable neuronal damage within just a few minutes after onset.

The symptoms of IS progress swiftly in just a few hours.[6] A transient ischemic attack is considered at least one risk factor.[7] Several of the risk factors can be managed by changing lifestyle activities, including mainly the control of high BP, high cholesterol levels, heart disease, diabetes, and smoking.[8]

Iron status is suggested as one major factor or cause involved in the occurrence and progression of various diseases.[9-12] Hepcidin (HP), produced in the liver, is a factor associated with iron status. It is the main antimicrobial regulatory hormone/peptide for iron metabolism.[13] In association with IL-6 and other inflammatory cytokines, HP has been recognized as having a significant involvement in the homeostasis of systemic iron, and it serves as a bridge or link between iron regulation and inflammation.[4]

Iron status and IL-6 have been shown to regulate the expression of HP.[14] Serum iron (SI), HP, and IL-6 have a highly significant role in inflammation since inflammation elevates the levels of HP for expressing the ischemic condition.[15]

Several therapeutic products have been introduced in the past decade to reduce the disability and death associated with stroke. Still, only a little progress has been made in understanding the neuronal mechanisms involved.[15,16]

Despite the mentioned reports providing evidence for the role of HP in stroke patients, serum levels of HP in association with IL-6 and SI are still not known. Hence, the present study was carried out to investigate the impact of an interactive association between HP, SI, and IL-6 in non-anemic women with AIS. It is hoped that further research may clarify the role of HP in AIS prognosis and therapeutic approaches.[17,18]

Materials and Methods

The present case-control, descriptive study comprised 25 non-anemic women with AIS and 25 healthy non-anemic women controls. The age range of AIS and control subjects was 50 to 54 years. Baseline characteristics of the subjects are presented in Table 1. A detailed questionnaire was prepared to contain information about clinical, biochemical, and hematological estimations. After obtaining ethical approval, the research was carried out in affiliated hospitals from January 2022 to January 2023. The consent of the women patients and healthy women subjects was obtained before the start of the consultation. The subjective and objective information for AIS patients and control subjects was obtained following the regulations and guidelines of the Biomedical Ethics Committee.

The present work is the next step to our previous study.[19] For the present study, the specialist neurologists and other medical experts helped in the differential diagnosis of patients with AIS, using CT scans, MRI, CT or MR angiogram, carotid ultrasound of the arteries, transcranial doppler (TCD) ultrasound, EEG, and other techniques. The data for the present report was collected from properly diagnosed patients with AIS. Blood tests were CBC, coagulation, blood glucose, blood protein, C-reactive protein (CRP), cholesterol, serum electrolytes, and other lab tests (Table 1).

The subjects (normal control and AIS subjects) selected for the present report had a normal range BMI of 18.5 to <25 kg/m^2 for the healthy Saudi population.[20] BMI was calculated as weight (kg) divided by height (m) squared.[21] Hence, the patients and healthy control subjects with higher or lower BMI values than the mentioned levels were not included in the present work.

Iron status was defined properly,[22] and the AIS and control subjects without anemia were included in the present study, following the definition of anemia as Hb<12 g/dL.[23,24] According to ACC/AHA, SBP/DBP below 120/80 mmHg was considered normal, and SBP/DBP ≥130/80 mmHg was considered hypertension.[25] Office blood pressure was measured using a mercury sphygmomanometer.[26] The subjects with hypotension and hypertension stage 2 were not included in the study.

The SI, IL-6, HP, HDL-C, and LDL-C levels were measured. The ELISA method was used to determine serum IL-6, SI, and HP, and a fully automated method was employed to measure serum HDL-C and LDL-C. [27,28]

A comprehensive analysis was conducted using GraphPad Prism (version 6.0) software, San Diego, CA, USA. For the descriptive analysis, results are presented as mean (M) ± standard deviation (SD). Student's unpaired and paired t-tests were used to compare two groups for data with normal distribution. The one-way analysis of variance (ANOVA) and related Tukey-Kramer post-hoc test was carried out. The coefficient of determination R^2 was estimated to measure the strength of the linear relationship. A probability value of $P<0.05$ was considered statistically significant. The results were compared and analyzed statistically following general statistical principles/concepts.[29]

Results

The age, Hb, and HDL-C in the women patients with AIS did not differ significantly from the healthy control subjects (Table 1). However, significantly increased values were obtained for SBP ($P=0.0267$) and DBP ($P=0.0183$) in

AIS women, compared to the control subjects. Serum CRP and LDL-C levels in AIS were significantly higher than in healthy control women (P<0.0001).

Table 1.

Baseline characteristics of the study participants

Baseline characteristics	Serum levels (mean ± SD)		t-value	*P*-value
	AIS (n = 25)	C (n = 25)		
Age (years)	52.72±1.07	52.34±1.44	1.08	0.2847
SBP (mmHg)	137.44±12.35	130.88±7.30	2.29	0.0267
DBP (mmHg)	86.72±8.48	81.80±5.42	2.44	0.0183
Hb (g/dL)	13.67±1.15	13.31±1.09	1.13	0.2621
CRP (mg/dL)	9.58±1.26	3.49± 0.97	19.15	<0.0001
HDL-C (mg/dL)	55.71±7.08	57.42±5.88	0.93	0.360
LDL-C (mg/dL)	111.85±17.17	95.47±6.40	4.47	<0.0001

A significant increase in serum HP, SI, and IL-6 for AIS<8 hrs was found, compared to AIS-72 hrs (P<0.001 in all cases) (Table 2) Comparison for AIS<8 hrs vs. controls showed a highly significant increase in serum HP, SI, and IL-6 for AIS<8 hrs (P<0.001 in all cases). On the other hand, AIS-72 hrs vs. controls indicated a significant increase in SI (P=0.0028) and IL-6 (P=0.0065) but a non-significant increase in serum HP (P>0.05) in AIS-72 hrs (Table 2).

One-way analysis of variance (ANOVA) for serum HP, IL-6, and iron in women with AIS (AIS<8 hrs and AIS-72 hrs) and healthy women controls showed a highly significant difference (P<0.0001, Table 3).

The coefficient of determination (R^2) was estimated to measure the strength of the linear relationship (Table 4). The strength of the relationship between serum HP and SI for AIS<8 hrs (R^2=0.82, P<0.0001) and AIS-72 hrs (R^2=0.73, P<0.0001) was high, but a negligible linear association for controls (R^2=0.01, P=0.5990). There was a high relationship between HP and IL-6 for AIS<8 hrs (R^2=0.67, P<0.0001) and AIS-72 hrs (R^2=0.67, P<0.0001), but a small linear association for controls (R^2=0.28, P=0.0063). The R^2 value of 0.47 (P<0.0002) and 0.42 (P<0.0004) was found between SI and IL-6 for AIS<8 hrs and AIS-72 hrs, and a negligible linear association (R^2=0.006, P=0.7250) for controls.

Table 3.

One-way ANOVA for serum hepcidin, IL-6, and iron in women with AIS (AIS < 8 hrs and AIS-72 hrs) and control women.

Variables	One-way ANOVA*	
	F	*P*
Serum HP (ng/ml)	11.028	<0.0001
Serum iron (µg/dL)	19.629	<0.0001
Serum IL-6 (pg/ml)	23.556	<0.0001

** - Tukey-Kramer post-hoc test indicates a highly significant difference for the comparisons for AIS< 8 hrs and AIS-72 hrs.*

Table 4.

The strength of the relationship between serum hepcidin, IL-6 and iron in women with AIS and control.

Variables			R^2	*P*-value
HP and SI	AIS	AIS < 8 hrs	0.8242	<0.0001
		AIS-72 hrs	0.7341	<0.0001
	C		0.0122	0.5990
HP and IL-6	AIS	AIS < 8 hrs	0.6692	<0.0001
		AIS-72 hrs	0.6778	<0.0001
	C		0.2820	0.0063
SI and IL-6	AIS	AIS < 8 hrs	0.4680	<0.0002
		AIS-72 hrs	0.4230	>0.0004
	C		0.0055	0.7250

C - control; R^2 - coefficient of determination.

Table 2.

Serum hepcidin, IL-6, and iron in women with acute ischemic stroke.

Variables	Serum levels and statistical analysis								
	AIS				C	AIS vs. C			
	AIS < 8 hrs	AIS-72 hrs	AIS < 8 hrs vs. AIS-72 hrs			AIS < 8 hrs vs. C		AIS-72 hrs vs. C	
			t*	*P*		t**	*P*	t**	*P*
Serum HP (ng/ml)	28.01±13.78	18.63±10.53	8.88	<0.0001	13.92±7.00	4.56	<0.0001	1.86	0.0684
SI (µg/dL)	122.12± 31.88	96.21± 25.46	12.64	<0.0001	76.20±19.00	6.19	<0.0001	3.15	0.0028
Serum IL-6 (pg/ml)	16.21± 7.07	9.66± 3.98	9.14	<0.0001	7.10± 2.13	6.17	<0.0001	2.85	0.0065

**- paired t-test; ** - unpaired t-test; C - control.*

Discussion

Inflammation increases the HP level and may express the ischemic condition [14,30] that has been confirmed in the present study. Elevated levels of free SI have also been documented in IS, though its mechanism is unclear.[31] The present study confirms the increased levels of SI in non-anemic women with AIS.

Another important factor related to inflammation is IL-6. It is quite well established that IL-6 is the main important cytokine involved in the inflammatory responses that control the HP levels, and it is elevated in brain tissues in ischemia and IS.[30]

The present study shows significantly increased levels of serum HP in non-anemic women with AIS, especially during the first 8 hours, compared to controls.[17,18] This corresponds to other studies reporting similar changes and emphasizes the role of HP and SI in causing brain ischemia. It seems quite interesting that serum HP level might serve as a strong factor for predicting the status of an IS and future therapeutic approaches.[17] It is also necessary to pay attention to iron transport proteins.

Higher levels of SI in AIS patients compared to controls in the present study are like those found in a study by Chi et al.[32] Moreover, Rouault and Cooperman consider the possibility that iron accumulation contributes to the formation of free radicals and oxidative damage to brain tissue.[33] According to Adibhatla and Hatcher,[34] free iron can react with H_2O_2 via the Fenton reaction, a primary cause of lipid peroxidation, and may be particularly important for these brain injuries.

The present study found a significant positive correlation between SI and HP, SI and IL-6, and HP and IL-6 in AIS. Several aspects of these findings are in accordance with the published studies [35,36] that help explore the HP role in iron-dependent damage and neurotoxicity and the role of SI in hypoxia via HP and concomitant changes occurring in IS.[30,37] Further studies may explore ways to develop novel therapeutics for controlling iron toxicity in IS and to understand the pathophysiological mechanisms whereby iron causes neurotoxicity in patients with AIS.[4]

A major limitation of the present report is that the patients consulted have a quite limited age range. Future studies need extensive research work in both male and female subjects/patients of a wider age range and a larger and multicentre-based sample size.

Conclusion

The present study provides evidence of the association of acute ischemic stroke in non-anemic women with increased hepcidin. The interactive pathophysiological role of hepcidin, IL-6, and serum iron in non-anemic women with acute ischemic stroke has also been shown. Furthermore, the present study discusses the introduction of better treatment modalities for modulating the signaling pathways for hepcidin expression and modifying neuronal iron homeostasis in patients with acute ischemic stroke.

Competing Interests

The author declares that there are no competing interests.

Acknowledgments

The author acknowledges the honorary help of neurologists, other medical experts, and laboratory personnel for their kind help and assistance.

References

1. Krishnamurthi RV, Ikeda T, Feigin VL. Global, Regional and Country-Specific Burden of Ischaemic Stroke, Intracerebral Haemorrhage and Subarachnoid Haemorrhage: A Systematic Analysis of the Global Burden of Disease Study 2017. Neuroepidemiology. 2020;54(2):171-179. doi: 10.1159/000506396.
2. Holmqvist L, Boström KB, Kahan T, Schiöler L, Hasselström J, Hjerpe P, et al. Cardiovascular outcome in treatment-resistant hypertension: results from the Swedish Primary Care Cardiovascular Database (SPCCD). J Hypertens. 2018 Feb;36(2):402-409. doi: 10.1097/HJH.0000000000001561.
3. Patlolla SH, Lee HC, Noseworthy PA, Wysokinski WE, Hodge DO, Greene EL, et al. Impact of Diabetes Mellitus on Stroke and Survival in Patients With Atrial Fibrillation. Am J Cardiol. 2020 Sep 15;131:33-39. doi: 10.1016/j.amjcard.2020.06.049. Epub 2020 Jun 30. PMID: 32723556.
4. Almutairi MMA, Xu G, Shi H. Iron Pathophysiology in Stroke. Adv Exp Med Biol. 2019;1173:105-123. doi: 10.1007/978-981-13-9589-5_6.
5. Hajar R. Risk Factors for Coronary Artery Disease: Historical Perspectives. Heart Views. 2017 Jul-Sep;18(3):109-114. doi: 10.4103/HEARTVIEWS.HEARTVIEWS_106_17.
6. Musuka TD, Wilton SB, Traboulsi M, Hill MD. Diagnosis and management of acute ischemic stroke: speed is critical. CMAJ. 2015 Sep 8;187(12):887-93. doi: 10.1503/cmaj.140355. Epub 2015 Aug 4.
7. Simmatis LER, Scott SH, Jin AY. The Impact of Transient Ischemic Attack (TIA) on Brain and Behavior. Front Behav Neurosci. 2019 Mar 11;13:44. doi: 10.3389/fnbeh.2019.00044.
8. Boehme AK, Esenwa C, Elkind MS. Stroke Risk Factors, Genetics, and Prevention. Circ Res. 2017 Feb 3;120(3):472-495. doi: 10.1161/CIRCRESAHA.116.308398.
9. Chopra VK, Anker SD. Anaemia, iron deficiency and heart failure in 2020: facts and numbers. ESC Heart Fail. 2020 Oct;7(5):2007-2011. doi: 10.1002/ehf2.12797.
10. Barandiarán Aizpurua A, Sanders-van Wijk S, Brunner-La Rocca HP, Henkens MTHM, Weerts J, Spanjers MHA, et al. Iron deficiency impacts prognosis but less exercise capacity in heart failure with preserved ejection fraction. ESC Heart Fail. 2021 Apr;8(2):1304-1313. doi: 10.1002/ehf2.13204.
11. Guedes M, Muenz D, Zee J, Lopes MB, Waechter S, Stengel B, et al. Serum biomarkers of iron stores are associated with worse physical health-related quality of life in nondialysis-dependent chronic kidney disease patients with or without anemia. Nephrol Dial Transplant. 2021 Aug 27;36(9):1694-1703. doi: 10.1093/ndt/gfab050.

12. Neidlein S, Wirth R, Pourhassan M. Iron deficiency, fatigue and muscle strength and function in older hospitalized patients. Eur J Clin Nutr. 2021 Mar;75(3):456-463. doi: 10.1038/s41430-020-00742-z.
13. Kemna EH, Tjalsma H, Willems HL, Swinkels DW. Hepcidin: from discovery to differential diagnosis. Haematologica. 2008 Jan;93(1):90-7. doi: 10.3324/haematol.11705.
14. Mabjeesh NJ, Escuin D, LaVallee TM, Pribluda VS, Swartz GM, Johnson MS, et al. 2ME2 inhibits tumor growth and angiogenesis by disrupting microtubules and dysregulating HIF. Cancer Cell. 2003 Apr;3(4):363-75. doi: 10.1016/s1535-6108(03)00077-1.
15. Chamorro Á. Neuroprotectants in the Era of Reperfusion Therapy. J Stroke. 2018 May;20(2):197-207. doi: 10.5853/jos.2017.02901.
16. Wilkinson DA, Pandey AS, Thompson BG, Keep RF, Hua Y, Xi G. Injury mechanisms in acute intracerebral hemorrhage. Neuropharmacology. 2018 May 15;134(Pt B):240-248. doi: 10.1016/j.neuropharm.2017.09.033.
17. Petrova JJ, Manolov VE, Hadjidekova SP, Hadjiev EA, Bogov BI, Marinov BM, et al. Is There a Link Between Changes in Levels of Hepcidin and Stroke? Clin Lab. 2015;61(12):1935-9. doi: 10.7754/clin.lab.2015.150522.
18. Słomka A, Świtońska M, Żekanowska E. Hepcidin Levels Are Increased in Patients with Acute Ischemic Stroke: Preliminary Report. J Stroke Cerebrovasc Dis. 2015 Jul;24(7):1570-6. doi: 10.1016/j.jstrokecerebrovasdis.2015.03.031.
19. Khan NI, Naz L, Mushtaq S, Rukh L, Ali S, Hussain Z. Ischemic stroke: prevalence of modifiable risk factors in male and female patients in Pakistan. Pak J Pharm Sci. 2009 Jan;22(1):62-7.
20. Harakeh S, Kalamegam G, Pushparaj PN, Al-Hejin A, Alfadul SM, Al Amri T, et al. Chemokines and their association with body mass index among healthy Saudis. Saudi J Biol Sci. 2020 Jan;27(1):6-11. doi: 10.1016/j.sjbs.2019.03.006.
21. Nuttall FQ. Body Mass Index: Obesity, BMI, and Health: A Critical Review. Nutr Today. 2015 May;50(3):117-128. doi: 10.1097/NT.0000000000000092.
22. Moliner P, Jankowska EA, van Veldhuisen DJ, Farre N, Rozentryt P, Enjuanes C, et al. Clinical correlates and prognostic impact of impaired iron storage versus impaired iron transport in an international cohort of 1821 patients with chronic heart failure. Int J Cardiol. 2017 Sep 15;243:360-366. doi: 10.1016/j.ijcard.2017.04.110.
23. Beutler E, Waalen J. The definition of anemia: what is the lower limit of normal of the blood hemoglobin concentration? Blood. 2006 Mar 1;107(5):1747-50. doi: 10.1182/blood-2005-07-3046.
24. von Haehling S, Ebner N, Evertz R, Ponikowski P, Anker SD. Iron Deficiency in Heart Failure: An Overview. JACC Heart Fail. 2019 Jan;7(1):36-46. doi: 10.1016/j.jchf.2018.07.015.
25. Whelton PK, Carey RM, Aronow WS, Casey DE Jr, Collins KJ, Dennison Himmelfarb C, et al. 2017 ACC/AHA/AAPA/ABC/ACPM/AGS/APhA/ASH/ASPC/NMA/PCNA Guideline for the Prevention, Detection, Evaluation, and Management of High Blood Pressure in Adults: A Report of the American College of Cardiology/American Heart Association Task Force on Clinical Practice Guidelines. J Am Coll Cardiol. 2018 May 15;71(19):e127-e248. doi: 10.1016/j.jacc.2017.11.006. Epub 2017 Nov 13. Erratum in: J Am Coll Cardiol. 2018 May 15;71(19):2275-2279. PMID: 29146535.
26. Oh SY, Ryue J, Hsieh CH, Bell DE. Eggs enriched in omega-3 fatty acids and alterations in lipid concentrations in plasma and lipoproteins and in blood pressure. Am J Clin Nutr. 1991 Oct;54(4):689-95. doi: 10.1093/ajcn/54.4.689.
27. Warnick GR, Nguyen T, Albers AA. Comparison of improved precipitation methods for quantification of high-density lipoprotein cholesterol. Clin Chem. 1985 Feb;31(2):217-22.
28. Tremblay AJ, Morrissette H, Gagné JM, Bergeron J, Gagné C, Couture P. Validation of the Friedewald formula for the determination of low-density lipoprotein cholesterol compared with beta-quantification in a large population. Clin Biochem. 2004 Sep;37(9):785-90. doi: 10.1016/j.clinbiochem.2004.03.008.
29. Zahir H, Javaid A, Rehman R, Hussain Z. Statistical concepts in biology and health sciences. J Ayub Med Coll Abbottabad. 2014 Jan-Mar;26(1):95-7. PMID: 25358229.
30. Ding H, Yan CZ, Shi H, Zhao YS, Chang SY, Yu P, et al. Hepcidin is involved in iron regulation in the ischemic brain. PLoS One. 2011;6(9):e25324. doi: 10.1371/journal.pone.0025324.
31. Chen Z, Gao C, Hua Y, Keep RF, Muraszko K, Xi G. Role of iron in brain injury after intraventricular hemorrhage. Stroke. 2011 Feb;42(2):465-70. doi: 10.1161/STROKEAHA.110.602755.
32. Chi SI, Wang CK, Chen JJ, Chau LY, Lin TN. Differential regulation of H- and L-ferritin messenger RNA subunits, ferritin protein and iron following focal cerebral ischemia-reperfusion. Neuroscience. 2000;100(3):475-84. doi: 10.1016/s0306-4522(00)00317-1.
33. Rouault TA, Cooperman S. Brain iron metabolism. Semin Pediatr Neurol. 2006 Sep;13(3):142-8. doi: 10.1016/j.spen.2006.08.002. PMID: 17101452.
34. Adibhatla RM, Hatcher JF. Lipid oxidation and peroxidation in CNS health and disease: from molecular mechanisms to therapeutic opportunities. Antioxid Redox Signal. 2010 Jan;12(1):125-69. doi: 10.1089/ars.2009.2668.
35. Rehu M, Punnonen K, Ostland V, Heinonen S, Westerman M, Pulkki K, et al. Maternal serum hepcidin is low at term and independent of cord blood iron status. Eur J Haematol. 2010 Oct;85(4):345-52. doi: 10.1111/j.1600-0609.2010.01479.x.
36. Choi HS, Song SH, Lee JH, Kim HJ, Yang HR. Serum hepcidin levels and iron parameters in children with iron deficiency. Korean J Hematol. 2012 Dec;47(4):286-92. doi: 10.5045/kjh.2012.47.4.286.
37. Tan G, Liu L, He Z, Sun J, Xing W, Sun X. Role of hepcidin and its downstream proteins in early brain injury after experimental subarachnoid hemorrhage in rats. Mol Cell Biochem.2016 Jul;418(1-2):31-8.doi: 10.1007/s11010-016-2730-1

***Correspondence:** Prof. Dr. Zahir Hussain, Department of Physiology, Faculty of Medicine, Umm Al-Qura University, Makkah 21955, Saudi Arabia. E-mail: zahirhussa@gmail.com*

International Journal of Biomedicine 14(2) (2024) 265-269
http://dx.doi.org/10.21103/Article14(2)_OA4

ORIGINAL ARTICLE

Diabetes Mellitus

INTERNATIONAL JOURNAL OF BIOMEDICINE

Evaluation of Serum Visfatin and Chemerin Levels in Diabetes Patients in Mosul City

Rana Ibrahim Khalil[1*], Saria Naji Mohsin[2], Sura Hameed Nayyef[2]

[1]*Al-Salam Teaching Hospital, Nineveh Health Department, Nineveh, Iraq*
[2]*Department of Biology, College of Science, Tikrit University, Salah Al-Din, Iraq*

Abstract

Background: Diabetes mellitus is a major public health concern worldwide. Although there are many possible causes of diabetes, the three most prevalent ones are insulin resistance, pancreatic cell damage, and insulin insufficiency. Visfatin, an adipocytokine with insulin-mimicking characteristics, and chemerin, an adipokine responsible for maintaining normal cholesterol and glucose levels, are linked to inflammation and immunological dysfunction in metabolic illnesses. Hence, in this study, we aimed to evaluate the possible association between type 2 diabetes mellitus (T2DM) and the adipokines visfatin and chemerin.

Methods and Results: This study was conducted at the Al-Salam Teaching Hospital in Mosul from December 1, 2022, to the end of June 2023. The study included 65 patients of both sexes with T2DM aged between 35 and 80. Twenty-five healthy individuals of both sexes were chosen for a control group. Visfatin and chemerin levels in the serum were measured using an ELISA kit (Koma biotech, ELISA, USA) per the manufacturer's instructions.

The levels of visfatin and chemerin in T2DM patients were significantly higher than in controls (1.478±0.631 ng/ml and 158.768±36.941 pg/ml vs. 0.538±0.151 ng/ml and 71.272±12.994 pg/ml, respectively, P=0.000 in both cases). The study showed no significant difference in the levels of chemerin and visfatin between females and males in T2DM patients. Among men, the visfatin levels were significantly higher in T2DM patients with diabetic retinopathy than in T2DM patients with such complications as cardiovascular disease and diabetic nephropathy. These features also occurred among women. Men and women with T2DM did not differ in the chemerin levels, depending on the nature of the diabetes complication.

Conclusion: T2DM patients are characterized by significantly higher visfatin and chemerin levels than healthy controls. No differences in the levels of these adipokines that depend on the gender of diabetic patients have been found. **(International Journal of Biomedicine. 2024;14(2):265-269.)**

Keywords: type 2 diabetes mellitus • visfatin • chemerin • insulin resistance

For citation: Khalil RI, Mohsin SN, Nayyef SH. Evaluation of Serum Visfatin and Chemerin Levels in Diabetes Patients in Mosul City. International Journal of Biomedicine. 2024;14(2):265-269. doi:10.21103/Article14(2)_OA4

Abbreviations

CVD, cardiovascular disease; **DN**, diabetic nephropathy; **DR**, diabetic retinopathy; **IR**, insulin resistance; **T2DM**, type 2 diabetes mellitus; **VSMCs**, vascular smooth muscle cells.

Introduction

Diabetes mellitus is a major public health concern, affecting over 400 million individuals throughout the world. The number of individuals with diabetes is rising, and by 2030, it is projected that 366 million people aged 65 and more will have the disease. Diabetes has been associated with several factors, including insulin deficiency, pancreatic cell injury, and insulin resistance. Nephropathy, neuropathy, cardiovascular disease, and diabetic retinopathy are only a few of the many complications of diabetes.(1) Constant microvascular and macrovascular problems could develop due to this metabolic disorder. The inability of the pancreas to produce enough insulin and a lifetime of poor dietary and lifestyle choices contribute to the development of insulin resistance and type 2 diabetes mellitus (T2DM).

The molecular mechanisms involved in insulin generation, release, and response in tissues must be tightly

regulated to ensure that insulin activity precisely matches metabolic demand. The pathophysiology of T2DM may be affected by defects in any of these systems, leading to a metabolic imbalance.[2] Adipokines regulate hunger, energy expenditure and storage, insulin secretion and sensitivity, blood pressure, endothelial function, and homeostasis. Adipokines have several systemic effects on the liver, brain, muscle, heart, arteries, and immune system.[3] The visceral adipose tissue produces the proinflammatory adipokine visfatin, a 52-kDa protein. Visfatin increases cytokine production, and elevated levels are linked to inflammation and endothelial dysfunction in metabolic illness. Visfatin has been linked to many different types of brain and heart damage in clinical investigations. Evidence suggests it has various harmful long-term effects and a regulatory function in the heart, neurons, and mitochondria. There is a need for more excellent research into the impact of adipocytokine on critically sick individuals.[4]

The newly discovered adipokine chemerin possesses endocrine, paracrine, and autocrine functions, making it crucial for maintaining normal cholesterol and glucose levels. It is generated mainly by white adipose tissue, the liver, and the placenta, with some also coming from brown adipose tissue, skeletal muscles, and other organs, such as kidneys, adrenal glands, lungs, ovaries, and the heart. In addition to its role in blood pressure control, chemerin may have a role in angiogenesis, inflammation, immunological modulation, and other processes. Some research has shown that chemerin levels are more significant in diabetic patients than in healthy controls, while others have shown no significant differences.[5] In this case-control and exploratory investigation, we examined a group of diabetic patients in Mosul (Iraq) for a possible association between T2DM and visfatin and chemerin.

Materials and Methods

This study was conducted at the Al-Salam Teaching Hospital in Mosul from December 1, 2022, to the end of June 2023. The study included 65 patients of both sexes with T2DM aged between 35 and 80. Twenty-five healthy individuals of both sexes were chosen for a control group. Venous blood was collected from patients and controls after an 8-hour fasting. The blood was allowed to rest for 20 minutes at room temperature. The serum separated was centrifuged at 3000rpm for 15 minutes and transferred to fresh tubes for further analysis. Fasting blood glucose was estimated using Glucose Reagent Kit (Biomerieux, France). Visfatin and chemerin levels in the serum were measured using an ELISA kit (Koma biotech, ELISA, USA) per the manufacturer's instructions.

Statistical analysis was performed using the statistical software package SPSS version 25.0 (SPSS Inc, Armonk, NY: IBM Corp). For the descriptive analysis, results are presented as mean (M) ± standard deviation (SD). For data with normal distribution, inter-group comparisons were performed using Student's t-test. Multiple comparisons were performed with one-way ANOVA and Tukey HSD post-hoc test. A value of $P<0.05$ was considered significant.

Results and Discussion

We found significantly higher levels of visfatin and chemerin in T2DM patients than in controls (1.478±0.631 ng/ml and 158.768±36.941 pg/ml vs. 0.538±0.151 ng/ml and 71.272±12.994 pg/ml, respectively, P=0.000 in both cases) (Table 1). The study showed no significant difference in the levels of chemerin and visfatin between females and males in T2DM patients (Table 2). The patients were divided into groups according to the T2DM complications, and the level of visfatin was compared between these groups and for each sex separately. Among men, the visfatin levels were significantly higher in T2DM patients with diabetic retinopathy than in T2DM patients with such complications as cardiovascular disease and diabetic nephropathy. These features also occurred among women (Table 3). Men and women with T2DM did not differ in the chemerin levels, depending on the nature of the diabetes complication (Table 4).

Table 1.

The levels of visfatin and chemerin in controls and T2DM patients.

Variable	Control group (n=25)	T2DM patients (n=65)	*P*-value
Visfatin (ng/mL)	0.538 ± 0.151	1.478 ± 0.631	0.000
Chemerin (pg/mL)	71.272±12.994	158.768 ± 36.941	0.000

Table 2.

Levels of chemerin and visfatin in T2DM patients depending on gender.

Variable	Female (n=25)	Male (n=40)	*P*- value
Visfatin (ng/ml)	1.546 ± 0.671	1.436± 0 .609	0.499
Chemerin (pg/ml)	157.122 ±43.678	159.797 ± 32.598	0.779

Table 3.

The visfatin levels according to the T2DM complications.

Gender	Group	n	Visfatin (ng/mL)	ANOVA
Males T2DM complication	Control group[1]	11	0.609±0.098	F=11.7128 P=0.0000 P_{1-2}=0.0036 P_{1-3}=0.0224 P_{1-4}=0.0000 P_{2-3}=0.9690 P_{2-4}=0.0372 P_{3-4}=0.0212
	CVD[2]	15	1.424± 0.587	
	DN[3]	11	1.324±0.565	
	DR[4]	9	2.083±0.789	
Females T2DM complication	Control group[1]	14	0.483±0.164	F=7.5841 P=0.0001 P_{1-2}=0.0016 P_{1-3}=0.0222 P_{1-4}=0.0044 P_{1-5}=0.0011 P_{2-3}=0.9942 P_{2-4}=0.9966 P_{2-5}=0.9269 P_{3-4}=0.9616 P_{3-5}=0.8124
	CVD[2]	11	1.487±0.836	
	DN3	7	1.370±0.796	
	DR[4]	6	1.594±0.400	
	Other complications[5]	6	1.733±0.652	

Table 4.

The chemerin levels according to the T2DM complications.

Gender	Group	n	Chemerin (pg/ml)	ANOVA
Males T2DM complication	Control group[1]	11	68.941 ±11.304	F=43.2797 P=0.000 P_{1-2}=0.0000 P_{1-3}=0.0000 P_{1-4}=0.0000 P_{2-3}=0.9579 P_{2-4}=0.5114 P_{3-4}=0.8246
	CVD[2]	15	159.127 ±35.327	
	DN[3]	11	164.001 ±15.726	
	DR[4]	9	173.449 ±21.770	
Females T2DM complication	Control group[1]	14	73.103 ±14.325	F=23.4721 P=0.0000 P_{1-2}=0.0011 P_{1-3}=0.0120 P_{1-4}=0.5790 P_{1-5}=0.0000 P_{2-3}=0.9988 P_{2-4}=0.3076 P_{2-5}=0.0000 P_{3-4}=0.5383 P_{3-5}=0.0000
	CVD[2]	11	139.765 ±49.931	
	DN[3]	7	134.732 ±57.010	
	DR[4]	6	101.291 ±38.130	
	Other complications[5]	6	252.693 ±29.641	

Adipokines play a critical role in maintaining systemic energy homeostasis, and the impaired adipokine production observed in obesity contributes to diabetes pathogenesis. Visfatin was first discovered as an adipocytokine with insulin-mimicking characteristics.[6] Chemerin is a recently discovered adipokine that regulates adipocyte differentiation and modulates chemotaxis and the activation of dendritic cells and macrophages.[7] Susairaj et al.[8] found that chemerin was associated with BMI and fat components but is not an independent risk factor for T2DM.

In our study, the levels of visfatin and chemerin in T2DM patients were significantly higher than in controls. These results are consistent with those of Sulaiman et al.,[9] who showed elevated levels of visfatin and chemerin in T2DM patients and showed that serum visfatin plays an important role in many pathological processes in T2DM.

Our study showed no differences in the levels of chemerin and visfatin regardless of the gender of patients with diabetes, which is consistent with the data of Tabandeh et al.[10] and Mir et al.[11] but disagrees with Lehrke et al.,[7] who found that the blood chemerin levels were significantly higher in females than in males. In addition, the researchers found that chemerin was strongly associated with markers of inflammation and components of metabolic syndrome (body mass index, triglycerides, HDL-cholesterol, and hypertension).

Diabetic microvascular complications (retinopathy, nephropathy, neuropathy) and macrovascular complications (ischemic heart disease, peripheral vascular disease, and cerebrovascular disease) result in organ and tissue damage in approximately one-third to one-half of people with diabetes. Akbarian et al.[12] showed high levels of visfatin and NO metabolites in patients with diabetic nephropathy. In addition, there was a positive correlation between visfatin and NO metabolite levels in nephropathic and non-nephropathic diabetic patients. The results of a study by Al Obaidi et al.[13] showed that serum visfatin levels were significantly correlated with CRP in patients with chronic kidney disease and with deterioration of kidney function.

Besides, Wang et al.[14] found that serum and vitreous visfatin levels were associated with the presence and severity of diabetic retinopathy, which is consistent with our results, indicating that diabetic retinopathy, among other complications of diabetes, was characterized by high values of this adipokine. In a study by Yasir et al.,[15] linear regression data showed that chemerin was also an independent predictor of diabetic retinopathy severity.

Kärberg et al.[16] found that visfatin could be used as a marker of subclinical atherosclerosis in patients with T2DM, especially in males. In particular, visfatin positively correlated with intima-media thickness ≥1.0 mm or plaque (P=0.008). According to research findings, visfatin has a strong connection to cardiovascular disease.

Several studies have shown a connection between chemerin and endothelial dysfunction in pathological conditions such as obesity, DM, and hypertension.[17-19] Neves et al.[20] found that chemerin induces endothelial dysfunction by downregulating endothelial nitric oxide synthase and decreasing NO production in endothelial cells. Chemerin is also associated with excessive ROS accumulation in endothelial cells, contributing to endothelial dysfunction.[18,20] Increased ROS accumulation and elevated expressions of inflammatory cytokines such as IL-1β, IL-6, and monocyte chemoattractant protein-1 were observed in chemerin-treated vascular smooth muscle cells, suggesting that chemerin can induce vascular smooth muscle cell dysfunction by augmenting oxidative stress and promoting inflammation.[21-24] Chemerin may contribute to the development of atherosclerosis by promoting the formation of vascular inflammation by recruiting macrophages to inflamed blood vessels.[25] Gasbarino et al.[26] showed circulating chemerin is associated with carotid plaque instability.

A prospective cohort study by Zhou et al.,[27] which included 834 patients with chronic heart failure, investigated the association between serum chemerin and clinical outcomes. Cox regression analysis showed that chemerin significantly predicted major adverse cardiac events after adjustment for conventional risk factors. In addition, chemerin was an independent predictor of all-cause mortality after multivariable adjustment. The authors concluded that chemerin may be a novel serum marker for predicting major adverse cardiac events in patients with chronic heart failure. Chemerin can also potentially be used as a biomarker in chronic kidney disease, which is common in people with diabetes.[28]

Conclusion

T2DM patients are characterized by significantly higher visfatin and chemerin levels than healthy controls. No differences in the levels of these adipokines that depend on

the gender of diabetic patients have been found. The level of visfatin has been significantly higher in patients with diabetic retinopathy than in such diabetes complications as cardiovascular disease and diabetic nephropathy. Elevated chemerin levels in T2DM patients do not depend on the type of diabetes complication.

Ethical Considerations

The study was conducted in accordance with ethical principles of the WMA Declaration of Helsinki (1964, ed. 2013). Written informed consent was obtained from all participants according to Administrative Order No. 3/7/107 dated 18/1/2022.

Competing Interests

The authors declare that they have no competing interests.

References

1. Padhi S, Nayak AK, Behera A. Type II diabetes mellitus: a review on recent drug based therapeutics. Biomed Pharmacother. 2020 Nov;131:110708. doi: 10.1016/j.biopha.2020.110708. Epub 2020 Sep 11. PMID: 32927252.
2. Galicia-Garcia U, Benito-Vicente A, Jebari S, Larrea-Sebal A, Siddiqi H, Uribe KB, Ostolaza H, Martín C. Pathophysiology of Type 2 Diabetes Mellitus. Int J Mol Sci. 2020 Aug 30;21(17):6275. doi: 10.3390/ijms21176275. PMID: 32872570; PMCID: PMC7503727.
3. Lelis DF, Freitas DF, Machado AS, Crespo TS, Santos SHS. Angiotensin-(1-7), Adipokines and Inflammation. Metabolism. 2019 Jun;95:36-45. doi: 10.1016/j.metabol.2019.03.006. Epub 2019 Mar 21. PMID: 30905634.
4. Hajri T, Gharib M, Kaul S, Karpeh MS Jr. Association between adipokines and critical illness outcomes. J Trauma Acute Care Surg. 2017 Sep;83(3):507-519. doi: 10.1097/TA.0000000000001610. PMID: 28697011.
5. Ashraf H, Soltani D, Sobh-Rakhshankhah A, Jafari S, Boroumand MA, Goudarzi V, Vasheghani Farahani A, Masoudkabir F. Visfatin as marker of isolated coronary artery ectasia and its severity. Cytokine. 2019 Jan;113:216-220. doi: 10.1016/j.cyto.2018.07.007. Epub 2018 Jul 9. PMID: 30001864.
6. Yu PL, Wang C, Li W, Zhang FX. Visfatin Level and The Risk of Hypertension and Cerebrovascular Accident: A Systematic Review and Meta-Analysis. Horm Metab Res. 2019 Apr;51(4):220-229. doi: 10.1055/a-0867-1333. Epub 2019 Apr 25. PMID: 31022738.
7. Lehrke M, Becker A, Greif M, Stark R, Laubender RP, von Ziegler F, Lebherz C, Tittus J, Reiser M, Becker C, Göke B, Leber AW, Parhofer KG, Broedl UC. Chemerin is associated with markers of inflammation and components of the metabolic syndrome but does not predict coronary atherosclerosis. Eur J Endocrinol. 2009 Aug;161(2):339-44. doi: 10.1530/EJE-09-0380. Epub 2009 Jun 4. PMID: 19497986.
8. Susairaj P, Snehalatha C, Nanditha A, Satheesh K, Raghavan A, Vinitha R, Ramachandran A. Analysis of an Indian diabetes prevention programme on association of adipokines and a hepatokine with incident diabetes. Sci Rep. 2021 Oct 13;11(1):20327. doi: 10.1038/s41598-021-99784-x. PMID: 34645898; PMCID: PMC8514464.
9. Sulaiman MM, Salih KN, Alazzawy MA. Role of Visfatin Chemerin with Type Two Diabetes Mellitus. Al-Kufa University Journal for Biology. 2019;11(1).
10. Tabandeh MR, Taha AS, Addai Ali H, Razijalali M, Mohammadtaghvaei N. Type 2 Diabetes Mellitus Coincident with Clinical and Subclinical Thyroid Dysfunctions Results in Dysregulation of Circulating Chemerin, Resistin and Visfatin. Biomedicines. 2023 Jan 25;11(2):346. doi: 10.3390/biomedicines11020346. PMID: 36830883; PMCID: PMC9952980.
11. Mir MM, Mir R, Alghamdi MAA, Wani JI, Sabah ZU, Jeelani M, Marakala V, Sohail SK, O'haj M, Alharthi MH, Alamri MMS. Differential Association of Selected Adipocytokines, Adiponectin, Leptin, Resistin, Visfatin and Chemerin, with the Pathogenesis and Progression of Type 2 Diabetes Mellitus (T2DM) in the Asir Region of Saudi Arabia: A Case Control Study. J Pers Med. 2022 May 1;12(5):735. doi: 10.3390/jpm12050735. PMID: 35629157; PMCID: PMC9143828.
12. Akbarian N, Zarghami N, Mota A, Abediazar S, Abroon S, Mihanfar A, Amanzadeh M, Darbin A, Bannazadeh Baghi H, Rahmati-Yamchi M. Correlation Between Circulating Visfatin and Nitric Oxide Metabolites Levels in Patients With Diabetic Nephropathy. Iran J Kidney Dis. 2018 May;12(3):163-168. PMID: 29891746.
13. Muayad Shukur Al Obaidi R. The Physiological Effects of Visfatin on Immune Response and Inflammatory Impacts on Nephropathy. Arch Razi Inst. 2021 Sep 1;76(3):639-647. doi: 10.22092/ari.2021.355463.1688. PMID: 34824756; PMCID: PMC8605846.
14. Wang Y, Yuan Y, Jiang H. Serum and vitreous levels of visfatin in patients with diabetic retinopathy. Med Sci Monit. 2014 Dec 19;20:2729-32. doi: 10.12659/MSM.891292. PMID: 25524991; PMCID: PMC4280054.
15. Yasir M, Senthilkumar GP, Jayashree K, Ramesh Babu K, Vadivelan M, Palanivel C. Association of serum omentin-1, apelin and chemerin concentrations with the presence and severity of diabetic retinopathy in type 2 diabetes mellitus patients. Arch Physiol Biochem. 2022 Apr;128(2):313-320. doi: 10.1080/13813455.2019.1680698. Epub 2019 Nov 5. PMID: 31686535.
16. Kärberg K, Forbes A, Lember M. Visfatin and Subclinical Atherosclerosis in Type 2 Diabetes: Impact of Cardiovascular Drugs. Medicina (Kaunas). 2023 Jul 18;59(7):1324. doi: 10.3390/medicina59071324. PMID: 37512134; PMCID: PMC10386106.
17. Gu P, Cheng M, Hui X, Lu B, Jiang W, Shi Z. Elevating circulation chemerin level is associated with endothelial dysfunction and early atherosclerotic changes in essential hypertensive patients. J Hypertens. 2015 Aug;33(8):1624-32. doi: 10.1097/HJH.0000000000000588. PMID: 26136068.
18. Haybar H, Shahrabi S, Rezaeeyan H, Shirzad R, Saki N. Endothelial Cells: From Dysfunction Mechanism to

***Corresponding author**: Rana Ibrahim Khalil, Al-Salam Teaching Hospital, Nineveh Health Department, Nineveh, Iraq. E-mail: ranaibkh82@gmail.com*

Pharmacological Effect in Cardiovascular Disease. Cardiovasc Toxicol. 2019 Feb;19(1):13-22. doi: 10.1007/s12012-018-9493-8. PMID: 30506414.
19. Macvanin MT, Rizzo M, Radovanovic J, Sonmez A, Paneni F, Isenovic ER. Role of Chemerin in Cardiovascular Diseases. Biomedicines. 2022 Nov 18;10(11):2970. doi: 10.3390/biomedicines10112970. PMID: 36428537; PMCID: PMC9687862.
20. Neves KB, Lobato NS, Lopes RA, Filgueira FP, Zanotto CZ, Oliveira AM, Tostes RC. Chemerin reduces vascular nitric oxide/cGMP signalling in rat aorta: a link to vascular dysfunction in obesity? Clin Sci (Lond). 2014 Jul;127(2):111-22. doi: 10.1042/CS20130286. PMID: 24498891.
21. Satoh K, Nigro P, Berk BC. Oxidative stress and vascular smooth muscle cell growth: a mechanistic linkage by cyclophilin A. Antioxid Redox Signal. 2010 Mar 1;12(5):675-82. doi: 10.1089/ars.2009.2875. PMID: 19747062; PMCID: PMC2861539.
22. Das S, Zhang E, Senapati P, Amaram V, Reddy MA, Stapleton K, Leung A, Lanting L, Wang M, Chen Z, Kato M, Oh HJ, Guo Q, Zhang X, Zhang B, Zhang H, Zhao Q, Wang W, Wu Y, Natarajan R. A Novel Angiotensin II-Induced Long Noncoding RNA Giver Regulates Oxidative Stress, Inflammation, and Proliferation in Vascular Smooth Muscle Cells. Circ Res. 2018 Dec 7;123(12):1298-1312. doi: 10.1161/CIRCRESAHA.118.313207. Erratum in: Circ Res. 2019 Dec 6;125(12):e112. PMID: 30566058; PMCID: PMC6309807.
23. Cui L, Zhou Q, Zheng X, Sun B, Zhao S. Mitoquinone attenuates vascular calcification by suppressing oxidative stress and reducing apoptosis of vascular smooth muscle cells via the Keap1/Nrf2 pathway. Free Radic Biol Med. 2020 Dec;161:23-31. doi: 10.1016/j.freeradbiomed.2020.09.028. Epub 2020 Oct 2. PMID: 33011276.
24. Dai L, Schurgers LJ, Shiels PG, Stenvinkel P. Early vascular ageing in chronic kidney disease: impact of inflammation, vitamin K, senescence and genomic damage. Nephrol Dial Transplant. 2020 Mar 1;35(Suppl 2):ii31-ii37. doi: 10.1093/ndt/gfaa006. PMID: 32162665; PMCID: PMC7066546.
25. Hart R, Greaves DR. Chemerin contributes to inflammation by promoting macrophage adhesion to VCAM-1 and fibronectin through clustering of VLA-4 and VLA-5. J Immunol. 2010 Sep 15;185(6):3728-39. doi: 10.4049/jimmunol.0902154. Epub 2010 Aug 18. PMID: 20720202.
26. Gasbarrino K, Mantzoros C, Gorgui J, Veinot JP, Lai C, Daskalopoulou SS. Circulating Chemerin Is Associated With Carotid Plaque Instability, Whereas Resistin Is Related to Cerebrovascular Symptomatology. Arterioscler Thromb Vasc Biol. 2016 Aug;36(8):1670-8. doi: 10.1161/ATVBAHA.115.306741. Epub 2016 Jun 16. PMID: 27312219.
27. Zhou X, Tao Y, Chen Y, Xu W, Qian Z, Lu X. Serum Chemerin as a Novel Prognostic Indicator in Chronic Heart Failure. J Am Heart Assoc. 2019 Aug 6;8(15):e012091. doi: 10.1161/JAHA.119.012091. Epub 2019 Jul 23. PMID: 31333053; PMCID: PMC6761658.
28. Behnoush AH, Shobeiri P, Bahiraie P, Amirkhani N, Khalaji A, Peiman S. Chemerin levels in chronic kidney disease: A systematic review and meta-analysis. Front Endocrinol (Lausanne). 2023 Jan 25;14:1120774. doi: 10.3389/fendo.2023.1120774.

International Journal of Biomedicine 14(2) (2024) 270-274
http://dx.doi.org/10.21103/Article14(2)_OA5

ORIGINAL ARTICLE

Internal Medicine

INTERNATIONAL JOURNAL OF BIOMEDICINE

Hypothyroidism and 25-Hydroxyvitamin D Correlation Study

Abdelgdair A. Altoum*, Ahmed Luay Osman, Praveen Kumar Kandakurti, Fatma Mubarak, Ruqeya Murad, Salwa Abdulrahman, Sofiyat Ajoke, Zulekha Shemote

College of Health Sciences, Gulf Medical University, Ajman, UAE

Abstract

Background: Thyroid disease is one of the most common illnesses in the UAE, which could be linked to vast numbers of people suffering from vitamin D deficiency. This study aimed to explore the association between serum 25(OH)D levels and thyroid function parameters in men and women with diagnosed hypothyroidism.

Methods and Results: This cross-sectional observational study included 86 patients (78[90.7%] women and 8[9.3%] men) with diagnosed hypothyroidism. The patients were divided into two groups, male and female. These two groups were compared in terms of age, TSH, free-T4 (FT4), vitamin D, free-T3 (FT3), and body mass index (BMI). In addition, the correlation between levels of vitamin D and TSH was also examined in these two groups.

The mean age of the patients was 27.5 years, and BMI was 28.00 kg/m^2, indicating overweight. Vitamin D deficiency was found in 61(70.9%) patients and severe vitamin D deficiency in 10(11.6%) patients with hypothyroidism. 25(OH)D levels were significantly low in patients with high TSH levels, showing a weak negative correlation (r=-0.132, *P*=0.043). A negligible positive correlation was identified between 25(OH)D levels and FT4 r=0.089, *P*>0.05) and FT3 (r=0.071, *P*>0.05), and a negligible negative correlation with BMI (r=-0.059, *P*>0.05).

Conclusion: There is a clear indication that vitamin D deficiency is prevalent in hypothyroid patients and that these subjects have lower levels of serum 25(OH)D. Suggesting that lower serum 25(OH)D is related to hypothyroidism and the deficiency in vitamin D plays a role in the development of the disease. **(International Journal of Biomedicine. 2024;14(2):270-274.)**

Keywords: 25-hydroxyvitamin D • vitamin D deficiency • thyroid-stimulating hormone • hypothyroidism

For citation: Altoum AA, Osman AL, Kandakurti PK, Mubarak F, Murad R, Abdulrahman S, Ajoke S, Shemote Z. Hypothyroidism and 25-Hydroxyvitamin D Correlation Study. International Journal of Biomedicine. 2024;14(2):270-274. doi:10.21103/Article14(2)_OA5

Abbreviations

25(OH)D, 25-hydroxyvitamin D; **TSH**, thyroid-stimulating hormone; **BMI**, body mass index; **VDR**, vitamin D receptor; **HT**, Hashimoto's thyroiditis.

Introduction

Hypothyroidism is a disease caused by inadequate synthesis and/or release of thyroid hormones. Thyroid dysfunction is a common condition that affects between 3% and 21% of the population.[1] A negative feedback mechanism exists between thyroid-stimulating hormone (TSH) and thyroid hormones. The level is the most sensitive marker of thyroid status in an individual.[2] Subclinical hypothyroidism is diagnosed when TSH levels are high and circulating free T4 is normal.[3,4] Vitamin D, a lipid-soluble prohormone, besides its well-recognized role in calcium metabolism, also affects immune regulation.[5] The emerging prevalence of hypovitaminosis D in populations with hypothyroidism might be attributed to a strong homology between the molecular structure of vitamin D receptor (VDR) and the thyroid hormone receptor.[6,7] Most immune cells, including T cells, B cells, and antigen-presenting cells, such as dendritic cells and macrophages, express VDR.[8,9] Some polymorphisms in the *VDR* gene were shown to predispose people to autoimmune thyroid disease, including Graves' disease and Hashimoto's thyroiditis.[10-14]

*__Corresponding author__: *Dr. Abdelgdair A. Altoum, Medical Laboratory Sciences Program, College of Health Sciences, Gulf Medical University. Ajman, United Arab Emirates. E-mail: gadoora1977@live.com*

Thyroid disease is one of the most common illnesses in the UAE, which could be linked to vast numbers of people suffering from vitamin D deficiency.[15] This deficiency is a consequence of many different traditional and cultural traits, alongside religious teachings, followed by the vast majority of the Emirati population. First, traditional factors include the men wearing white clothing, also known as the thobe, to protect themselves from the sun. As for women, religious teachings instruct them to cover up, exposing only their faces and hands, and some even cover up their faces, further reducing the chance of sun exposure.[16] However, perhaps the main cause of the deficiency is the lack of outdoor physical activities, further reducing their exposure to the sun's rays.[17,18]

Serum levels of 25(OH)D can reflect the whole body's nutritional status and are used to indicate whether vitamin D is adequate in the body.[19-22] A growing body of research supports the important role of adequate vitamin D in health. Vitamin D has also been found to be associated with a variety of inflammation, which is reduced by vitamin D supplements. Vitamin D deficiency is more common in obese people or obesity-related diseases, such as diabetes, so vitamin D supplements may also be a potential treatment.[23-25] Most experts agree that 25(OH)D of <20 ng/ml is considered to be vitamin D deficiency, whereas a 25(OH)D of 21-29 ng/ml is considered to be insufficient.[26] The goal should be >30ng/ml in children and adults.

Studies suggest that vitamin D deficiency participates in the pathogenesis of hypothyroidism. However, contradictory research exists about the relationship between hypothyroidism and vitamin D deficiency. This study aimed to explore the association between serum 25(OH)D levels and thyroid function parameters in men and women with diagnosed hypothyroidism.

Materials and Methods

This cross-sectional observational study was conducted in Ajman state of the UAE at the Thumbay Hospital from February 2021 to April 2021. It included a total of 86 patients (78[90.7%] women and 8[9.3%] men) with diagnosed hypothyroidism of random ages in the Endocrinology Outpatient Clinic of Thumbay Hospital. The patients were divided into two groups, male and female. These two groups were compared in terms of age, TSH, free-T4 (FT4), vitamin D, free-T3 (FT3), and body mass index (BMI) after taking their informed written consent. In addition, the correlation between levels of vitamin D and TSH was also examined in these two groups.

Serum 25-hydroxyvitamin D [25(OH)D] levels were determined using chemiluminescent immunoassay. The subjects were divided into clinically relevant groups according to their serum 25(OH)D levels: ≥30.0 ng/ml (sufficiency), 20-29.9 ng/ml (insufficiency), <20 ng/ml (vitamin D deficiency), and <10 ng/ml (severe vitamin D deficiency).

The measurements of TSH, FT3, and FT4 were conducted by electrochemical luminescence (ECLIA) on Cobas 8000 (Roche Diagnostics, Germany). The provided TSH reference ranges for TSH, FT3, and FT4 were 0.27–4.2 mIU/L, 3.1–6.8 pmol/L, and 12.0–22.0 pmol/L. respectively. The criteria for overt hypothyroidism were TSH >4.20 mIU/L, FT3 <3.1 pmol/L, and FT4 <12.0 pmol/L. The criteria for subclinical hypothyroidism were TSH >4.20 mIU/L, and FT3 and FT4 levels in the reference ranges.

Statistical analysis was performed using the statistical software package SPSS version 21.0 (SPSS Inc, Armonk, NY: IBM Corp). For the descriptive analysis, results are presented as mean ± standard deviation (SD). The Student's unpaired and paired t-tests were used to compare two groups for data with normal distribution. A simple linear regression with a calculation of Pearson's correlation coefficient was performed. A probability value of $P<0.05$ was considered statistically significant.

Results

The mean age of the patients was 27.5 years, and BMI was 28.00 kg/m^2, indicating overweight. Vitamin D deficiency was found in 61(70.9%) patients and severe vitamin D deficiency in 10(11.6%) patients with hypothyroidism. Table 1 shows the mean values of all studied parameters in female and male patients. There was no statistical difference between groups regarding TSH, FT3, FT4, BMI, and 25(OH)D levels ($P>0.05$ in all cases).

Table 1.
Clinical characteristics of the study participants.

Parameter	Male	Female	P-value
Sex	8	78	<0.0001
Age (years)	29	26	0.26
25(OH)D, ng/ml	33.257	27.222	0.862
TSH, mIU/L	6.32571	6.26482	0.934
FT4, pmol/L	15.33714	15.81668	0.709
FT3, pmol/L	3.7857	3.9897	0.509
BMI, kg/m^2	28.443	27.564	0.374

25(OH)D levels were significantly low in patients with high TSH levels, showing a weak negative correlation (r=-0.132, $P=0.043$) (Figure 1). A negative correlation was found between 25(OH)D levels and the disease duration (Figure 2). A negligible positive correlation was identified between 25(OH)D levels and FT4 r=0.089, $P>0.05$) and FT3 (r=0.071, $P>0.05$) (Figures 3 and 4), and a negligible negative correlation with BMI (r=-0.059, $P>0.05$) (Figure 5).

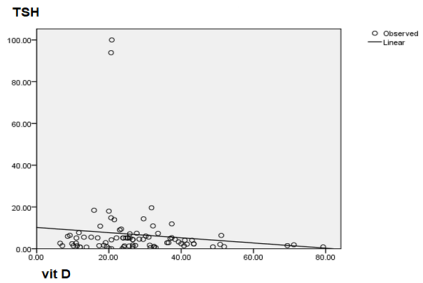

Fig. 1. *A negative correlation between 25-(OH)D and serum TSH (r=-0.132, P=0.043).*

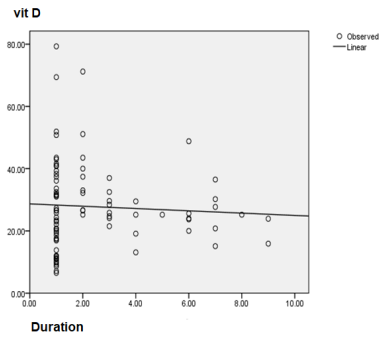

Fig. 2. *A negative correlation between 25-(OH)D and the duration of the disease.*

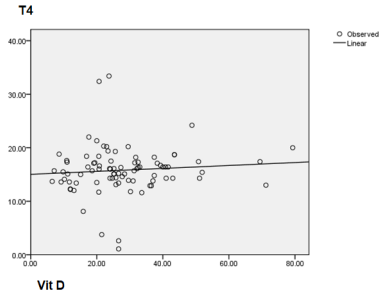

Fig. 3. *A positive correlation between 25(OH)D and serum T4 (r=0.089, P>0.05).*

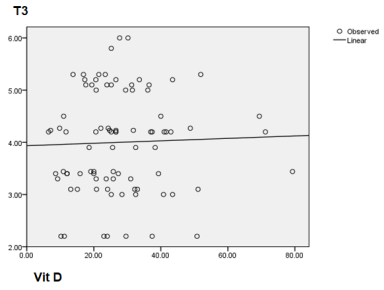

Fig. 4. *A **positive** correlation between 25(OH)D and serum T3 (r=0.071, P>0.05)*

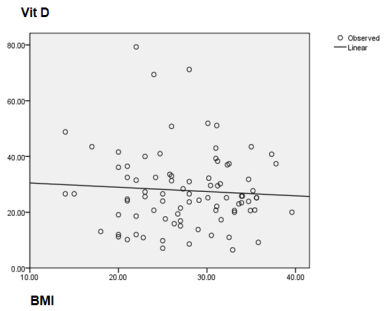

Fig. 5. *A negative correlation between 25(OH) and BMI (r=-0.059, P>0.05).*

Discussion

Hypothyroidism is one of the most common endocrine diseases in the UAE. It is more common in adults over 25. In our study, 90.7% of patients were women, while only 9.3% were male, with a male-to-female ratio of 10.1%.

25(OH)D is the principal stored form of vitamin D. The measurement of serum 25(OH)D levels is considered to be the best diagnostic test to assess the vitamin D status.[27] It reflects vitamin D produced cutaneously and obtained from food and supplements[28] and has a fairly long circulating half-life of 15 days. In contrast to 25(OH)D, circulating 1,25(OH)2D is generally not a good indicator of vitamin D status because it has a short half-life of 15 hours, and serum concentrations are closely regulated by a parathyroid hormone, calcium, and phosphate.[29] Levels of 1,25(OH)2D do not typically decrease until severe vitamin D deficiency.[30,31]

There are several studies suggesting that the prevalence of vitamin D deficiency is high in patients with thyroid diseases and that there is a relationship between hypothyroidism and vitamin D in these patients.[26] In our study, we found that 70.9% of patients with hypothyroidism had vitamin D deficiency, and 11.6% of patients had severe vitamin D deficiency (<10 ng/mL). We also found a negative correlation between vitamin D and TSH levels in these patients.

A study by Bozkurt et al.[32] demonstrated that serum 25(OH)D levels in the patients with Hashimoto's thyroiditis (HT) were significantly lower than those of controls, and 25(OH)D deficiency severity correlated with the duration of Hashimoto's thyroiditis. Supporting our study is another study by Ke et al.,[33] which found significant differences in serum 25(OH)D levels among mild HT, treated HT and controls. Compared with the control, treated and mild HT patients exhibited significantly lower 25(OH)D levels (45.77 ± 3.48 vs. 83.49 ± 6.24 nmol/L and 55.25 ± 3.88 vs. 83.49 ± 6.24 nmol/L, respectively, P<0.001 in both cases).

Hypothyroidism is associated with decreased thermogenesis and decreased metabolic rate and has also been shown to correlate with a higher BMI and a higher prevalence of obesity. There is clinical evidence suggesting that even mild thyroid dysfunction in the form of subclinical hypothyroidism is linked to significant changes in body weight and represents a risk factor for overweight and obesity.

Clinical evidence linking 25(OH)D level to thyroid function is limited and conflicting. A study performed among euthyroid adults showed a strong positive association of vitamin D deficiency with TSH levels after adjusting for age, gender, and season.[34] Another study also demonstrated a negative relationship between 25(OH)D levels and TSH in patients with hypothyroidism.[35] Our study is also consistent with a study by Mackawy et al.,[35] who recorded significant negative correlations between serum 25(OH)D and TSH and a positive correlation between serum 25(OH)D with T4. The studies by Sedrani,[36] Al-Jurayyan et al.,[37] Fida,[38] and Naeem et al.[39] stated that vitamin D serum levels were significantly lower in females than males. These studies showed that the prevalence of vitamin D insufficiency in HT cases (92%) was significantly higher than that observed in healthy controls (63%) (P<0.001). In a study by Mirhosseini et al.,[40] the number of patients with clinical and subclinical hypothyroidism significantly decreased after 12 months of vitamin D supplementation.

Conclusion

Our results indicated that patients with hypothyroidism suffered from hypovitaminosis D and were overweight. Moreover, there is a weak negative but significant correlation between serum 25(OH)D and TSH levels, suggesting that vitamin D deficiency is associated with the severity of hypothyroidism. Screening for vitamin D deficiency is highly recommended for all hypothyroid patients.

Ethical Considerations

The study protocol was reviewed and approved by the Ethics Committee at the Gulf Medical University, Ajman, UAE. Written informed consent was obtained from all the participants.

Competing Interests

The authors declare that they have no competing interests.

References

1. Unal AD, Tarcin O, Parildar H, Cigerli O, Eroglu H, Demirag NG. Vitamin D deficiency is related to thyroid antibodies in autoimmune thyroiditis. Cent Eur J Immunol. 2014;39(4):493-7. doi: 10.5114/ceji.2014.47735. Epub 2014 Dec 15. PMID: 26155169; PMCID: PMC4439962.
2. Kulie T, Groff A, Redmer J, Hounshell J, Schrager S. Vitamin D: an evidence-based review. J Am Board Fam Med. 2009 Nov-Dec;22(6):698-706. doi: 10.3122/jabfm.2009.06.090037. Erratum in: J Am Board Fam Med. 2010 Jan-Feb;23(1):138. PMID: 19897699.
3. Tunbridge WM, Evered DC, Hall R, Appleton D, Brewis M, Clark F, Evans JG, Young E, Bird T, Smith PA. The spectrum of thyroid disease in a community: the Whickham survey. Clin Endocrinol (Oxf). 1977 Dec;7(6):481-93. doi: 10.1111/j.1365-2265.1977.tb01340.x. PMID: 598014.
4. Canaris GJ, Manowitz NR, Mayor G, Ridgway EC. The Colorado thyroid disease prevalence study. Arch Intern Med. 2000 Feb 28;160(4):526-34. doi: 10.1001/archinte.160.4.526. PMID: 10695693.
5. Gil Á, Plaza-Diaz J, Mesa MD. Vitamin D: Classic and Novel Actions. Ann Nutr Metab. 2018;72(2):87-95. doi: 10.1159/000486536. Epub 2018 Jan 18. PMID: 29346788.
6. Kim D. The Role of Vitamin D in Thyroid Diseases. Int J Mol Sci. 2017 Sep 12;18(9):1949. doi: 10.3390/ijms18091949. PMID: 28895880; PMCID: PMC5618598.
7. McDonnell DP, Pike JW, O'Malley BW. The vitamin D receptor: a primitive steroid receptor related to thyroid hormone receptor. J Steroid Biochem. 1988;30(1-6):41-6. doi: 10.1016/0022-4731(88)90074-x. PMID: 2838696.
8. Prietl B, Treiber G, Pieber TR, Amrein K. Vitamin D and immune function. Nutrients. 2013 Jul 5;5(7):2502-21. doi: 10.3390/nu5072502. PMID: 23857223; PMCID: PMC3738984.
9. Baeke F, Takiishi T, Korf H, Gysemans C, Mathieu C. Vitamin D: modulator of the immune system. Curr Opin Pharmacol. 2010 Aug;10(4):482-96. doi: 10.1016/j.coph.2010.04.001. Epub 2010 Apr 27. PMID: 20427238.
10. Feng M, Li H, Chen SF, Li WF, Zhang FB. Polymorphisms in the vitamin D receptor gene and risk of autoimmune thyroid diseases: a meta-analysis. Endocrine. 2013 Apr;43(2):318-26. doi: 10.1007/s12020-012-9812-y. Epub 2012 Oct 12. PMID: 23065592.
11. Meng S, He ST, Jiang WJ, Xiao L, Li DF, Xu J, Shi XH, Zhang JA. Genetic susceptibility to autoimmune thyroid diseases in a Chinese Han population: Role of vitamin D receptor gene polymorphisms. Ann Endocrinol (Paris). 2015 Dec;76(6):684-9. doi: 10.1016/j.ando.2015.01.003. Epub 2015 Dec 1. PMID: 26593863.
12. Muscogiuri G, Tirabassi G, Bizzaro G, Orio F, Paschou SA, Vryonidou A, Balercia G, Shoenfeld Y, Colao A. Vitamin D and thyroid disease: to D or not to D? Eur J Clin Nutr. 2015 Mar;69(3):291-6. doi: 10.1038/ejcn.2014.265. Epub 2014 Dec 17. PMID: 25514898.
13. Fawzy E, Mohammad SAS, Rabat AME. Hypovitaminosis d in autoimmune hypothyroidism. Journal of American Science. 2013;9:60-65.
14. Zhou H, Xu C, Gu M. Vitamin D receptor (VDR) gene polymorphisms and Graves' disease: a meta-analysis. Clin Endocrinol (Oxf). 2009 Jun;70(6):938-45. doi: 10.1111/j.1365-2265.2008.03413.x. Epub 2008 Sep 8. PMID: 18782354.
15. Dawodu A, Kochiyil J, Altaye N. Pilot study of sunlight exposure and vitamin D status in Arab women of childbearing age. East Mediterr Health J. 2011 Jul;17(7):570-4. PMID: 21972479.
16. Al Attia HM, Ibrahim MA. The high prevalence of vitamin D inadequacy and dress style of women in the sunny UAE. Arch Osteoporos. 2012;7:307-10. doi: 10.1007/s11657-012-0104-1. PMID: 23150183.
17. Glerup H, Mikkelsen K, Poulsen L, Hass E, Overbeck S, Thomsen J, Charles P, Eriksen EF. Commonly recommended daily intake of vitamin D is not sufficient if sunlight exposure is limited. J Intern Med. 2000 Feb;247(2):260-8. doi: 10.1046/j.1365-2796.2000.00595.x. PMID: 10692090.
18. Tanabe S, Yano S, Mishima S, Nagai A. Physical inactivity and vitamin D deficiency in hospitalized elderlies. J Bone Miner Metab. 2019 Sep;37(5):928-934. doi: 10.1007/s00774-019-00996-z. Epub 2019 Mar 26. PMID: 30915552.
19. Holick MF. Resurrection of vitamin D deficiency and rickets. J Clin Invest. 2006 Aug;116(8):2062-72. doi: 10.1172/JCI29449. PMID: 16886050; PMCID: PMC1523417.
20. Holick MF. High prevalence of vitamin D inadequacy and implications for health. Mayo Clin Proc. 2006 Mar;81(3):353-73. doi: 10.4065/81.3.353. PMID: 16529140.
21. Bouillon R. Vitamin D: From photosynthesis, metabolism, and action to clinical applications. In: DeGroot LJ, Jameson JL, editors. Endocrinology. Philadelphia: WB Saunders; 2001:1009–1028.
22. Dawson-Hughes B, Heaney RP, Holick MF, Lips P, Meunier PJ, Vieth R. Estimates of optimal vitamin D status. Osteoporos Int. 2005 Jul;16(7):713-6. doi: 10.1007/s00198-005-1867-7. Epub 2005 Mar 18. PMID: 15776217.
23. Jahn D, Dorbath D, Schilling AK, Gildein L, Meier C, Vuille-Dit-Bille RN, Schmitt J, Kraus D, Fleet JC, Hermanns HM, Geier A. Intestinal vitamin D receptor modulates lipid metabolism, adipose tissue inflammation and liver steatosis in obese mice. Biochim Biophys Acta Mol Basis Dis. 2019

Jun 1;1865(6):1567-1578. doi: 10.1016/j.bbadis.2019.03.007. Epub 2019 Mar 21. PMID: 30905785.
24. Kremer R, Campbell PP, Reinhardt T, Gilsanz V. Vitamin D status and its relationship to body fat, final height, and peak bone mass in young women. J Clin Endocrinol Metab. 2009 Jan;94(1):67-73. doi: 10.1210/jc.2008-1575. Epub 2008 Nov 4. PMID: 18984659; PMCID: PMC2630864.
25. Vimaleswaran KS, Berry DJ, Lu C, Tikkanen E, Pilz S, Hiraki LT, Cooper JD, et al.; Genetic Investigation of Anthropometric Traits-GIANT Consortium; Streeten EA, Theodoratou E, Jula A, Wareham NJ, Ohlsson C, Frayling TM, et al. Causal relationship between obesity and vitamin D status: bi-directional Mendelian randomization analysis of multiple cohorts. PLoS Med. 2013;10(2):e1001383. doi: 10.1371/journal.pmed.1001383. Epub 2013 Feb 5. PMID: 23393431; PMCID: PMC3564800.
26. Holick MF. Vitamin D deficiency. N Engl J Med. 2007 Jul 19;357(3):266-81. doi: 10.1056/NEJMra070553. PMID: 17634462.
27. Nalbant A, Aydın A, Tilla H, Cinemre H. Hashimoto tiroiditli olguların klinik ve laboratuvar bulgularınındeğerlendirilmesi. Online Türk Sağlık Bilimleri Dergisi. 2016;1(3):8–20.
28. EFSA Panel on Dietetic Products, Nutrition and Allergies (EFSA NDA Panel); Turck D, Bresson JL, Burlingame B, Dean T, Fairweather-Tait S, Heinonen M, et al. Update of the tolerable upper intake level for vitamin D for infants. EFSA J. 2018 Aug 7;16(8):e05365. doi: 10.2903/j.efsa.2018.5365. PMID: 32626014; PMCID: PMC7009676.
29. Institute of Medicine, Food and Nutrition Board. Dietary Reference Intakes for Calcium and Vitamin D. Washington, DC: National Academy Press, 2010.
30. Jones G. Pharmacokinetics of vitamin D toxicity. Am J Clin Nutr. 2008 Aug;88(2):582S-586S. doi: 10.1093/ajcn/88.2.582S. PMID: 18689406.
31. Cranney A, Horsley T, O'Donnell S, Weiler H, Puil L, Ooi D, Atkinson S, Ward L, Moher D, Hanley D, Fang M, Yazdi F, Garritty C, Sampson M, Barrowman N, Tsertsvadze A, Mamaladze V. Effectiveness and safety of vitamin D in relation to bone health. Evid Rep Technol Assess (Full Rep). 2007 Aug;(158):1-235. PMID: 18088161; PMCID: PMC4781354.
32. Bozkurt NC, Karbek B, Ucan B, Sahin M, Cakal E, Ozbek M, Delibasi T. The association between severity of vitamin D deficiency and Hashimoto's thyroiditis. Endocr Pract. 2013 May-Jun;19(3):479-84. doi: 10.4158/EP12376.OR. PMID: 23337162.
33. Ke W, Sun T, Zhang Y, He L, Wu Q, Liu J, Zha B. 25-Hydroxyvitamin D serum level in Hashimoto's thyroiditis, but not Graves' disease is relatively deficient. Endocr J. 2017 Jun 29;64(6):581-587. doi: 10.1507/endocrj.EJ16-0547. Epub 2017 Apr 11. PMID: 28413173.
34. Barchetta I, Baroni MG, Leonetti F, De Bernardinis M, Bertoccini L, Fontana M, Mazzei E, Fraioli A, Cavallo MG. TSH levels are associated with vitamin D status and seasonality in an adult population of euthyroid adults. Clin Exp Med. 2015 Aug;15(3):389-96. doi: 10.1007/s10238-014-0290-9. Epub 2014 Jun 13. PMID: 24925636.
35. Mackawy AM, Al-Ayed BM, Al-Rashidi BM. Vitamin d deficiency and its association with thyroid disease. Int J Health Sci (Qassim). 2013 Nov;7(3):267-75. doi: 10.12816/0006054. PMID: 24533019; PMCID: PMC3921055.
36. Sedrani SH. Low 25-hydroxyvitamin D and normal serum calcium concentrations in Saudi Arabia: Riyadh region. Ann Nutr Metab. 1984;28(3):181-5. doi: 10.1159/000176801. PMID: 6610383.
37. Al-Jurayyan NA, El-Desouki ME, Al-Herbish AS, Al-Mazyad AS, Al-Qhtani MM. Nutritional rickets and osteomalacia in school children and adolescents. Saudi Med J. 2002 Feb;23(2):182-5. PMID: 11938395.
38. Fida NM. Assessment of nutritional rickets in Western Saudi Arabia. Saudi Med J. 2003 Apr;24(4):337-40. PMID: 12754529.
39. Naeem Z, Almohaimeed A, Sharaf FK, Ismail H, Shaukat F, Inam SB. Vitamin D status among population of Qassim Region, Saudi Arabia. Int J Health Sci (Qassim). 2011 Jul;5(2):116-24. PMID: 23267289; PMCID: PMC3521830.
40. Mirhosseini N., Brunel L., Muscogiuri G., Kimball S. Physiological serum 25-hydroxyvitamin D concentrations are associated with improved thyroid function-observations from a community-based program. *Endocrine.* 2017;58:563–573. doi: 10.1007/s12020-017-1450-y.

International Journal of Biomedicine 14(2) (2024) 275-281
http://dx.doi.org/10.21103/Article14(2)_OA6

ORIGINAL ARTICLE

Pediatrics

INTERNATIONAL JOURNAL OF BIOMEDICINE

Results of Turner Syndrome Treatment with Recombinant Human Growth Hormone in Albania

Agim Gjikopulli[1*], Sonila Tomori[2], Donjeta Bali[2], Paskal Cullufi[2], Laurant Kollcaku[2], Mirela Tabaku[3], Anila Babameto[3]

[1]*Pediatric Endocrinology Unit, Department of Pediatric, University Hospital Center "Mother Teresa," Tirana, Albania*
[2]*Pediatric Specialty Service Nr.2, Department of Pediatric, University Hospital Centre "Mother Teresa," Tirana, Albania*
[3]*Genetic Service, Department of Pediatric, University Hospital Center "Mother Teresa," Tirana, Albania*

Abstract

Background: There is no doubt that the use of rhGH in patients with TS brings satisfactory results regarding the improvement of height growth, realizing the improvement of the final adult height. This study aimed to evaluate the influence of the type/characteristic of the genetic anomaly on sex chromosome X on the outcome of treatment with rhGH among Albanian children diagnosed with TS.

Methods and Results: This analytical-observational study was conducted at the Pediatric Endocrine Unit at University Hospital Centre Mother Teresa in Tirana, the only one of its kind treating TS pediatrics in Albania. Only TS patients who had attained near-adult height (NAH) by December 2023 were included in the analysis of this study. Near-adult height was obtained for 44(72.1%) patients. The mean age of starting treatment was 12.68±3.03 years. After a treatment duration of 3.60±2.26 years, the patients recovered 0.88±0.56 in height-for-age Z-score (HAZ), resulting in HAZ at the end of treatment of -2.73±0.87. They achieved their NAH of 144.56±6.53 cm.

Conclusion: Despite starting treatment late, our patients managed to gain 17.70±12.53 cm in length. The progression of height improvement under rhGH treatment showed differences between chromosomal groups. The non-monosomy group had better results regarding NAH and HAZ at the treatment's end than the monosomy group.**(International Journal of Biomedicine. 2024;14(2):275-281.)**

Keywords: Turner syndrome • karyotype • rhGH • height-for-age Z-score • near-adult height

For citation: Gjikopulli A, Tomori S, Bali D, Cullufi P, Kollcaku L, Tabaku M, Babameto A. Results of Turner Syndrome Treatment with Recombinant Human Growth Hormone in Albania. International Journal of Biomedicine. 2024;14(2):275-281. doi:10.21103/Article14(2)_OA6

Abbreviations

BA, bone age; **BAD**, BA deficit; **BMI**, body mass index; **GH**, growth hormone; **HAZ**, height-for-age Z-score; **IGF**, insulin-like growth factor; **MPH**, mid-parental height; **MG**, monosomy group; **n-MG**, non-monosomy group; **NAH**, near-adult height; **rhGH**, recombinant human growth hormone; **TS**, Turner syndrome.

Introduction

Turner syndrome (TS) is a congenital genetic disorder with a combination of characteristic phenotypic features caused by the loss of all or a critical part of one X chromosome. It occurs in phenotypically female individuals and affects approximately 1 in 2,000-2,500 live female births.[1] It can cause various medical and developmental problems, but short stature is the most frequent clinical feature in patients with TS. To date, there is no convincing evidence to support the view

that the growth disorder in TS is associated with a disorder in the growth hormone-insulin-like growth factor (GH-IGF) axis, but, instead, it is related to haploinsufficiency of the short stature homeobox-containing (*SHOX*) gene.[2] TS is one of the most common syndromes in Albania's list of diseases treated with rhGH during the last 22 years. This study is the first attempt to evaluate the results of this treatment on the near-adult height (NAH) of Albanian TS patients. In Albania, the use of GH has been increasing slowly since 2001 due to the high cost of treatment, lack of funding for patients, and lack of public awareness until recently. Furthermore, data regarding treatment response and factors influencing final height in TS children treated with rhGH have just been analyzed.

This study aimed to evaluate the influence of the type/characteristic of the genetic anomaly on sex chromosome X on the outcome of treatment with rhGH among Albanian children diagnosed with TS.

Materials and Methods

This is a register-based cohort study. The medical records of all patients diagnosed with TS from January 2001 in the Pediatric Endocrine Unit, Department of Pediatrics, University Hospital Centre "Mother Teresa," Albania, were reviewed. Only patients who had attained NAH by December 2023 were included in the analysis of this study. Patients with TS who discontinued the treatment with rhGH for any reason before attaining NAH, patients with TS who are still under treatment, patients with another syndrome, and patients with GH deficiency were excluded (Figure 1).

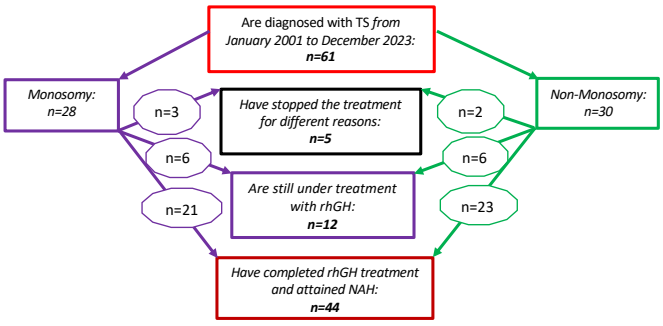

Fig. 1. *Flow chart of study methodology.*

The following data were retrieved from the patients' medical records: diagnosis, chronological age, bone age (BA) and height at starting treatment, height after the first year of treatment, age and height at onset of puberty, age of attaining NAH, duration of growth hormone (GH) treatment and mean GH dose. The height of patients was plotted using the WHO growth charts and was standardized by calculating their standard deviation (SDS) score (Z-score).[3] Administration of conjugated estrogens was initiated at 2.0 mcg/day and increased by 4.0 mcg/day every six months. At 1.5 years, estrogen replacement was given cyclically, and progesterone was added. The onset of puberty was taken to be the time when spontaneous breast development (Tanner stage B2) was first observed or the date at which estrogen replacement therapy was initiated. Bone age (BA) was calculated by reading the plain radiograph of the left hand and wrist using the Greulich and Pyle atlas [4] by a single observer. Bone age deficit (BAD) was defined as (chronological age) – (BA).

Mid-parental height (MPH) was determined by using Tanner's method for girls (cm) = (father's height + mother's height - 13)/2. Target height range = MPH ± 6.5 cm. The dosage of rhGH varied from 0.035 to 0.06 mg/kg/day (0.735-1.26 UI/kg/week). The dosage of rhGH was individualized based on the level of IGF1 and IGFBP3 and growth velocity. Thyroid function tests, biochemical panels, and complete blood counts were performed every six months. All registered subjects were visited as outpatients at the Pediatric Endocrine Unit at "Mother Teresa" University Hospital Centre in Tirana for follow-up every two months, and their height and weight were measured. Height was checked using a Harpenden stadiometer and marked to the nearest 0.1 cm. Body weight was measured with an electronic weighing scale to 0.1 kg. NAH was defined as height reached when growth velocity was less than 2 cm/year calculated over a minimum of 9 months, where the chronological age was more than 16 years or BA more than 15 years, and analysis of individual growth curves showed evidence of asymptotic proximity to final height. The height at diagnosis, NAH, MPH, and the height when puberty was started were then standardized by calculating their height SDS (Z-score) using the WHO growth charts.

Turner syndrome was diagnosed based on clinical and hormonal findings and was confirmed by cytogenetic analysis, such as classical chromosome banding, high-resolution chromosome analysis, spectral karyotype analysis (fluorescent in situ hybridization (FISH)), and array comparative genomic hybridization (aCGH), all of which allow the entire genome to be scanned for chromosome dosage abnormalities, including increases (duplications) or decreases (deletions), which may also be suggestive of an unbalanced displacement. These examinations were conducted in the Genetic Unit, Department of Paediatrics, University Hospital Centre "Mother Teresa," Albania, and other genetic laboratories outside Albania.

To simplify the data analysis, since the number of patients in the subgroups was relatively small, a regrouping of karyotype types was made in the group with monosomy (MG [Subgroup A]) and non-monosomy group (n-MG), which includes the karyotypes of Subgroups B, C, D, and E (Table 1). To eliminate the confusion between the terminology "age of diagnosis" and "age of initiation of therapy" (because for all patients, the therapy was started as soon as the genetic diagnosis was confirmed), the terminology was unified as "age of diagnosis" = "age of initiation of treatment."

Statistical analysis was performed using statistical software package SPSS version 20.0 (SPSS Inc, Armonk, NY: IBM Corp). For descriptive analysis, results are presented as mean (M) ± standard deviation (SD). Inter-group comparisons were performed using Student's t-test. Pearson correlation analysis was performed on the data to explore the relationship between various parameters with final height SDS. A P-value < 0.05 was considered statistically significant.

Table 1.

Frequency of karyotype for all TS patients and TS patients who attained NAH.

Subgroup	Karyotype	All TS patients		TS treated till NAH	
		Count (n)	Percentage (%)	Count (n)	Percentage (%)
A Monosomy	45,X	30	49.18%	21	47.73%
	Total	30	49.18%	21	47.73%
B Mosaic form with structural abnormalities of the X chromosome	45,Xt(5;16)(q11.2;q21.1)/46,XX	1	1.64%	1	2.27%
	45,X(15ps+)/46,XX	1	1.64%	1	2.27%
	45,X,/46X,der(X)	2	3,28%	0	0%
	45,X,1qh+,9qh+/46,X,i(Xq), 1qh+,9qh+	1	1.64%	1	2.27%
	45,X/47,X,i(Xq),i(Xq)/46,X,i(Xq)	1	1.64%	1	2.27%
	45,X/46,X,i(Xq)	10	16.39%	8	18.18%
	45,X/46X,der(X),t(X;X)(p;q)	1	1.64%	1	2.27%
	Total	17	27.87%	13	29.55%
C Mosaic form with numeric anomaly	45,X/46,XX	2	3.28%	1	2.27%
	45,X/47,XXX	1	1.64%	0	0%
	Total	3	4.92%	1	2.27%
D Mosaic form with presence of Y chromosome	45,X/46,XY	5	8.19%	4	9.09%
	Total	5	8.19%	4	9.09%
E Non-mosaic 46,X,der(X)	46,X,i(Xq)	5	8.19%	4	9.09%
	46,X,r(X)	1	1.64%	1	2.27%
	Total	6	9.83%	5	11.36%
Total		61	100%	44	100%

Results

Characteristics of all TS patients at baseline

During the period mentioned above, 61 patients with TS were diagnosed. Out of 61 patients, 30(49.18%) resulted in numeric anomaly with monosomy (45,X0) (Subgroup A or MG), 17(27.87%) had mosaic form with structural anomaly (Subgroup B), 3(4.92%) had mosaic form with the numeric anomaly of the X chromosome (Subgroup C), 5(8.19%) had mosaic form with the presence of Y chromosome (Subgroup D), and only 6(9.83%) had non-mosaic with X-structural abnormalities (Subgroup E) (Table 1).

The mean diagnosis age of all 61 patients with TS was 11.77±3.33 years (min. 3.52; max. 17.64 years). No statistically significant difference was identified in the age of diagnosis/ start of therapy between karyotypic groups (P=0.398). The height-for-age Z-score (HAZ) at the start of the treatment for all TS patients was -3.64±1.01 z-score (min. -6.00; max. -0.93 z-score). The most pronounced shortness at the beginning of therapy was identified in Subgroup A (-3.90±0.93 z-score), followed by Subgroup E (-3.72±0.62 z-score), Subgroup B (-3.59±0.99 z-score), and Subgroups C and D (-2.70±0.97 z-score and -2.67±1.26 z-score, respectively). Even beyond this fact, the MG (Subgroup A) was -0.518 z-score shorter than the n-MG (Subgroups B, C, D, and E), and this difference was statistically significant about the means of HAZ at the time of starting treatment between the MG and n-MG (P=0.043). BMI for age z-score at the start of the treatment was 0.20±1.19 z-score (min. -2,61; max. 3.81 z-score) for all 61 patients. No statistically significant difference was identified in BMI for age between the MG and n-MG (P=0.214).

Characteristics of patients treated to NAH

A total of 44 TS patients reached NAH. The relative frequency of the documented karyotypes for these patients is listed in Table 1. The distribution of karyotypes was not significantly different from the total group of 61 TS patients in our study. Table 2 presents the characteristics of patients at the time of starting treatment with rhGH, the dose of rhGH that was used, the age of onset/induction of puberty, the age of first menarche, the progress of growth indicators before and during puberty as well as at the end of treatment with rhGH, height changes expressed in z-score and cm, including NAH according to karyotypic groups, and, in total, including the statistical evaluation for the differences in means between the two groups.

The mean diagnosis age of all 44 TS patients who completed the rhGH therapy and achieved NAH was 12.68±3.03 years (min. 3.52; max. 14,64 years). At the time of starting the treatment, HAZ was -3.62±0.96 z-score (min. -5.49; max. -0,93 z-score), BMI for age z-score was 0.19±1.28 z-score (min. -2.61; max. 3.81 z-score), and BA for all 44 patients was 10.22±2.57 years with BAD 2.46±0.71 years. The treatment duration with rhGH was 3.60±2.26 years (min. 1.01; max. 9.88 years). All patients started puberty at 13.58±1.78 years (min. 9.65; max. 15.81 years), and at the age of 14.68±1.55 years, they experienced their first menstrual bleeding. Out of 44

patients, 6 (13.6%) had spontaneous breast development, and 4 (9.1%) had complete spontaneous pubertal development with menarche. Nine of them had pubertal arrest and subsequently received estrogen-progestin replacement. At the time before onset/induction of puberty, they had -3.11±1.04 z-score, gaining from the start of treatment to that time 0.50±0.46 z-score and over the entire period of puberty 0.38±0.56 z-score in the height. Moreover, these changes were statistically significant (P=0.000). After the entire treatment period mentioned above, all 44 patients reached NAH expressed in the HAZ at the end of treatment with -2.73±0.87 z-score, benefiting from the start of treatment, a total of HAZ gained by 0.88±0.56 in z-score, and this means change is statistically significant (Table 2). At the end of the rhGH therapy, all the patients grew by 17.70±12.53 cm, but only 6 (13.6%) patients reached the target projection for MPH.

The Pearson correlation analysis was performed between HAZ at the end of treatment and near-final height in cm with various parameters. The results showed that only six variables had a good correlation with HAZ at the end of treatment in our patients: HAZ at the start of treatment, treatment duration, HAZ before induced puberty, BMI z-score at the start of therapy, rhGH dose, and MPH; HAZ before induced puberty and HAZ at the start of treatment showed the strongest correlation with HAZ at the end of treatment (Figure 2).

Other variables, such as the age at starting treatment, BA at starting treatment, BAD, and age of induced puberty, had negative correlations with HAZ at the end of treatment, but they were not statistically significant.

On the other hand, NAH expressed in cm also correlated well with variables mentioned above: HAZ at start of treatment, treatment duration, HAZ before induced puberty, BMI z-score at start of therapy, rhGH dose, and MPH; HAZ before induced puberty and HAZ at start of treatment showed the strongest correlation with HAZ at the end of treatment (Figure 3). Other variables, such as age at starting treatment, BA at starting treatment, BAD, and age of induced puberty, had weak negative correlations with HAZ at the end of treatment.

Table 2.

The characteristics of patients at the start of treatment and the progress of growth indicators during treatment.

	Monosomy (A)	Non – monosomy (B, C, D, E)	*P*-value	Total
N	21	23		44
Age at starting treatment, years	12.62±3.26	12.74±2.88	0.899	12.68±3.03
Dose of rhGH, mg/kg/day	0.04±0.008	0.05±0.074	0.344	0.05±0.077
HAZ-score at the start of treatment	-3.87±0.88	-3.38±1.00	0.091	-3.62±0.96
BMI z-score at the start of treatment	-0.08±1.13	0.44±1.39	0.176	0.19±1.28
BA at starting treatment, years	10.15±2.84	10.29±2.37	0.858	10.22±2.57
BAD, years	2.47±0.63	2.44±0.78	0.915	2.46±0.71
MPH, cm	162.04±6.59	164.13±7.30	0.328	163.13±6.97
Age of induced puberty, years	13.35±1.80	13.78±1.78	0.426	13.58±1.78
Age of first menarche, years	14.38±1.63	15.02±1.46	0.226	14.68±1.55
Age at the end of treatment, years	15.88±1.47	16.64±1.72	0.124	16.28±1.63
Treatment duration, years	3.26±2.20	3.91±2.32	0.353	3.60±2.26
BMI z-score before puberty induced	-0.06±1.16	0.56±1.17	0.085	0.26±1.19
BMI z-score at the end of treatment	0.40±1.15	0.88±0.89	0.129	0.65±1.04
HAZ-score before puberty induced	-3.42±0.99	-2.83±1.04	0.061	-3.11±1.04
Δ-HAZ change before puberty	0.45±0.41	0.55±0.51	0.489	0.50±0.46
Δ-HAZ change during puberty	0.325±10.48	0.43±0.64	0.553	0.38±0.56
Δ-HAZ change during treatment	0.78±0.34	0.98±0.70	0.245	0.88±0.56
HAZ-score at the end of treatment	-3.10±0.73	-2.40±0.87	0.007	-2.73±0.87
Δ-cm change during treatment	17.68±13.14	17.72±12.25	0.992	17.70±12.53
NAH, cm	142.15±5.28	146.76±6.88	0.017	144.56±6.53

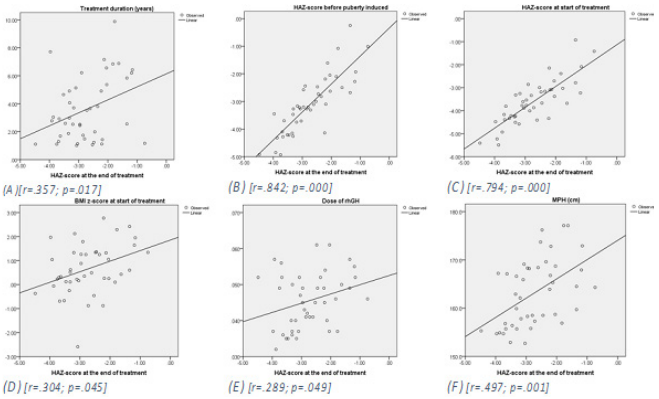

Fig. 2. *Correlations of HAZ score at the end of treatment with (A) Treatment duration, (B) HAZ score before puberty induced, (C) HAZ score at the start of treatment, (D) BMI z-score at start of treatment, (E) Mean rhGH dose and (F) MPH.*

Characteristics of patients and results of treatment under the perspective of chromosomal groups

When starting treatment, the patient age in the MG and n-MG was 12.62±3.26 and 12.74±2.88 years, respectively. No statistically significant difference was identified about the age of diagnosis/start of therapy between karyotypic groups (*P*=0.899).

At the start of the treatment, BA was 0.14 years older in the n-MG, and the BAD was 0.023 years smaller in the n-MG. However, this difference in means between the two groups for those parameters was not statistically significant (*P*=0.858 and *P*=0.915, respectively). Treatment duration with rhGH was longer in the n-MG (3.91±2.32 years), compared to the MG (3.26±2.20 years), but this difference was not statistically significant (*P*=0.353).

The most pronounced shortness at the beginning of therapy was identified in the MG (*3.87*±0.88 z-score), compared to the n-MG (*3.38*±1.00 z-score), but this difference was not statistically significant (*P*=0.091) (Figure 3A). No statistically significant difference was identified in BMI for age between the two groups (*P*=0.176). The MG started puberty slightly earlier than the n-MG (13.35±1.80 vs 13.78±1.78 years), but this difference was not statistically significant. The MG experienced their first menstrual bleeding a little earlier than the n-MG (14.38±1.63 vs 15.02±1.46), but this difference was not statistically significant. Before the onset/induction of puberty, the MG was shorter than the n-MG (-3.42±0.99 vs. -2.83± 1.04 z-score), and this difference was not statistically significant (Figure 3B); both groups gained height throughout the pubertal period with no statistically significant differences between the two groups.

The n-MG had a better total height gained than the MG in Δ-HAZ (0.98±0.70 z-score vs. 0.78±0.34 z-score) (Figure 3D) and in cm (17.72±12.25 cm vs. 17.68±13.14 cm) (Figure 3E), but these changes were not statistically significant. NAH expressed in HAZ at the end of treatment was better in the n-MG (-2.40±0.87 z-score) than in the MG (-3.10±0.73 z-score), with statistically significant differences (Figure 3C). Moreover, the NAH expressed in cm was better in the n-MG (146.76±6.88 cm) than in the MG (142.15±5.28 cm), and these changes were statistically significant (*P*=0.017) (Figure 3F).

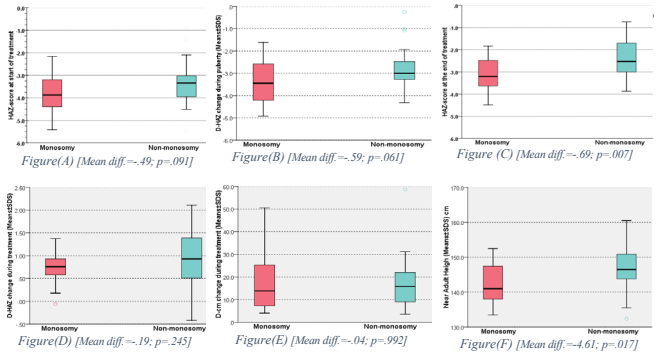

Fig. 3. *Differences in means between monosomy and non-monosomy groups for (A) HAZ score at baseline, (B) Δ-HAZ change during puberty, (C) HAZ-score at the end of the treatment, (D) Δ-HAZ change during treatment, (E) HAZ-cm change during treatment, (F) NAH.*

Analysis according to chromosomal subgroups, showed that the best result of NAH expressed in z-score was in Subgroup D ("Mosaic form with presence of Y chromosome") with -1.94 z-score followed by Subgroup C ("Mosaic form with numeric anomaly") with -2.43 z-score, Subgroup B ("Mosaic form with Structural Abnormalities of the X Chromosome") with -2.45 z-score, Subgroup E ("Non-mosaic 46, X, der(X)") with -2.70 z-score and finally Subgroup A ("Monosomy") with -3.09 z-score (Figure 4). Differences in the means of heights in z-score between chromosomal subgroups were statistically significant (*P*=0.035).

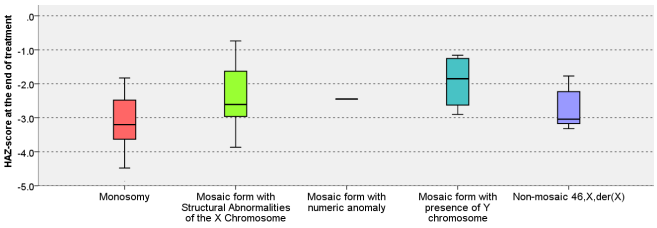

Fig. 4. *HAZ-score at the end of treatment based on chromosomal subgroups.*

Discussion

This study reflected our experiences using rhGH in TS patients. It is now well known that using rhGH effectively improves adult height in patients with TS. Our patients improved NAH by 0.88 z-score throughout treatment, or 17.7 cm in height from the start of treatment for a total duration of 3.6 years. As in the other indications for the use of rhGH, such as GH deficiency, the results depend on many different factors, such as the age at the start of the therapy, such as the duration of the treatment, the dose of the medication, the height for the age at the beginning of the treatment, the time of the onset of puberty, and MPH (which reflects the genetic

predisposition for height). From these points of view, we analyzed the results of our study.

The final height in our study showed good positive correlations with HAZ at the start of treatment, the treatment duration, HAZ before puberty was induced, BMI z-score at the beginning of treatment, rhGH dose, and MPH. Other indicators, such as the age at starting treatment, BA at starting treatment, BAD, and age of induced puberty, had a weak negative correlation with HAZ at the end of treatment.

A significant factor that could influence the therapy and its results is the age at which treatment was started. It was shown that the best response to the treatment was correlated with the age of starting treatment, whereby the girls with TS who began the therapy earlier tended to grow better.[5,6] The duration of the treatment is generally a function of the age at the start of the treatment, which means that the younger the age at the start of the treatment, the longer the treatment period. From this point of view, our patients started the treatment relatively late, compared to other studies. A study by Rosenfeld et al.[7] showed that long-term treatment with doses higher than the replacement doses applied in treating GH deficiency could increase height during childhood and final adult height in TS. In that study, with two groups of patients with TS separated into those who used only GH and the group that used GH and oxandrolone, the age at the start of GH therapy was 9.1 years and 9.9 years, respectively; the duration of treatment was 7.6 years and 6.1 years, and final height was 150.4 cm and 152.1 cm, respectively. Compared to that study, the age of our patients was 12.6 years, older than the ten years of the Rosenfeld et al. study. Our patients continued the therapy for about 3.6 years, approximately half of the treatment time of the study above, and gained during the entire treatment period about 17.7 cm in height with an average annual growth of 4.9 cm/year and reaching a near-final height of 144.56 cm, significantly shorter than the patients in the study above. Another study[8] indicated that when GH therapy was initiated at nine years of age, final height improved by approximately 8 cm/year, against a height gain of approximately 6 cm/year when therapy was started at 11-13 years, therefore, recommendations for the diagnosis and management of TS state that ''initiation of GH therapy should be considered as soon as a patient with TS has dropped below the fifth percentile of the normal female growth curve."[9] Growth failure sometimes begins prenatally, and most girls with TS demonstrate growth failure within the first 3 years of life.

Other factors that could influence the therapy and its results are the height of the parents and HAZ before starting puberty. In our study, MPH showed an excellent correlating variable with NAH and HAZs at the end of treatment, which shows the genetic influence on height growth. However, only six patients (13.6%) reached the MPH target after treatment. The pubertal spurt is absent even in those girls with spontaneous pubertal development. These alterations make short stature (a 20cm deficit in the final height) one of the main features of TS.[10] Patients with TS gain more height during the prepubertal period than in the pubertal period. Even in our study, the gain in height z-score was more significant during the period before the induction of puberty (0.50±0.46 z-score), compared to that during the pubertal period (0.38±0.56 z-score).

Besides the classic karyotype 45,X, other karyotype abnormalities can occur in TS, such as duplications of the long arm (q) of the X chromosome with concurrent loss of the short arm (p) to constitute an isochromosome (isoXq); ring formation (rX); deletions of the short and long arm of the X chromosome (Xp- or Xq-); mosaicisms (45, X/46, XX); or karyotypes with the presence of the entire Y chromosome or parts of it.[11] Patients with TS and deletions at the end of the short arm of the X chromosome (Xp-), including haploinsufficiency of the *SHOX* gene, have short stature and different orthopedic abnormalities.[12] Most girls with TS inherit just one copy of the *SHOX* gene. This state of haploinsufficiency seems to be substantially responsible for the height deficit in these patients.[13,14]

In our study, we analyzed the result of the treatment from the point of view of chromosomal abnormalities. The analysis of the results showed that the outcomes of rhGH treatment were better in the non-monosomy group than in the monosomy group. In a study similar to our research carried out in Poland [15] involving 57 patients with TS, treated for three years, the authors concluded that the use of rhGH improves the length of all abnormal karyotypic groups of TS patients, but these results were more satisfactory in patients with marker chromosome or Y chromosome and patients with X-mosaicism. It should be noted that the 3.6-year therapy using rhGH improved the height of all groups of our patients with TS expressed in terms of NAH and HAZ at the end of treatment. Although there were no statistical differences in means regarding HAZ at the start of therapy, treatment dose, duration of treatment, and MPH between groups with monosomy and non-monosomy, the best outcomes were achieved in patients with mosaic form with the presence of the Y chromosome and in patients with mosaic form with structural abnormalities of the X chromosome.

TS patients with monosomy (45,X) and non-mosaic 46,X, der(X) had a shorter final height than patients with other chromosome abnormalities. Some other studies [16,17] reached the same conclusion: TS patients with the karyotype 45,X, and patients with isochromosomes of the long arm of X tend to have a shorter final height than patients with other types of chromosome abnormalities.

Conclusion

Treatment with rhGH is effective in Albanian pediatric patients with TS. Our study showed that treatment started relatively late, approximately 12.7 years, with the recommended doses (0.05 mg/kg/day) in a relatively short period, compared to studies in the literature (approximately 3.6 years), resulting in NAH for all patients, which is considered a significant improvement, compared to HAZ at the beginning of treatment. Our pediatric population with TS recovered in height of approximately 0.9 z-score or 17.7 cm for about 3.6 years of therapy with a growth velocity of 4.9 cm/year. Based on our results, we conclude that only a minority of 6 out of 44 children with TS treated with GH achieved their genetic height

potential, benefiting more in height during the prepubertal period than in the pubertal period. Better outcomes of rhGH treatment were observed in the non-monosomy group than in the monosomy group.

Moreover, the best results were obtained in the subgroups with marker or Y chromosomes and in patients with X-mosaicism within the non-monosomy group. This study highlighted the importance of early diagnosis and starting early treatment in children with TS. This is to ensure adequate duration of therapy to optimize the prepubertal growth so that the height prognosis of these children can be further improved. Of course, the treatment results depend on many other factors, including the type of karyotypic anomaly.

Competing Interests

The authors declare that they have no competing interests.

References

1. Saenger P. Turner's syndrome. N Engl J Med. 1996 Dec 5;335(23):1749-54. doi: 10.1056/NEJM199612053352307. PMID: 8929268.
2. Rao E, Weiss B, Fukami M, Rump A, Niesler B, Mertz A, Muroya K, Binder G, Kirsch S, Winkelmann M, Nordsiek G, Heinrich U, Breuning MH, Ranke MB, Rosenthal A, Ogata T, Rappold GA. Pseudoautosomal deletions encompassing a novel homeobox gene cause growth failure in idiopathic short stature and Turner syndrome. Nat Genet. 1997 May;16(1):54-63. doi: 10.1038/ng0597-54. PMID: 9140395.
3. WHO. Child growth standards. Available at: http://www.who.int/childgrowth/software/en/
4. Greulich WW, Pyle S. I. Radiographic Atlas of Skeletal Development of the Hand and Wrist. Stanford: Stanford University Press; 1959.
5. Wasniewska M, Aversa T, Mazzanti L, Guarneri MP, Matarazzo P, De Luca F, Lombardo F, Messina MF, Valenzise M. Adult height in girls with Turner syndrome treated from before 6 years of age with a fixed per kilogram GH dose. Eur J Endocrinol. 2013 Sep 13;169(4):439-43. doi: 10.1530/EJE-12-1032. PMID: 23904278.
6. Ross J, Lee PA, Gut R, Germak J. Impact of age and duration of growth hormone therapy in children with Turner syndrome. Horm Res Paediatr. 2011;76(6):392-9. doi: 10.1159/000333073. Epub 2011 Nov 29. PMID: 22156541.
7. Rosenfeld RG, Attie KM, Frane J, Brasel JA, Burstein S, Cara JF, Chernausek S, Gotlin RW, Kuntze J, Lippe BM, Mahoney CP, Moore WV, Saenger P, Johanson AJ. Growth hormone therapy of Turner's syndrome: beneficial effect on adult height. J Pediatr. 1998 Feb;132(2):319-24. doi: 10.1016/s0022-3476(98)70452-4. PMID: 9506648.
8. Ricotti S, Petrucci L, Carenzio G, Klersy C, Calcaterra V, Larizza D, Dalla Toffola E. Prevalence and incidence of scoliosis in Turner syndrome: a study in 49 girls followed-up for 4 years. Eur J Phys Rehabil Med. 2011 Sep;47(3):447-53. Epub 2011 Apr 20. PMID: 21508910.
9. Saenger P, Wikland KA, Conway GS, Davenport M, Gravholt CH, Hintz R, Hovatta O, Hultcrantz M, Landin-Wilhelmsen K, Lin A, Lippe B, Pasquino AM, Ranke MB, Rosenfeld R, Silberbach M; Fifth International Symposium on Turner Syndrome. Recommendations for the diagnosis and management of Turner syndrome. J Clin Endocrinol Metab. 2001 Jul;86(7):3061-9. doi: 10.1210/jcem.86.7.7683. PMID: 11443168.
10. Blum WF, Cao D, Hesse V, Fricke-Otto S, Ross JL, Jones C, Quigley CA, Binder G. Height gains in response to growth hormone treatment to final height are similar in patients with SHOX deficiency and Turner syndrome. Horm Res. 2009;71(3):167-72. doi: 10.1159/000197874. Epub 2009 Feb 3. PMID: 19188742.
11. Hjerrild BE, Mortensen KH, Gravholt CH. Turner syndrome and clinical treatment. Br Med Bull. 2008;86:77-93. doi: 10.1093/bmb/ldn015. Epub 2008 Apr 9. PMID: 18400842.
12. Hintz RL. SHOX mutations. Rev Endocr Metab Disord. 2002 Dec;3(4):363-7. doi: 10.1023/a:1020909925921. PMID: 12424438.
13. Guedes AD, Bianco B, Callou EQ, Gomes AL, Lipay MV, Verreschi IT. O hormônio de crescimento na síndrome de Turner: dados e reflexões [Growth hormone treatment inTurner syndrome: data and reflections]. Arq Bras Endocrinol Metabol. 2008 Jul;52(5):757-64. Portuguese. doi: 10.1590/s0004-27302008000500007. PMID: 18797582.
14. Jorge AA, Nishi MY, Funari MF, Souza SC, Arnhold IJ, Mendonça BB. Baixa estatura por haploinsuficiência do gene SHOX: do diagnóstico ao tratamento [Short stature caused by SHOX gene haploinsufficiency: from diagnosis to treatment]. Arq Bras Endocrinol Metabol. 2008 Jul;52(5):765-73. Portuguese. doi: 10.1590/s0004-27302008000500008. PMID:
15. Kasprzyk J, Włodarczyk M, Sobolewska-Włodarczyk A, Wieczorek-Szukała K, Stawerska R, Hilczer M, Lewiński A. Karyotype Abnormalities in the X Chromosome Predict Response to the Growth Hormone Therapy in Turner Syndrome. J Clin Med. 2021 Oct 29;10(21):5076. doi: 10.3390/jcm10215076. PMID: 34768596; PMCID: PMC8584940.
16. Donaldson MD, Gault EJ, Tan KW, Dunger DB. Optimising management in Turner syndrome: from infancy to adult transfer. Arch Dis Child. 2006 Jun;91(6):513-20. doi: 10.1136/adc.2003.035907. PMID: 16714725; PMCID: PMC2082783.
17. Gravholt CH, Viuff MH, Brun S, Stochholm K, Andersen NH. Turner syndrome: mechanisms and management. Nat Rev Endocrinol. 2019 Oct;15(10):601-614. doi: 10.1038/s41574-019-0224-4. Epub 2019 Jun 18. PMID: 31213699.

***Corresponding author**: Agim Gjikopulli, Pediatric Endocrinology Unit, Department of Pediatric, University Hospital Center "Mother Teresa," Tirana, Albania. E-mail: agimgjikopulli21@gmail.com*

International Journal of Biomedicine 14(2) (2024) 282-285
http://dx.doi.org/10.21103/Article14(2)_OA7

ORIGINAL ARTICLE

Surgery

INTERNATIONAL JOURNAL OF BIOMEDICINE

Loose Seton Technique in the Management of Complex High Anal Fistula: Enhancing Outcomes with Magnetic Resonance Imaging

Ahmed Salim Khazaal[1*], Inas Abd Al Majed Rasheed[1], Anas Ahmed Salih[1]

[1]*Department of Surgery, College of Medicine, University of Tikrit, 314 – Yarmuk, Tikrit, Iraq*

Abstract

Background: Complex high anal fistulas challenge treatment efforts, necessitating innovative approaches that balance healing with sphincter preservation.

Methods and Results: In a prospective study at Tikrit Teaching Hospital, 39 patients with complex high anal fistulas underwent treatment with loose silicone setons, guided by preoperative MRI mapping. The efficacy of this method was evaluated through follow-up visits at 1, 3, and 6 months, focusing on fistula healing, recurrence rates, continence preservation (assessed by the Wexner Continence Score), and patient satisfaction.

Complete healing was achieved in 31 patients (79.5%), with a recurrence rate of 7.7%. There was a significant improvement in continence, with the mean Wexner score reducing from 3.5 to 1.2 (P<0.001). Moreover, 85% of patients expressed satisfaction with their treatment outcomes.

Conclusion: The combined use of loose silicone setons and MRI mapping presents an effective, satisfactory method for managing complex high anal fistulas. This technique ensures high healing rates, significantly preserves sphincter function, and achieves high patient satisfaction.**(International Journal of Biomedicine. 2024;14(2):282-285.)**

Keywords: fistula healing • sphincter preservation • MRI • patient satisfaction

For citation: Khazaal AS, Rasheed IAAM, Salih AA. Loose Seton Technique in the Management of Complex High Anal Fistula: Enhancing Outcomes with Magnetic Resonance Imaging. International Journal of Biomedicine. 2024;14(2):282-285. doi:10.21103/Article14(2)_OA7

Introduction

Complex high anal fistulas represent a significant therapeutic challenge in colorectal surgery due to their intricate course and close relationship with the anal sphincters.[1] The loose seton technique has been recognized as a sphincter-preserving method, offering a balance between effective treatment and the preservation of anal function.[2-4] However, one of the key challenges in the management of complex fistulas is the accurate identification and assessment of the fistulous tract.[5,6]

Magnetic resonance imaging (MRI) has emerged as a crucial tool in the preoperative assessment of anal fistulas, it provides detailed visualization of the fistula's path, its relationship with the sphincter complex, and any associated abscesses.[7,8] This information is vital for surgical planning; allowing for a targeted approach that minimizes sphincter disruption (Figure 1 and Figure 2).

This study aims to evaluate the effectiveness of the loose seton technique for the treatment of complex high anal fistulas, assisted by MRI for defining the fistula tract. Specifically, it seeks to assess the accuracy of fistula tract identification, the success rate of the procedure, the preservation of sphincter function, and the incidence of recurrence.

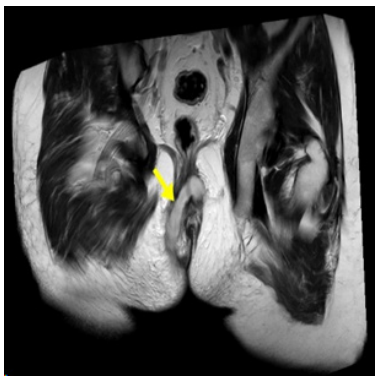

Fig. 1. *MRI T2 coronal oblique image shows a large sinus tract crossing the midline.*

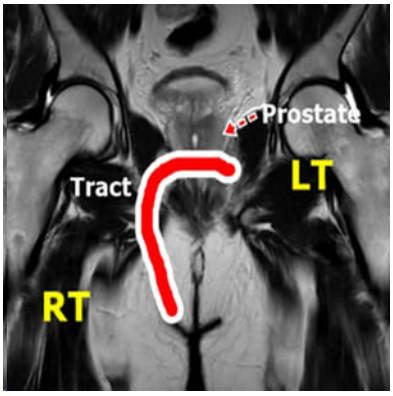

Fig. 2. *MRI T2 coronal oblique image: the red line shows the course of the sinus tract.*

Materials and Methods

Study Design and Setting

This prospective study was conducted at Tikrit Teaching Hospital, focusing on patients diagnosed with complex high anal fistulas. The study aimed to evaluate the effectiveness of the loose seton technique, enhanced by MRI, for defining the fistula tract.

A total of 39 patients were included in the study, based on the following inclusion criteria: adults aged 18 years and older; diagnosed with complex high anal fistula, as confirmed by clinical examination and preoperative MRI; no previous anal fistula surgery; consent to participate in the study.

Exclusion criteria were the presence of an acute anal abscess, low anal fistulas not involving the sphincter complex, and patients with contraindications to MRI.

Intervention

All patients underwent a detailed preoperative assessment, including MRI, to map the fistula tract. Silicone setons were used in the loose seton technique for all patients, which involved the careful placement of the seton to allow for drainage and gradual fistula-tract fibrosis without cutting through the sphincter muscle.

Surgical Procedure

The procedure was performed under general anesthesia. Following the MRI and proctoscopic evaluations, the external opening of the fistula was identified and cannulated with a probe. A silicone seton was then threaded through the tract and loosely tied around the sphincter muscle to avoid tension. Silicone was chosen as the material for the seton due to its biocompatibility, flexibility, and minimal irritation to the surrounding tissues.

Postoperative Care and Follow-up

Patients were discharged with instructions on seton care, including hygiene and monitoring for signs of infection. Follow-up visits were scheduled at 1, 3, and 6 months postoperatively, including clinical examination and a repeat MRI at the last follow-up to assess fistula healing and any changes in the fistula tract.

Outcome Measures

The primary outcomes measured were the healing rate of the fistula, defined as the closure of the external opening and absence of discharge; recurrence rate within the follow-up period; preservation of continence assessed using the Wexner Continence Score; and patient satisfaction, measured through a post-treatment questionnaire.

Statistical Analysis

Statistical analysis was performed using the statistical software package SPSS version 25.0 (SPSS Inc, Armonk, NY: IBM Corp). Descriptive statistics were used to summarize patient demographics and clinical characteristics. The Kaplan-Meier method was employed to estimate healing and recurrence rates. The significance of differences between preoperative and postoperative continence scores was evaluated using the paired t-test, with a P-value < 0.05 considered statistically significant.

Results

The study included 39 patients (28 males and 11 females) with an average age of 45±12 years (range 18-65 years). All patients presented with symptoms of complex high anal fistulas and underwent the specified treatment protocol at Tikrit Teaching Hospital (Table 1).

Table 1.

Patient Demographics and Clinical Characteristics.

Characteristic	Value
Total number of patients	39
Age (years), (mean ± SD)	45 ± 12
Gender (Male/Female)	28/11
Previous fistula surgery	No
Type of fistula (according to MRI) Transsphincteric Suprasphincteric	 25 4

Fistula Healing and Recurrence Rates

At the end of the 6-month follow-up period, 31(79.5%) out of 39 patients showed complete fistula healing. The recurrence rate was observed in 3(7.7%) patients. The Kaplan-Meier survival analysis indicated a significant improvement in fistula healing over the follow-up period (P<0.05) (Table 2).

Table 2.

Fistula Healing and Recurrence Rates.

Outcome	Number of Patients	Percentage
Complete healing	31	79.5%
Recurrence	3	7.7%
No change	5	12.8%

Continence Preservation

Continence was assessed using the Wexner Continence Score. Preoperative scores ranged from 0 to 12 (mean 3.5±2.1). Postoperatively, scores improved significantly, with a mean postoperative score of 1.2±1.5, indicating a significant preservation of continence following the procedure (P<0.05) (Table 3).

Table 3.

Continence Scores Pre- and Post-Procedure.

Time Point	Mean Wexner Score	SD	*P*-value
Preoperative	3.5	2.1	<0.001
Postoperative	1.2	1.5	

Patient Satisfaction

The patient satisfaction questionnaire revealed that 85% of patients were satisfied or very satisfied with the outcome of their treatment, reporting improved quality of life without significant discomfort or incontinence issues (Table 4).

Table 4.

Patient Satisfaction Survey Results.

Satisfaction Level	Number of Patients	Percentage
Very satisfied	20	51.3%
Satisfied	13	33.3%
Neutral	4	10.3%
Unsatisfied	2	5.1%
Very unsatisfied	0	0%

Discussion

The present study's findings indicate a promising approach to managing complex high anal fistulas, with a significant healing rate of 79.5% and a low recurrence rate of 7.7% over a 6-month follow-up period. These outcomes are notable, considering the complexity of the fistulas treated and the priority placed on sphincter preservation. Integrating MRI for surgical planning and using loose silicone setons has contributed to these favorable outcomes.

The use of MRI in the preoperative assessment aligns with the recommendations of recent studies, which highlight its utility in accurately mapping fistula tracts and identifying associated abscesses. This accuracy in mapping is crucial for surgical planning, particularly for complex fistulas, where traditional examination methods may not suffice.[11,12]

The significant preservation of continence observed, with an improvement in Wexner Continence Scores postoperatively, underscores the importance of sphincter-preserving approaches. These findings are consistent with the work of several studies, which also reported high rates of continence preservation using similar techniques.[13-16]

Patient satisfaction levels reported in this study reinforce the clinical relevance of these outcomes. The high satisfaction rate among participants suggests that combining MRI with the use of loose silicone setons not only addresses the physical aspects of fistula management but also positively impacts patients' quality of life. This aspect of treatment is increasingly recognized in the literature as an essential measure of success.[17-19]

Conclusion

This study contributes valuable insights into the management of complex high anal fistulas, highlighting the efficacy of a multimodal approach involving MRI and loose silicone setons. As the field evolves, continued innovation and research are essential to refine these techniques and improve patient outcomes.

Acknowledgments

We thank the staff and workers of the Department of Surgery at Tikrit Teaching Hospital for their general support.

Disclaimer

We state that the views expressed in the submitted article are ours and not an official position of the institution.

Competing Interests

The authors declare that they have no competing interests.

References

1. Cadeddu F, Salis F, Lisi G, Ciangola I, Milito G. Complex anal fistula remains a challenge for colorectal surgeon. Int J Colorectal Dis. 2015 May;30(5):595-603. doi: 10.1007/s00384-014-2104-7. Epub 2015 Jan 9. PMID: 25566951.
2. Huang H, Ji L, Gu Y, Li Y, Xu S. Efficacy and Safety of Sphincter-Preserving Surgery in the Treatment of Complex Anal Fistula: A Network Meta-Analysis. Front Surg. 2022 Feb 8;9:825166. doi: 10.3389/fsurg.2022.825166. PMID: 35211503; PMCID: PMC8861434.
3. Hong Y, Xu Z, Gao Y, Sun M, Chen Y, Wen K, Wang X, Sun X. Sphincter-Preserving Fistulectomy Is an Effective Minimally Invasive Technique for Complex Anal Fistulas. Front Surg. 2022 Mar 22;9:832397. doi: 10.3389/fsurg.2022.832397. PMID: 35392057; PMCID: PMC8980274.
4. Kršul D, Karlović D, Bačić Đ, Zelić M. Sphincter preserving techniques in anal fistula treatment [Internet]. Current Topics in Colorectal Surgery. IntechOpen; 2023. Available from: http://dx.doi.org/10.5772/intechopen.99547.
5. Garg P, Sodhi SS, Garg N. Management of Complex Cryptoglandular Anal Fistula: Challenges and Solutions. Clin Exp Gastroenterol. 2020 Nov 11;13:555-567. doi: 10.2147/CEG.S198796. PMID: 33204136; PMCID: PMC7667587.

6. Bubbers EJ, Cologne KG. Management of Complex Anal Fistulas. Clin Colon Rectal Surg. 2016 Mar;29(1):43-9. doi: 10.1055/s-0035-1570392. PMID: 26929751; PMCID: PMC4755767.
7. Kummari S, Burra KG, Reddy VRK, Das S, Ramadugu R, Ramadugu S. The Role of Magnetic Resonance Imaging in Pre-operative Assessment of Anorectal Fistula With Surgical Correlation. Cureus. 2024 Jan 30;16(1):e53237. doi: 10.7759/cureus.53237. PMID: 38425597; PMCID: PMC10903756.
8. Vo D, Phan C, Nguyen L, Le H, Nguyen T, Pham H. The role of magnetic resonance imaging in the preoperative evaluation of anal fistulas. Sci Rep. 2019 Nov 29;9(1):17947. doi: 10.1038/s41598-019-54441-2. PMID: 31784600; PMCID: PMC6884577.
9. Bouchra B, Madany A, Murad A, Kabbash M, Maher H. Magnetic resonance imaging in the workup of patients with perianal fistulas. Egyptian Journal of Radiology and Nuclear Medicine. 2023;54. doi: 10.1186/s43055-023-00975-5.
10. Garg P. Comparison of Preoperative and Postoperative MRI After Fistula-in-Ano Surgery: Lessons Learnt from An Audit of 1323 MRI At a Single Centre. World J Surg. 2019 Jun;43(6):1612-1622. doi: 10.1007/s00268-019-04926-y. PMID: 30706106.
11. Bayrak M, Altintaş Y, Alabaz Ö, Çelİktaş M. Contribution of preoperative magnetic resonance imaging in diagnosis and surgical treatment of anal fistula. Cukurova Med J. 2020;45(3):1210–1216.
12. Varghese S, Nunna KC. Patterns of perianal fistula in magnetic resonance imaging and its usefulness in their pre surgical evaluation. J Evolut Med Dent Sci-JEMDS. 2018;7(21):2621–2627.
13. Zheng L, Shi Y, Zhi C, Yu Q, Li X, Wu S, Zhang W, Liu Y, Huang Z. Loose combined cutting seton for patients with high intersphincteric fistula: a retrospective study. Ann Transl Med. 2020 Oct;8(19):1236. doi: 10.21037/atm-20-6123. PMID: 33178768; PMCID: PMC7607110.
14. Eitan A, Koliada M, Bickel A. The use of the loose seton technique as a definitive treatment for recurrent and persistent high trans-sphincteric anal fistulas: a long-term outcome. J Gastrointest Surg. 2009 Jun;13(6):1116-9. doi: 10.1007/s11605-009-0826-6. Epub 2009 Feb 24. PMID: 19238493.
15. Schrader L, Brandstrup B, Olaison G. Slowly cutting, loose seton ligature and staged fistulotomy for healing of idiopathic perianal fistula and influence on anal continence. Langenbecks Arch Surg. 2023 Sep 7;408(1):352. doi: 10.1007/s00423-023-03005-0. PMID: 37673848; PMCID: PMC10482758.
16. George Pinedo M, Gino Caselli M, Gonzalo Urrejola S, Sergio Niklitschek L, María Elena Molina P, Felipe Bellolio R, et al. Modified loose-seton technique for the treatment of complex anal fistulas. Colorectal Dis. 2010;12(10 Online):e310-3. doi:10.1111/j.1463-1318.2010.02195.x.
17. García-Aguilar J, Davey CS, Le CT, Lowry AC, Rothenberger DA. Patient satisfaction after surgical treatment for fistula-in-ano. Dis Colon Rectum. 2000 Sep;43(9):1206-12. doi: 10.1007/BF02237422. PMID: 11005484.
18. Ferrer-Márquez M, Espínola-Cortés N, Reina-Duarte A, Granero-Molina J, Fernández-Sola C, Hernández-Padilla JM. Design and Psychometric Evaluation of the Quality of Life in Patients With Anal Fistula Questionnaire. Dis Colon Rectum. 2017 Oct;60(10):1083-1091. doi: 10.1097/DCR.0000000000000877. PMID: 28891853.
19. Ferrer-Márquez M, Espínola-Cortés N, Reina-Duarte Á, Granero-Molina J, Fernández-Sola C, Hernández-Padilla JM. Analysis and description of disease-specific quality of life in patients with anal fistula. Cir Esp (Engl Ed). 2018 Apr;96(4):213-220. English, Spanish. doi: 10.1016/j.ciresp.2017.12.003. Epub 2018 Feb 13. PMID: 29452968.

***Corresponding author:** Ahmed Salim Khazaal, MBChB, FICMS, Assistant Professor in Surgery, Head of Department University of Tikrit, College of Medicine. 314 – Yarmuk, Tikrit, Iraq. E-mail: ahmed.salim@tu.edu.iq*

International Journal of Biomedicine 14(2) (2024) 286-290
http://dx.doi.org/10.21103/Article14(2)_OA8

ORIGINAL ARTICLE

Radiology

INTERNATIONAL JOURNAL OF BIOMEDICINE

Quantitative Analysis of ^{99m}Tc-MDP SPECT-CT Data in Diagnosing Bone Metastases in Breast Cancer Patients

Nora Almuqbil[1], Sahar Mansour[1*], Sadem Alnuwaiser[1], Rema bin Ghamlas[1], Methail Alduwaysan[1], Ruyuf Alghofaili[1], Sadeem Alotaibi[1], Nouf Alqahtani[1], Huda Saad[1]

[1]*Radiological Sciences Department, College of Health and Rehabilitation Sciences, Princess Nourah bint Abdulrahman University, Riyadh, Saudi Arabia*

Abstract

Background: In patients with advanced breast cancer (BC), distant metastases happen mainly in the skeleton. This study aimed to investigate the role of ^{99m}Tc-MDP SPECT/CT in the differential diagnosis of malignant bone lesions from degenerative benign bone diseases in female BC patients.

Methods and Results: The study included 39 female BC patients who underwent a baseline ^{99m}Tc-MDP SPECT/CT bone scans. After lesion detection, a quantitative radiotracer uptake analysis was conducted, and the standardized uptake value (SUVmax) was identified in each patient, and the data were then statistically analyzed. SUVmax values were significantly higher in BC patients with malignant metastasis than in patients with degenerative changes (33.04±15.3 vs. 13.25±5.46 g/mL, $P<0.05$). The SUVmax cut-off value of 22.75 g/mL (25th percentile) obtained through box plot analysis can help to discriminate metastatic from degenerative lesions. The logistic regression analysis indicated that the SUVmax was a significant predictor of metastatic BL ($P<0.001$, OR = 159.90, B=5.07).

Conclusion: Our results suggested that quantitative analysis of the ^{99m}Tc-MDP SPECT-CT data can improve diagnostic accuracy in differentiating malignant metastatic bone lesions from degenerative bone lesions in high-risk BC patients.**(International Journal of Biomedicine. 2024;14(2):286-290.)**

Keywords: breast cancer • metastatic bone lesions • ^{99m}Tc-MDP • SPECT/CT • quantitative analysis

For citation: Almuqbil N, Mansour S, Alnuwaiser S, Ghamlas R, Alduwaysan M, Alghofaili R, Alotaibi S, Alqahtani N, Saad H. Quantitative Analysis of ^{99m}Tc-MDP SPECT-CT Data in Diagnosing Bone Metastases in Breast Cancer Patients. International Journal of Biomedicine. 2024;14(2):286-290. doi:10.21103/Article14(2)_OA8

Abbreviations

^{99m}Tc-MDP, ^{99m}Tc-labelled methylene diphosphonate; **BC**, breast cancer; **BL**, bone lesions; **DC**, degenerative changes; **SPECT/CT**, single photon emission computed tomography combined with computed tomography; **SUVmax**, standardized uptake value; **VOI**, volume of interest.

Introduction

Worldwide, BC is the most frequent tumor and occupies the first position in terms of incidence among women and the fifth position in terms of mortality.[1,2] For females, BC, colorectal cancer, and lung cancer account for 51% of all new diagnoses, with BC alone accounting for 32% of patients.[3] In Saudi Arabia, epidemiological studies reported that BC incidence was 19.8% of all tumor patients.[4,5]

In patients with advanced BC, distant metastases happen mainly in the skeleton. It was reported that 30%-85% of BC cases will develop bone metastases.[6,7] The thoracic spine, pelvis, and sternum are the most susceptible sites to metastases. However, some other bones are also involved in metastases, such as the femur, skull, and pelvis.[8-10] Bone metastases usually cause skeleton-related events such as hypercalcemia, pain, bone fractures, and spinal cord compression; thus, bone metastases in BC patients heavily affect patients' prognosis, life quality, and therapy procedure.[11] Consequently, skeletal metastasis response assessment and early diagnosis are even more important.[12,13] Moreover, sometimes, it is very difficult to make a differential diagnosis between degenerative benign and

malignant bone disease.[14] Despite planar bone scanning's, well-known limitations, such as poor specificity in response assessment and staging, it remains the main technique for detecting and staging skeleton lesions in cases of bone metastases risk.[7,15] Bone scanning accuracy is significantly improvable with the addition of single photon emission computed tomography combined with computed tomography (SPECT/CT).[16,17]

For visualizing skeletal lesions, bone scintigraphy using ^{99m}Tc-labelled methylene diphosphonate (^{99m}Tc-MDP) is the most frequent examination, including primarily either cancers or metastatic sites in other tumors, like BC.[7,13] To evaluate bone metastasis, whole-body bone scans using ^{99m}Tc-MDP are the most routine test.[18] The ^{99m}Tc-MDP biological distribution reveals high uptake in the urinary system and skeletal structure.[7]

This study aimed to investigate the role of ^{99m}Tc-MDP SPECT/CT in the differential diagnosis of malignant BL from degenerative benign bone diseases in female BC patients using an SUV (standardized uptake value) cut-off value.

Materials and Methods

Study design and patients' coherent and imaging protocol

Data were collected retrospectively, from January 2016 to March 2023. The information was gathered from two distinct database sources. The study included 39 female patients with BC. All patients underwent a baseline ^{99m}Tc-MDP SPECT/CT bone scan before their treatment, for staging purposes. However, any patients who had received therapy were excluded from the study.

The first database source was from Riyadh City Hospitals (Saudi Arabia). Patients had a baseline SPECT/CT. The dose was calculated using the patient's body weight, and an intravenous injection of 555-851 MBq equivalent to 15-23 mCi of ^{99m}Tc-MDP was administered. Images were taken 3 hours following the injection. A hybrid, SPECT/CT, dual-head gamma camera (GE Discovery D670) was used. Emission data were acquired using a parallel-hole, low-energy, high-resolution collimator with the patient in the supine position. The acquisition orbits were body contour orbits over 360° arcs, with 60 stops, each 6°. For 60 stops, emission data were acquired for 30 seconds per stop. The image acquisition matrix was 128×128, and the pixel size was 4.8 mm. Images were acquired on the 140 keV photo-peak with a 20% symmetrical window. SPECT was followed by CT examination with acquisition parameters of 130 kV, 100 mAs, Pitch-1, and 512×512 matrix using standard filters.

Additional secondary data were collected from an open-source platform, the Cancer Imaging Archive (TCIA), to improve the research analysis. TCIA is a service that provides a massive, publicly accessible archive of cancer-related medical images; it is financed by the Cancer Imaging Program. SPECT/CT data from University of Illinois Hospital was gathered from the second source. The patients had a bone scan for staging before they received their treatments, based on their body weight; (444–703 MBq), equivalent to 12–19 mCi of ^{99m}Tc-MDP intravenous injection, was administered, and a Siemens SPECT-CT camera was utilized to obtain the images after 3 hours of injection.

Image interpretation and quantitative assessment

The first database source images, from Riyadh City Hospital, were displayed on a workstation (GE Xeleris 4.0) for diagnosis by two experienced physicians, the initial qualitative examination was performed. As the physicians indicated, many regions with increased radiotracer activity were seen; out of the total number of patients, five were confirmed to have BC with bone metastases, with a mean age of 61±5 years. In contrast, four patients had confirmed BC but without bone metastases, with a mean age of 63±7 years. Next, Volumetrix GE Healthcare's Xeleris software was used to perform the quantitative SUV analysis using the following formula:[20]

$$SUV = \frac{C(T)}{[injected\ dose\ (Mbq)/patient\ weight(kg)]}\ ,$$

where C (T) reflects the radioactive concentration at a point in time.

The different SUVmax based on lean body mass for each patient was obtained. According to the vendor's recommendation, a volume of interest (VOI) was drawn using a multimodality computer platform, and then the SUVmax results were measured.

Regarding the second database, TCIA images revealed 13 patients with confirmed BC and bone metastasis with a mean age of 65±8 years, and 17 patients with confirmed BC and without bone metastasis with a mean age of 67±10 years. To obtain the quantitative analysis, we transferred the TCIA images to the 3D-slicer platform (version 4.10).[21] The SUVmax values were calculated from each segment using PET DICOM Extension installed on a 3D slicer.

Statistical analysis was performed using the statistical software package SPSS version 20.0 (SPSS Inc, Armonk, NY: IBM Corp). The normality of the distribution of continuous variables was tested by a one-sample Kolmogorov-Smirnov test. For comparisons between 2 independent groups, Student's t-test was applied. The boxplot was performed to define the cut-off value.[22] A logistic regression analysis was conducted to determine whether the SUV could predict the presence of degenerative or metastatic bone lesions. A probability value of $P<0.05$ was considered statistically significant.

Results

SUVmax values differentiated malignant lesions from degenerative bone changes

^{99m}Tc-MDP SPECT/CT (Figure 1) was performed for all patients, and the VOI was manually delineated for each image. We Collected the calculated SUVmax values for 39 patients with metastasis or degenerative changes (DC). In the normality test, SUVmax values of both metastasis (Figure 2A) and degenerative alterations (Figure 2B) were normally distributed. Quantitatively, SUVmax values were significantly higher in BC patients with malignant metastasis than in patients with DC (33.04±15.3 vs. 13.25±5.46 g/mL; P<0.05; Table 1). In the box plot, the cut-off was determined (25th percentile - 22.75 g/mL). The lower and upper quartiles and the median for metastasis (22.75, 45.11, and

30.27 g/mL, respectively) were higher than DC (9.50, 16.48, and 12.31 g/mL, respectively).

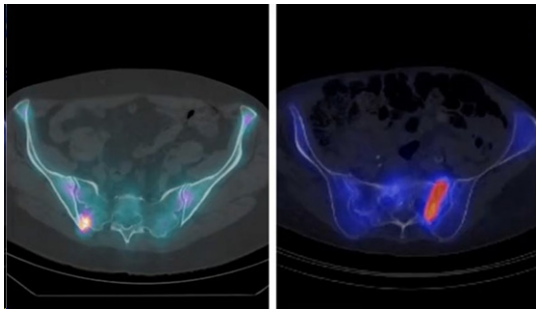

Fig. 1. *^{99m}Tc-MDP SPECT/CT bone scan of a 57-year-old female with a history of breast cancer who suffers from degenerative hip joints.*

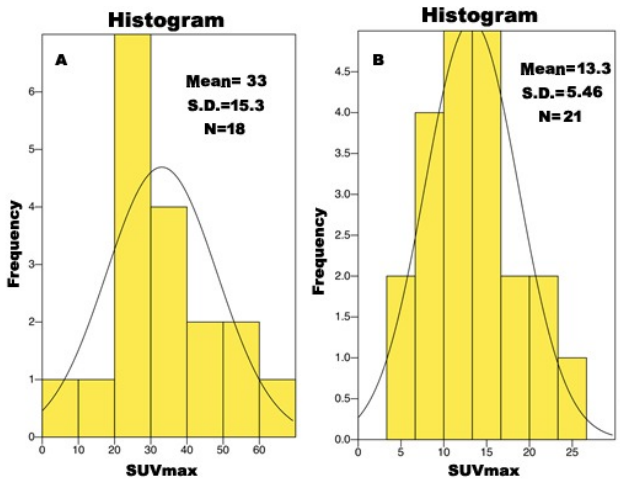

Fig. 2. *(A) SUVmax values for metastatic lesions and (B) degenerative alterations.*

Table 1.

Comparison of SUVmax values between BC patients with malignant bone metastasis and patients with benign degenerative changes.

Lesion type	Number	Minimum	Maximum	Mean	SD	t-test	*P*-value
Metastatic	18	7.44	65.8	33.04	15.3	5.21	<0.05
Degenerative	21	3.74	25.2	13.25	5.46		

Table 2.

Results of the logistic regression analysis.

Model Summary

-2 Log likelihood	Cox & Snell R Square	Nagelkerke R Square
26.76	.50	.67

Classification Table

Observed			Predicted		
			Metastasis	DC	Percentage Correct
Step 1	Patient	Metastasis	15	3	83.33
		DC	3	18	85.71
	Overall percentage				84.62

Variables in the Equation

		B	S.E.	Wald	df	Sig.	Exp(B)	95% CI for Exp(B) Lower	Upper
Step 1	SUVmax	-.24	.08	10.33	1	.001	.78	.68	.91
	Constant	5.07	1.55	10.74	1	.001	159.90		

The logistic regression analysis indicated that the SUVmax was a significant predictor of metastatic BL (P<0.001, OR = 159.90, B=5.07; Table 2).

Discussion

BC represents one of the most frequently diagnosed tumors in female patients, with up to 75% of the patients with advanced stages of BC developing malignant metastatic BL.[23] In cancer patients, a planar whole-body bone scan is a sensitive and robust imaging technique to evaluate the presence of skeletal involvement. Unfortunately, this method suffers from low specificity and cannot differentiate benign skeletal lesions from malignant ones.[7,17] Thus, early detection of bone metastasis and differentiation from degenerative benign BL using molecular imaging modalities, such as SPECT-CT, is important for patient follow-up and therapeutic purposes.[24]

This study aimed to investigate the role of ^{99m}Tc-MDP SPECT/CT in the differential diagnosis of malignant BL from degenerative benign bone diseases in female BC patients using an SUVmax cut-off value. SUVmax values calculated from ^{99m}Tc-MDP SPECT/CT bone scan were normally distributed in both metastasis and degenerative alterations. SUVmax values were significantly (P<0.05) higher in BC patients with malignant metastasis (33.04±15.3 g/mL) than in patients with degenerative changes (13.25±5.46 g/mL). The box plot revealed a cut-off equal to 22.75 g/mL, and the logistic regression analysis indicated that SUVmax was a significant predictor of metastatic BL (P<0.001, OR= 159.90, B=5.07).

Skeletal structure uptake of radioactivity usually overlaps with radiopharmaceutical accumulation in several other benign disorders and situations, such as degenerative changes, trauma, and infection.[7,25] To a certain degree, SPECT-CT imaging resolves overlying activity superimposition, which causes a more accurate anatomical localization of skeletal lesions and helps differentiate malignant and benign lesions.[7,25]

Like our findings, other authors have reported that quantitative analysis of SPECT-CT data can enhance diagnostic accuracy in differentiating degenerative benign lesions from metastatic BL, leading to better follow-up and appropriate therapy in metastatic BC patients.[24] Arvola et al.[26] compared SUVmax between ^{18}F-NaF PET/CT and ^{99m}Tc-HDP SPECT/CT in bone metastases of BC and prostate cancer. They found that the measured SUVs very strongly correlated between PET and SPECT (R^2≥0.80, P<0.001), and this demonstrates that SPECT is an applicable tool for clinical quantification of bone metabolism in bone metastases in prostate cancer and BC patients. In metastatic BL, Gherghe et al.[24] reported that the SUVmax value of SPECT-CT was significantly greater than degenerative lesions. At a comparable cut-off value (16.6 g/mL) with our results, they found that SPECT-CT revealed a specificity of 93.3% and a sensitivity of 91.5%.[24] In prostate cancer patients, Rohani et al. evaluated bone scans with ^{99m}Tc-MDP SPECT/CT in differentiating patients with bone metastases from those with degenerative joint disease.[27] SUVmax was significantly greater in bone metastases than in normal vertebrae. SUVmax cut-off value ≥20 gave a specificity of 85.4% and a sensitivity of 73.8%

in differentiating bone metastases from degenerative joint disease.[27] Also, in patients with prostate cancer, Kuji et al.[28] evaluated the role of the skeletal SUVs by ^{99m}Tc-MDP SPECT/CT for differentiating active bone metastases from degenerative changes. They found that skeletal SUVmax may be helpful indices for bone metastatic prognostication, enhancing the discrimination of active bone osteoblastic metastases from frequently coexisting degenerative changes in patients with prostate cancer. Some studies revealed that SPECT/CT using different radiotracers significantly reduced equivocal findings in diagnosing bone metastases, which implies improved diagnostic confidence.[29-31]

In conclusion, our results suggested that quantitative analysis of the ^{99m}Tc-MDP SPECT-CT data can improve diagnostic accuracy in differentiating malignant metastatic BL from degenerative BL in high-risk BC patients. In BC patients, the SUVmax cut-off value of 22.75 g/mL obtained through box plot analysis can help to discriminate metastatic from degenerative lesions. Interpatient comparison, patient follow-up, and evaluation of treatment effectiveness may represent further benefits in performing ^{99m}Tc-MDP SPECT-CT SUVmax calculation. To use these findings in clinical practice, further extensive studies are required.

Ethical Considerations

The study protocol was reviewed and approved by the Ethics Committee at Princess Nourah bint Abdulrahman University.

Competing Interests

The authors declare that they have no competing interests.

References

1. Abdelrazek MA, Nageb A, Barakat LA, Abouzid A, Elbaz R. BC-DETECT: combined detection of serum HE4 and TFF3 improves breast cancer diagnostic efficacy. Breast Cancer. 2022 May;29(3):507-515. doi: 10.1007/s12282-021-01328-8. Epub 2022 Jan 7. PMID: 34994942.
2. Shrestha R, Paudel B, Panthi B, Gyawali B, Pandey A, Khanal S, Gyawali S. Breast Cancer among Cancer Patients Visiting the Department of Internal Medicine of a Tertiary Centre. JNMA J Nepal Med Assoc. 2024 Feb 24;62(270):64-67. doi: 10.31729/jnma.8466. PMID: 38409971; PMCID: PMC10924505.
3. Siegel RL, Giaquinto AN, Jemal A. Cancer statistics, 2024. CA Cancer J Clin. 2024 Jan-Feb;74(1):12-49. doi: 10.3322/caac.21820. Epub 2024 Jan 17. Erratum in: CA Cancer J Clin. 2024 Mar-Apr;74(2):203. PMID: 38230766.
4. Ravichandran K, Hamdan NA, Dyab AR. Population based survival of female breast cancer cases in Riyadh Region, Saudi Arabia. Asian Pac J Cancer Prev. 2005 Jan-Mar;6(1):72-6. PMID: 15780037.
5. AlRajhi B, Aljadani FF, Almarwan SR, Alzahrani AA, Sindi MHM, Kano A, Alzahrani RS, Baaqeel R. Breast Cancer Awareness Among Women in Saudi Arabia: A Systematic Review. Breast Cancer (Dove Med Press). 2023 Dec 14;15:913-924. doi: 10.2147/BCTT.S426079. PMID: 38111500; PMCID: PMC10726713.
6. Hansen JA, Naghavi-Behzad M, Gerke O, Baun C, Falch K, Duvnjak S, Alavi A, Høilund-Carlsen PF, Hildebrandt MG. Diagnosis of bone metastases in breast cancer: Lesion-based sensitivity of dual-time-point FDG-PET/CT compared to low-dose CT and bone scintigraphy. PLoS One. 2021 Nov 18;16(11):e0260066. doi: 10.1371/journal.pone.0260066. PMID: 34793550; PMCID: PMC8601566.
7. Abedi SM, Mardanshahi A, Zeanali R. Added diagnostic value of SPECT to evaluate bone metastases in breast cancer patients with normal whole body bone scan. Caspian J Intern Med. 2021 Apr;12(3):290-293. doi: 10.22088/cjim.12.3.290. PMID: 34221278; PMCID: PMC8223046.
8. Gilkes DM. Implications of Hypoxia in Breast Cancer Metastasis to Bone. Int J Mol Sci. 2016 Sep 30;17(10):1669. doi: 10.3390/ijms17101669. PMID: 27706047; PMCID: PMC5085702.
9. Fornetti J, Welm AL, Stewart SA. Understanding the Bone in Cancer Metastasis. J Bone Miner Res. 2018 Dec;33(12):2099-2113. doi: 10.1002/jbmr.3618. Epub 2018 Nov 26. PMID: 30476357.
10. Brook N, Brook E, Dharmarajan A, Dass CR, Chan A. Breast cancer bone metastases: pathogenesis and therapeutic targets. Int J Biochem Cell Biol. 2018 Mar;96:63-78. doi: 10.1016/j.biocel.2018.01.003. Epub 2018 Jan 5. PMID: 29309917.
11. Even-Sapir E. Imaging of malignant bone involvement by morphologic, scintigraphic, and hybrid modalities. J Nucl Med. 2005 Aug;46(8):1356-67. PMID: 16085595.
12. Bombardieri E, Gianni L. The choice of the correct imaging modality in breast cancer management. Eur J Nucl Med Mol Imaging. 2004 Jun;31 Suppl 1:S179-86. doi: 10.1007/s00259-004-1541-x. Epub 2004 May 4. PMID: 15127242.
13. Ben-Haim S, Israel O. Breast cancer: role of SPECT and PET in imaging bone metastases. Semin Nucl Med. 2009 Nov;39(6):408-15. doi: 10.1053/j.semnuclmed.2009.05.002. PMID: 19801220.
14. Sharma R, Mondal A, Bhatnagar A, Chakravarty KL, Mishra P, Chopra MK, Rawat HS, Kashyap R. Differentiation of malignant and degenerative benign bone disease using Tc-99m MDP and Tc-99m citrate scintigraphy. Clin Nucl Med. 1998 Nov;23(11):758-63. doi: 10.1097/00003072-199811000-00008. PMID: 9814564.
15. Cook GJ, Azad GK, Goh V. Imaging Bone Metastases in Breast Cancer: Staging and Response Assessment. J Nucl Med. 2016 Feb;57 Suppl 1:27S-33S. doi: 10.2967/jnumed.115.157867. PMID: 26834098.
16. Agrawal K, Marafi F, Gnanasegaran G, Van der Wall H, Fogelman I. Pitfalls and Limitations of Radionuclide Planar and Hybrid Bone Imaging. Semin Nucl Med. 2015 Sep;45(5):347-72. doi: 10.1053/j.semnuclmed.2015.02.002. PMID: 26278850.
17. Rager O, Nkoulou R, Exquis N, Garibotto V, Tabouret-Viaud C, Zaidi H, Amzalag G, Lee-Felker SA, Zilli T, Ratib O. Whole-Body SPECT/CT versus Planar Bone Scan with Targeted SPECT/CT for Metastatic Workup. Biomed Res Int. 2017;2017:7039406. doi: 10.1155/2017/7039406. Epub 2017 Jul 24. PMID: 28812019; PMCID: PMC5546128.
18. Kannivelu A, Loke KS, Kok TY, Osmany SY, Ali SZ,

Suat-Jin L, Ng DC. The role of PET/CT in the evaluation of skeletal metastases. Semin Musculoskelet Radiol. 2014 Apr;18(2):149-65. doi: 10.1055/s-0034-1371017. Epub 2014 Apr 8. PMID: 24715447.
19. NIH. CIP Cancer Imaging Program. About the cancer imaging archive (TCIA) [Internet]. 2022 [cited 2023 May 18]. Available from: https://www.cancerimagingarchive.net/about-the-cancer-imaging-archive-tcia/.
20. Kinahan PE, Fletcher JW. Positron emission tomography-computed tomography standardized uptake values in clinical practice and assessing response to therapy. Semin Ultrasound CT MR. 2010 Dec;31(6):496-505. doi: 10.1053/j.sult.2010.10.001. PMID: 21147377; PMCID: PMC3026294.
21. 3D Slicer image computing platform. 2023; Available from: https://www.slicer.org/
22. Krzywinski M, Altman N. Visualizing samples with box plots. Nat Methods. 2014 Feb;11(2):119-20. doi: 10.1038/nmeth.2813. PMID: 24645192.
23. Wang Z, Cheng Y, Chen S, Shao H, Chen X, Wang Z, Wang Y, Zhou H, Chen T, Lin N, Ye Z. Novel prognostic nomograms for female patients with breast cancer and bone metastasis at presentation. Ann Transl Med. 2020 Mar;8(5):197. doi: 10.21037/atm.2020.01.37. PMID: 32309344; PMCID: PMC7154431.
24. Gherghe M, Mutuleanu MD, Stanciu AE, Irimescu I, Lazar A, Bacinschi X, Anghel RM. Quantitative Analysis of SPECT-CT Data in Metastatic Breast Cancer Patients-The Clinical Significance. Cancers (Basel). 2022 Jan 6;14(2):273. doi: 10.3390/cancers14020273. PMID: 35053436; PMCID: PMC8773966.
25. Koppula BR, Morton KA, Al-Dulaimi R, Fine GC, Damme NM, Brown RKJ. SPECT/CT in the Evaluation of Suspected Skeletal Pathology. Tomography. 2021 Oct 11;7(4):581-605. doi: 10.3390/tomography7040050. PMID: 34698290; PMCID: PMC8544734.
26. Arvola S, Jambor I, Kuisma A, Kemppainen J, Kajander S, Seppänen M, Noponen T. Comparison of standardized uptake values between 99mTc-HDP SPECT/CT and 18F-NaF PET/CT in bone metastases of breast and prostate cancer. EJNMMI Res. 2019 Jan 24;9(1):6. doi: 10.1186/s13550-019-0475-z. PMID: 30680469; PMCID: PMC6346696.
27. Mohd Rohani MF, Mat Nawi N, Shamim SE, Wan Sohaimi WF, Wan Zainon WMN, Musarudin M, Said MA, Hashim H. Maximum standardized uptake value from quantitative bone single-photon emission computed tomography/computed tomography in differentiating metastatic and degenerative joint disease of the spine in prostate cancer patients. Ann Nucl Med. 2020 Jan;34(1):39-48. doi: 10.1007/s12149-019-01410-4. Epub 2019 Oct 14. PMID: 31612417.
28. Kuji I, Yamane T, Seto A, Yasumizu Y, Shirotake S, Oyama M. Skeletal standardized uptake values obtained by quantitative SPECT/CT as an osteoblastic biomarker for the discrimination of active bone metastasis in prostate cancer. Eur J Hybrid Imaging. 2017;1(1):2. doi: 10.1186/s41824-017-0006-y. Epub 2017 Oct 12. PMID: 29782587; PMCID: PMC5954671.
29. Löfgren J, Mortensen J, Rasmussen SH, Madsen C, Loft A, Hansen AE, Oturai P, Jensen KE, Mørk ML, Reichkendler M, Højgaard L, Fischer BM. A Prospective Study Comparing 99mTc-Hydroxyethylene-Diphosphonate Planar Bone Scintigraphy and Whole-Body SPECT/CT with 18F-Fluoride PET/CT and 18F-Fluoride PET/MRI for Diagnosing Bone Metastases. J Nucl Med. 2017 Nov;58(11):1778-1785. doi: 10.2967/jnumed.116.189183. Epub 2017 Aug 10. PMID: 28798033.
30. Jambor I, Kuisma A, Ramadan S, Huovinen R, Sandell M, Kajander S, Kemppainen J, Kauppila E, Auren J, Merisaari H, Saunavaara J, Noponen T, Minn H, Aronen HJ, Seppänen M. Prospective evaluation of planar bone scintigraphy, SPECT, SPECT/CT, 18F-NaF PET/CT and whole body 1.5T MRI, including DWI, for the detection of bone metastases in high risk breast and prostate cancer patients: SKELETA clinical trial. Acta Oncol. 2016;55(1):59-67. doi: 10.3109/0284186X.2015.1027411. Epub 2015 Apr 2. PMID: 25833330.
31. Helyar V, Mohan HK, Barwick T, Livieratos L, Gnanasegaran G, Clarke SE, Fogelman I. The added value of multislice SPECT/CT in patients with equivocal bony metastasis from carcinoma of the prostate. Eur J Nucl Med Mol Imaging. 2010 Apr;37(4):706-13. doi: 10.1007/s00259-009-1334-3. Epub 2009 Dec 17. PMID: 20016889.

***Corresponding author**: Sahar Mansour, Radiological Sciences Department, College of Health and Rehabilitation Sciences, Princess Nourah bint Abdulrahman University, Riyadh, Saudi Arabia. E-mail: smabdelaty@pnu.edu.sa*

International Journal of Biomedicine 14(2) (2024) 291-294
http://dx.doi.org/10.21103/Article14(2)_OA9

ORIGINAL ARTICLE

Oncology

INTERNATIONAL JOURNAL OF BIOMEDICINE

Determination of the Optimal Parameters for Microwave Ablation of Liver Tumor

Nikola Bošković, Branislav Radjenović, Marija Radmilović-Radjenović*

Institute of Physics, University of Belgrade, Belgrade, Serbia

Abstract

Microwave ablation is a minimally invasive cancer treatment with high survival and low recurrence rates. Despite the unquestionable benefits of microwave ablation, the interaction between the medical tool and the tissue may cause damage to the surrounding tissue, which can be removed by clarifying the conditions for their development. In addition to clinical methods, computer simulation has proven to be a very effective tool to optimize microwave ablation performance. This study aimed to determine the optimal input power for complete microwave tumor ablation with an adequate safety margin while avoiding injury to surrounding healthy tissue. The liver tumor model was based on a real tumor labeled 1.02 in the 3D-IRCADb-01 database. Calculations were performed for a 10-slot microwave antenna with a frequency of 2.45 GHz using COMSOL Multiphysics. The obtained simulation results revealed that with proper input power, the necrotic tissue was mainly located in the tumor with minimal damage to the surrounding healthy tissue. This study may represent a step forward in planning individual microwave ablation procedures for each patient.**(International Journal of Biomedicine. 2024;14(2):291-294.)**

Keywords: liver tumor • microwave ablation • ablation zone • necrotic tissue

For citation: Bošković N, Radjenović B, Radmilović-Radjenović M. Determination of the Optimal Parameters for Microwave Ablation of Liver Tumor. International Journal of Biomedicine. 2024;14(2):291-294. doi:10.21103/Article14(2)_OA9

Introduction

Liver cancer is not only one of the most common cancers in the world, but it is also the fastest-growing cause of cancer-related death.[1-4] Microwave ablation (MWA) at 2.45 GHz is considered as a minimally invasive procedure with a higher overall survival rate than external beam radiation therapy and proton beam therapy.[5,6] Furthermore, MWA is highly recommended as a rapid treatment with a short recovery time for COVID-19 patients with liver tumors.[7] Although the success rate of eliminating small liver tumors by MWA is higher than 85% for large tumors, the completion rates slightly decrease.[8,9]

The mechanism underlying MWA is associated with an increase in temperature above the normal physiological threshold to kill cancer cells with minimal damage to surrounding tissue.[10] A microwave antenna radiates a rapidly oscillating electromagnetic field that causes frictional heating of water molecules in the soft tissues around the field source.[11] The production of reliable near-spherical ablation zones depends on the antenna design. Recently, a compact multi-slot coaxial antenna was built to achieve an optimal ablation shape and proper impedance matching to the target tumor without damaging the surrounding healthy tissues.[12] Besides clinical studies, the role of computational models in predicting microwave ablation outcomes has significantly increased.[13,14]

In this study, simulations were performed using a full three-dimensional (3D) MWA model,[15] which was developed and tested using the COMSOL Multiphysics platform.[16] A realistic tumor model based on a 3D CT scan of the tumor labeled as 1.02 in the 3D-IRCADb-01 liver tumors database (3D-IRCADb)[17] was given special emphasis. The main goal of this study was to determine the optimal input power to ensure complete tumor 1.02 (3D-IRCADb) ablation with minimal damage to the surrounding healthy tissue. Estimating the optimal power will ensure the best ratio of necrotic tissue to healthy tissue.

Methodology

To simulate microwave tissue ablation,[18] the model must contain three fundamental components. The antenna probe model contains a microwave field production in the

tissue. In the heat transfer equation, the second component describes the microwave field and blood perfusion as sources of heat and heat sinks, respectively. The third component deals with the effect of the heat on the destruction of the tumor cells. All components of the MWA model are affected by various material parameters that depend on tissue characteristics. Modeling MWA as a multiphysics problem involves modeling multiple physical phenomena, such as electromagnetic wave propagation, heat transfer, and tissue damage, that occur during the procedure.[18] Equations governing the calculations of the electric field distribution through the tissue and the heat generated by the electromagnetic field during MWA[18,19] have been described in previous publications.

In contrast to the frequently used spherical tumor geometry, which is artificial, our simulation model is based on a real tumor labeled as 1.02, which belongs to a female in the database 3D-IRCADb-01, which contains several sets of CT scans of patients (3D-IRCADb).[17] This tumor is relatively large (2.80 cm × 2.34 cm × 2.30 cm) and has an irregular shape, as shown in Figure 1.

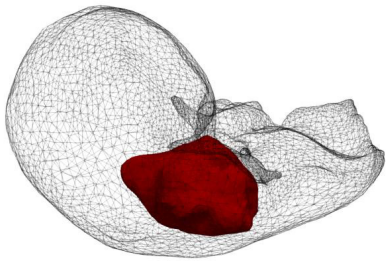

Fig. 1. *Schematic view of the liver (triangulated surface) with tumor 1.02 taken from the database (3D-IRCADb) [17] (solid surface).*

To determine the optimal input power, numerical simulations were performed for tumor 1.02 from the database (3D-IRCADb)[17] exposed to a frequency of 2.45 GHz and an input power in the range of 25–45 W. The parameters of the biological materials used in the numerical simulations were obtained from the literature.[10,19]

Results

Figure 2 shows the isocontours representing the tumor (triangulated surface) and surrounding healthy tissue (solid light brown surface). The optimal value of the input power corresponded to total tumor ablation with minimal damage to healthy tissues. An input power of 25 W did not ensure complete ablation of the tumor backside. When 35 W was applied, the ablation zone covered the entire tumor, but there was significant damage to healthy tissue. When the whole tumor was destroyed, the isocontours that best fit the necrotic tissue were achieved for an input power of 30 W, while healthy tissue was preserved.

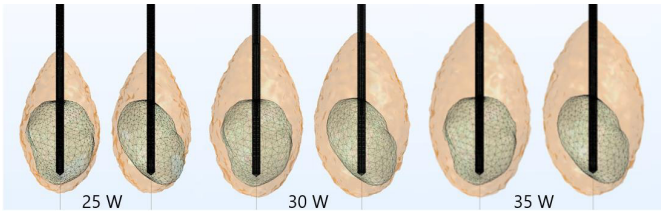

Fig. 2. *Isocontours composed of the totally ablated region (solid surface) after 600 s of MWA of tumor 1.02 (3D-IRCADb)[17] (triangulated surface) (for input power of 25, 30, and 35 W).*

Figure 3 shows the significance of the proper choice of the input power and ablation time. The ablation time was shortened from 600 to 560, 540, or 520 s when a power of 35, 40, or 45 W was applied, respectively. However, even though the ablation time was shorter, the healthy surrounding tissues were heavily damaged compared with those treated with 30 W for 600 s. These results indicate that the most efficient and safest MWA procedure is not always related to higher input power and shorter ablation time. Due to the dimensions of the tumor and its irregular shape, the formed ablation zones were elongated with a greater length along the shaft of the antenna than the transverse diameter. Elongated shapes are undesirable ablation patterns that cause damage to healthy tissues even if the ablation time is shorter.

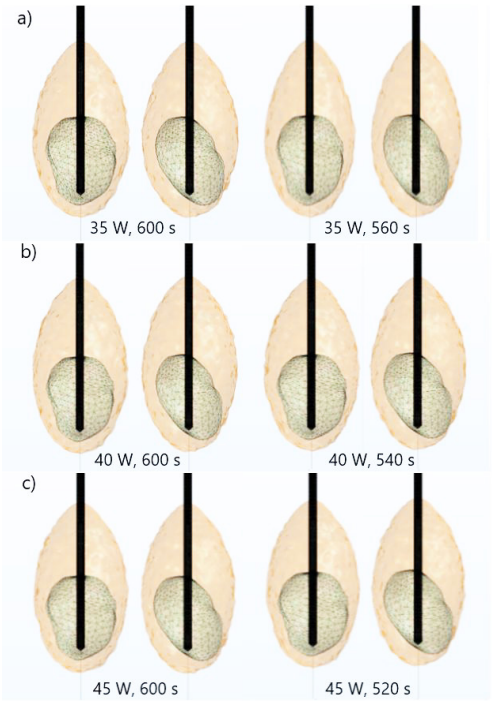

Fig. 3. *Totally ablated regions (solid surface) around liver tumor 1.02 (3D-IRCADb)[17] (triangulated surface) for MWA with an input power of a) 35 W, b) 40 W, and c) 45 W during various ablation times.*

Figure 4a shows the isocontours calculated for the optimal power of 30 W at temperatures of 40°C, 60°C, 70°C, 80°C, and 90°C.

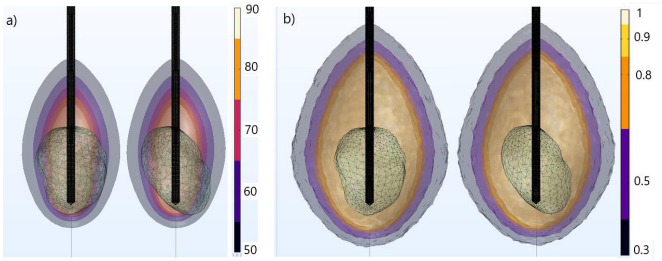

Fig. 4. *Isocontours of a) temperature (50 oC, 60 oC, 70 oC, 80 oC, and 90 oC) and b) fraction of damage (0.3, 0.5, 0.8, 0.9, and 1) corresponding to the front (left) and back (right) sides of the liver tumor 1.02 [17] (triangulated surface).*

The absorbed energy is converted into thermal energy, leading to an increase in tissue temperature. Close to the antenna, where the heat source is strong, the temperature is higher. The temperature increases with the ablation time, reaching a maximum inside the tumor region, where all cancer cells are killed. The temperature decreased as the distance from the antenna decreased, where the heat source weakened. Blood perfusion limits the extent of the heated area. Figure 4b illustrates isocontours related to damage fractions of 0.6, 0.7, 0.8, 0.9, and 1 for an optimal input power of 30 W. The ablation zones were elongated because of the size and irregular shape of the tumor (1.02 3D-IRCADb).[17] The active and passive heating zones can be distinguished. An active heating zone emerges within the tissue closest to the device, with high energy intensity and rapid absorption by tissue. On the other hand, the passive zone appears outside the active zone, far from the antenna.

Discussion

The study aimed to determine the optimal input power for efficient and safe microwave liver tumor ablation. For this purpose, full three-dimensional simulations within COMSOL Multiphysics, a finite element method-based platform, were applied.[16] Calculations were performed for a model of a real liver tumor labeled as 1.02 in the database 3D-ICRADb-01 (3D-IRCADb)[17] exposed to radiation from a 10-slot antenna operating at a frequency of 2.45 GHz. The optimal value of the input power of 30 W was estimated so that the whole tumor could be completely treated with minimal damage to the healthy tissue. The difference between ablation times when the input power was 35, 40, and 45 W, compared with that at 30 W, was approximately 7%, 10%, and 13%, respectively. Ablation time decreased with increasing input power. However, higher input power values may result in undesirable ablation zone shapes, leading to significant damage to healthy tissue. Regardless of the input power, the maximum temperature values were reached inside the tumor regions, where all cancer cells were destroyed. The fraction of damage increased as the ablation time increased. Although a multi-slot coaxial antenna produces a more localized heating pattern for spherical tumors, for realistic tumor shapes, the ablation zones are usually elongated.

Determining the optimal ratio of necrotic tissue to healthy tissue is important for improving the microwave ablation procedure to destroy the maximal part of the tumor while conserving the healthy tissue. It was confirmed that two-dimensional models are not sufficient and that full three-dimensional simulations are necessary for predicting the optimal conditions for microwave ablation, which may be incorporated into medical procedure planning.

Sources of Funding

The authors acknowledge that this research was supported by the Science Fund of the Republic of Serbia (GRANT No. 7739583, SimSurgery).

Conflicts of interest

The authors declare no conflict of interest.

References

1. Watson J, Hydon K, Lodge P. Primary and secondary liver tumours. InnovAiT 2016; 9(8):477-82. doi: 10.1177/1755738016653419
2. Sia D, Villanueva A, Friedman SL, Llovet JM. Liver Cancer Cell of Origin, Molecular Class, and Effects on Patient Prognosis. Gastroenterology. 2017 Mar;152(4):745-761. doi: 10.1053/j.gastro.2016.11.048. Epub 2016 Dec 30. PMID: 28043904.
3. Chen JG, Zhu J, Zhang YH, Chen YS, Lu JH, Zhu YR, Chen HZ, Shen AG, Wang GR, Groopman JD, Kensler TW. Liver cancer mortality over six decades in an epidemic area: what we have learned. PeerJ. 2021 Feb 3;9:e10600. doi: 10.7717/peerj.10600. PMID: 33604165; PMCID: PMC7866902.
4. Linn YL, Chee MY, Koh YX, Teo JY, Cheow PC, Chow PKH, Chan CY, Chung AYF, Ooi LLPJ, Goh BKP. Actual 10-year survivors and 10-year recurrence free survivors after primary liver resection for hepatocellular carcinoma in the 21st century: A single institution contemporary experience. J Surg Oncol. 2021 Jan;123(1):214-221. doi: 10.1002/jso.26259. Epub 2020 Oct 23. PMID: 33095920.
5. Villard C, Soler L, Gangi A. Radiofrequency ablation of hepatic tumors: simulation, planning, and contribution of virtual reality and haptics. Comput Methods Biomech Biomed Engin. 2005 Aug;8(4):215-27. doi: 10.1080/10255840500289988. PMID: 16298844.
6. Facciorusso A, Di Maso M, Muscatiello N. Microwave ablation versus radiofrequency ablation for the treatment of hepatocellular carcinoma: A systematic review and meta-analysis. Int J Hyperthermia. 2016 May;32(3):339-44. doi: 10.3109/02656736.2015.1127434. Epub 2016 Jan 21. PMID: 26794414.
7. Afaghi P, Lapolla MA, Ghandi K. Percutaneous microwave ablation applications for liver tumors: recommendations for

***Corresponding author**: Prof. Marija Radmilović-Radjenović, Institute of Physics, University of Belgrade, Belgrade, Pregrevica 118, Serbia. E-mail: marija@ipb.ac.rs*

COVID-19 patients. Heliyon. 2021 Mar 6;7(3):e06454. doi: 10.1016/j.heliyon.2021.e06454. PMID: 33748501; PMCID: PMC7966996.
8. Gartshore A, Kidd M, Joshi LT. Applications of Microwave Energy in Medicine. Biosensors (Basel). 2021 Mar 26;11(4):96. doi: 10.3390/bios11040096. PMID: 33810335; PMCID: PMC8065940.
9. Itoh S, Ikeda Y, Kawanaka H, Okuyama T, Kawasaki K, Eguchi D, Korenaga D, Takenaka K. Efficacy of surgical microwave therapy in patients with unresectable hepatocellular carcinoma. Ann Surg Oncol. 2011 Dec;18(13):3650-6. doi: 10.1245/s10434-011-1831-z. Epub 2011 Jun 15. PMID: 21674268.
10. Tehrani MHH, Soltani M, Kashkooli FM, Raahemifar K. Use of microwave ablation for thermal treatment of solid tumors with different shapes and sizes-A computational approach. PLoS One. 2020 Jun 15;15(6):e0233219. doi: 10.1371/journal.pone.0233219. PMID: 32542034; PMCID: PMC7295236.
11. Karampatzakis A, Kühn S, Tsanidis G, Neufeld E, Samaras T, Kuster N. Antenna design and tissue parameters considerations for an improved modelling of microwave ablation in the liver. Phys Med Biol. 2013 May 21;58(10):3191-206. doi: 10.1088/0031-9155/58/10/3191. Epub 2013 Apr 19. PMID: 23603829.
12. Ge M, Jiang H, Huang X, Zhou Y, Zhi D, Zhao G, Chen Y, Wang L, Qiu B. A multi-slot coaxial microwave antenna for liver tumor ablation. Phys Med Biol. 2018 Sep 6;63(17):175011. doi: 10.1088/1361-6560/aad9c5. PMID: 30102247.
13. Racila M, Crolet JM. Numerical simulation of thermoablation in living tissues. Computer Methods in Biomechanics and Biomedical Engineering 2011;14(sup1): 279-80.
14. Chiang J, Wang P, Brace CL. Computational modelling of microwave tumour ablations. Int J Hyperthermia. 2013 Jun;29(4):308-17. doi: 10.3109/02656736.2013.799295. PMID: 23738698; PMCID: PMC3768158.
15. Radjenović B, Sabo M, Šoltes L, Prnova M, Čičak P, Radmilović-Radjenović M. On Efficacy of Microwave Ablation in the Thermal Treatment of an Early-Stage Hepatocellular Carcinoma. Cancers (Basel). 2021 Nov 18;13(22):5784. doi: 10.3390/cancers13225784. PMID: 34830937; PMCID: PMC8616542.
16. Heat Transfer Module 1986-2020. Burlington (MA): COMSOL, Inc. https://www.comsol.com/heat-transfer-module
17. 3D-IRCADb. Available online: https://www.ircad.fr/research/3dircadb/
18. Radmilović-Radjenović M, Bošković N, Sabo M, Radjenović B. An Analysis of Microwave Ablation Parameters for Treatment of Liver Tumors from the 3D-IRCADb-01 Database. Biomedicines. 2022 Jul 1;10(7):1569. doi: 10.3390/biomedicines10071569. PMID: 35884874; PMCID: PMC9312906.
19. Bošković N, Radmilović-Radjenović M, Radjenović B. Finite Element Analysis of Microwave Tumor Ablation Based on Open-Source Software Components. Mathematics. 2023;11:2654.

International Journal of Biomedicine 14(2) (2024) 295-299
http://dx.doi.org/10.21103/Article14(2)_OA10

ORIGINAL ARTICLE

Transplantology

INTERNATIONAL JOURNAL OF BIOMEDICINE

The Impact of Warm Ischemia Time on Kidney Function in Experiment

Ulugbek Abduganiev[1], Muhammadaziz Aliev[2], Pulat Sultanov[1,2*]

[1]*Republican Research Center of Emergency Medicine, Tashkent, Uzbekistan*
[2]*Center for the Development of Professional Qualifications for Medical Workers, Tashkent, Uzbekistan*

Abstract

Background: The main difficulty with donation after circulatory death is the inevitable period of warm ischemia, which may adversely affect tissue viability and graft function after transplantation. The aim of this study was to evaluate dynamic changes in the functional parameters of the kidneys because of renal warm ischemia (RWI) in the experiment.

Methods and Results: The experiments were carried out on 78 white male rats weighing 214.5±31.8g. To achieve the study's aim, we applied a method of modeling the intraoperative RWI by clamping renal arteries from both sides through a median laparotomy under ether anesthesia. Vascular clamping lasted 12, 24, 36, or 48 minutes in four experimental groups of rats, each containing 18 rats. The intact group of rats became the control group (n=6). In each of the 4 experimental groups, rats were euthanized by decapitation on Days 3, 7, and 14 of the experiment. Before euthanasia, a 24-hour urine collection was performed in metabolic chambers. Laboratory tests included the determination of blood urea nitrogen (BUN), serum creatinine (sCR), serum potassium (SP), and urinary creatinine (uCr); glomerular filtration rate (GFR) was calculated using the Rehberg-Tareev method.

Warm ischemia time (WIT) for no more than 12 minutes did not lead to significant negative changes in most of the studied parameters of renal function at all time stages of the experiment, with the exception of a significant decrease in GFR, as well as an increase in SP levels on Days 3 and 7 of the experiment. The WIT up to 24 minutes led to a more pronounced drop in GFR at all time stages of the experiment ($P<0.05$ in all cases), as well as a moderate increase in the levels of BUN and SP and a decrease in uCr levels on Days 3 and 7 ($P<0.05$ in all cases). The WIT up to 36 minutes led to a drop in GFR by 84% and 86% on Days 3 and 7 of the experiment, as well as a decrease in diuresis, an increase in levels of BUN and SP, as well as a twofold decrease in uCr, compared to the control at the specified time intervals ($P<0.05$ in all cases). The WIT up to 48 minutes led to a drop in GFR by 95%, 97%, and 100% on Days 3, 7, and 14 of the experiment, respectively ($P<0.05$ in all cases). The drop in diuresis worsened on Days 3 and 7 to anuria on Day 14 ($P<0.05$ in all cases). The levels of BUN and SP increased from Day 3 to Day 14, and uCr dropped significantly to zero on Day 14 ($P<0.05$ in all cases).

Conclusion: Among all parameters analyzed, GFR was the early and most sensitive indicator of renal dysfunction in RWI. A 12-minute WIT leads to a slight decrease in renal function on Days 3 and 7, which is relatively restored by Day 14. The 24-minute and 36-minute WIT leads to a noticeable decrease in renal function with a tendency to recover on Day 14. The 48-minute WIT leads to a sharp decline in renal function, progressing on Day 7 and reaching critical changes by Day 14 of the experiment. **(International Journal of Biomedicine. 2024;14(2):295-299.)**

Keywords: kidney transplantation • donation after circulatory death • warm ischemia time • glomerular filtration rate

For citation: Abduganiev U, Aliev M, Sultanov P. The Impact of Warm Ischemia Time on Kidney Function in Experiment. International Journal of Biomedicine. 2024;14(2):295-299. doi:10.21103/Article14(2)_OA10

Abbreviations

BUN, blood urea nitrogen; **sCr**, serum creatinine; **uCr**, urinary creatinine; **DGF**, delayed graft function; **DCD**, donation after circulatory death; **GFR**, glomerular filtration rate; **HR**, hazard ratio; **RWI**, renal warm ischemia; **SP**, serum potassium; **WIT**, warm ischemia time.

Introduction

Kidney transplantation has a history of more than half a century and is still developing. In terms of a patient's lifespan and quality of life, the effectiveness of alternative renal replacement therapies other than kidney transplantation has been shown to be comparably low.[1] Kidney transplantation is accepted as alone the most optimal radical therapy for end-stage renal disease.[2,3] However, there is a chronic shortage of cadaveric organ donors for renal transplantation,[4] which might be solved using donation after circulatory death (non-heart-beating donation).[5-9] In contrast, a conventional heart-beating donor is one who sustains an irreversible brain injury, and death is based on neurologic criteria.[10]

Donation after circulatory death (DCD) can be categorized into 2 groups: controlled (cDCD) and uncontrolled (uDCD).[8] cDCD takes place when the death occurs within an intensive care unit/hospital setting, and cDCD occurs in a controlled fashion with surgical team assembly before a planned withdrawal of life-sustaining therapy. uDCD takes place when death occurs outside the hospital or within the emergency room after an unexpected cardiac arrest and resuscitative efforts fail. uDCD is identified as a significant potential source of organ donors in the out-of-hospital cardiac arrest population, but significant operational, ethical, logistical, and legal barriers exist across most jurisdictions.[11]

It is well established that living donor kidney transplants are associated with superior post-transplant outcomes, compared with deceased donor transplants.[12] According to the Scientific Registry of Transplant Recipients (SRTR) report, from 2010 to 2014, the unadjusted one-year allograft survival rate for recipients of a first deceased donor kidney transplant was 93.4%. The five-year unadjusted allograft survival rate for a primary deceased donor transplant was 72.4% among transplant recipients from 2005 to 2009. In recipients undergoing a primary living donor kidney transplant, the one-year unadjusted allograft survival rate was 97.2%. The five-year unadjusted allograft survival rate for a first living donor kidney transplant was 84.6%.

Early identification and treatment of surgical complications are critical for patient and graft survival.[13] The main difficulty with DCD is the inevitable period of warm ischemia, which may adversely affect tissue viability and graft function after transplantation.[14]

The aim of this study was to evaluate dynamic changes in the functional parameters of the kidneys because of renal warm ischemia (RWI) in the experiment.

Materials and Methods

The experiments were carried out on 78 white male rats weighing 214.5±31.8g. The experiments were performed in accordance with the norms for the humane treatment of animals, which are regulated by the International Guidelines of the Association for the Assessment and Accreditation of Laboratory Animal Care, following the protocol approved by the Institutional Animal Care and Use Committee at the Republican Research Center of Emergency Medicine (Tashkent, Uzbekistan).

The rats were allowed free access to standard rat chow and water. To achieve the study's aim, we applied a method of modeling the intraoperative RWI by clamping renal arteries from both sides through a median laparotomy under ether anesthesia. Vascular clamping lasted 12, 24, 36, or 48 minutes in four experimental groups of rats, each containing 18 rats (Group 1, Group 2, Group 3, and Group 4). Clamping of the arteries was carried out by temporarily ligating with a special loop (like an end-loop) of the renal hilum. Surgical procedures were performed on a heated pad to avoid cold-induced hemodynamic alterations. After the laparotomy, the wound was sutured tightly. The intact group of rats became the control group (n=6). There was no significant difference in age and weight between all groups. The rats' condition was monitored daily, with a qualitative determination of the presence of diuresis and recording changes in body weight. In each of the 4 experimental groups, rats were euthanized by decapitation on Days 3, 7, and 14 of the experiment. Thus, 3 subgroups (Subgroup A, Subgroup B, and Subgroup C, with 6 rats in each subgroup) were formed for each experimental group. Before euthanasia, a 24-hour urine collection was performed in metabolic chambers. Laboratory blood tests included the determination of BUN, sCR, and SP; uCr was also measured; GFR was calculated using the Rehberg-Tareev method.

Statistical analysis was performed using the statistical software package SPSS version 23.0 (SPSS Inc, Armonk, NY: IBM Corp). The Mann-Whitney U Test was used to compare the differences between the two independent groups A probability value of $P<0.05$ was considered statistically significant.

Results

During the experiment, all rats from Groups 1 and 2 survived until the planned date of euthanasia. In Group 3, 2(11.1%) rats died on Days 7 and 8. In Group 4, death was observed in 5(27.8%) cases on Days 7, 8, 10, 11 and 12 of the experiment. Autopsy of dead rats on Days 7 and 8 revealed the presence of thrombosis of the inferior vena cava, starting from the right renal vein and reaching the chambers of the heart and pulmonary artery. Congestion and an increase in the size of the liver and right kidney were noted. This was due to the short right renal vein and increasing thrombosis of the inferior vena cava as a result of prolonged ligation of the right renal hilum. After autopsying dead rats on Days 10-12, a decrease in and pallor of kidney parenchyma, dilation of the heart chambers, swelling of the lung tissue, and ascitic fluid in the abdominal cavity were noted to varying degrees.

Table 1 presents the functional parameters of the kidney on different days of the experiment. In Group 1, daily diuresis showed a significant increase in Subgroups B and C, compared to the control group ($P=0.048$ and $P=0.042$, respectively). In Group 2, a decrease in diuresis in all subgroups was insignificant ($P>0.05$ in all cases). In Group 3, a significant reduction in daily diuresis was found in Subgroups A and

B (P=0.048 and P=0.023, respectively); this reduction was without statistical significance in Subgroup C, compared to the control group (P=0.077). In Group 4, there was a sharp decrease in daily diuresis in Subgroups A and B, and we found anuria in Subgroup C (P=0.047, P=0.038, and P=0.031, respectively).

The BUN level did not change significantly in all subgroups of Group 1 (P>0.05 in all cases). In Group 2, we found a significant increase in BUN level in Subgroups A (P<0.05) and B (P<0.05), but in Subgroup C, BUN level returned to control value (P=0.275). In the subgroups of Group 3, we found changes like Group 2. In subgroups of Group 4, the increase in the BUN level was the most significant, and in Subgroup C, the BUN level increased almost 7 times, compared to the control (P=0.038).

The sCr level remained within the normal range in Groups 1-3 in all subgroups. At the same time, in Group 4, there was a gradual increase in the sCr level in Subgroups A and B, with a sharp rise in Subgroup C, compared to the control (P=0.031).

The SP increased significantly, compared to the control group in Subgroups A and B of all groups (P<0.05 in all cases). By Day 14 of the experiment, we found a decrease to normal levels in Groups 1-3, except for Group 4, where SP was 10.10±1.04 mmol/L vs. 5.1±0.16 mmol/L in the control (P=0.044).

The uCr level was within the normal limits in all subgroups of Group 1. At the same time, it decreased significantly in Subgroups A and B of Group 2, and this decrease was more pronounced in Subgroups A and B of Group 3. We found the most pronounced decrease in uCr levels in Group 4 to complete absence in Subgroup C.

During RWI, a decrease in GFR was observed in all subgroups of all 4 experimental groups, and the degree of decline increased from Group 1 to Group 4 to zero in Subgroup C of Group 4 (P<0.05 in all cases).

Table 1.

The functional parameters of the kidney on different days of RWI in the experiment.

	Control group (0)	Group 1 (1)	Group 2 (2)	Group 3 (3)	Group 4 (4)	P-value
Diuresis, ml/day						
Day 3 (Subgroup A)	5.30±1.10	5.08±0.24	4.73±0.38	3.31±0.32	1.50±0.40	P_{0-1}=0.827; P_{0-2}=0.513; P_{0-3}=0.048; P_{0-4}=0.047;
Day 7 (Subgroup B)		6.70±0.14	3.78±0.63	2.80±0.09	1.30±0.05	P_{0-1}=0.048; P_{0-2}=0.127; P_{0-3}=0.023; P_{0-4}=0.038;
Day 14 (Subgroup C)		6.80±0.39	4.83±0.12	3.63±0.58	0.00±0.00	P_{0-1}=0.042; P_{0-2}=0.827; P_{0-3}=0.077; P_{0-4}=0.031;
BUN, µmol/L						
Day 3 (Subgroup A)	6.08±0.54	5.79±1.03	8.09±0.36	8.5±0.04	15.2±2.37	P_{0-1}=0.827; P_{0-2}=0.049; P_{0-3}=0.023; P_{0-4}=0.047;
Day 7 (Subgroup B)		5.22±0.68	9.07±2.06	9.6±0.92	15.3±4.72	P_{0-1}=0.121; P_{0-2}=0.045; P_{0-3}=0.042; P_{0-4}=0.033;
Day 14 (Subgroup C)		4.92±0.23	6.5±0.20	6.8±1.12	42.3±0.03	P_{0-1}=0.055; P_{0-2}=0.275; P_{0-3}=0.509; P_{0-4}=0.038;
sCr, µmol/L,						
Day 3 (Subgroup A)	59.07±5.15	51.40±0.60	57.03±2.76	59.60±8.07	66.35±3.65	P_{0-1}=0.055; P_{0-2}=0.412; P_{0-3}=0.827; P_{0-4}=0.127;
Day 7 (Subgroup B)		49.93±5.44	58.55±4.15	62.80±2.87	70.2±14.25	P_{0-1}=0.227; P_{0-2}=1.000; P_{0-3}=0.487; P_{0-4}=0.275;
Day 14 (Subgroup C)		45.00±4.12	55.70±6.75	58.35±2.25	225.0±20.64	P_{0-1}=0.055; P_{0-2}=0.273; P_{0-3}=0.787; P_{0-4}=0.031;
SP, mmol/L						
Day 3 (Subgroup A)	5.1±0.16	6.37±0.32	6.62±0.83	7.04±0.63	7.60±1.18	P_{0-1}=0.041; P_{0-2}=0.045; P_{0-3}=0.049; P_{0-4}=0.047;
Day 7 (Subgroup B)		5.99±0.09	7.07±0.12	7.08±0.81	8.39±0.87	P_{0-1}=0.038; P_{0-2}=0.045; P_{0-3}=0.044; P_{0-4}=0.046;
Day 14 (Subgroup C)		5.50±0.92	6.42±0.64	6.89±1.15	10.10±1.04	P_{0-1}=0.529; P_{0-2}=0.052; P_{0-3}=0.058; P_{0-4}=0.044;
uCr, µmol/L						
Day 3(Subgroup A)	504.51±67	437.01±0.98	313.57±52.52	236.37±69.49	186.30±39.24	P_{0-1}=0.513; P_{0-2}=0.049; P_{0-3}=0.047; P_{0-4}=0.037;
Day 7(Subgroup B)		502.20±0.33	284.35±11.85	246.15±11.05	122.50±0.48	P_{0-1}=0.487; P_{0-2}=0.041; P_{0-3}=0.036; P_{0-4}=0.042;
Day 14 (Subgroup C)		512.40±0.28	445.20±13.90	402.10±66.40	0.0±0.0	P_{0-1}=0.474; P_{0-2}=0.431; P_{0-3}=0.127; P_{0-4}=0.036;
GFR, µl/min						
Day 3 (Subgroup A)	55.97±1.20	30.01±2.38	18.04±0.99	9.10±0.09	2.9±0.07	P_{0-1}=0.033; P_{0-2}=0.023; P_{0-3}=0.041; P_{0-4}=0.029;
Day 7 (Subgroup B)		46.79±1.15	12.70±0.31	7.6±0.03	1.6±0.1	P_{0-1}=0.028; P_{0-2}=0.034; P_{0-3}=0.042; P_{0-4}=0.038;
Day 14 (Subgroup C)		53.77±3.11	26.80±0.11	17.3±1.28	0.0±0.0	P_{0-1}=0.044; P_{0-2}=0.024; P_{0-3}=0.043; P_{0-4}=0.034;

Discussion

It is assumed that ischemic damage and DGF lead to a decrease in the number of functioning nephrons, and an inadequate "amount" of nephrons causes graft dysfunction in the late period.[15] According to Weight et al.,[16] the rat model demonstrated different renal changes depending on the RWI time: mild morphological changes (15-30 minutes), which became moderate (45 minutes) and severe with the presence of impaired glomerular perfusion, apoptosis, and pyknotic nuclei (60 minutes). In a study by Arefjev et al.,[17] ischemic damage to the donor kidney is morphologically manifested by acute tubular necrosis. The main target in ischemic damage to the donor kidney is tubular epithelial cells, because of which acute kidney injury develops.[18] Most of the studies indicated that WIT longer than 30 minutes should be considered as a major, potentially modifiable risk factor for inferior long-term results after kidney transplantation.[19]

Tennankore et al.,[20] in a study on 131,677 kidney transplant recipients, found that WIT >30 minutes was associated with a statistically higher adjusted relative hazard for the composite event of death or graft failure. In the case of WIT >60 minutes, a 23% increase in the adjusted relative hazard for death or graft failure was observed. Donor WIT >20 minutes was also found to correlate with increased delayed graft function.[21]

Donation after circulatory death (DCD) donors are an important source of kidneys for transplantation. In a study by Gill et al.,[22] among the 12,831 DCD kidneys transplanted, kidneys with WIT ≤48 minutes had survival like that of kidney transplants from brain-dead donors. DCD kidneys with WIT > 48 minutes had a higher risk of allograft failure (HR = 1.23; 95% CI: 1.07 - 1.41).

A study by Chen et al.[23] included 11,907 DCD kidney transplants. Compared to kidneys with WIT <60 minutes, kidneys with WIT 60-79 minutes had similar rates of graft failure (HR = 0.95, 95% CI: 0.67-1.37), whereas those with WIT ≥80 minutes had 1.66 times more failure (HR = 1.66, 95% CI: 1.16-2.38, P<0.05). One-year (90±0.3%, 87±2.7% vs. 82.1±4.2%) and 5-year (69.4±0.6%, 79.0±4% vs. 62.0±6.8%) survival were greater in kidneys with WIT <60 minutes and 60-79 minutes, compared to those with WIT ≥80 minutes, respectively.

In our study, WIT for no more than 12 minutes did not lead to significant negative changes in most of the studied parameters of renal function at all time stages of the experiment, with the exception of a significant decrease in GFR, as well as an increase in SP levels on Days 3 and 7 of the experiment.

The WIT up to 24 minutes led to a more pronounced drop in GFR at all time stages of the experiment, as well as a moderate increase in the levels of BUN and SP and a decrease in uCr levels on Days 3 and 7.

The WIT up to 36 minutes led to a drop in GFR by 84% and 86% on Days 3 and 7 of the experiment, as well as a decrease in diuresis, an increase in levels of BUN and SP, as well as a twofold decrease in uCr, compared to the control at the specified time intervals.

The WIT up to 48 minutes led to a drop in GFR by 95%, 97%, and 100% on Days 3, 7, and 14 of the experiment, respectively. The drop in diuresis worsened on Days 3 and 7 to anuria on Day 14. The levels of BUN and SP increased from Day 3 to Day 14, and uCr dropped significantly to zero on Day 14.

Conclusion

Among all parameters analyzed, GFR was the early and most sensitive indicator of renal dysfunction in RWI. A 12-minute WIT leads to a slight decrease in renal function on Days 3 and 7, which is relatively restored by Day 14. The 24-minute and 36-minute WIT leads to a noticeable decrease in renal function with a tendency to recover on Day 14. The 48-minute WIT leads to a sharp decline in renal function, progressing on Day 7 and reaching critical changes by Day 14 of the experiment.

Competing Interests

The authors declare that they have no competing interests.

References

1. Gauthier SV. Immunosuppression in solid organ transplantation, 2nd edition. Moscow, 2011. (In Russ.)
2. Onishchenko NA, Meshcherin SS, Ilyinsky IM, Sevastianov VI. INFLUENCE OF BONE MARROW MSCs ON THE DEVELOPMENT OF POSTTRANSPLANT CHANGES IN KIDNES. Russian Journal of Transplantology and Artificial Organs. 2016;18(1):45-52. (In Russ.) doi.org: 10.15825/1995-1191-2016-1-45-52
3. Khadjibaev F, Sharipova V, Sultanov P, Anvarov K, Ergashev D, Ruzibakieva M. The First Successful Kidney Transplant to a Child With Abnormality of Urinary Tract in Uzbekistan: Case Report. Exp Clin Transplant. 2020 Jan;18(Suppl 1):44-46. doi: 10.6002/ect.TOND-TDTD2019.O22. PMID: 32008493.
4. Khadjibaev A, Khadjibaev F, Anvarov K, Sultanov P. Organ Donation in Uzbekistan: Achievements and Prospects for Further Development. Exp Clin Transplant. 2020 Jul;18(Suppl 2):54-57. doi: 10.6002/ect.rlgnsymp2020.L8. PMID: 32758120.
5. Skvortsov AE, Bagnenko SF, Komedev SS, Teplov VM, Kolachev II, Shchurov AYu, Merkulov AL, Filatov VP, Boykov AA, Reznik ON. First Russian experience of liver and kidneys transplantation obtained from the donor with out-of-hospital irreversible cardiac arrest. Russian Journal of Transplantology and Artificial Organs. 2019;21(1):88-95. (In Russ.) doi: 10.15825/1995-1191-2019-1-88-95
6. Skvortsov AE, Loginov IV, Kukushkin AA, Ananiev AN, Kutenkov AA, Kuzmin DO, Daineko VS, Shiganov MYu, Reznik ON. NORMOTHERMIC EXTRACORPOREAL PERFUSION IN SITU IN DECEASED ORGAN DONORS WITH IRREVERSIBLE CARDIAC ARREST AND ONE HOUR OF ASYSTOLE. 5-YEAR OUTCOMES OF KIDNEY

TRANSPLANTATION. Russian Journal of Transplantology and Artificial Organs. 2016;18(3):57-67. (In Russ.) doi: 10.15825/1995-1191-2016-3-57-67
7. Khadjibaev AM, Rakhmanov RO, Sultanov PK, Sharipova VKh. Diagnosis and Treatment of Chest Injury and Emergency Diseases of Chest Organs. General Reanimatology. 2016;12(4):57-67. doi: 10.15360/1813-9779-2016-4-57-67
8. Morrison LJ, Sandroni C, Grunau B, Parr M, Macneil F, Perkins GD, Aibiki M, Censullo E, Lin S, Neumar RW, Brooks SC; International Liaison Committee on Resuscitation. Organ Donation After Out-of-Hospital Cardiac Arrest: A Scientific Statement From the International Liaison Committee on Resuscitation. Circulation. 2023 Sep 5;148(10):e120-e146. doi: 10.1161/CIR.0000000000001125. Epub 2023 Aug 8. PMID: 37551611.
9. Terasaki PI, Cho YW, Cecka JM. Strategy for eliminating the kidney shortage. Clin Transpl. 1997:265-7. PMID: 9919410.
10. Kootstra G. The asystolic, or non-heartbeating, donor. Transplantation. 1997 Apr 15;63(7):917-21. doi: 10.1097/00007890-199704150-00001. PMID: 9112339.
11. Coll E, Miñambres E, Sánchez-Fructuoso A, Fondevila C, Campo-Cañaveral de la Cruz JL, Domínguez-Gil B. Uncontrolled Donation After Circulatory Death: A Unique Opportunity. Transplantation. 2020 Aug;104(8):1542-1552. doi: 10.1097/TP.0000000000003139. PMID: 32732830.
12. Wang JH, Skeans MA, Israni AK. Current Status of Kidney Transplant Outcomes: Dying to Survive. Adv Chronic Kidney Dis. 2016 Sep;23(5):281-286. doi: 10.1053/j.ackd.2016.07.001. PMID: 27742381.
13. Reyna-Sepúlveda F, Ponce-Escobedo A, Guevara-Charles A, Escobedo-Villarreal M, Pérez-Rodríguez E, Muñoz-Maldonado G, Hernández-Guedea M. Outcomes and Surgical Complications in Kidney Transplantation. Int J Organ Transplant Med. 2017;8(2):78-84. Epub 2017 May 1. PMID: 28828167; PMCID: PMC5549004.
14. Brook NR, Waller JR, Nicholson ML. Nonheart-beating kidney donation: current practice and future developments. Kidney Int. 2003 Apr;63(4):1516-29. doi: 10.1046/j.1523-1755.2003.00854.x. PMID: 12631369.
15. Danovitch GM. Handbook of Kidney Transplantation. Sixth Edition. Wolters Kluwar, 2017. ISBN: 9781496326157.
16. Weight SC, Furness PN, Nicholson ML. New model of renal warm ischaemia-reperfusion injury for comparative functional, morphological and pathophysiological studies. Br J Surg. 1998 Dec;85(12):1669-73. doi: 10.1046/j.1365-2168.1998.00851.x. PMID: 9876072.
17. Arefjev ML, Minina MG, Iljinsky IM. Ischemic Injury of Kidney Allografts and Expression of Matrix Metalloproteinases. Russian Journal of Transplantology and Artificial Organs. 2011;13(2):103-109. (In Russ.) doi: 10.15825/1995-1191-2011-2-103-109
18. Arefjev M.L., Minina M.G., Mogeiko N.P., Iljinsky I.M. PATHOMORPHOLOGY OF ZERO BIOPSIES OF DONOR KIDNEYS. Russian Journal of Transplantology and Artificial Organs. 2011;13(1):36-42. (In Russ.) doi: 10.15825/1995-1191-2011-1-36-42
19. Kamińska D, Kościelska-Kasprzak K, Chudoba P, Hałoń A, Mazanowska O, Gomółkiewicz A, Dzięgiel P, Drulis-Fajdasz D, Myszka M, Lepiesza A, Polak W, Boratyńska M, Klinger M. The influence of warm ischemia elimination on kidney injury during transplantation - clinical and molecular study. Sci Rep. 2016 Nov 3;6:36118. doi: 10.1038/srep36118. PMID: 27808277; PMCID: PMC5093711.
20. Tennankore KK, Kim SJ, Alwayn IP, Kiberd BA. Prolonged warm ischemia time is associated with graft failure and mortality after kidney transplantation. Kidney Int. 2016 Mar;89(3):648-58. doi: 10.1016/j.kint.2015.09.002. Epub 2015 Dec 30. PMID: 26880458.
21. Cantafio AW, Dick AA, Halldorson JB, Bakthavatsalam R, Reyes JD, Perkins JD. Risk stratification of kidneys from donation after cardiac death donors and the utility of machine perfusion. Clin Transplant. 2011 Sep-Oct;25(5):E530-40. doi: 10.1111/j.1399-0012.2011.01477.x. Epub 2011 May 18. PMID: 21585547.
22. Gill J, Rose C, Lesage J, Joffres Y, Gill J, O'Connor K. Use and Outcomes of Kidneys from Donation after Circulatory Death Donors in the United States. J Am Soc Nephrol. 2017 Dec;28(12):3647-3657. doi: 10.1681/ASN.2017030238. Epub 2017 Oct 5. PMID: 28982695; PMCID: PMC5698075.
23. Chen J, Mikhail D, Sharma H, Hijazi A, Nap D, Stitt L, Jevnikar J, Cooper M, Luke P, Sener A. Donor Warm Ischemic Time >80min Is an Important Predictor of Kidney Graft Survival from Donors After Cardiac Death.[abstract]. Am J Transplant. 2017;17 (suppl 3).

***Corresponding author**: Pulat Sultanov, MD, PhD, DSc. Head of the Department of External Affairs; Center for the Development of Professional Qualification of Medical Workers. Tashkent, Uzbekistan. E-mail: sultanovpk@gmail.com*

International Journal of Biomedicine 14(2) (2024) 300-304
http://dx.doi.org/10.21103/Article14(2)_OA11

ORIGINAL ARTICLE

Experimental Biology and Medicine

INTERNATIONAL JOURNAL OF BIOMEDICINE

Effects Inhalation of Kerosene and Naphtha Fumes on Some Blood Indices in Rats

Aya Ammar Kadum, Zaid Makki AL-Hakkak

Department of Ecology and Pollution, Faculty of Science, University of Kufa, Najaf, Iraq

Abstract

***Background*:** Multiple studies, including both humans and animals, have demonstrated that gasoline, kerosene, and diesel fuel exhaust emissions include chemical components harmful to the bone marrow, lymph nodes, and spleen. This study aimed to evaluate the impact of kerosene and naphtha vapors on several blood parameters in rats.

***Methods and Results*:** The study was conducted on 10–12-week-old male Wistar albino rats (*Rattus norvegicus*) (n=20) weighing 150–200g. The experimental rats were categorized into two groups, each including five animals. The rats were exposed to kerosene and naphtha vapors for 15, 30, and 45 days, with six hours of daily exposure. Two control groups of animals, each including five animals, were exposed to room air. One group of rats was allowed to inhale the vapors emitted by the evaporating kerosene. Another group underwent an identical process for the naphtha vapors. Both groups of animals were exposed to daily vapors for six hours, from 9:00 a.m. to 3:00 p.m., six days a week, for three different durations: 15, 30, and 45 days. Blood samples were tested for hematological indices using a Cell Dyn Ruby Hematology Analyzer (Abbott, USA). On days 15, 30, and 45 of the experiment, rats exposed to kerosene and naphtha vapors had an increase in the total number of leukocytes, an increase in the percentage of lymphocytes, and a decrease in the percentage of neutrophils, compared to the control group ($P<0.05$ in all cases). At 15, 30, and 45 days of the experiment, the total number of RBCs increased significantly ($P<0.05$ in all cases). In addition, under the influence of kerosene and naphtha vapors, a higher level of PCV and MCV was noted at 30 and 45 days of the experiment, compared to the control group. At the same time, at the indicated stages of the experiment, there was a significant decrease in MCH and MCHC, compared to the control group ($P<0.05$ in all cases).

Conclusion: exposure to naphtha and kerosene vapor significantly affects a variety of WBC and RBC parameters, exhibiting toxic effects.**(International Journal of Biomedicine. 2024;14(2):300-304.)**

Keywords: white blood cell • red blood cell • kerosene • naphtha • toxic effects

For citation: Kadum AA, AL-Hakkak ZM. Effects Inhalation of Kerosene and Naphtha Fumes on Some Blood Indices in Rats. International Journal of Biomedicine. 2024;14(2):300-304. doi:10.21103/Article14(2)_OA11

Abbreviations

Hb, hemoglobin; **MCH**, mean corpuscular hemoglobin; **MCHC**, MCH concentration; **MCV**, mean corpuscles volume; **PCV**, packed cell volume; **RBC**, red blood cell; **WBC**, white blood cell.

Introduction

Refineries and petrochemical firms produce a wide range of toxic pollutants discharged into the environment. Petroleum fumes are widely present in our surroundings, and the main places for inhalation or contact are petrochemical businesses (refineries, oil fields, and filling stations) and residential areas.[1] The Al-Najaf refinery (Iraq) is a crucial source of petroleum products (naphtha and kerosene, gas oil, and heavy black petroleum) for Najaf city and its neighboring regions. It serves the local demand for these products and supplies electrical stations, factories, and other purposes.

Crude petroleum consists of a mixture of different metals and hydrocarbons. Crude oil undergoes a refining process to produce distinct fractions such as petroleum, diesel, kerosene, heavy gas, and lubricating oils. Petrol, diesel, and kerosene are commonly produced from fractional distillation of crude oil.[2] Petrol poses a significant hazard due to its composition of diverse harmful substances, such as volatile aliphatic and aromatic hydrocarbons referred to as BTEX (benzene, toluene,

ethylbenzene, and xylene).[3] Furthermore, the widespread presence of processed petroleum chemicals has adversely affected many human biological functions.[4]

Multiple studies, including both humans and animals, have demonstrated that gasoline, kerosene, and diesel fuel exhaust emissions include chemical components such as cadmium, benzene, and volatile nitrates harmful to the bone marrow, lymph nodes, and spleen.[5] The presence of pollutants derived from petroleum products has been reported to cause changes in the levels of liver enzymes and in the generation of hormones in the pituitary gland.[6]

Industry emits hazardous air pollutants such as organic compounds (benzene, toluene, formaldehyde, acetaldehyde, phenol, ethylbenzene, xylene), inorganic compounds (hydrogen chloride [HCl], hydrogen cyanide [HCN]), reduced sulfur compounds (carbon disulfide [CS2]), and metals (arsenic, beryllium, cadmium, chromium, cobalt). These pollutants are primarily associated with the development of leukemia.[7,8] This study aimed to evaluate the impact of kerosene and naphtha vapors on several blood parameters in rats.

Materials and Methods

Animals

The experiments were performed in accordance with the norms for the humane treatment of animals, which are regulated by the International Guidelines of the Association for the Assessment and Accreditation of Laboratory Animal Care, following the protocol approved by the Institutional Animal Care and Use Committee of the University of Kufa. The study was conducted on 10–12-week-old male Wistar albino rats (*Rattus norvegicus*) (n=20) weighing 150–200g. The experimental rats were categorized into two groups, each including five animals. The rats were exposed to kerosene and naphtha vapors for 15, 30, and 45 days, with six hours of daily exposure. Two control groups of animals, each including five animals, were exposed to room air. The animals were kept at the Faculty of Science, University of Kufa's animal facility under controlled environmental conditions, with a temperature range of 25–28°C and a 12-hour light-dark cycle. Animals were provided with normal water and feed.

Exposure to kerosene & naphtha vapors

The study used inhalation as the technique of exposure. The experimental groups were housed in animal cages and placed inside exposure chambers with dimensions of 150, 90, and 210 cm. Two extensively perforated 1000ml cans carrying 500 ml of fluid kerosene were put in the exposure chamber. One group of rats was allowed to inhale the vapors emitted by the evaporating kerosene. Another group underwent an identical process for the naphtha vapors. Both groups of animals were exposed to daily vapors for six hours, from 9:00 a.m. to 3:00 p.m., six days a week, for three different durations: 15, 30, and 45 days. The study used kerosene and naphtha produced by the Al-Najaf refinery. This investigation utilized a previously documented modified nose-inhalation exposure approach.[9]

Blood sample collection and analysis

After exposure, each animal received 0.5 ml ketamine and 0.1ml xylazine for moderate anesthesia.[10] After anesthesia, the rats were put in a dissecting dish and sutured at the wrists and ankles with small pins. Blood was drawn correctly using a 3ml and 5ml disposable syringe following a heart puncture. It was mixed correctly in an EDTA tube before being used by an automated analyzer to estimate blood levels. Blood samples taken from the EDTA tube were tested for hematological indices using a Cell Dyn Ruby Hematology Analyzer (Abbott, USA).[11]

Statistical analysis was performed using the statistical software package SPSS version 21.0 (SPSS Inc, Armonk, NY: IBM Corp). For the descriptive analysis, results are presented as mean (M) ± standard deviation (SD). The Mann-Whitney U Test was used to compare the differences between the two independent groups (for nonparametric data). The Wilcoxon criterion was used to compare the differences between the paired samples. A value of $P<0.05$ was considered significant.

Results

On days 15, 30, and 45 of the experiment, rats exposed to kerosene and naphtha vapors had an increase in the total number of leukocytes, an increase in the percentage of lymphocytes, and a decrease in the percentage of neutrophils, compared to the control group ($P<0.05$ in all cases) (Tables 1 and 2).

Some red blood cell (RBC) parameters under the influence of kerosene and naphtha vapors changed at 15, 30 and 45 days of the experiment: The total number of RBCs increased significantly ($P<0.05$ in all cases). In addition, under the influence of kerosene and naphtha vapors, a higher level of PCV and MCV was noted at 30 and 45 days of the experiment, compared to the control group ($P<0.05$ in all cases). At the same time, at the indicated stages of the experiment, there was a significant decrease in MCH and MCHC, compared to the control group (Tables 3 and 4).

Table 1.

Effect of kerosene fumes on the total number of WBCs and the differential count in rats.

Variable	Control (1)	Time exposure (days)			Statistics
		15 (2)	30 (3)	45 (4)	
WBC count ($\times10^3/mm^3$)	6.52±0.13	18.06±1.70	13.33±2.13	13.95±2.42	P_{1-2*} P_{1-3*} P_{1-4*} P_{3-2*} P_{4-2*} $P_{4-3\wedge}$
Neutrophils (%)	51.40±2.55	19.12±3.32	13.34±2.09	10.42±3.13	P_{1-2*} P_{1-3*} P_{1-4*} P_{3-2*} P_{4-2*} P_{4-3*}
Lympho-cytes (%)	41.26±0.25	67.38±2.18	79.74±3.86	84.24±3.18	P_{1-2*} P_{1-3*} P_{1-4*} P_{3-2*} P_{4-2*} P_{4-3*}
Mid cells (%)	7.28±2.50	13.50±4.05	6.84±2.27	5.06±2.71	P_{1-2*} $P_{1-3\wedge}$ P_{1-4*} P_{3-2*} P_{4-2*} $P_{4-3\wedge}$

**-<0.05; ^->0.05*

Table 2.

Effect of naphtha fumes on the total number of WBCs and the differential count in rats.

Variable	Control (1)	Time exposure (days)			Statistics
		15 (2)	30 (3)	45 (4)	
WBC count ($\times10^3$/mm^3)	6.25±0.38	16.07±2.38	13.34±2.54	14.43±0.82	P_{1-2*} P_{1-3*} P_{1-4*} $P_{3-2\wedge}$ $P_{4-2\wedge}$ $P_{4-3\wedge}$
Neutrophils (%)	51.40±2.55	13.24±3.35	13.24±3.34	13.80±4.61	P_{1-2*} P_{1-3*} P_{1-4*} $P_{3-2\wedge}$ $P_{4-2\wedge}$ $P_{4-3\wedge}$
Lympho-cytes (%)	41.26±2.37	74.28±3.65	82.16±3.72	80.30±3.07	P_{1-2*} P_{1-3*} P_{1-4*} P_{3-2*} $P_{4-2\wedge}$ $P_{4-3\wedge}$
Mid cells (%)	7.34±2.76	12.48±2.90	7.22±2.66	6.10±2.49	P_{1-2*} $P_{1-3\wedge}$ P_{1-4*} P_{3-2*} P_{4-2*} $P_{4-3\wedge}$

**-<0.05; ^->0.05*

Table 3.

Effect of kerosene fumes on the total number of RBCs and RBC indices in rats.

Variable	Control (1)	Time exposure (days)			Statistics
		15 (2)	30 (3)	45 (4)	
RBCs ($\times10^6$/mm^3)	6.21±0.42	7.18±0.49	7.26±0.48	7.98±0.78	P_{1-2*} P_{1-3*} P_{1-4*} $P_{3-2\wedge}$ $P_{4-2\wedge}$ $P_{4-3\wedge}$
Hb (g/dl)	12.54±0.02	12.78±0.33	13.28±0.26	13.32±0.50	$P_{1-2\wedge}$ $P_{1-3\wedge}$ $P_{1-4\wedge}$ $P_{3-2\wedge}$ $P_{4-2\wedge}$ $P_{4-3\wedge}$
PCV (%)	38.42±1.16	40.16±1.60	46.44±2.80	49.52±1.81	P_{1-2*} P_{1-3*} P_{1-4*} P_{3-2*} P_{4-2*} P_{4-3*}
MCV (fL)	51.50±1.49	55.76±1.80	64.42±2.22	63.90±2.14	$P_{1-2\wedge}$ P_{1-3*} P_{1-4*} P_{3-2*} P_{4-2*} $P_{4-3\wedge}$
MCH (pg)	19.44±2.71	19.14±2.18	18.02±2.86	16.66±2.41	$P_{1-2\wedge}$ $P_{1-3\wedge}$ $P_{1-4\wedge}$ $P_{3-2\wedge}$ P_{4-2*} $P_{4-3\wedge}$
MCHC (g/dl)	31.88±0.82	30.94±0.51	28.10±1.16	26.10±0.39	$P_{1-2\wedge}$ P_{1-3*} P_{1-4*} P_{3-2*} P_{4-2*} P_{4-3*}

**-<0.05; ^->0.05*

Discussion

The results of our research are mainly consistent with the data of various authors. According to a study by Rabee,[12] exposure to air pollution at the oil refinery led to a considerable elevation in white blood cell (WBC) and lymphocyte counts.

Table 4.

Effect of naphtha fumes on the total number of RBCs and RBC indices in rats.

Variable	Control (1)	Time exposure (days)			Statistics
		15 (2)	30 (3)	45 (4)	
RBCs ($\times10^6$/mm^3)	6.21±0.42	7.47±0.46	7.64±0.10	7.44±0.36	P_{1-2*} P_{1-3*} P_{1-4*} $P_{3-2\wedge}$ $P_{4-2\wedge}$ $P_{4-3\wedge}$
Hb (g/dl)	12.54±0.28	12.64±0.37	12.26±0.29	12.70±0.51	$P_{1-2\wedge}$ $P_{1-3\wedge}$ $P_{1-4\wedge}$ $P_{3-2\wedge}$ $P_{4-2\wedge}$ $P_{4-3\wedge}$
PCV (%)	38.42±0.14	39.84±1.77	44.18±2.86	49.56±1.83	$P_{1-2\wedge}$ P_{1-3*} P_{1-4*} P_{3-2*} P_{4-2*} P_{4-3*}
MCV (fL)	51.51±4.49	55.80±3.83	66.44±3.78	65.04±3.16	$P_{1-2\wedge}$ P_{1-3*} P_{1-4*} P_{3-2*} P_{4-2*} $P_{4-3\wedge}$
MCH (pg)	19.44±0.71	17.02±0.65	16.50±0.46	16.80±0.48	P_{1-2*} P_{1-3*} P_{1-4*} $P_{3-2\wedge}$ $P_{4-2\wedge}$ $P_{4-3\wedge}$
MCHC (g/dl)	31.88±0.82	30.86±0.56	27.52±0.82	25.88±0.53	$P_{1-2\wedge}$ P_{1-3*} P_{1-4*} P_{3-2*} P_{4-2*} P_{4-3*}

**-<0.05; ^->0.05*

As known, WBCs are responsible for safeguarding the body against infectious illnesses and external substances. Inhaling polluted air might stimulate the release of WBCs into the circulatory system, leading to inflammation. Furthermore, the elevated WBC counts may be attributed to activating a defensive mechanism in response to exposure to xenobiotics. A study by Uboh et al.[13] documented the hepatotoxic effects observed in albino Wistar rats following exposure to kerosene and gasoline vapors. Additionally, the hazardous constituents, particularly those present in petroleum vapors, can alter the chemistry of the blood.

A study by Johnson et al.[14]) also revealed a statistically significant increase ($P<0.05$) in WBC count and lymphocyte number in the group exposed to household kerosene, compared to the control group. Leukocytosis was seen in the exposure group with a dosage of 1ml/kg body weight of household kerosene. This increase in WBCs may be attributed to bone marrow response and inflammatory illness in the animals exposed to kerosene.[15]

A study by Getu et al.[16] revealed that the mean RBC count, hemoglobin level, and the absolute lymphocyte count, of petrol-filling workers in Gondar town (Northwest Ethiopia), showed a significant increase, compared with the control group. Moreover, the duration of exposure to petrol showed a significant positive correlation with RBC count and mean cell hemoglobin concentration; however, a significant negative correlation was observed with mean cell volume.

A study by Sajid Jabbar and Ali [17] aimed to investigate the effect of benzene exposure on some blood parameters of

workers at several fuel stations in Basra city. The authors found significant hematological changes in the exposed workers and concluded that anemia was a common disorder among them. In addition, there was a significant decline in WBC and different types of WBC, including lymphocytes, monocytes, and neutrophils, due to continuous exposure to vapors of petrol products.

The results of a study by Imo et al.[18] showed that exposure of albino rats to inhalation of petroleum products could cause slight alteration in hematological parameters but can cause significant alteration in levels of liver function parameters and distortion in normal histoarchitecture of the liver tissue.

A study by Okoh et al.[19] showed a significant increase (P<0.05) in the PCV and the total number of leukocytes of Wistar rats exposed to diesel fumes, as compared to the control. Exposure to diesel fumes also caused elevated levels of liver and kidney biomarkers.

High kerosene and naphtha fume exposure may obstruct airways, causing alveolar hypoxia. In response to hypoxia, renal erythropoietin secretion increases, stimulating RBC production and maintenance. In this study, we also found a significant decrement in MCH and MCHC in rats exposed to kerosene and naphtha vapors for 30 and 45 days compared with the control. This may be caused by affected heme biosynthesis under kerosene and naphtha vapors that, with increased production of erythrocytes, lead to the development of hypochromic erythrocytosis. A study by Ufelle et al.[20] showed that exposure to volatile petroleum hydrocarbons raised the absolute RBC indices and liver enzymes and could stimulate a combined increase in the release of erythropoietin and interleukin-3, leading to ineffective hematopoiesis.

In conclusion, exposure to naphtha and kerosene vapor significantly affects a variety of WBC and RBC parameters, exhibiting toxic effects.

Disclosure and Competing Interests

The authors declare that they have no competing interests. The views presented in this paper are the views of the authors and not an official position of the institution.

References

1. McDonald BC, de Gouw JA, Gilman JB, Jathar SH, Akherati A, Cappa CD, Jimenez JL, Lee-Taylor J, Hayes PL, McKeen SA, Cui YY, Kim SW, Gentner DR, Isaacman-VanWertz G, Goldstein AH, Harley RA, Frost GJ, Roberts JM, Ryerson TB, Trainer M. Volatile chemical products emerging as largest petrochemical source of urban organic emissions. Science. 2018 Feb 16;359(6377):760-764. doi: 10.1126/science.aaq0524. PMID: 29449485.

2. Berepubo NA, Johnson NC, Sese B.T. Growth potentials and organ weights of weaner rabbits exposed to crude oil contaminated feed. Int J Anim. Sci.1994; 9:73-76.

3. Kodidala SR, Ahanger AM, Gandhi A. Comparison of pulmonary functions in petrol pump workers and residents of oil refinery. Indian Journal of Medical Specialities.2020;11(4):197-200.

4. Ajeel MA, Ajeel AA, Nejres AM, Salih RA. Assessment of Heavy Metals and Related Impacts on Antioxidants and Physiological Parameters in Oil Refinery Workers in Iraq. J Health Pollut. 2021 Aug 17;11(31):210907. doi: 10.5696/2156-9614-11.31.210907. PMID: 34434599; PMCID: PMC8383791.

5. Menanteau-Ledouble S, El-Matbouli M. Chemical hazards associated with fish as a food. In: Chemical hazards in foods of animal origin. Wageningen Academic Publishers. 2019:296-303.

6. Al-Hulfi RA, Al Salem BAM, Al-Naiema IM. The Effect of Air Pollutants on liver Enzymes and Pituitary Gland Hormones of Smokers and non-smokers of Oil Refinery and Gas Station Workers in Basra/Iraq. Indian Journal of Forensic Medicine & Toxicology. 2022;16(3):297-301.

7. Dantes E, Fildan AP, Toma CL, Voicu GH, Oancea C. Respiratory impact in workers exposed to air pollutants from petroleum refinery. J Environ Prot Ecol.2016; 17(2), 523-531.

8. Vogelmeier CF, Criner GJ, Martinez FJ, Anzueto A, Barnes PJ, Bourbeau J, Celli BR, Chen R, Decramer M, Fabbri LM, Frith P, Halpin DM, López Varela MV, Nishimura M, Roche N, Rodriguez-Roisin R, Sin DD, Singh D, Stockley R, Vestbo J, Wedzicha JA, Agustí A. Global Strategy for the Diagnosis, Management, and Prevention of Chronic Obstructive Lung Disease 2017 Report. GOLD Executive Summary. Am J Respir Crit Care Med. 2017 Mar 1;195(5):557-582. doi: 10.1164/rccm.201701-0218PP. PMID: 28128970.

9. Uboh FE, Akpanabiatu MI, Ekaidem IS, Ebong PE, Umoh IB . Effect of inhalation exposure to gasoline fumes on sex hormones profile in Wistar albino rats. Acta Endocrinol. 2007;(Buc) 3(1): 23-30.

10. Gecit İ, Kavak S, Meral I, Pirinçci N, Güneş M, Demir H, Cengiz N, Ceylan K. Effects of shock waves on oxidative stress, antioxidant enzyme and element levels in kidney of rats. Biol Trace Elem Res. 2011 Dec;144(1-3):1069-76. doi: 10.1007/s12011-011-9124-8. Epub 2011 Jun 24. PMID: 21701835.

11. Mathieleers I, Lsabel G, Fadila S, Rick G. Abbott apromise for life. Com, Case Book. 2012; 1-91.

12. Rabee, A. M. Evaluation of Biomarkers in Workers Exposed to Air Pollutants in Oil Refineries. Indian Journal of Forensic Medicine & Toxicology. 2022;16(1).

13. Uboh FE. Evaluation of toxicological implications of inhalation exposure to kerosene fumes and petrol fumes in rats. Acta Biologica Szegediensis. 2005;49(3-4):19-22.

14. Johnson M, Damazio OA. Hepatotoxicity of House Hold Kerosene (HHK) on Liver Enzyme Markers and Its Effect on Hematological and Oxidative Stress Parameters on Wistar Albino Rats. Science Journal of Medicine and Clinical Trials. 2014: Article ID sjmct-232

15. Marieb EN. Human Anatomy and Physiology. 3rd ed. Benjamin and Cummnings Pub Co, California.1995. 585-611.

***Corresponding author:** Dr. Zaid Makki Mohammed AL-Hakkak, Department of Ecology and Pollution, Faculty of Science, University of Kufa, Najaf, Iraq. E-mail: zaid.alhakkak@uokufa.edu.iq*

16. Getu S, Shiferaw E, Melku M. Assessment of hematological parameters of petrol filling workers at petrol stations in Gondar town, Northwest Ethiopia: a comparative cross-sectional study. Environ Health Prev Med. 2020 Aug 29;25(1):44. doi: 10.1186/s12199-020-00886-1. PMID: 32861244; PMCID: PMC7456503.
17. Sajid Jabbar A, Ali ET. Impact of Petroleum Exposure on Some Hematological Indices, Interleukin-6, and Inflammatory Markers of Workers at Petroleum Stations in Basra City. J Environ Public Health. 2020 Aug 4;2020:7693891. doi: 10.1155/2020/7693891. PMID: 32831856;
18. Imo C, Uhegbu FO, Ifeanacho NG. Effect of exposure to inhalation of selected petroleum products on liver function of male albino rats: A comparative study. IOSR Journal of Environmental Science, Toxicology and Food Technology. 2015;19:2319-2399.
19. Okoh HI, Odoh IM, Ahmed J, Adewemimo T, Nwana AO, Akano OA. Biochemical and Histopathological Effects of Exposure to Diesel Fumes on Vital Organs of Wistar Rats (*Rattus Norvegicus*). FUOYE Journal of Engineering and Technology.2023; 8(2),136-141.
20. Ufelle S, Onyekwelu K, Chinweoke A, Ibegbu D, Okoli U, Ikekpeazu J. Assessment of hepatic functions, hematopoietic cytokines and haematological parameters in people occupationally exposed to volatile petroleum hydrocarbons. Arch Environ Occup Health. 2021;76(8):567-571. doi: 10.1080/19338244.2020.1832037. Epub 2020 Oct 12. PMID: 33043855.

International Journal of Biomedicine 14(2) (2024) 305-311
http://dx.doi.org/10.21103/Article14(2)_OA12

ORIGINAL ARTICLE

COVID-19

INTERNATIONAL JOURNAL OF BIOMEDICINE

Pulmonary Embolism Diagnosed by CT Pulmonary Angiography in Patients with COVID-19 and Features of the Associated Factors

Ahmed Ibrahim Haidar[1], Rafat Saeed Mohtasib[2], Rami Mohammed Abudraz[1], Saleh Abdullah Alsulaiman[1], Faisal Ibrahim AL Tamimi[1], Ahmed Yaqinuddin[3], Ateeg Mohammed Algarni[1], Rateb Abd AL Razak Daowd[1], Abdelmoneim Adam Sulieman[4*]

[1]*Imam Abdulrahman Al-Faisal Hospital, Riyadh, KSA*
[2]*King Faisal Specialist Hospital and Research Center, Riyadh, KSA*
[3]*College of Medicine, Al-Faisal University, Riyadh, KSA*
[4]*Radiological Sciences College of Applied Medical Sciences - Al Ahsa, King Saud bin Abdulaziz University for Health Sciences, Al-Ahsa, KSA*

Abstract

Background: Since December 2019, when a new coronavirus disease 2019 (COVID-19) was detected in Wuhan, China, over 774 million confirmed COVID-19 cases and over seven million deaths have been reported globally, as of 7 January 2024 (WHO, 2024). Venous thromboembolism is a recognized complication of COVID-19. This study aimed to investigate the prevalence of pulmonary embolism (PE) diagnosed by CT pulmonary angiography (CTPA) in COVID-19 patients and the features of the associated factors.

Methods and Results: The study included 162 patients from the Imam Abdulrahman Al-Faisal Hospital who had COVID-19-confirmed infections while hospitalized in the ICU. Patients were diagnosed as COVID-19 positive by RT-PCR and underwent CTPA examination on the Discovery 16-slice CT scanner (Siemens, Germany) following standard protocol. For contrast enhancement, non-ionic, iodinated, intravenous contrast material (Omnipaque 350 mg) was used.

PE was detected by CTPA in 87(53.7%) COVID-19 patients. The D-dimer level was significantly higher in the PE group than in the non-PE group. The frequency of renal impairment in the PE group was 2.3 times higher than in the non-PE group. The ICU duration was longer in the PE group than in non-PE group (12.9±11.3 and 8.6±7.2 days, P=0.005). The death rate was 17.2% in the PE group and 1.3% in the non-PE group (P=0.001). The heart and respiratory rates, blood pressure, BMI, BUN, and creatinine levels did not differ in the study groups. The frequency of diabetes, hypertension, asthma, COPD, and smoking were comparable in the groups.

Conclusion: CTPA is very important in diagnosing PE in COVID-19 patients. CTPA-diagnosed PE is significantly associated with D-dimer, ICU duration, and death.**(International Journal of Biomedicine. 2024;14(2):305-311.)**

Keywords: COVID-19 • CT pulmonary angiography • pulmonary embolism • D-dimer

For citation: Haidar AI, Mohtasib RS, Abudraz RM, Alsulaiman SA, Tamimi FIA, Yaqinuddin A, Algarni AM, Daowd RAAR, Sulieman AA. Pulmonary Embolism Diagnosed by CT Pulmonary Angiography in Patients with COVID-19 and Features of the Associated Factors. International Journal of Biomedicine. 2024;14(2):305-311. doi:10.21103/Article14(2)_OA12

Abbreviations

ARDS, acute respiratory distress syndrome; **AKI**, acute kidney injury; **BMI**, body mass index; **BP**, blood pressure; **DBP**, diastolic BP; **CT**, computed tomography; **CTPA**, CT pulmonary angiography; **COPD**, chronic obstructive pulmonary disease; **HR**, heart rate; **ICU**, intensive care unit; **PE,** pulmonary embolism; **RR**, respiratory rate; **RT-PCR**, reverse transcription–polymerase chain reaction; **SBP**, systolic BP.

Introduction

Since December 2019, when a new coronavirus disease 2019 (COVID-19) was detected in Wuhan, China, over 774 million confirmed COVID-19 cases and over seven million deaths have been reported globally, as of 7 January 2024.[1]

Patients with SARS-CoV-2 infection can experience a range of clinical manifestations, from no symptoms to critical illness. Venous thromboembolism is a recognized complication of COVID-19. Many studies have reported a higher incidence of deep vein thrombosis and PE in COVID-19.[2-4] PE in COVID-19 has been found to be different from traditional PE in terms of demographic and clinical characteristics and laboratory data.[5]

SARS-CoV-2 infection could increase predisposition to venous and arterial thromboembolism due to excessive inflammation, hypoxia, immobilization, and diffuse intravascular coagulation.[6] SARS-CoV-2 infection with a wide thrombotic response has become a factor in a sudden surge in the incidence of PE the world over. Data from numerous meta-analyses also strongly indicate a higher incidence of PE in COVID-19 patients, especially in ICU settings.[7] In a Chinese study, Miesbach et al.[8] reported that up to 40% of patients developed PE chiefly localized in small pulmonary artery branches. In a French study, Poissy et al.[9] reported PE in 20.6% of the patients during their stay in the ICU, with a median time of 6 days. Another French study by Bompard et al.[10] reported a PE incidence of 50% in ICU, COVID-19 patients.

CTPA, a gold standard,[11] should be performed on admission if PE is suspected, or if there is acute degradation of hemodynamic or respiratory status, or if the patient presents with minimal pulmonary infiltrates or signs of acute right ventricular overload.[12,13]

This study aimed to investigate the prevalence of PE diagnosed by CTPA in COVID-19 patients and the features of the associated factors.

Materials and Methods

The study included 162 patients from the Imam Abdulrahman Al-Faisal Hospital who had COVID-19-confirmed infections while hospitalized in the ICU. The baseline characteristics of COVID-19 patients are shown in Table 1.

Table 1.
Baseline characteristics of COVID-19 patients.

Patient group	Age (years)	Height (cm)	Weight (kg)	BMI (kg/m^2)	HR (bpm)	RR (bpm)
Male	52.2±13 (18-92)	169.4±6 (150-188)	80.8±11 (52-119)	28.1±4 (18.1-37.5)	79.5±8 (22-100)	21.3±6 (17-78)
Female	50.8±15 (22-84)	161±7 (134-188)	78.4±15 (52-120)	30±5 (21.4-45.7)	81.4±12 (52-146)	21.1±2 (18-25)
Total	51.8±14 (18-92)	167±7 (134-188)	80.1±12 (52-120)	28.7±4 (18.4-45.7	80.1±9 (22-146)	21.2±5 (17 -78)

Patients admitted for treatment or isolation had to meet the following criteria: (a) positive SARS-CoV-2 RT-PCR testing on pharyngeal swabs; (b) a thin-section chest CT scan indicating any signs of pneumonia; and (c) patients hospitalized for treatment or isolation. All patients were examined based on the World Health Organization's interim recommendations for the clinical care of COVID-19 patients (WHO, 2022).

All patients were identified via the electronic record system, and their demographic, clinical, and radiological data were extracted and reviewed. Patients were diagnosed as COVID-19 positive by RT-PCR and underwent CTPA examination on the Discovery 16-slice CT scanner (Siemens, Germany) following standard protocol. We used non-ionic, iodinated, intravenous contrast material (Omnipaque 350 mg) for contrast enhancement. CTPA images were double-reviewed by radiologists with more than 10 years of experience. If PE was detected in the CTPA, the location, distribution, size, and type were documented.[14]

Statistical analysis was performed using the statistical software package SPSS version 21.0 (SPSS Inc, Armonk, NY: IBM Corp). Baseline characteristics were summarized as frequencies and percentages for categorical variables and mean ± SD for continuous variables. For data with normal distribution, inter-group comparisons were performed using Student's t-test. The frequencies of categorical variables were compared using a chi-squared test. A probability value of $P<0.05$ was considered statistically significant.

Results

The patients ranged in age from 18 to 92 years. The largest age group was 56-60 years (Table 2). The distribution of symptoms in COVID-19 patients is shown in Table 3.

Table 2.
Patient distribution by age group.

Age group (year)	N	%	Cumulative Percentage
<20	2	1.2	1.2
20-25	2	1.2	2.5
26-30	6	3.7	6.2
31-35	8	4.9	11.1
36-40	18	11.1	22.2
41-45	20	12.3	34.6
46-50	19	11.7	46.3
51-55	23	14.2	60.5
56-60	25	15.4	75.9
61-65	18	11.1	87.0
66-70	7	4.3	91.4
>70	14	8.6	100.0
Total	162	100.0	

Table 3.

The distribution of symptoms in COVID-19 patients.

Signs and symptoms	N	Percent
Fever	19	11.7%
Cough	11	6.8%
General symptoms	49	30.2%
General symptoms & pneumonia	30	18.5%
Breath shortness	39	24.1%
Sore throat	2	1.2%
Diarrhea	4	2.5%
Body pain	4	2.5%
Vomiting	2	1.2%
Others	1	0.6%
General symptoms & pneumonia & other symptoms	1	0.6%
Total	162	100%

PE was detected by CTPA in 87(53.7%) COVID-19 patients. In general, the death rate was 9.87%, and the causes of death are presented in Table 4. Three images demonstrate features of COVID-19 on CT (Figures 1-3).

Table 4.

Causes of death.

Causes of death among 162 COVID-19 patients	N	Percent
Irreversible cardiogenic shock	1	0.617
Metabolic acidosis	1	0.617
Irreversible shock/cardiac arrest	1	0.617
ARDS/septic shock	2	1.234
ARDS/septic shock/cardiac arrest	1	0.617
Septic shock/ARDS /AKI	1	0.617
ARDS/PE/septic shock	1	0.617
ARDS/respiratory failure	1	0.617
Metabolic acidosis/shock	1	0.617
Cardiovascular collapse/refractory hypoxia	1	0.617
ARDS /cardiogenic shock	1	0.617
Shock/metabolic acidosis/AKI/cardiac arrest	1	0.617
ARDS/septic shock/cardiac arrest/PE	1	0.617
Severe ARDS/shock/AKI/pneumothorax/PE	1	0.617
Chronic renal failure/septic shock	1	0.617
Total	16	9.872%

A comparison of the demographic and clinical characteristics of COVID-19 patients with PE and without PE is presented in Table 5. Mean levels of SBP and DBP were within the recommended values in both groups. The D-dimer level was significantly higher in the PE group than in the non-PE group (4.7±11.2 vs.1.8±2.8 µg/mL, *P*=0.031). The frequency of renal impairment in the PE group was 2.3 times higher than in the non-PE group (27.6% vs.12.0%, *P*=0.014). The ICU duration was longer in the PE group than in non-PE group (12.9±11.3 and 8.6±7.2 days, *P*=0.005). The death rate was 17.2% in the PE group and 1.3% in the non-PE group (*P*=0.001). The heart and respiratory rates, blood pressure, BMI, BUN, and creatinine levels did not differ in the study groups. The frequency of diabetes, hypertension, asthma, COPD, and smoking were comparable in the groups.

Table 5.

Demographic and clinical characteristics of the studied groups.

Variable		PE (n= 87)	Non-PE (n=75)	*P*-value
Demographic data				
Age, years		50.8±12.9	52.2±15.2	0.527
Sex	Female	30 (34.5%)	22 (29.3%)	0.485
	Male	57 (65.5%)	53 (70.7%)	
Nationality	Non-Saudi	56 (64.4%)	37 (49.3%)	0.054
	Saudi	31 (35.6%)	38 (50.7%)	
Height, cm		166.6±8.1	167±6.6	0.734
Weight, kg		78.6±12.7	81.2±13.5	0.209
BMI, kg/m^2		28.3±4.3	29.0±3.8	0.277
Vital signs				
SBP, mmHg		128±12	129±11	0.583
DBP, mmHg		77.8±5.8	78.7±6.0	0.334
HR, bpm		80±10.8	80±6.8	1.000
RR, bpm		21.5±6.4	20.9±2.2	0.441
History of risk factors				
Diabetes Mellites		50 (57.5%)	33 (44.0%)	0.088
Hypertension		31 (35.6%)	30 (40.0%)	0.569
Asthma		11 (12.6%)	10 (13.3%)	0.897
COPD		1 (1.1%)	0.0(0.0%)	0.353
Smoking		2 (2.3%)	1 (1.3%)	0.813
Laboratory investigations				
D-dimer, µg/mL		4.7±11.2	1.8±2.8	0.031
BUN, mg/dL		8.2±8.4	7.1±4.0	0.301
Creatinine, µmol/L		73.6±28.9	79.2±43.2	0.328
AKI, n %		24 (27.6%)	9 (12.0%)	0.014
Outcomes				
ICU duration, days		12.9±11.3	8.6±7.2	0.005
Death		15 (17.2%)	1 (1.3%)	0.001

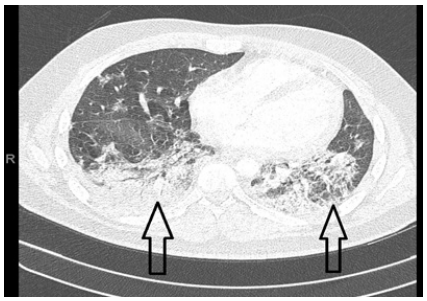

Fig.1. *A 22-year-old Saudi female patient. Bilateral patchy consolidated opacities at the lower lobes.*

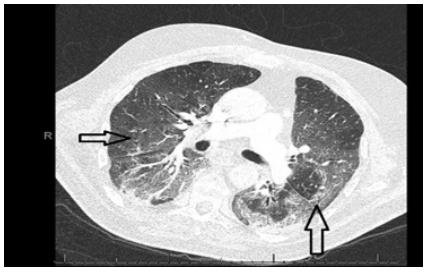

Fig.2. *A 65-year-old non-Saudi male patient. Bilateral ground glass opacity, the middle and lower consolidation.*

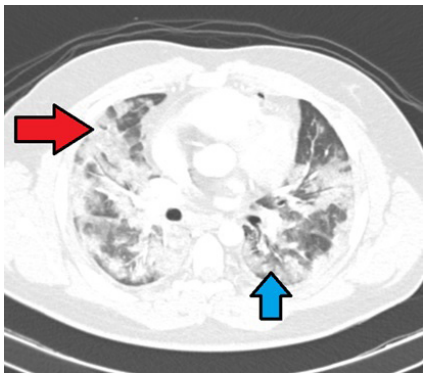

Fig.3. *A 31-year-old non-Saudi male patient. Crazy paving (red arrow) and areas of consolidation (blue arrow)*

Discussion

Pulmonary embolism is highly associated with COVID-19 disease and should be further explored and characterized for each patient.[15] Our study detected PE, diagnosed by CTPA, in 87(53.7%) COVID-19 patients. This result is much higher than that of Kyriakopoulos et al.[16] in Greece (6%). In a study by Abohamr et al.,[17] the incidence of acute PE was 22% [95% confidence interval (95% CI): 19%-39%], detected by chest CT. Overall, a higher prevalence of PE can be assumed among COVID-19 patients in Saudi Arabia. This study examined a wide range of variables associated with PE in patients with COVID-19. Regarding the gender of patients in this study population, males were more affected by COVID-19 than females, which agrees with a study by Abohamr et al.[17] from Saudi Arabia and Espallargas et al.[18] from Spain. This might be attributed to a higher probability of contact and exposure to sources of SARS-CoV-2 virus due to the nature of work among male rather than female patients.

Among factors predisposing to increased mortality with COVID-19 infection, male sex, hypertension, obesity, and increasing age are most important, but multiple studies have shown that excess weight is also significantly associated with severe COVID-19 disease.[19] The body mass index (BMI) of 28.7±4.0 kg/m^2 of participants in our research, which corresponds to the overweight range according to NHLBI (2022),[20] was found to be close to the mean BMI of 30.8 kg/m^2, which is within the obese range found in a US study of 20,736 COVID-19 patients.[21]

By analyzing the relationship between known risk factors for poor prognosis in COVID-19 and the development of PE, we found that COVID-19 patients with PE were characterized by significantly higher D-dimer level and ICU duration than non-PE patients [4.7±11.2 vs.1.8±12.8 µg/mL (P=0.031), 12.9±11.3 vs. 8.6±7.2 days (P=0.005), respectively]. Abohamr et al.[17] found that COVID-19 patients with PE had significantly higher levels of D-dimer, C-reactive protein, cardiac troponin, and lactate dehydrogenase than those in patients without PE. In a study by Mouhat,[22] elevated D-dimers (>2590 ng/mL) and the absence of anticoagulant therapy predicted PE in hospitalized COVID-19 patients with clinical signs of severity. D-dimers ≥2000 ng/mL (26.3 [4.1–537.8]) and neutrophils ≥7.0 g/L (5.8 [1.4–29.5]) were two biomarkers associated with a higher risk of PE (P=0.0002) and death or intensive care unit (ICU) transfer (HR [95%CI], 12.9 [2.5–67.8], P<0.01) in a study by Thoreau et al.[23] According to Kaminetzky et al.,[24] the D-dimer level can be used to stratify patients according to PE risk and severity.

The relationships we found between CTPA-diagnosed PE and studied parameters in our study were consistent with the results of a number of studies. Bompard et al.[10] showed that patients with PE were more frequently hospitalized in the ICU and more frequently under mechanical ventilation, with a longer median (IQR) hospitalization duration (15(9–17) vs. 8(4–12) days [P=0.04] in the PE-negative patients).

In our study, high levels of blood D-dimer, and ICU duration in PE patients were accompanied by more than 13 times higher mortality: 17.2% in the PE group and 1.3% in the non-PE group (P=0.001). Causes of death were irreversible cardiogenic shock, acute kidney injury, metabolic acidosis, large PE, respiratory failure, acute respiratory distress syndrome, septic shock, cardiovascular collapse, refractory hypoxia, and right-side pneumothorax. These causes of death were in accordance with data from Menter et al.[25] and Elezkurtaj et al.[26] Moreover, PE, in the study of Elezkurtaj et al.,[26] was the cause of death in 3.8% of cases.

As is known, comorbidities complicate the prognosis of COVID-19 patients. In our study, diabetes, identified in 57.5% of COVID-19 patients with PE and 44.0% of non-PE patients, was the most prevalent comorbidity, followed by hypertension. The high incidence of diabetes in our study is

explained by the high incidence of diabetes in the country. According to the International Diabetes Federation,[27] 17.7% of Saudi Arabia's adult population suffers from diabetes, which is the second highest diabetes prevalence in the region and seventh worldwide.

Hypertension is also the most common comorbidity in COVID-19 patients and increases in-hospital mortality. Blood pressure (BP) variability is associated with clinical outcomes in hypertensive patients. A study by He et al.[28] included 702 COVID-19 patients with hypertension from Huoshenshan Hospital (Wuhan, China). The authors demonstrated that day-by-day in-hospital systolic blood pressure variability can independently predict mortality and acute respiratory distress syndrome in COVID-19 patients with hypertension. In our study, the frequency of hypertension in the PE and non-PE groups was 35.6% and 40.0%, respectively, without statistical significance. However, mean levels of systolic blood pressure and diastolic blood pressure were within the recommended values in PE and non-PE patients. The heart and respiratory rates did not differ in the study groups.

Early reports indicate that acute kidney injury is common among patients with COVID-19 and is associated with worse outcomes and high mortality. In a study by Chan et al.,[29] of 3993 hospitalized patients with COVID-19, acute kidney injury occurred in 1835(46%) patients; 347(19%) of the patients with acute kidney injury required dialysis. In our study, renal impairment was found in 27.6% of COVID-19 patients with PE and only 12.0% of non-PE patients (P=0.014).

Compared to factors predisposing to increased mortality with COVID-19 infection, such as male sex, hypertension, obesity, and increasing age, airway diseases gave some contradictory results. Finnerty et al.,[30] in a systematic global review and meta-analysis, showed that for asthma and COPD, prevalence in patients hospitalized with COVID-19 varies markedly by region. The authors found no evidence that asthma predisposes one to increased mortality in COVID-19 disease. For COPD, there was clear evidence of an association with increased mortality. In our study, the prevalence of asthma and COPD was 12.6% and 1.1% in the PE group and 13.3% and 0% in the non-PE group, and no differences were found.

Conclusion

CT pulmonary angiography (CTPA) is very important in diagnosing PE in COVID-19 patients. CTPA-diagnosed PE is significantly associated with D-dimer, ICU duration, and death. The specified parameters, such as D-dimer levels in COVID-19 patients, as well as ICU duration, can be recommended as indicators or predictors of the development of PE in circumstances where immediate CT is unavailable.

Ethical Considerations

The study was conducted in accordance with ethical principles of the WMA Declaration of Helsinki (1964, ed. 2013) and was approved by the King Saud Medical City's institutional review board.

Competing Interests

The authors declare that they have no competing interests.

References

1. WHO: COVID-19 epidemiological update – 19 January 2024Available from: https://www.who.int/publications/m/item/covid-19-epidemiological-update---19-january-2024
2. Yousaf M, Thomas MM, Almughalles S, Hameed MA, Alharafsheh A, Varikkodan I, Waseem A, Babikir M, Chengamaraju D, Khatib MY. Pulmonary embolism in COVID-19, risk factors and association with inflammatory biomarkers. Medicine (Baltimore). 2023 Feb 17;102(7):e32887. doi: 10.1097/MD.0000000000032887. PMID: 36800623; PMCID: PMC9936004.
3. Xiong X, Chi J, Gao Q. Prevalence and risk factors of thrombotic events on patients with COVID-19: a systematic review and meta-analysis. Thromb J. 2021 May 19;19(1):32. doi: 10.1186/s12959-021-00284-9. PMID: 34011381; PMCID: PMC8132033.
4. Bilaloglu S, Aphinyanaphongs Y, Jones S, Iturrate E, Hochman J, Berger JS. Thrombosis in Hospitalized Patients With COVID-19 in a New York City Health System. JAMA. 2020 Aug 25;324(8):799-801. doi: 10.1001/jama.2020.13372. PMID: 32702090; PMCID: PMC7372509.
5. Fauvel C, Weizman O, Trimaille A, Mika D, Pommier T, Pace N, Douair A, Barbin E, Fraix A, Bouchot O, Benmansour O, Godeau G, Mecheri Y, Lebourdon R, Yvorel C, Massin M, Leblon T, Chabbi C, Cugney E, Benabou L, Aubry M, Chan C, Boufoula I, Barnaud C, Bothorel L, Duceau B, Sutter W, Waldmann V, Bonnet G, Cohen A, Pezel T; Critical Covid-19 France Investigators. Pulmonary embolism in COVID-19 patients: a French multicentre cohort study. Eur Heart J. 2020 Jul 1;41(32):3058-3068. doi: 10.1093/eurheartj/ehaa500. PMID: 32656565; PMCID: PMC7528952.
6. Klok FA, Kruip MJHA, van der Meer NJM, Arbous MS, Gommers DAMPJ, Kant KM, Kaptein FHJ, van Paassen J, Stals MAM, Huisman MV, Endeman H. Incidence of thrombotic complications in critically ill ICU patients with COVID-19. Thromb Res. 2020 Jul;191:145-147. doi: 10.1016/j.thromres.2020.04.013. Epub 2020 Apr 10. PMID: 32291094; PMCID: PMC7146714.
7. Akhter MS, Hamali HA, Mobarki AA, Rashid H, Oldenburg J, Biswas A. SARS-CoV-2 Infection: Modulator of Pulmonary Embolism Paradigm. J Clin Med. 2021 Mar 4;10(5):1064. doi: 10.3390/jcm10051064. PMID: 33806540; PMCID: PMC7961449.

***Corresponding author**: Prof. Abdelmoneim A. Sulieman, Radiological Sciences College of Applied Medical Sciences - Al Ahsa, King Saud bin Abdulaziz University for Health Sciences, Al-Ahsa, KSA. E-mail: abdelmoneim_a@yahoo.com*

8. Miesbach W, Makris M. COVID-19: Coagulopathy, Risk of Thrombosis, and the Rationale for Anticoagulation. Clin Appl Thromb Hemost. 2020 Jan-Dec;26:1076029620938149. doi: 10.1177/1076029620938149. PMID: 32677459; PMCID: PMC7370334.
9. Poissy J, Goutay J, Caplan M, Parmentier E, Duburcq T, Lassalle F, Jeanpierre E, Rauch A, Labreuche J, Susen S; Lille ICU Haemostasis COVID-19 Group. Pulmonary Embolism in Patients With COVID-19: Awareness of an Increased Prevalence. Circulation. 2020 Jul 14;142(2):184-186. doi: 10.1161/CIRCULATIONAHA.120.047430. Epub 2020 Apr 24. PMID: 32330083.
10. Bompard F, Monnier H, Saab I, Tordjman M, Abdoul H, Fournier L, Sanchez O, Lorut C, Chassagnon G, Revel MP. Pulmonary embolism in patients with COVID-19 pneumonia. Eur Respir J. 2020 Jul 30;56(1):2001365. doi: 10.1183/13993003.01365-2020. PMID: 32398297; PMCID: PMC7236820.
11. Righini M, Robert-Ebadi H. Diagnosis of acute Pulmonary Embolism. Hamostaseologie. 2018 Feb;38(1):11-21. English. doi: 10.5482/HAMO-17-07-0023. Epub 2018 Feb 26. PMID: 29536476.
12. Adams E, Broce M, Mousa A. Proposed Algorithm for Treatment of Pulmonary Embolism in COVID-19 Patients. Ann Vasc Surg. 2021 Jan;70:282-285. doi: 10.1016/j.avsg.2020.08.088. Epub 2020 Sep 4. PMID: 32891745; PMCID: PMC7471764.
13. Rosovsky RP, Grodzin C, Channick R, Davis GA, Giri JS, Horowitz J, Kabrhel C, Lookstein R, Merli G, Morris TA, Rivera-Lebron B, Tapson V, Todoran TM, Weinberg AS, Rosenfield K; PERT Consortium. Diagnosis and Treatment of Pulmonary Embolism During the Coronavirus Disease 2019 Pandemic: A Position Paper From the National PERT Consortium. Chest. 2020 Dec;158(6):2590-2601. doi: 10.1016/j.chest.2020.08.2064. Epub 2020 Aug 27. PMID: 32861692; PMCID: PMC7450258.
14. Wong KT, Antonio GE, Hui DS, Lee N, Yuen EH, Wu A, Leung CB, Rainer TH, Cameron P, Chung SS, Sung JJ, Ahuja AT. Thin-section CT of severe acute respiratory syndrome: evaluation of 73 patients exposed to or with the disease. Radiology. 2003 Aug;228(2):395-400. doi: 10.1148/radiol.2283030541. Epub 2003 May 8. PMID: 12738877.
15. Benzakoun J, Hmeydia G, Delabarde T, Hamza L, Meder JF, Ludes B, Mebazaa A. Excess out-of-hospital deaths during the COVID-19 outbreak: evidence of pulmonary embolism as a main determinant. Eur J Heart Fail. 2020 Jun;22(6):1046-1047. doi: 10.1002/ejhf.1916. Epub 2020 Jun 29. PMID: 32463538; PMCID: PMC7283748.
16. Kyriakopoulos C, Gogali A, Exarchos K, Potonos D, Tatsis K, Apollonatou V, Loukides S, Papiris S, Sigala I, Katsaounou P, Aggelidis M, Fouka E, Porpodis K, Kontakiotis T, Sampsonas F, Karampitsakos T, Tzouvelekis A, Bibaki E, Karagiannis K, Antoniou K, Tzanakis N, Dimeas I, Daniil Z, Gourgoulianis K, Kouratzi M, Steiropoulos P, Antonakis E, Papanikolaou IC, Ntritsos G, Kostikas K. Reduction in Hospitalizations for Respiratory Diseases during the First COVID-19 Wave in Greece. Respiration. 2021;100(7):588-593. doi: 10.1159/000515323. Epub 2021 Apr 7. PMID: 33827103; PMCID: PMC8089411.
17. Abohamr SI, Aldossari MA, Amer HA, Saadeddin HM, Abulhamid SW, Bhat FA, Elsheikh E. The Incidence of Acute Pulmonary Embolism with COVID-19 Pneumonia in Saudi Arabia: A Retrospective Single-Center Study. J Saudi Heart Assoc. 2020 May 6;33(2):128-134. doi: 10.37616/2212-5043.1253. PMID: 34183909; PMCID: PMC8143725.
18. Espallargas I, Rodríguez Sevilla JJ, Rodríguez Chiaradía DA, Salar A, Casamayor G, Villar-Garcia J, Rodó-Pin A, Marsico S, Carbullanca S, Ramal D, Del Carpio LA, Gayete Á, Maiques JM, Zuccarino F. CT imaging of pulmonary embolism in patients with COVID-19 pneumonia: a retrospective analysis. Eur Radiol. 2021 Apr;31(4):1915-1922. doi: 10.1007/s00330-020-07300-y. Epub 2020 Sep 22. PMID: 32964337; PMCID: PMC7508235.
19. Yu W, Rohli KE, Yang S, Jia P. Impact of obesity on COVID-19 patients. J Diabetes Complications. 2021 Mar;35(3):107817. doi: 10.1016/j.jdiacomp.2020.107817. Epub 2020 Nov 26. PMID: 33358523; PMCID: PMC7690270.
20. NHLBI. Calculate Your Body Mass Index. Available from: https://www.nhlbi.nih.gov/health/educational/lose_wt/BMI/bmi-m.htm
21. Roth GA, Emmons-Bell S, Alger HM, Bradley SM, Das SR, de Lemos JA, Gakidou E, Elkind MSV, Hay S, Hall JL, Johnson CO, Morrow DA, Rodriguez F, Rutan C, Shakil S, Sorensen R, Stevens L, Wang TY, Walchok J, Williams J, Murray C. Trends in Patient Characteristics and COVID-19 In-Hospital Mortality in the United States During the COVID-19 Pandemic. JAMA Netw Open. 2021 May 3;4(5):e218828. doi: 10.1001/jamanetworkopen.2021.8828. PMID: 33938933; PMCID: PMC8094014.
22. Mouhat B, Besutti M, Bouiller K, Grillet F, Monnin C, Ecarnot F, Behr J, Capellier G, Soumagne T, Pili-Floury S, Besch G, Mourey G, Lepiller Q, Chirouze C, Schiele F, Chopard R, Meneveau N. Elevated D-dimers and lack of anticoagulation predict PE in severe COVID-19 patients. Eur Respir J. 2020 Oct 22;56(4):2001811. doi: 10.1183/13993003.01811-2020. PMID: 32907890; PMCID: PMC7487272.
23. Thoreau B, Galland J, Delrue M, Neuwirth M, Stepanian A, Chauvin A, Dellal A, Nallet O, Roriz M, Devaux M, London J, Martin-Lecamp G, Froissart A, Arab N, Ferron B, Groff MH, Queyrel V, Lorut C, Regard L, Berthoux E, Bayer G, Comarmond C, Lioger B, Mekinian A, Szwebel TA, Sené T, Amador-Borrero B, Mangin O, Sellier PO, Siguret V, Mouly S, Kevorkian JP, Lariboisière Covid Group, Vodovar D, Sene D. D-Dimer Level and Neutrophils Count as Predictive and Prognostic Factors of Pulmonary Embolism in Severe Non-ICU COVID-19 Patients. Viruses. 2021 Apr 26;13(5):758. doi: 10.3390/v13050758. PMID: 33926038; PMCID: PMC8146364.
24. Kaminetzky M, Moore W, Fansiwala K, Babb JS, Kaminetzky D, Horwitz LI, McGuinness G, Knoll A, Ko JP. Pulmonary Embolism at CT Pulmonary Angiography in Patients with COVID-19. Radiol Cardiothorac Imaging. 2020 Jul 2;2(4):e200308. doi: 10.1148/ryct.2020200308. PMID: 33778610; PMCID: PMC7336753.
25. Menter T, Haslbauer JD, Nienhold R, Savic S, Hopfer H, Deigendesch N, Frank S, Turek D, Willi N, Pargger H, Bassetti S, Leuppi JD, Cathomas G, Tolnay M, Mertz KD, Tzankov A. Postmortem examination of COVID-19 patients reveals

diffuse alveolar damage with severe capillary congestion and variegated findings in lungs and other organs suggesting vascular dysfunction. Histopathology. 2020 Aug;77(2):198-209. doi: 10.1111/his.14134. Epub 2020 Jul 5. PMID: 32364264; PMCID: PMC7496150.

26. Elezkurtaj S, Greuel S, Ihlow J, Michaelis EG, Bischoff P, Kunze CA, Sinn BV, Gerhold M, Hauptmann K, Ingold-Heppner B, Miller F, Herbst H, Corman VM, Martin H, Radbruch H, Heppner FL, Horst D. Causes of death and comorbidities in hospitalized patients with COVID-19. Sci Rep. 2021 Feb 19;11(1):4263. doi: 10.1038/s41598-021-82862-5. PMID: 33608563; PMCID: PMC7895917.

27. IDF Diabetes Atlas 2021. Available from: https://diabetesatlas.org/atlas/tenth-edition/

28. He C, Liu C, Yang J, Tan H, Ding X, Gao X, Yang Y, Shen Y, Xiang H, Ke J, Yuan F, Chen R, Cheng R, Lv H, Li P, Zhang L, Huang L. Prognostic significance of day-by-day in-hospital blood pressure variability in COVID-19 patients with hypertension. J Clin Hypertens (Greenwich). 2022 Mar;24(3):224-233. doi: 10.1111/jch.14437. Epub 2022 Feb 7. PMID: 35293689; PMCID: PMC8925012.

29. Chan L, Chaudhary K, Saha A, Chauhan K, Vaid A, Zhao S, Paranjpe I, Somani S, Richter F, Miotto R, Lala A, Kia A, Timsina P, Li L, Freeman R, Chen R, Narula J, Just AC, Horowitz C, Fayad Z, Cordon-Cardo C, Schadt E, Levin MA, Reich DL, Fuster V, Murphy B, He JC, Charney AW, Böttinger EP, Glicksberg BS, Coca SG, Nadkarni GN; on behalf of the Mount Sinai COVID Informatics Center (MSCIC). AKI in Hospitalized Patients with COVID-19. J Am Soc Nephrol. 2021 Jan;32(1):151-160. doi: 10.1681/ASN.2020050615. Epub 2020 Sep 3. PMID: 32883700; PMCID: PMC7894657.

30. Finnerty JP, Hussain ABMA, Ponnuswamy A, Kamil HG, Abdelaziz A. Asthma and COPD as co-morbidities in patients hospitalised with Covid-19 disease: a global systematic review and meta-analysis. BMC Pulm Med. 2023 Nov 22;23(1):462. doi: 10.1186/s12890-023-02761-5. PMID: 37993829; PMCID: PMC10664669.

International Journal of Biomedicine 14(2) (2024) 312-318
http://dx.doi.org/10.21103/Article14(2)_OA13

ORIGINAL ARTICLE
Population Health

INTERNATIONAL JOURNAL OF BIOMEDICINE

Community Awareness and Perception Regarding Vaccination against COVID-19, Concerns about Side Effects in Gezira State, Sudan

Asaad MA. Babker[1], Sarah Elsiddig Dafallah[2], Hala Elsir Khair[3], Rania Saad Suliman[4], Yousif Mohammed Elmosaad[5], Abdullah A. Alqasem[6], Mohammed Ageeli Hakami[7], Alhomidi Almotiri[8], Hisham Ali Waggiallah[6*]

[1]*College of Health Sciences, Gulf Medical University, Ajman, United Arab Emirates*
[2]*Faculty of Medicine, Gadarif University, Gadarif, Sudan*
[3]*Faculty of Medical Laboratory Sciences, University of Gezira, Wad Madani, Sudan*
[4]*Prince Sultan Military College for Health Sciences, Dhahran, Saudi Arabia*
[5]*College of Applied Medical Sciences, King Faisal University, Al-Hofuf, Saudi Arabia*
[6]*College of Applied Medical Science, Prince Sattam Bin Abdulaziz University, Alkharj, Saudi Arabia*
[7]*College of Applied Medical Sciences, Al- Quwayiyah, Shaqra University, Riyadh, Saudi Arabia*
[8]*College of Applied Medical Sciences, Dawadmi, Shaqra University, Riyadh, Saudi Arabia*

Abstract

Introduction: Vaccine hesitancy is undermining individual and community protection from vaccine-preventable diseases. This study aimed to investigate the level of awareness and perception of the COVID-19 vaccine and its determinants among people in Wad Madani City, Gezira State, as well as its known side effects.

Methods and Results: This cross-sectional, descriptive, and correlative study included 400 participants (56.8% females and 43.2% males) who visited Wad Madani neighborhood COVID-19 centers during the data collection period (June 2022). The data was collected using a structured questionnaire based on prior published studies. Approximately 93.0% of the participants knew the importance of the COVID-19 vaccines, 84.8% knew about their effectiveness, and 83.8% knew that the vaccines help to reduce the risk of virus infection. However, only 58.0% were vaccinated against COVID-19. The results showed that 56.8% of the participants did not develop side effects. Among those who did, the most common side effects were headache and fever (10.2%), injection site pain (7.9%), myalgia (7.1%), and chills and swelling (5.6%). The results showed that 52.5% had negative perceptions of the COVID-19 vaccines. Urban residents were 2.17 times more likely to have a positive perception of the COVID-19 vaccine than rural residents (P=0.05). Furthermore, study participants with nuclear family type have shown a positive attitude toward the COVID-19 vaccines and were 2.32 times more likely to have had a positive attitude than participants with extended family (P=0.036). Moreover, participants not vaccinated were found to be less likely to have had a positive attitude toward the COVID-19 vaccine, when compared with vaccinated participants (P=0.005).

Conclusion: Although society is aware of the need for COVID-19 immunization, the community has a low positive perception toward COVID-19 vaccination. Similarly, people in rural areas are less aware of the significance of immunization. Local health officials must collaborate to address public fears about vaccinations through the media.**(International Journal of Biomedicine. 2024;14(2):312-318.)**

Keywords: COVID-19 • vaccination • hesitancy • awareness • perception

For citation: Babker AMA, Dafallah SE, Khair HE, Suliman RS, Elmosaad YM, Alqasem AA, Hakami MA, Almotiri A, Waggiallah HA. Community Awareness and Perception Regarding Vaccination against COVID-19, Concerns about Side Effects in Gezira State, Sudan. International Journal of Biomedicine. 2024;14(2):312-318. doi:10.21103/Article14(2)_OA13

Abbreviations

COVID-19, coronavirus disease 2019; **Pct**, percentage; **SARS-CoV-2**, severe acute respiratory syndrome coronavirus 2.

Introduction

The spread of SARS-CoV-2 has caused significant casualties and placed enormous strain on public health systems around the world, necessitating the implementation of various prevention and control strategies, including vaccine development and vaccination. As of November 2023, at least 70.5% of the world's population had received at least one dose of a COVID-19 vaccine.[1]

On February 28, 2024, the CDC recommended that people 65 and older should get an additional dose of any updated COVID-19 vaccine at least four months after their previous shot. This recommendation reflects that the risk of severe disease from COVID-19 continues throughout the year and is highest among older adults.

Each COVID-19 vaccine causes the immune system to create antibodies to fight COVID-19. The main types of COVID-19 vaccines currently available or being studied include messenger RNA (mRNA) vaccine (Pfizer-BioNTech and Moderna COVID-19), vector vaccine (Janssen/Johnson & Johnson COVID-19 vaccine, Oxford-AstraZeneca ChAdOx1 nCoV-19), protein subunit vaccine 9 (Novavax COVID-19).[2-4]

Large-scale vaccination against COVID-19 required comprehensive monitoring of vaccine safety. The Global COVID Vaccine Safety (GCoVS) Project, established in 2021 under the multinational Global Vaccine Data Network™, facilitated a comprehensive assessment of vaccine safety.[5]

Vaccines, regardless of the disease or vaccination program, are generally controversial. Vaccine hesitancy is a term used to describe delaying or refusing a vaccine despite its availability and is classified as one of the top ten threats to global health.[6,7]

Globally, vaccine hesitancy, reluctance to take vaccine, is determined by characteristics such as self-satisfaction, expediency, self-confidence, and various sociocultural and demographic factors. Vaccine hesitancy is undermining individual and community protection from vaccine-preventable diseases.

Understanding the fundamental factors determining the community's preferences and desires for a future vaccine may contribute to developing measures to improve the global immunization program.[8] This study aimed to investigate the level of awareness and perception of the COVID-19 vaccine and its determinants among people in Wad Madani City, Gezira State, as well as its known side effects.

Materials and Methods

We present a cross-sectional, descriptive, and correlative study based on health facilities. The research population consisted of people who visited Wad Madani neighborhood COVID-19 centers during the data collection period (June 2022). The study included 400 participants (56.8% females and 43.2% males). The data was collected using a structured questionnaire based on prior published studies. The total number of questions in the questionnaire was 27; sociodemographic data consists of six questions, 11 questions for awareness, and ten questions for perception.

Statistical analysis was performed using the statistical software package SPSS version 21.0 (SPSS Inc, Armonk, NY: IBM Corp). Group comparisons with respect to categorical variables are performed using the chi-square test. Multivariable-adjusted ORs, their respective 95%CIs, and P-values were calculated. A probability value of $P<0.05$ was considered statistically significant.

Ethical Considerations

The study protocol was reviewed and approved by the Ethics Committee at the University of Gezira's Department of Family Medicine (ECUG/FM/20/2/2023). Written informed consent was obtained from each research participant. All identifiable information about participants was removed, and the data were coded to ensure anonymity.

Results

Table 1 displays the socio-demographic details of the study participants. Most respondents (78/2%) were older than 25. Regarding marital status, 71.2% of the study participants were married. Participant's education level was 69.8% for high school or less graduates, 28.8% for college graduates, and 1.5% for postgraduate degrees. Most study participants (87.8%) lived in urban areas, while only 12.3% lived in rural areas. More than two-thirds of the participants came from a nuclear family, while a minority came from an extended family. The analysis showed that vaccination status was not associated with gender, age, marital status, places of residence, or family type. Only one significant association was found between education level and vaccination status (P=0.032). More than half of those who graduate from college were vaccinated against COVID- 19.

Table 1.

The socio-demographic details of the study participants (n=400).

Variables	Responses	Count	Pct	Vaccinated	Unvaccinated	*P*
Gender	Male	173	43.2	100 (57.8)	73 (42.2)	0.944
	Female	227	56.8	132 (58.1)	95(41.9)	
Age	18-25 years	87	21.8	47 (54.0)	40 (46.0)	0.395
	Over 25 years	313	78.2	185 (59.1)	128 (40.9)	
Marital status	Married	285	71.2	169 (59.3)	116 (40.7)	0.408
	Unmarried	115	28.8	63 (54.8)	52 (45.2)	
Education level	High school or less	279	69.8	153 (54.8)	126 (45.2)	0.032
	Diploma/ bachelor's degree	115	28.8	73 (63.5)	42 (36.5)	
	Postgraduate studies	6	1.5	0 (0.0)	6 (100)	
Places of residence	Urban	351	87.8	201 (57.3)	150 (42.7)	0.425
	Rural	49	12.2	31 (63.3)	18 (36.70	
Family type	Nuclear	350	87.5	201 (57.4)	149 (42.6)	0.540
	Extended	50	12.5	31 (62.0)	19 (3.0)	

A set of statements was developed to assess the study participants' awareness of the COVID-19 vaccine (Table 2). Of the study participants, 86.0% have received all the necessary vaccines during their lifetime. Approximately 93.0% [95.0, CI: 90.3-95.7] of the participants knew the importance of the COVID-19 vaccines, 84.8% knew about their effectiveness, and 83.8% knew that the vaccines help to reduce the risk of virus infection. However, only 58.0% [95.0%, CI: 52.8-63.2] were vaccinated against COVID-19. The results indicated that 53.2% [95.0%, CI: 548.1-58.5] of the participants knew that the COVID-19 vaccines have side effects, while 20.5% of the vaccinated participants recognized they had side effects after receiving the vaccine. However, it is remarkable that the participants were less aware of the vaccines' effectiveness in reducing mortality and complications related to COVID-19.

Table 2.

The study participants' awareness of the COVID-19 vaccine (n=400).

Questions	Count	Pct	(95.0% CI)
Have you received all the recommended vaccines? (Yes)	344	86.0	82.4-89.6
Did you receive the COVID-19 vaccine? (Yes)	232	58.0	52.8-63.2
Do you have any chronic diseases? (Yes)	141	35.2	30.3-40.3
Do you know about the COVID-19 vaccines? (Yes)	372	93.0	90.3-95.7
Do you know how effective the COVID-19 vaccination is? (Yes)	339	84.8	81.0-88.6
Do COVID-19 vaccines help to reduce the risk of virus infection? (Yes)	284	83.8	80.0-87.6
Do COVID-19 vaccines vaccine is effective in reducing mortality from COVID-19? (Yes)	15	4.4	2.3-6.5
Would COVID-19 vaccines produce immunity against COVID-19? (Yes)	19	5.6	3.2-8.0
Will COVID-19 vaccines reduce the complications of COVID-19? (Yes)	21	6.2	3.7-8.7
Do know COVID-19 vaccines have side effects? (Yes)	213	53.2	48.1-58.5
Did you get any side effects after receiving the COVID-19 vaccine? (Yes)	82	20.5	16.3-24.7

The COVID-19 vaccine side effects. results showed that 56.8% of the participants did not develop side effects. Among those who did, the most common side effects were headache and fever (10.2%), injection site pain (7.9%), myalgia (7.1%), and chills and swelling (5.6%). Moreover, a lesser percentage of the vaccinated participants experienced other side effects, such as nausea (3.0%), tiredness/fatigue (2.6%), and sore throat (2.3%) (Figure 1).

Table 3 summarizes the participants' perceptions of the COVID-19 vaccines. The results showed that 52.5% had negative perceptions. The mean perception score was 9.03±1.54, on a scale from 1 to 10. Most study participants (98.8%) agreed that coronavirus prevention measures and masks are still necessary even after vaccination. Moreover, 97.7% agreed that COVID-19 is a major public health issue that necessitates vaccines, 96.0% perceived that patients with the risk factors should be the first ones to get the vaccines, and 95.5% agreed that everyone should be required to get the vaccines. Notably, 22.0% of study participants perceived that diseases provide better immunity than vaccines. Based on Bloom's cut-off point criteria and levels of perception, the participants who got the mean and above score were considered to have positive perception (>9.03) points, and those who got less than the mean score were considered to have a negative perception (<9.03 points).

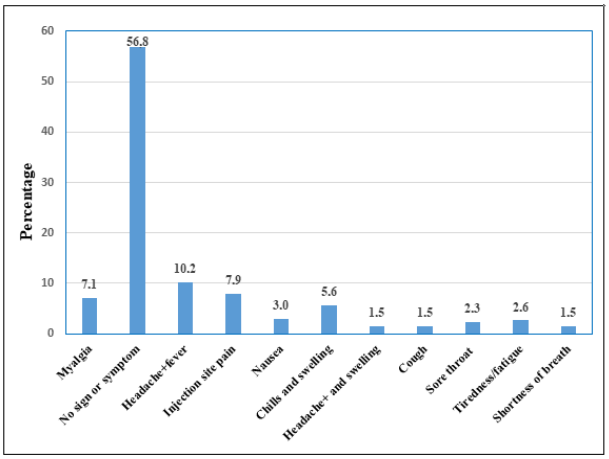

Fig. 1. *COVID-19 vaccine side effects.*

Table 3.

The participants' perceptions of the COVID-19 vaccines

Perception regarding COVID vaccination statements*	Agree (n / %)	Disagree (n / %)
Is COVID-19 a major public health issue that necessitates vaccines?	391/97.9	9/223
Is the government providing enough information about the vaccine's safety and efficacy?	353/88.2	47/11.8
COVID-19 vaccine was effective at preventing COVID-19.	375/93.8	25 (6.2)
Diseases provide better immunity than vaccines do	88/22.0	312 (78.0)
Everyone should be required to get the COVID-19 Vaccine	382/95.5	18 (4.5)
COVID-19 vaccinations are safe to use in the long term.	273/68.2	127 (31.8)
I believe that even after vaccination, coronavirus prevention measures and masks are still necessary.	395/98.8	5 (1.2)
I will recommend to my family to get COVID-19 vaccine	381/95.2	19 (4.8)
I believe that the COVID-19 vaccine would reduce the number of productive hours missed due to COVID-19 disease.	365/91.2	35 (8.8)
Patients with risk characteristics, in my opinion, should be the first to receive the COVID-19 vaccine.	384/96.0	16 (4.0)
Overall perception Positive perception Negative perception	190/47.5 210/52.5	

**These statements were used to compute the overall score of perception*

As revealed in Table 4, there were differences among the participants' sources of information about the COVID-19 vaccine. Most participants from urban areas got their information from public media (70.2%), followed by social media platforms (5.2%), colleagues, friends, and relatives (5.2%), and lastly, from newspapers (2.8%). In the same order, in smaller percentages, were the results for participants from rural areas. This indicates that public and social media platforms are important sources of information about the COVID-19 vaccine for both urban and rural residents.

Table 4.

The participants' sources of information about the COVID-19 vaccine.

Source of information	Residence		Total
	Urban (n/%)	Rural (n/%)	
Public media	281 (70.2)	13 (3.2)	294 (73.5)
Colleagues, friends, and relatives	21 (5.2)	12 (3.0)	33 (8.2)
Social media platforms	21 (5.2)	10 (2.5)	31 (7.8)
Different sources of information	17 |(4.2)	8 (2.0)	25 (6.2)
Newspapers	11 (2.8)	6 (1.5)	17 (4.2)
Total	351 (87.8)	49 (12.2)	400 (100)
P-value <0.0001			

The results showed a significant association between residents and reasons for willingness to take the COVID-19 vaccine. Among urban residents, the most common reason was protecting themselves from COVID-19 (76.7%), followed by protecting their relatives from infection (5.6%), and last was putting an end to the pandemic (4.3%). In the same order, in smaller percentages, were the results for participants from rural areas. This indicates that the important reasons that encouraged residents from both urban and rural areas were to protect themselves from COVID-19, protect their relatives from infection, and end the pandemic (Figure 2).

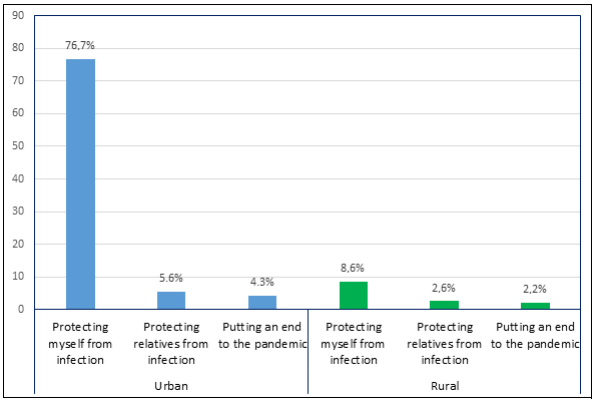

Fig. 2. *Reasons for willingness to take COVID-19 vaccine (P =0.002).*

Table 5 illustrates the results of a multivariate analysis of factors significantly associated with the study participants' perceptions of the COVID-19 vaccines

Table 5.

The results of a multivariate analysis of factors significantly associated with the study participants' perceptions of the COVID-19 vaccines adjusted by knowledge.

Predictors	Responses	Unadjusted model			Adjusted model		
		B	OR (95% CI)	*P*-value	B	OR (95% CI)	*P*-value
Gender	Male	R					
	Female	-0.09	0.92 (0.62-1.36)	0.660	-0.27	0.76 (0.50-1.17)	0.213
Age group	18-27 years	R					
	More than 25 years	-0.82	0.44 (0.27-0.73)	0.001	-0.31	0.73 (0.35-1.53)	0.408
Marital status	Married	R					
	Unmarried	0.73	2.08 (1.33-3.26)	0.001	0.39	1.48 (0.77-2.83)	0.241
Education level	High school or less	R					
	Bachelor's degree and above	0.50	1.66 (1.07-2.56)	0.023	0.20	1.22 (0.73-2.04)	0.453
Residence	Urban	R					
	Rural	-1.41	0.24 (0.12-0.50)	0.000	0.77	2.17 (1.98-4.79)	0.050
Family type	Nuclear	R					
	Extended	1.44	4.24 (2.05-8.74)	0.000	0.84	2.32 (1.06-5.08)	0.036
Do you know about the COVID-19 vaccines	No	R					
	Yes	-3.33	0.04 (0.01-0.27)	0.001	0.13	1.14 (0.74-1.76)	0.547
Did you receive the COVID-19 vaccine	No	R					
	Yes	-0.05	0.95 (0.64-1.42)	0.808	2.91	0.05 (0.01-0.42)	0.005

adjusted by knowledge. It is worth noting that some factors were significantly associated with the study participants' perceptions of the vaccines. These were place of residence, family type, and receiving the COVID-19 vaccine. Urban residents were 2.17 times more likely to have a positive perception of the COVID-19 vaccine [B =0.77, P=0.05, (OR= 2.17, 95% CI: 1.98-4.79)] than rural residents. Furthermore, study participants with nuclear family type have shown a positive attitude toward the COVID-19 vaccines and were 2.32 times more likely to have had a positive attitude than participants with extended family [B=0.84, *P*=0.036, (OR=2.32, 95% CI: 1.06-5.08)]. Moreover, participants not vaccinated were found to be less likely to have had a positive attitude toward the COVID-19 vaccine, when compared with vaccinated participants [B =-2.91, *P*=0.005, (OR=0.05, 95% CI: 0.01-042)]. However, gender, age group, marital status, and education level were not associated with factors related to the study participants' perceptions toward the COVID-19 vaccine (*P*>0.05).

Discussion

COVID-19, as a global challenge, requires a global response. Sudanese medical authorities have ensured immunization coverage through COVID-19 vaccination programs. Despite huge efforts and money invested in COVID-19 training, this study discovered that a significant percentage of participants lacked an understanding of the disease's transmission mode and showed insufficient awareness of risk factors and disease avoidance, with a positive perception of only 47.5%.

According to the most recent findings, the older people polled were more likely to be vaccinated against COVID-19, which agreed with the outcomes of Lazarus et al.[9] In the current study, participants over 25 were more likely to be vaccinated than those under 25. Older people are more vulnerable to bacterial infections due to declines in physical ability and poor immunological response. Whether it involves pathogenic organisms or not, older people are more likely to become very unwell and have a higher fatality rate.[10] While the elderly are more prone to severe COVID-19 infections and death, higher disease concern in this group has been linked to favorable opinions for COVID-19 vaccines.[11] Moreover, because older people are more likely to acquire vaccine information from reputable sources such as radio and television, they are less likely to be overwhelmed with misinformation, contributing to vaccine reception.

In this study, male and female vaccination rates for COVID-19 were nearly identical, in contrast to recent research that found women to be more motivated to be vaccinated against COVID-19 than men, which contradicts previous studies that found men to have higher rates of influenza vaccination.[12] This could be because women perceive health threats differently than men. According to the current study, highly educated groups were significantly more likely to receive COVID-19 immunizations than less educated ones. This could be because higher educated people gain more information from social media and other sources, and they are more concerned about the efficacy and negative repercussions of COVID-19 vaccines, which influences their willingness to be vaccinated. Previous influenza vaccine research had comparable results.[13]

The investigation discovered that our participants exhibited negative attitudes and perceptions, which contradicts the revelation that a high level of knowledge was highly associated with more positive attitudes and perceptions. At the same time, in a study by Papagiannis et al.,[14] Greek healthcare workers had a high level of knowledge concerning the SARS-CoV-2 pandemic, which was significantly associated with positive attitudes and practices toward preventive health measures. Health professionals' high level of knowledge about SARS-CoV-2 may have contributed considerably to the successful management of the pandemic in Greece. Published data from a knowledge, attitude, and practice survey conducted during COVID-19 among the general population in China revealed a high rate of correct answers in the knowledge questionnaire, which the authors attributed to the participants' high educational level and the severity of the public health program.[15]

The dangers of SARS-CoV-2 and the necessity for immunization should be actively promoted throughout vaccine promotion initiatives. Validation of the vaccine's efficacy by credible sources, medical advice, and government media marketing of the vaccine's utility can all influence citizens to choose immunization.[16]

Based on our findings, the percentage of participants who had a solid comprehension of COVID-19 was significantly higher among those who received the COVID-19 vaccine than those who did not, and extended family members had more knowledge than nuclear family members.

In our study, widespread belief in the efficacy of conventional healthcare in preventing and curing COVID-19, as well as misinformation from social media platforms, newspapers, colleagues, friends, and relatives, may have contributed to the lower knowledge rating among non-vaccinated and nuclear family participants.

According to the WHO, the side effects of COVID-19 vaccines are mostly minor and last only a few days. In our study, the most prevalent adverse effects were headache, muscle discomfort, fever, tiredness, and joint pain. These findings are consistent with the results reported by Riad et al.,[17] Zhu et al.,[18] and numerous other studies. The most frequently stated local side effect was injection discomfort. A study by Almughais et al.[19] included 2,530 participants from different regions of Saudi Arabia. The most common vaccine among the study group was Pfizer-BioNTech COVID-19 vaccine, for which 73.8% of the population was provided; the remaining 26.2% received the Oxford-AstraZeneca vaccine. Regarding the Pfizer-BioNTech vaccine, the common systemic side effects that followed the first dose included headaches, followed by muscle pain, fever, and joint pain. Vaccine side effects were more frequently reported by smokers and those who received the AstraZeneca vaccine. The documented side effects among our study participants indicate that vaccinations have safe characteristics. These findings are consistent with the results reported in a study by

Alhazmi et al.,[20] in which Oxford-AstraZeneca and Pfizer-BioNTech vaccines were received by 75% and 25% of the study participants, respectively. Side effects associated with COVID-19 vaccines have been reported by 60% of the study subjects, and most of them reported fatigue (90%) and pain at the site of the injections (85%).

More research is needed to determine the efficacy of current vaccines in protecting against COVID-19. Another study on the assessment in Jordan of side effects and perceptions after COVID-19 found that most post-vaccination side effects were common and non-life threatening (fatigue, chills, disorientation, fever, headache, joint pain, and myalgia). Only 10% of participants had severe side effects, whereas 39% and 21% had moderate and mild side effects. At the same time, the results of the GCoVS Project should also be noted.[5] This multi-country analysis confirmed pre-established safety signals for myocarditis, Guillain-Barré syndrome, and cerebral venous sinus thrombosis. Other potential safety signals that require further investigation were identified.

Conclusion

Although society is aware of the need for COVID-19 immunization, it has been observed that the community has a low positive perception toward COVID-19 vaccination. Similarly, people in rural areas are less aware of the significance of immunization. Local health officials must collaborate to address public fears about vaccinations through the media, which has a significant and powerful influence, particularly now that different variants of SARS-CoV-2 are developing and spreading.

Competing Interests

The authors declare that they have no competing interests.

Acknowledgments

This study was supported by the Deanship of Scientific Research at Prince Sattam bin Abdulaziz University.

References

1. Our World in Data. Coronavirus (COVID-19) Vaccinations - Our World in Data 2023. Available from: https://ourworldindata.org/covid-vaccinations

2. Hatmal MM, Al-Hatamleh MAI, Olaimat AN, Hatmal M, Alhaj-Qasem DM, Olaimat TM, Mohamud R. Side Effects and Perceptions Following COVID-19 Vaccination in Jordan: A Randomized, Cross-Sectional Study Implementing Machine Learning for Predicting Severity of Side Effects. Vaccines (Basel). 2021 May 26;9(6):556. doi: 10.3390/vaccines9060556. PMID: 34073382; PMCID: PMC8229440.

3. Heidary M, Kaviar VH, Shirani M, Ghanavati R, Motahar M, Sholeh M, Ghahramanpour H, Khoshnood S. A Comprehensive Review of the Protein Subunit Vaccines Against COVID-19. Front Microbiol. 2022 Jul 14;13:927306. doi: 10.3389/fmicb.2022.927306. PMID: 35910658; PMCID: PMC9329957.

4. Hanawi MK, Keetile M, Kadasah NA, Alshareef N, Qattan AMN, Alsharqi O. Side Effects and Perceptions of COVID-19 Vaccination in Saudi Arabia: A Cross-Sectional Study. Front Med (Lausanne). 2022 Jun 7;9:899517. doi: 10.3389/fmed.2022.899517. PMID: 35746946; PMCID: PMC9210956.

5. Faksova K, Walsh D, Jiang Y, Griffin J, Phillips A, Gentile A, Kwong JC, Macartney K, Naus M, Grange Z, Escolano S, Sepulveda G, Shetty A, Pillsbury A, Sullivan C, Naveed Z, Janjua NZ, Giglio N, Perälä J, Nasreen S, Gidding H, Hovi P, Vo T, Cui F, Deng L, Cullen L, Artama M, Lu H, Clothier HJ, Batty K, Paynter J, Petousis-Harris H, Buttery J, Black S, Hviid A. COVID-19 vaccines and adverse events of special interest: A multinational Global Vaccine Data Network (GVDN) cohort study of 99 million vaccinated individuals. Vaccine. 2024 Apr 2;42(9):2200-2211. doi: 10.1016/j.vaccine.2024.01.100. Epub 2024 Feb 12. PMID: 38350768.

6. Butler R, MacDonald NE; SAGE Working Group on Vaccine Hesitancy. Diagnosing the determinants of vaccine hesitancy in specific subgroups: The Guide to Tailoring Immunization Programmes (TIP). Vaccine. 2015 Aug 14;33(34):4176-9. doi: 10.1016/j.vaccine.2015.04.038. Epub 2015 Apr 18. PMID: 25896376.

7. WHO. Ten Threats to Global Health in 2019. Available from: https://www.who.int/news-room/spotlight/ten-threats-to-global-health-in-2019

8. Al-Mohaithef M, Padhi BK. Determinants of COVID-19 Vaccine Acceptance in Saudi Arabia: A Web-Based National Survey. J Multidiscip Healthc. 2020 Nov 20;13:1657-1663. doi: 10.2147/JMDH.S276771. PMID: 33262600; PMCID: PMC7686470.

9. Lazarus JV, Ratzan SC, Palayew A, Gostin LO, Larson HJ, Rabin K, Kimball S, El-Mohandes A. A global survey of potential acceptance of a COVID-19 vaccine. Nat Med. 2021 Feb;27(2):225-228. doi: 10.1038/s41591-020-1124-9. Epub 2020 Oct 20. Erratum in: Nat Med. 2021 Jan 11;: PMID: 33082575; PMCID: PMC7573523.

10. Neumann-Böhme S, Varghese NE, Sabat I, Barros PP, Brouwer W, van Exel J, Schreyögg J, Stargardt T. Once we have it, will we use it? A European survey on willingness to be vaccinated against COVID-19. Eur J Health Econ. 2020 Sep;21(7):977-982. doi: 10.1007/s10198-020-01208-6. PMID: 32591957; PMCID: PMC7317261.

11. Fisher KA, Bloomstone SJ, Walder J, Crawford S, Fouayzi H, Mazor KM. Attitudes Toward a Potential SARS-CoV-2 Vaccine : A Survey of U.S. Adults. Ann Intern Med. 2020 Dec 15;173(12):964-973. doi: 10.7326/M20-3569. Epub 2020 Sep 4. PMID: 32886525; PMCID: PMC7505019.

12. Li Q, Guan X, Wu P, Wang X, Zhou L, Tong Y, Ren R, Leung KSM, Lau EHY, Wong JY, Xing X, Xiang N, Wu Y,

***Corresponding author:** Dr. Hisham Ali Waggiallah, Department of Medical Laboratory Science, College of Applied Medical Science, Prince Sattam Bin Abdulaziz University, Alkharj 11942, Saudi Arabia. E-mail: hishamwagg30@hotmail.com*

Li C, Chen Q, Li D, Liu T, Zhao J, Liu M, Tu W, Chen C, Jin L, Yang R, Wang Q, Zhou S, Wang R, Liu H, Luo Y, Liu Y, Shao G, Li H, Tao Z, Yang Y, Deng Z, Liu B, Ma Z, Zhang Y, Shi G, Lam TTY, Wu JT, Gao GF, Cowling BJ, Yang B, Leung GM, Feng Z. Early Transmission Dynamics in Wuhan, China, of Novel Coronavirus-Infected Pneumonia. N Engl J Med. 2020 Mar 26;382(13):1199-1207. doi: 10.1056/NEJMoa2001316. Epub 2020 Jan 29. PMID: 31995857; PMCID: PMC7121484.

13. Yan S, Wang Y, Zhu W, Zhang L, Gu H, Liu D, Zhu A, Xu H, Hao L, Ye C. Barriers to influenza vaccination among different populations in Shanghai. Hum Vaccin Immunother. 2021 May 4;17(5):1403-1411. doi: 10.1080/21645515.2020.1826250. Epub 2020 Dec 3. PMID: 33270473; PMCID: PMC8078689.

14. Papagiannis D, Malli F, Raptis DG, Papathanasiou IV, Fradelos EC, Daniil Z, Rachiotis G, Gourgoulianis KI. Assessment of Knowledge, Attitudes, and Practices towards New Coronavirus (SARS-CoV-2) of Health Care Professionals in Greece before the Outbreak Period. Int J Environ Res Public Health. 2020 Jul 8;17(14):4925. doi: 10.3390/ijerph17144925. PMID: 32650614; PMCID: PMC7400230.

15. Zhong BL, Luo W, Li HM, Zhang QQ, Liu XG, Li WT, Li Y. Knowledge, attitudes, and practices towards COVID-19 among Chinese residents during the rapid rise period of the COVID-19 outbreak: a quick online cross-sectional survey. Int J Biol Sci. 2020 Mar 15;16(10):1745-1752. doi: 10.7150/ijbs.45221. PMID: 32226294; PMCID: PMC7098034.

16. Kabamba Nzaji M, Kabamba Ngombe L, Ngoie Mwamba G, Banza Ndala DB, Mbidi Miema J, Luhata Lungoyo C, Lora Mwimba B, Cikomola Mwana Bene A, Mukamba Musenga E. Acceptability of Vaccination Against COVID-19 Among Healthcare Workers in the Democratic Republic of the Congo. Pragmat Obs Res. 2020 Oct 29;11:103-109. doi: 10.2147/POR.S271096. PMID: 33154695; PMCID: PMC7605960.

17. Riad A, Pokorná A, Attia S, Klugarová J, Koščík M, Klugar M. Prevalence of COVID-19 Vaccine Side Effects among Healthcare Workers in the Czech Republic. J Clin Med. 2021 Apr 1;10(7):1428. doi: 10.3390/jcm10071428. PMID: 33916020; PMCID: PMC8037149.

18. Zhu FC, Li YH, Guan XH, Hou LH, Wang WJ, Li JX, Wu SP, Wang BS, Wang Z, Wang L, Jia SY, Jiang HD, Wang L, Jiang T, Hu Y, Gou JB, Xu SB, Xu JJ, Wang XW, Wang W, Chen W. Safety, tolerability, and immunogenicity of a recombinant adenovirus type-5 vectored COVID-19 vaccine: a dose-escalation, open-label, non-randomised, first-in-human trial. Lancet. 2020 Jun 13;395(10240):1845-1854. doi: 10.1016/S0140-6736(20)31208-3. Epub 2020 May 22. PMID: 32450106; PMCID: PMC7255193.

19. Almughais ES, Alharbi AH, Aldarwish HA, Alshammari AF, Alsuhaymi RS, Almuaili JA, Alanizy AM. Side-effects of COVID-19 vaccines among the Saudi population: A cross-sectional study. Saudi Med J. 2022 Apr;43(4):386-393. doi: 10.15537/smj.2022.43.4.20210905. PMID: 35414617; PMCID: PMC9998061.

20. Alhazmi A, Alamer E, Daws D, Hakami M, Darraj M, Abdelwahab S, Maghfuri A, Algaissi A. Evaluation of Side Effects Associated with COVID-19 Vaccines in Saudi Arabia. Vaccines (Basel). 2021 Jun 18;9(6):674. doi: 10.3390/vaccines9060674. PMID: 34207394; PMCID: PMC8235009.

International Journal of Biomedicine 14(2) (2024) 319-323
http://dx.doi.org/10.21103/Article14(2)_OA14

ORIGINAL ARTICLE

Dentistry

INTERNATIONAL JOURNAL OF BIOMEDICINE

Palatoscopy and Palatal Rugae Pattern among Adolescents of Southeastern Kosovo

Miranda Sejdiu Abazi[1], Agim Prokshaj[1*], Vesel Rrustemaj[1], Arben Abazi[2*], Egzon Veliu[2], Mirand N. Heta[3]

[1]*Department of Dentistry, UBT Campus, Pristina, Kosovo*
[2]*Department of Dentistry, Faculty of Medicine, University of Pristina, Pristina, Kosovo*
[3]*Department of Maxillofacial Surgery, Clinical Centre of Kosovo, Pristina, Kosovo*

Abstract

Background: Palatal rugae are elevations found on the anterior part of the hard palate and are the most stable features in the mouth. Our study aimed to analyze the palatal rugae pattern among an adolescent sample of the Albanian population in southeastern Kosovo.

Methods and Results: A total of 100 adolescents (50 females and 50 males) aged from 12 to 18 were selected from schools in southeastern Kosovo. Palatal impressions were taken with elastomers, and models of the upper jaw were poured into stone casts for further examination. The rugae patterns were classified according to the Thomas and Kotze classification. The current study indicates that the predominant rugae pattern among the young population in southeastern Kosovo is the straight rugae. The predominant rugae pattern among female subjects is straight rugae and among males, wavy rugae; the frequency of various rugae patterns differed significantly between men and women. The total number of palatal rugae in men was significantly higher than in women. At the same time, there is no significant difference in the number of palatal rugae on the left and right sides between male and female subjects.**(International Journal of Biomedicine. 2024;14(2):319-323.)**

Keywords: palatoscopy • palatal rugae • rugae pattern

For citation: Abazi MS, Prokshaj A, Rrustemaj V, Abazi A, Veliu E, Heta MN. Palatoscopy and Palatal Rugae Pattern among Adolescents of Southeastern Kosovo. International Journal of Biomedicine. 2024;14(2):319-323. doi:10.21103/Article14(2)_OA14

Introduction

Palatoscopy, or palatal rugoscopy, studies palatal rugae patterns. Palatal rugae become apparent in the mouth between the 12th and 14th weeks of prenatal life. Epithelial-mesenchymal interactions are known to play a critical role in the development of many organs, including the palate. Periodic patterning of iterative structures, the palatal rugae, develops by Turing-type reaction-diffusion mechanisms that occur through epithelial-mesenchymal interactions.[1] Physiologically, relieving the palate helps swallowing, speech, tasting food, and sucking of the finger in children.[2]

***Corresponding authors**

Agim Prokshaj. Department of Dentistry, UBT Campus, Pristina, Kosovo. E-mail: agim.prokshaj@ubt-uni.net

Arben Abazi. Department of Dentistry, Faculty of Medicine, University of Pristina, Pristina, Kosovo. E-mail: arbenabazi033@gmail.com

Palatal rugae, like fingerprints, do not change throughout life. No two palates are alike regarding their rugae pattern, which remains stable even during an eruption or tooth loss.[3] The most widely known classification is the Thomas and Kotze classification.[4] Palatoscopy is also an important tool for gender determination.[5,6] Every person has a unique palatal rugae pattern, even in monozygotic twins. Herrera et al.[7] showed that palatal rugae were unique to each individual, even in monozygotic twins. Lestari et al.,[8] in their study of monozygotic twins, concluded that patterns of palatal rugae were unique in identical twins even though they showed a mirror-image effect. Therefore, they could be used as an adjunctive tool for medico-legal identification.

Currently, palatoscopy is considered a promising alternative method for identifying human individuals. Palatoscopy doesn't need complex instrumentation for examination but requires a very well-trained dentist with broad background knowledge in forensics. Mahajan et al.,[9] analyzing many studies in their review article, concluded that

palatoscopy can be successfully used for identifying humans. When dental identification is not possible in an edentulous patient, palatoscopy is the method of choice.[10] Poojya et al.[11] concluded that cast records are beneficial in these cases, but if they are unavailable, the mucosal surface of the dentures could be a good source for taking records. Our study aimed to analyze the palatal rugae pattern among an adolescent sample of the Albanian population in southeastern Kosovo.

Materials and Methods

A total of 100 adolescents (50 females and 50 males) aged from 12 to 18 were selected from schools in southeastern Kosovo. All 100 subjects were healthy, without any congenital abnormalities, orthognathic operations, previous orthodontic treatment, inflammation, trauma, malformations, deformities, or surgical scars.

Materials used for the study were elastomers (Zhermack), graphite pencils, and scissors (Figure 1). Palatal impressions were taken with elastomers, and models of the upper jaw were poured into stone casts for further examination. The shape of the rugae was traced with a graphite pencil (Figure 2).

Fig. 1. *Materials used for data collection.*

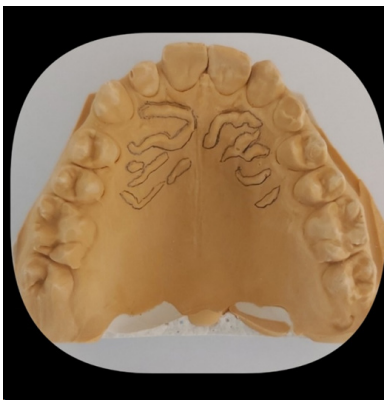

Fig. 2. *The highlighted rugae with graphite pencil.*

According to the Thomas and Kotze classification, the rugae patterns were classified based on shape, unification, and length. Based on shape, rugae were divided into Wavy (curved shape at the origin or termination), Straight (the rugae run directly from the origin to termination), Circular (rugae that form a continuous ring), Curved (crescent and curved gently); unification was defined as when two rugae are joined at their origin or termination. Unification was classified into divergent (rugae were considered to be diverging if two rugae had the same origin but immediately branched) and convergent (rugae were considered to be converging if two rugae with different origins joined on their lateral portions). The rugae were also classified based on their length as primary rugae (>5 mm), secondary (3-5 mm), and fragmentary (<3 mm).

Statistical analysis was performed using statistical software package SPSS version 23.0 (SPSS Inc, Armonk, NY: IBM Corp). Baseline characteristics were summarized as frequencies and percentages for categorical variables. Differences in attributive series between the patient groups were tested using Pearson Chi-square / Monte Carlo Sig. (2-sided). In all cases, a probability value of $P<0.05$ was considered statistically significant.

Results

Table 1 and Figure 3 show the shapes of the palatal rugae pattern in the subjects included in the study. A total of 519 the palatal rugae pattern were registered in 50 female subjects: 277(53.37%) on the right and 242(46.63%) on the left side. A total of 592 the palatal rugae pattern were registered in 50 male subjects: 294(49.66%) on the right and 298(50.34%) on the left side. On the right side of the palates of female subjects, the straight rugae were dominant (98/35.38%), followed by wavy rugae (68/24.55%), curved rugae (41/14.80%), circular rugae (30/10.83%), divergent rugae (29/10.47%), and convergent rugae (11/3.97%). The distribution pattern of different variants of rugae shapes on the left side of the palates of female subjects was similar to that on the right side. On the right side of the palates of male subjects, the wavy rugae were dominant (87/29.59%), followed by straight rugae (75/25.51%), curved rugae (57/19.39%), circular rugae (42/14.29%), divergent rugae (18/6.12%), and convergent rugae (15/5.10%). The distribution pattern of different variants of rugae shapes on the left side of the palates of male subjects was similar to that on the right side.

Table 1.
Shapes of the palatal rugae pattern in the study subjects.

Variable	Valid N	Female	%	Valid N	Male	%
Straight/Right	50	98	35.38	50	75	25.51
Straight/Left	50	68	28.10	50	80	26.85
Wavy/Right	50	68	24.55	50	87	29.59
Wavy/Left	50	67	27.69	50	76	25.50
Curved/Right	50	41	14.80	50	57	19.39
Curved/Left	50	50	20.66	50	68	22.82
Circular/Right	50	30	10.83	50	42	14.29
Circular/Left	50	24	9.92	50	42	14.09
Divergent/Right	50	29	10.47	50	18	6.12
Divergent/Left	50	23	9.50	50	20	6.71
Convergent/Right	50	11	3.97	50	15	5.10
Convergent/Left	50	10	4.13	50	12	4.03

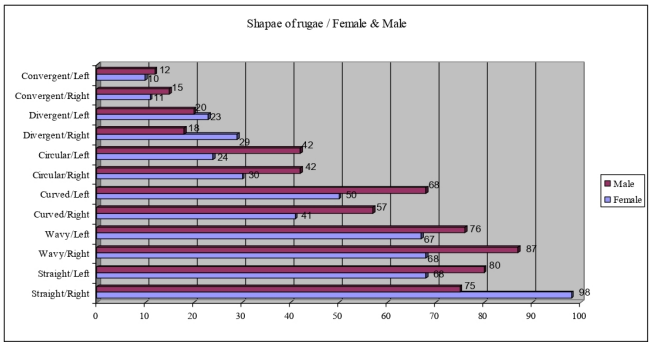

Fig. 3. *Shapes of the palatal rugae pattern in the subjects included in the study.*

Thus, among all those examined, 1111 palatal rugae were registered: the straight rugae (321/28.89%) were dominant, followed by wavy rugae (298/26.82%), curved rugae (216/19.44%), circular rugae (138/12.42%), divergent rugae (90/8.1%), and convergent rugae (48/4.32%) (Table 2 and Figure 4). The total distribution of the rugae patterns in female and male subjects is presented in Table 2. We found a significant difference in the total number of palatal rugae between female and male subjects (Pearson chi-squared =13.07 and *P*=0.023 / Monte Carlo Sig. (2-sided) / 0.019–0.026 /) (Table 2 and Figure 4). The frequency of various rugae patterns also differed significantly between men and women.

Table 2.

Total distribution of the rugae patterns in female and male subjects.

			Shape of rugae						Total
			Straight	Wavy	Curved	Cir	Div	Con	
Gender	Female	Count	166	135	91	54	52	21	519
		%	32.0	26.0	17.5	10.4	10.0	4.0	100.0
	Male	Count	155	163	125	84	38	27	592
		%	26.2	27.5	21.1	14.2	6.4	4.6	100.0
Total		Count	321	298	216	138	90	48	1111
		%	28.9	26.8	19.4	12.4	8.1	4.3	100.0

Cir - Circular; Div - Divergent; Con - Convergent.

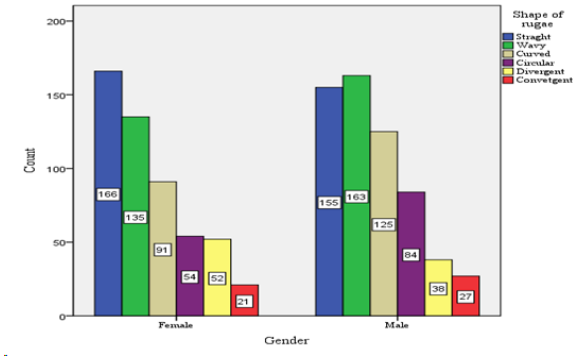

Fig. 4. *Total distribution of the rugae patterns in female and male subjects.*

Tables 3-4 and Figures 5-6 show the palatal rugae distribution based on their length on the right and left sides in female and male subjects.

In female subjects, on the right side, primary rugae were found in 197(69.12%) women, secondary rugae in 47(16.49%), and fragmentary rugae in 41(14.39%). The distribution patterns of primary, secondary, and fragmentary rugae on the left side of the palate were as follows: primary rugae - 193(72.83%), secondary rugae - 32(12.08%), and fragmentary rugae - 40(15.09%).

Table 3.

Palatal rugae distribution based on their length on the right and left sides in female subjects.

Gender	Side	n	Primary Rugae 5-10 mm	%	Secondary Rugae 3-5 mm	%	Fragmentary Rugae <3 mm	%	Total
Female	Right	50	197	69.12	47	16.49	41	14.39	285
	Left	50	193	72.83	32	12.08	40	15.09	265
Total		100	390		79		81		550

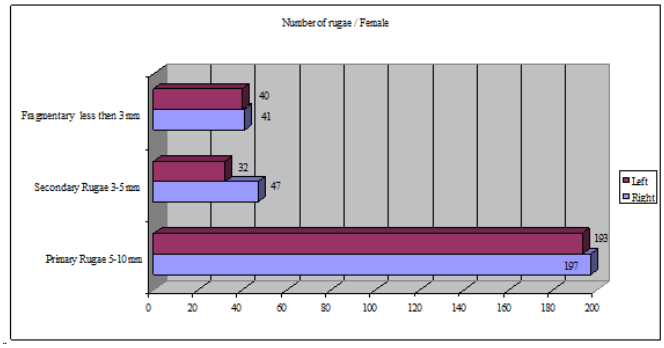

Fig. 5. *Palatal rugae distribution based on their length on the right and left sides in female subjects.*

Table 4.

Palatal rugae distribution based on their length on the right and left sides in male subjects.

Gender	Side	n	Primary Rugae 5-10 mm	%	Secondary Rugae 3-5 mm	%	Fragmentary Rugae <3 mm	%	Total
Male	Right	50	200	70.18	42	14.73	43	15.09	285
	Left	50	200	69.20	46	15.92	43	14.88	289
Total		100	400		88		86		574

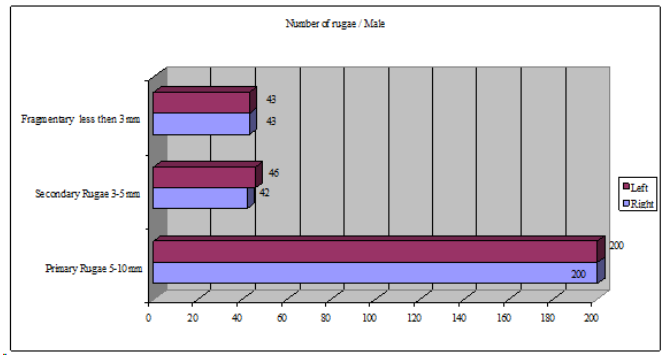

Fig. 6. *Palatal rugae distribution based on their length on the right and left sides in male subjects.*

In male subjects, on the right side, primary rugae were found in 200(70.18%) men, fragmentary rugae in 43(15.09%), and secondary rugae in 42(14.73%). The distribution patterns of primary, secondary, and fragmentary rugae on the left side of the palate were as follows: primary rugae - 200(69.20%), secondary rugae - 46(15.92%), and fragmentary rugae - 43(14.88%).

We found no significant difference in the number of primary, secondary, and fragmentary palatine rugae on the right and left sides of female and male subjects (P=0.34 and P=0.93, respectively).

Discussion

Palatoscopy studies palatal rugae, which are characteristic elevations in the anterior part of the hard palate. They are also unique for every person, like fingerprints. In the present study, 1111 palatal rugae were found in the study sample. The predominant rugae, among all subjects, were straight rugae (28.89%), followed by wavy shape (26.82%), curved rugae (19.44%), circular rugae (12.42%), divergent rugae (8.1%), and convergent rugae with the lowest frequency (4.32%). Similar results have been shown in studies by Pillai et al.,[12] Khalid et al.,[13] and Sheikhi et al.,[14] where the most common rugae were the straight type, followed by the wavy type. In contrast, a study by Byatnal et al.[15] found that a wavy shape was predominant among five different populations of India. Our study showed that the predominant rugae pattern in females was straight rugae (32%), while the wavy type was predominant in males (27.5%). The total number of palatal rugae in men was significantly greater than in women. The results of a study by Sharma et al.[16] showed contradictory data. We found no significant difference in the number of primary, secondary, and fragmentary palatine rugae on the right and left sides of female and male subjects. These findings were consistent with a study by Jadoon et al.[17]

Conclusion

The results of the current study indicate that the predominant rugae pattern among the young population in southeastern Kosovo is the straight rugae. The predominant rugae pattern among female subjects is straight rugae and among males, wavy rugae; the frequency of various rugae patterns differed significantly between men and women. The total number of palatal rugae in men was significantly higher than in women. At the same time, there is no significant difference in the number of palatal rugae on the left and right sides between male and female subjects.

Ethical Considerations

Ethical approval for this study was obtained from the Ethical Committees of the Faculty of Dentistry of Ss. Cyril and Methodius University in Skopje (N#02-150115) and the Dental Chamber of Kosovo, Republic of Kosovo (N#19). All participants provided written informed consent.

Competing Interests

The authors declare that they have no competing interests.

References

1. Kawasaki M, Kawasaki K, Meguro F, Yamada A, Ishikawa R, Porntaveetus T, Blackburn J, Otsuka-Tanaka Y, Saito N, Ota MS, Sharpe PT, Kessler JA, Herz J, Cobourne MT, Maeda T, Ohazama A. Lrp4/Wise regulates palatal rugae development through Turing-type reaction-diffusion mechanisms. PLoS One. 2018 Sep 20;13(9):e0204126. doi: 10.1371/journal.pone.0204126. PMID: 30235284; PMCID: PMC6147471.
2. Gandikota C, Venkata YP, Challa P, Juvvadi SR, Mathur A. Comparative study of palatal rugae pattern in class II div 1 and class I individuals. J Pharm Bioallied Sci. 2012 Aug;4(Suppl 2):S358-63. doi: 10.4103/0975-7406.100271. PMID: 23066290; PMCID: PMC3467934.
3. Indira A, Gupta M, David MP. Usefullness of palatal rugae patterns in establishing identity: Preliminary results from Bengaluru city, India. J Forensic Dent Sci. 2012 Jan;4(1):2-5. doi: 10.4103/0975-1475.99149. PMID: 23087574; PMCID: PMC3470413.
4. Thomas CJ, Kotze TJ. The palatal ruga pattern: a new classification. J Dent Assoc S Afr. 1983 Mar;38(3):153-7. PMID: 6579725.
5. Pereira T, Shetty S, Surve R, Gotmare S, Kamath P, Kumar S. Palatoscopy and odontometrics for sex identification and hereditary pattern analysis in a Navi Mumbai population: A cross-sectional study. J Oral Maxillofac Pathol. 2018 May-Aug;22(2):271-278. doi: 10.4103/jomfp.JOMFP_197_16. PMID: 30158785; PMCID: PMC6097358.
6. Smriti K, Gupta R, Pentapati KC, Singh A, Kapoor I, Vineetha R, Gadicherla S. Sex Assessment by Morphological Analysis of Palatal Rugae Patterns in a South Indian Adult Population. Clin Cosmet Investig Dent. 2021 Mar 17;13:77-81. doi: 10.2147/CCIDE.S304599. PMID: 33762852; PMCID: PMC7982778.
7. Herrera LM, Strapasson RA, Mazzilli LE, Melani RF. Differentiation between palatal rugae patterns of twins by means of the Briñón method and an improved technique. Braz

Oral Res. 2017 Mar 20;31:e9. doi: 10.1590/1807-3107BOR-2017.vol31.0009. PMID: 28327781.
8. Lestari W, Adanan NA, Mokhtar NI, Ardini YD, Ichw2an SJ, Haris MS. Tooth Morphometry and Pattern of Palatal Rugae Among Monozygotic Twins in Malaysia. J Orofac Sci. 2021;13;39-46
9. Mahajan R, Dar MA, Risam, SS. PALATOSCOPY / RUGOSCOPY: A POTENTIAL TOOL IN HUMAN IDENTIFICATION. Journal of Evolution of Medical and Dental Sciences. 2014;(3):10076-10088
10. Caldas IM, Magalhães T, Afonso A. Establishing identity using cheiloscopy and palatoscopy. Forensic Sci Int. 2007 Jan 5;165(1):1-9. doi: 10.1016/j.forsciint.2006.04.010. Epub 2006 May 24. PMID: 16725290.
11. Poojya R, Shruthi CS, Rajashekar VM, Kaimal A. Palatal Rugae Patterns in Edentulous Cases, Are They A Reliable Forensic Marker? Int J Biomed Sci. 2015 Sep;11(3):109-12. PMID: 26508904; PMCID: PMC4614010.
12. Pillai J, Banker A, Bhattacharya A, Gandhi R, Patel N, Parikh S. Quantitative and qualitative analysis of palatal rugae patterns in Gujarati population: A retrospective, cross-sectional study. J Forensic Dent Sci. 2016 Sep-Dec;8(3):126-134. doi: 10.4103/0975-1475.195110. PMID: 28123265.
13. Khalid K, Phillips VM. Palatal Rugae Patterns Among a Sudanese Population Sample. Int J Dentistry Oral Sci. 2016; 3(7):276-280
14. Sheikhi M, Zandi M, Ghazizadeh M. Assessment of palatal rugae pattern for sex and ethnicity identification in an iranian population. Dent Res J (Isfahan). 2018 Jan-Feb;15(1):50-56. doi: 10.4103/1735-3327.223611. PMID: 29497447; PMCID: PMC5806430.
15. Byatnal A, Byatnal A, Kiran AR, Samata Y, Guruprasad Y, Telagi N. Palatoscopy: An adjunct to forensic odontology: A comparative study among five different populations of India. J Nat Sci Biol Med. 2014 Jan;5(1):52-5. doi: 10.4103/0976-9668.127287. PMID: 24678197; PMCID: PMC3961952.
16. Sharma P, Saxena S, Rathod V. Comparative reliability of cheiloscopy and palatoscopy in human identification. Indian J Dent Res. 2009 Oct-Dec;20(4):453-7. doi: 10.4103/0970-9290.59451. PMID: 20139570.
17. Jadoon OK, Zaman MU, Zaman FU, Khan D, Farooq U, Seema N, Ahmed I. Analysis Of Palatal Rugae Pattern In Population Of Abbottabad: A Forensic Study. J Ayub Med Coll Abbottabad. 2018 Jul-Sep;30(3):428-431. PMID: 30465380.

International Journal of Biomedicine 14(2) (2024) 324-328
http://dx.doi.org/10.21103/Article14(2)_OA15

ORIGINAL ARTICLE

Dentistry

INTERNATIONAL JOURNAL OF BIOMEDICINE

Cytological and Cytometric Analysis of Epithelial Cell Changes Under the Surface of Acrylate Prosthesis in Diabetic Patients

Erejeta Deva Kurshumliu[1], Gordana Kovacevska[2], Kujtim Shala[1], Blerta Musliu Krasniqi[3], Fisnik Kurshumiu[4*]

[1]*Department of Prosthodontics, University Clinical Dentistry Center of Kosovo, Prishtina, Kosovo*
[2]*Department of Prosthodontics, Dental School, University of Skopje "Ss. Cyril and Methodius," Republic of Macedonia*
[3]*Department of Pedodontics, Alma Mater Europaea, Campus College "Rezonanca," Prishtina, Kosovo*
[4]*Institute of Pathology, University Clinical Center of Kosovo; Medical Faculty, University of Prishtina, Prishtina, Kosovo*

Abstract

***Background*:** The aim of this study was to assess cytological alterations of the squamous epithelium of the alveolar ridge mucosal surface under the acrylate prosthesis in patients with type 2 diabetes (T2D).

Methods and Results: The subjects of interest were patients in whom the total acrylate prosthesis had been applied 3-5 years or more prior to the examination. The subjects were divided into two groups: 30 adult subjects with T2D (T2D group) and 30 adult subjects without T2D (control group). Both groups were over 49 years of age. Cytological smears were obtained by cytobrush from the mucosal surface of the gingival crest underlying the acrylate prosthesis. The following parameters were assessed: type of cells (basal, intermediate, superficial, superficial without nucleus, and parakeratotic), proportions of the types of cells, cytoplasmic diameter, nuclear diameter, and nucleus-to-cytoplasm ratio. An independent sample t-test was used to compare the two study groups. The percentage of superficial cells was significantly lower in the T2D group than in the control group (P=0.001). The T2D group tended to have a higher rate of parakeratotic cells (13.0±11.12 % vs. 8.07±7.92%, P=0.052). Superficial cells in the T2D group had a significantly lower mean cytoplasmic diameter than the control group (32.7947±8.61929µ vs. 36.6383±4.32228µ, P=0.03). Additionally, the nucleus-to-cytoplasm ratio of intermediate and superficial cells in the T2D group was significantly higher than in the control group (0.2407±0.07206 vs. 0.2000±0.03291, P=0.007 and 0.2573±0.06330 vs. 0.2280±0.03178, P=0.027).

Conclusion: The results of our study show that total acrylate prostheses in diabetic patients are responsible for the disrupted maturation of squamous epithelial cells. This is reflected in smaller superficial cells, increased parakeratosis, and the higher nucleus-to-cytoplasm ratio of intermediate and superficial cells.**(International Journal of Biomedicine. 2024;14(2):324-328.)**

Keywords: exfoliative cytology • liquid-based cytology • cytometric analysis • diabetes mellitus

For citation: Kurshumliu ED, Kovacevska G, Shala K, Krasniqi BM, Kurshumiu F. Cytological and Cytometric Analysis of Epithelial Cell Changes Under the Surface of Acrylate Prosthesis in Diabetic Patients. International Journal of Biomedicine. 2024;14(2):324-328. doi:10.21103/Article14(2)_OA15

Introduction

Type 2 diabetes (T2D) is an expanding global health problem. Contributing factors include genetics, obesity, physical inactivity, and advancing age.(1) Several oral diseases and disorders manifest themselves with greater frequency and severity in individuals with diabetes mellitus.(2) The situation is even worse in edentulous patients with diabetes mellitus who, on some occasions, happen to be wearers of total acrylic prostheses, given all the microvascular complications that may occur in relation to the disease.(3) Although the prevalence of complete tooth loss has declined over the last decade, edentulism remains a major disease worldwide, especially among older individuals.(4) The reasons for edentulism are

many. While it is primarily the result of microbial or genetic diseases that have strong individual and behavioral impacts, edentulism can be the result of iatrogenic, traumatic, or therapeutic causes, too.[5] Edentulism is manifested with masticatory difficulty, altered facial expression and difficulty in speech.[6,7] Most edentulous patients are rehabilitated by the application of total acrylic prostheses as a replacement for lost bone and teeth. Complete dentures restore the function of the jaw-tooth system and improve the aesthetic aspect of the face, which are very important to the life of an individual.[8] The effect of total prostheses on the oral mucosa has been the subject of a number of scientific studies with rather controversial results.[9-19] These studies analyzed the cytological features of oral mucosa. The major advantage of exfoliative cytology is the non-invasive character of the technique, which allows a simple and painless collection of mucosal cells from different layers of the epithelium for microscopic examination.[20] The cytological examination may be carried out by the conventional method and liquid-based cytology (LBC).[21]

In our study, we used LBC, which allows immediate fixation of cells while removing unwanted harvested material, e.g., blood cells, mucus, and debris. This technique provides for a thin cellular layer of evenly dispersed cells in a clear background.[22]

Although several studies have suggested a potential association between diabetes and oral mucosa,[23] the effect of total acrylic prosthesis on the underlying mucosa in diabetic patients is rarely reported.[24] The aim of this study was to assess cytological alterations of the squamous epithelium of the alveolar ridge mucosal surface under the acrylate prosthesis in T2D patients.

Materials and Methods

The subjects were selected from the patient records at the University Dentistry Clinical Center of Kosovo. The subjects of interest were patients in whom the total acrylate prosthesis had been applied 3-5 years or more prior to the examination. The subjects were divided into two groups: 30 adult subjects with T2D (T2D group) and 30 adult subjects without T2D (control group). Both groups were total acrylate prosthesis wearers and over 49 years of age. Exclusion criteria were patients with oral pathologies that may interfere with morphological features of the epithelial cells, such as stomatitis, candidiasis, and other infections, and patients with traumatic or tumor lesions.

Clinical protocol

Prior to cell collection, a questionnaire was filled out with relevant information, such as the patient's age, duration of T2D, type of treatment for T2D, duration of wearing a total prosthesis, causes of tooth loss, oral hygiene habits, smoking habits, alcohol consumption, daytime and/or nighttime wearing, and maintenance and hygiene of prostheses. Subjects underwent a clinical oral examination before sampling. The oral mucosa status was generally evaluated. The mucosa in the undersurface of the acrylate prosthesis was assessed for the following: color, surface, transparency, vascularity, edema, and evidence of recent or old traumatic lesions or tumors. Photographs were taken from the areas of interest and stored for analysis. Subsequently, disinfecting mouthwash was applied for a few seconds before sampling. A cytological sample was obtained using a cytobrush; the smear was taken from the mucosal surface of the gingival crest underlying the acrylate prosthesis. After the smear was scraped off from the surface, the cytobrush was placed in a cell collection vial for LBC.

Laboratory protocol

The cell suspension from the cell collection vial was placed in a Hettich cytospin centrifuge and subsequently applied on a glass slide. After additional fixation of the cell smear with 96% ethanol, the same was stained by the Papanicolaou method. This stain was applied because it provides the best morphological details and level of keratinization of the squamous epithelial cells. After staining, the slides were mounted with a mounting medium and coverslipped.

Cytological and cytometric analysis (Figures 1-4)

The microscope slides were scanned by a Microvisioneer slide scanner, using the Olympus CX41 microscope and the Microvisioneer Manual WSI 2020C-34 FL software. After scanning, the images were transferred and saved on the InstaSlide cloud platform. Cytometric analysis was performed using the Aperio Image Scope software (v12.4.3.5008). The following parameters were assessed: overall cellularity; ratio of basal-to-intermediate-to-superficial cells; presence and percentage of parakeratinized squamous epithelial cells; presence and percentage of anuclear surface epithelial cells (keratinization); the median diameter of basal, intermediate, and superficial cell cytoplasm; the median diameter of basal, intermediate, and superficial cell nuclei; the nucleus-to-cytoplasm ratio of basal, intermediate, and superficial cells.

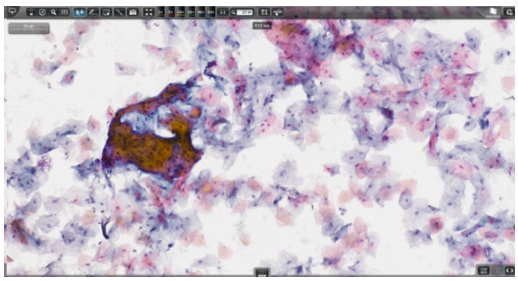

Fig 1. *Squamous epithelial cells in the cytological smear (Papanicolaou stain, 20x magnification; SlideViewer software).*

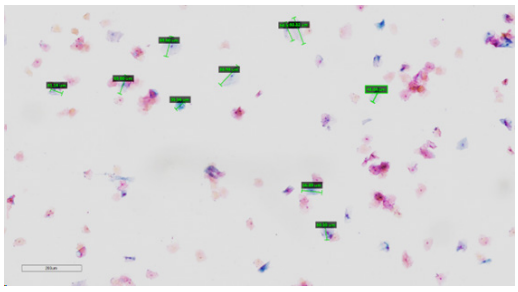

Fig. 2. *Measurement of cytoplasmic diameter (Papanicolaou stain, 10x magnification; Aperio Image Scope software).*

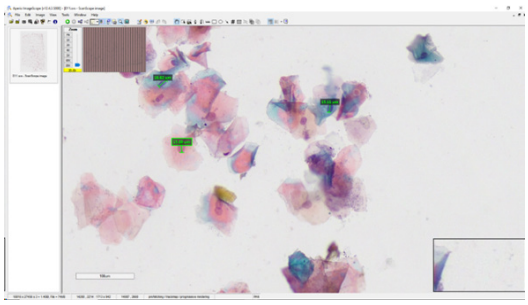

Fig. 3. *Measurement of nuclear diameter (Papanicolaou stain, 40x magnification; Aperio Image Scope software)*

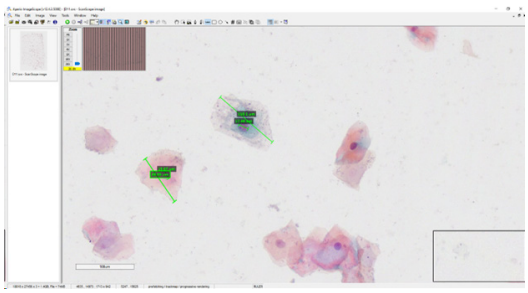

Fig. 4. *Measurement of nucleus-to-cytoplasm ratio (Papanicolaou stain, 40x magnification; Aperio Image Scope software)*

Statistical analysis was performed using the statistical software package SPSS version 23.0 (SPSS Inc, Armonk, NY: IBM Corp). For the descriptive analysis, results are presented as mean, standard deviation (SD), standard error of the mean (SEM). Means of 2 continuous normally distributed variables were compared by independent samples Student's t-test. A probability value of $P<0.05$ was considered statistically significant.

Results

Our results show no significant difference between the sample cellularity of the two study groups ($P=0.838$) (Table 1).

Table 1.

Cellularity of cytological smears in the study groups.

Cellularity	N	Mean	SD	SEM	*P*-value
T2D group	30	2.4667	0.68145	0.12441	0.838
Control group	30	2.5000	0.57235	0.10450	

In contrast, the percentage of superficial cells was significantly lower in the T2D group than in the control group ($P=0.001$) (Table 2). Also, the T2D group tended to have a higher rate of parakeratotic cells (13.0±11.12 vs. 8.07±7.92, $P=0.052$) (Table 2). Superficial cells in the T2D group had a significantly lower mean cytoplasmic diameter than the control group (32.7947±8.61929µ vs. 36.6383±4.32228µ, $P=0.03$) (Table 3). Additionally, the nucleus-to-cytoplasm ratio of intermediate and superficial cells in the T2D group was significantly higher than in the control group (0.2407±0.07206 vs. 0.2000±o.03291, $P=0.007$ and 0.2573±0.06330 vs. 0.2280±0.03178, $P=0.027$) (Table 4).

Table 2.

Percentage of types of squamous epithelial cells in the study groups.

Type of squamous epithelial cells (%)	N	Mean	SD	SEM	*P*-value
Intermediate (T2D)	30	27.2667	25.45304	4.64707	0.27
Intermediate (Control)	30	21.2333	15.48009	2.82627	
Superficial (T2D)	30	32.3333	25.20992	4.60268	0.001
Superficial (Control)	30	52.2667	19.22630	3.51023	
Parakeratotic (T2D)	30	13.0000	11.12003	2.03023	0.052
Parakeratotic (Control)	30	8.0667	7.91739	1.44551	
Anuclear (T2D)	30	27.7333	30.77161	5.61810	0.18
Anuclear (Control)	30	18.4333	21.69170	3.96034	

Table 3.

Cytoplasmic (CD) and nuclear (ND) diameter of intermediate and superficial cells in the study groups.

Type of squamous epithelial cells	N	Mean (µ)	SD	SEM	*P*-value
Intermediate CD (T2D)	30	38.4547	15.41475	2.81433	0.24
Intermediate CD (Control)	30	42.1333	7.62489	1.39211	
Superficial CD (T2D)	30	32.7947	8.61929	1.57366	0.03
Superficial CD (Control)	30	36.6383	4.32228	0.78914	
Intermediate ND (T2D)	30	8.6450	2.30501	0.42084	0.39
Intermediate ND (Control)	30	8.2587	0.82743	0.15107	
Superficial ND (T2D)	30	8.1860	2.11151	0.38551	0.87
Superficial ND (Control)	30	8.2523	0.70371	0.12848	

Table 4.

Nucleus-to-cytoplasm ratio (N:C) of intermediate and superficial cells in the study groups.

Type of squamous epithelial cells / N:C	N	Mean	SD	SEM	*P*-value
Intermediate / N:C (T2D)	30	0.2407	0.07206	0.01316	0.007
Intermediate / N:C (Control)	30	0.2000	0.03291	0.00601	
Superficial / N:C (T2D)	30	0.2573	0.06330	0.01156	0.027
Superficial / N:C (Control)	30	0.2280	0.03178	0.00580	

Discussion

Considering that changes in the oral mucosa of patients with diabetes mellitus are common, epithelial mucosal changes under the surface of acrylate prosthesis should be even more pronounced. The squamous epithelium undergoes constant replacement by cell migration and differentiation. Keratinization is a process of cytodifferentiation during which

the keratinocytes undergo maturation from their germinative state to finally differentiated stratum corneum.[9,10]

Cytological and cytometric changes of the oral mucosal epithelial cells in the immediate undersurface of the acrylate prostheses provide important morphological data about the level of irritation of the mucosa in diabetic patients. Various published studies have observed changes in the degree of keratinization of oral epithelium under prosthesis. Some of these studies show that oral epithelium under the prosthesis becomes more keratinized, while others show that the epithelium remains non-keratinized.[11] Many authors have concluded that total dentures affect keratinization, and most have reported increased keratinization in patients who wear total dentures. According to a study by Kumaresan and Jagannathan,[25] exfoliative cytology plays a major role in diagnosing clinically misinterpreted changes. Considering that the sensitivity and specificity of cytology are limited, the combination of computer-aided cytology and morphometry improves its accuracy. According to this study, this method should be used as a routine method for diagnosing mucosal lesions in the early stages. In a cytological study by Markov et al.,[12] if dentures were regularly removed at night, ortho keratinization (normal keratinization) occurred. They believed that rest at night made it possible for the oral mucosa to recover from the wear and tear caused by the dentures. According to a study by Watson and MacDonald,[13] the degree of keratinization was lower, and the stratum corneum was thinner in the epithelium under dentures. The complete dentures in these studies seemed to reduce the quantity and quality of the keratin layer. Our study has shown that the presence of a denture produced a more regular epithelium with few rete ridges and a thinner, less keratinized stratum corneum. In diabetic patients, due to the previously mentioned oral manifestations and increased susceptibility, these changes may have altered morphology and gravity. According to a study by Farhan and Yas,[26] diabetes is related to certain cytomorphometric changes in the oral mucosal cells. Our study shows that nuclear diameter increases while cytoplasmic diameter decreases in oral mucosal epithelial cells in T2D patients, compared to patients without diabetes. Parallel to these observations, our study shows that in the T2D group, superficial cells were smaller than in the control group. Similarly, there was also an increase in the nucleus-to-cytoplasm ratio in superficial and intermediary cells in T2D patients, compared to the control group. Additionally, our study shows an alteration of the differentiation process of the keratinocytes in diabetes mellitus with lesser numbers of superficial cells and an increased percentage of parakeratotic cells, compared to the control group. In our study, there was a higher percentage of superficial cells without a nucleus in the diabetes mellitus than in the control group; however, it was not statistically significant. We believe that with a larger study group, statistical significance could be established even regarding the percentage of superficial cells without a nucleus.

The alveolar ridge under the acrylic prosthesis seems to be a useful site for cell collection, considering that during chewing, the oral mucosa beneath the denture plays a critical role in distributing occlusal loads to the underlying bony ridge over a large denture-supporting tissue interface.[14,27,28] Acrylic-based resins are frequently used in daily dental practice for prostheses as they can provide essential properties and have the necessary characteristics for their use in diverse functions. During the polymerization of these materials, the residual monomer is released, which may be cytotoxic to oral mucosa. There is an assumption that residual monomers in the denture base, which is in direct contact with oral mucosa, might have a clinical impact on the tissue.[29-33] Some of the studies found that there is not only a quantitative reduction of keratinization but also acanthosis. Its frequency is considered even more significant in patients suffering from diabetes mellitus, considering the oral mucosa sensitivity in these patients. The results of our study support these observations.

In conclusion, the results of our study show that total acrylate prostheses in diabetic patients are responsible for the disrupted maturation of squamous epithelial cells. This is reflected in smaller superficial cells, increased parakeratosis, and the higher nucleus-to-cytoplasm ratio of intermediate and superficial cells. We believe that these results should be a driver for further research in exploring alternative materials or approaches for managing edentulism in diabetic patients.

Competing Interests

The authors declare that they have no competing interests.

References

1. Rathee M, Jain P, Singh S, Divakar S, Chahal S, Wakure P. Role of diabetes in the prosthodontic management of a completely edentulous patient. International Journal of Dental Research. Jun 2021; 3(1):50-5

2. Jivanescu A, Bratu EA, Goguta L, Borgnakke WS. Effect of Improvement of Complete Dentures on Quality of Life in Type 2 Diabetes. Diabetes, Stoffwechsel und Herz. 2013;22(4):207-211

3. Al-Maskari AY, Al-Maskari MY, Al-Sudairy S. Oral Manifestations and Complications of Diabetes Mellitus: A review. Sultan Qaboos Univ Med J. 2011 May;11(2):179-86. Epub 2011 May 15. PMID: 21969888; PMCID: PMC3121021.

4. Emami E, de Souza RF, Kabawat M, Feine JS. The impact of edentulism on oral and general health. Int J Dent. 2013;2013:498305. doi: 10.1155/2013/498305. Epub 2013 May 8. PMID: 23737789; PMCID: PMC3664508

5. Al-Rafee MA. The epidemiology of edentulism and the associated factors: A literature Review. J Family Med Prim Care. 2020 Apr 30;9(4):1841-1843. doi: 10.4103/jfmpc.jfmpc_1181_19. PMID: 32670928; PMCID: PMC7346915

6. Shinde J, Mowade T, Gupta P, Tekale R, Pande N, Deshmukh K, Lokhande T, Radke U. Satisfaction in conventional acrylic complete denture patient with and without denture liners - a systematic review. Pan Afr Med J. 2022 Aug 22;42:296. doi: 10.11604/pamj.2022.42.296.33035. PMID: 36415342; PMCID: PMC9643794

7. Olms C, Hix N, Neumann H, Yahiaoui-Doktor M, Remmerbach TW. Clinical comparison of liquid-based and conventional cytology of oral brush biopsies: a randomized

controlled trial. Head Face Med. 2018 May 29;14(1):9. doi: 10.1186/s13005-018-0166-4. PMID: 29843756; PMCID: PMC5975412.
8. Sun X, Meng L, Chen Y, Wang J, Wang Q. Efficacy and risk factors of traditional denture restoration versus biofunctional complete denture restoration system. Am J Transl Res. 2023 Jul 15;15(7):4755-4762. PMID: 37560251; PMCID: PMC10408514.
9. Menon RS, Dhakshaini MR, Gujjari AK, Hegde U. A clinical evaluation on the effect of astringent on keratinization of oral mucosa before and after the insertion of complete denture. Indian J Dent Res. 2019 May-Jun;30(3):347-351. doi: 10.4103/ijdr.IJDR_620_17. PMID: 31397406.
10. Shetty S; Gokul S. Keratinization and its disorders. Oman Med J. 2012 Sep;27(5):348-57. doi: 10.5001/omj.2012.90. PMID: 23074543; PMCID: PMC3472583.
11. Mneizel T.A study of the palatal keratinization levels beneath complete acrylic resin dentures. JRMS. June 2005; 12(1): 25-29
12. Markov NJ. Cytologic study of keratinization under complete dentures. J Prosthet Dent 1968;20:8-13.
13. Watson IB, MacDonald DG. Oral mucosa and complete dentures. J Prosthet Dent. 1982 Feb;47(2):133-40. doi: 10.1016/0022-3913(82)90176-7. PMID: 6173477
14. Mori S, Sato T, Hara T, Nakashima K, Minagi S. Effect of continuous pressure on histopathological changes in denture-supporting tissues. J Oral Rehabil. 1997 Jan;24(1):37-46. doi: 10.1046/j.1365-2842.1997.00443.x. PMID: 9049918.
15. Menon RS, Dhakshaini MR, Gujjari AK, Hegde U. A clinical evaluation on the effect of astringent on keratinization of oral mucosa before and after the insertion of complete denture. Indian J Dent Res. 2019 May-Jun;30(3):347-351. doi: 10.4103/ijdr.IJDR_620_17. PMID: 31397406.
16. Radke U, Kahar A, Zade P, Lambade D, Deshpande S, Radke P. Evaluation of Effect of Astringent on Oral Mucosa as a Non-surgical Preprosthetic Treatment Modality in Edentulous Patients: An In Vivo Study. J Indian Prosthodont Soc. 2014;14(Suppl 1):93-97. doi:10.1007/s13191-014-0372-0
17. Stig Gson Östlund. The Effect of Complete Dentures on the Gum Tissues, Acta Odontologica Scandinavica. 1958;16(1):1-41. doi: 10.3109/00016355809028181
18. Jani RM, Bhargava K. A histologic comparison of palatal mucosa before and after wearing complete dentures. J Prosthet Dent. 1976 Sep;36(3):254-60. doi: 10.1016/0022-3913(76)90179-7. PMID: 1066479.
19. Nedelman C, Gamer S, Bernick S. The alveolar ridge mucosa in denture and non-denture wearers. J Prosthet Dent. 1970 Mar;23(3):265-73. doi: 10.1016/0022-3913(70)90181-2. PMID: 5263308.
20. Verma R, Singh A, Badni M, Chandra A, Gupta S, Verma R. Evaluation of exfoliative cytology in the diagnosis of oral premalignant and malignant lesions: A cytomorphometric analysis. Dent Res J (Isfahan). 2015 Jan-Feb;12(1):83-8. doi: 10.4103/1735-3327.150339. PMID: 25709680; PMCID: PMC4336977.
21. Kokubun K, Nakajima K, Yamamoto K, Akashi Y, Matsuzaka K. Evaluation of oral brush liquid-based cytology for oral squamous cell carcinoma: a comparative study of cytological and histological diagnoses at a single center. BMC Oral Health. 2023 Mar 11;23(1):145. doi: 10.1186/s12903-023-02839-w. PMID: 36906554; PMCID: PMC10007825.
22. Olms C, Hix N, Neumann H, Yahiaoui-Doktor M, Remmerbach TW. Clinical comparison of liquid-based and conventional cytology of oral brush biopsies: a randomized controlled trial. Head Face Med. 2018 May 29;14(1):9. doi: 10.1186/s13005-018-0166-4. PMID: 29843756; PMCID: PMC5975412.
23. Nandita KP, Boaz K, Srikant N, Lewis AJ, Nidhi M. Oral epithelium in diabetics: A cytomorphometric correlation, Dental Hypotheses. Apr-Jun 2014;5(2):59-65. doi:10.4103/2155-8213.133428
24. Lee JH, Han JS, Han K, Lee SY. Association between Diabetes and the Use of Removable Dental Prostheses among the Korean Population. J Korean Med Sci. 2019 Oct 28;34(41):e262. doi: 10.3346/jkms.2019.34.e262. PMID: 31650717; PMCID: PMC6813424.
25. Kumaresan GD, Jagannathan N. Exfoliative cytology - A predictive diagnostic tool. International Journal of Pharmacy and Pharmaceutical Sciences,.2014;6(5): 1-3.
26. Farhan RS, Yas LS. Oral Finding and Cytomorphometric Analysis of Oral Mucosal Cells in Type 2 Diabetic Patients. International Journal of Medical Research & Health Sciences. 2018;7(6): 86-93
27. Kydd WL, Daly CH, Nansen D. Variation in the response to mechanical stress of human soft tissues as related to age. J Prosthet Dent. 1974 Nov;32(5):493-500. doi: 10.1016/0022-3913(74)90003-1. PMID: 4531483.
28. Jenny N. Beneath the Complete Denture Prosthesis: A Review. International Journal of Dental Sciences and Research. 2018;6(4):87-89. doi: 10.12691/ijdsr-6-4-2.
29. Gonçalves TS, Morganti MA, Campos LC, Rizzatto SM, Menezes LM. Allergy to auto-polymerized acrylic resin in an orthodontic patient. Am J Orthod Dentofacial Orthop. 2006 Mar;129(3):431-5. doi: 10.1016/j.ajodo.2005.10.017.
30. Lunder T, Rogl-Butina M. Chronic urticaria from an acrylic dental prosthesis. Contact Dermatitis. 2000 Oct;43(4):232-3. PMID: 11011931.
31. Martin N, Bell HK, Longman LP, King CM. Orofacial reaction to methacrylates in dental materials: a clinical report. J Prosthet Dent. 2003 Sep;90(3):225-7. doi: 10.1016/s0022-3913(03)00331-7. PMID: 12942054.
32. Koutis D, Freeman S. Allergic contact stomatitis caused by acrylic monomer in a denture. Australas J Dermatol. 2001 Aug;42(3):203-6. doi: 10.1046/j.1440-0960.2001.00517.x. PMID: 11488717.
33. Ruiz-Genao DP, Moreno de Vega MJ, Sánchez Pérez J, García-Díez A. Labial edema due to an acrylic dental prosthesis. Contact Dermatitis. 2003 May;48(5):273-4. doi: 10.1034/j.1600-0536.2003.00100.x. PMID: 12868970.

***Corresponding author:** *Fisnik Kurshumliu. Institute of Pathology, University Clinical Center of Kosovo; Medical Faculty, University of Prishtina, Prishtina, Kosovo. E-mail: fisnik.kurshumliu@uni-pr.edu*

International Journal of Biomedicine 14(2) (2024) 329-334
http://dx.doi.org/10.21103/Article14(2)_O16

ORIGINAL ARTICLE

Dentistry

INTERNATIONAL JOURNAL OF BIOMEDICINE

Comparative Evaluation of Resin Infiltration and Bifluoride Varnish in White Spots in Children between the Ages of 8 and 15 Years

Blerta Krasniqi[1], Meri Pavlevska[2], Erejeta Deva Kurshumliu[3], Blerta Latifi Xhemajli[4], Teuta Kutllovci[1*]

[1]*Department of Pediatric and Preventive Dentistry, Alma Mater Europaea, Campus College "Rezonanca," Pristina, Kosovo*
[2]*Department of Pediatric and Preventive Dentistry, Dental School, University of Skopje "Ss. Cyril and Methodius," Skopje, Republic of Macedonia*
[3]*Department of Prosthodontics, University Dentistry Clincal Center of Kosovo, Prishtina, Republic of Kosovo*
[4]*Department of Pediatric and Preventive Dentistry, University Dentistry Clinical Center of Kosovo, Prishtina, Kosovo*

Abstract

The aim of this study was to compare the efficacy of resin infiltration and bifluoride varnish in white spot lesions (WSLs) in children between the ages of 8 and 15.

Methods and Results: This study was conducted at Alma Mater Europaea Campus College "Rezonanca" (Pristina, Kosovo) and enrolled 60 participants (34 females and 26 males) between the ages of 8 and 15 years with WSLs in the vestibular surface on permanent anterior teeth. The participants were randomly assigned to the resin infiltration (Icon®) group (Group 1, n=30) and the bifluoride varnish (F&A Biflu) group (Group 2, n=30). Both materials were applied on permanent anterior teeth with WSLs in enamel. WSLs were assessed using ICDAS-II (International Caries Detection and Assessment System) criteria by visual inspection, which were coded as 1 and 2. Lesions were evaluated before the material was applied (T0), just after application (T1), and at a 6-month follow-up (T2). A total of 173 teeth from 60 participants were included in our study. Group 1 showed a significant decrease in ICDAS-II scores throughout time intervals T0-T1 (P=0.001), T0-T2 (P=0.001), and T1-T2 (P=0.041). In Group 2, there was no visible difference between T0-T1 (P=1.00) but a significant decrease between T0-T2 (P=0.001) and T1-T2 (P=0.001). Comparisons between the two groups in relation to T0, T1, and T2 were analyzed using the independent samples t-test. Significant differences have been presented in two cases at T1 (P=0.001) and T2 (P=0.003). ICDAS-II scores decreased significantly in Group 1.

Conclusion: The application of resin infiltration in WSLs was found to be more effective than the application of bifluoride varnish. While the effects of bifluoride varnish in WSLs persisted over time, the effect of resin infiltration was evident as soon as WSLs were treated. Moving forward, we recommend considering resin infiltration as a favorable option for WSL treatment. Future studies with long-term follow-ups are necessary to corroborate these results.**(International Journal of Biomedicine. 2024;14(2):329-334.)**

Keywords: white spot lesion • ICDAS-II criteria • bifluoride varnish • resin infiltration

For citation: Krasniqi B, Pavlevska M, Kurshumliu ED, Xhemajli BL, Kutllovci T. Comparative Evaluation of Resin Infiltration and Bifluoride Varnish in White Spots in Children between the Ages of 8 and 15 Years. International Journal of Biomedicine. 2024;14(2):329-334. doi:10.21103/Article14(2)_OA16

Abbreviations

BFV, bifluoride varnish; **FV**, fluoride varnish; **RI**, resin infiltration; **WSL**, white spot lesion.

Introduction

Dental caries, often known as tooth decay, is one of the most common chronic disorders afflicting people worldwide; people are susceptible to it throughout their lives.[1] The balance of pathogenic and preventative factors determines the start and progression of caries.[2] Dental disease treatment is quite expensive in all nations, and prevention is very easy and

efficient.[3] First, mineral loss causes microporosities, which may be seen clinically as white, opaque, and rough areas. If the mineral loss persists, these white spot lesions (WSLs) will ultimately grow into lesions with cavitation.[4-6]

White spot lesions are described as demineralization of the enamel surface and subsurface without cavitation. Such symptoms are the early clinical signs of the development of dental caries, with a possibility of reversal. These lesions are distinguished by their white chalky, opaque appearance. [7] Active WSLs are 'chalky'/dull and uneven on probing, but inactive lesions are glossy and smooth on probing.[8] White spot lesions are common in orthodontic patients, especially beneath broken bands, around bracket bases, and in areas where brushing is difficult.[9,10]

Noninvasive or minimally invasive therapies are essential for stopping tooth decay before caries develops and for reducing treatment time and costs.[11] So far, numerous strategies for treating WSLs have been researched.[11,12] It has been demonstrated that in noninvasive treatments of WSLs, topical fluoride products, along with diet and good dental hygiene, improve lesion remineralization.[13]

Bifluoride varnish (BFV) is good for accelerating tooth remineralization and fluoridation. The unique mix of the two fluoride salts allows for both immediate high fluoride release through NaF and long-term fluoridation through CaF_2. The easily soluble sodium fluoride releases fluoride ions quickly, which are converted to calcium fluoride on the tooth surface to assist remineralization efficiently. Fluorides have been used for many years as an effective way to prevent and stop caries. Researchers have proven that fluoride achieves its preventive effects by being incorporated into the structure of teeth, making them stronger and more resistant to attack by acids released by bacteria.

Resin infiltration (RI) in treating early proximal caries lesions is a new concept in dentistry, with beneficial clinical applicability for clinicians and high patient acceptance. Such infiltration is effective in arresting smooth-surface enamel lesions in permanent teeth in children [14-16] and is an alternative approach to treating early caries lesions that are not expected to remineralize or arrest by noninvasive measures when performed with low-viscosity light-curing resins (so-called infiltrants). Resin infiltration has lately been recognized as a minimally invasive treatment. The RI therapy, which involves filling the enamel intercrystalline spaces with a low-viscosity resin with a high penetration coefficient, prevents the lesion from growing further.[17-20] The effectiveness of RI in stopping caries lesions has been studied in vitro,[21] in situ,[22] and in vivo,[14] and clinical evidence of its ability to cover up WSLs has been provided.[23,24] However, more research is required to fully understand the camouflage impact of the RI approach and the potential remineralization action of fluoride compounds within the non-cavitated active WSLs. [25]

The aim of this study was to compare the efficacy of RI and BFV in WSLs in children between the ages of 8 and 15.

Materials and Methods

This study was conducted at Alma Mater Europaea Campus College "Rezonanca" (Pristina, Kosovo) with prior approval from the Ethical Committee (AD-3408/22, 14.06.2022) of this institution and enrolled 60 participants. The parents of the children were informed about the whole procedure and signed an agreement to include their children in the study.

Participant selection

The participants were randomly assigned to the RI (Icon®) group (Group 1, n=30) and the BFV (F&A Biflu) group (Group 2, n=30). Both materials were applied on permanent anterior teeth with WSLs in enamel. Inclusion criteria were participants between the ages of 8 and 15 years with WSLs in the vestibular surface on permanent anterior teeth. Exclusion criteria were participants with active carious lesions, restoration of the surface of the teeth being treated, and deciduous teeth.

The clinical selection was done using artificial light, a dental mirror, a ball-ended probe, and air drying. WSLs were assessed using ICDAS-II (International Caries Detection and Assessment System) criteria by visual inspection, which were coded as 1 and 2. Lesions were evaluated before the material was applied (T0), just after application (T1), and at a 6-month follow-up (T2).

Treatment procedures

Resin infiltration

All participants received the same preparation protocol for teeth cleaning, with a brush and paste. A lip retractor, cotton roll, and gum shield were used to maintain a dry working environment. The RI procedure was performed according to the manufacturer's instructions. A 15% hydrochloric acid gel was applied over WSLs for two min. Next, the acid was rinsed for 30 seconds, and the treated surfaces were dried, then ethanol was applied for 30 seconds and was dried. In the last step, RI was applied to the surface of the lesion using a micro brush and left for three min. Excessive material was wiped away from the surface using a cotton roll before light curing. After light curing for 40 sec, the application of RI was repeated once for 1 minute and light cured for 40 sec. Rough surfaces were smoothed using silicone discs and polishes.

Bifluoride varnish

The surfaces to be treated with BFV were carefully cleaned and air-dried. One or two drops of medication were applied using the applicator as a thin layer to the surfaces to be treated. The varnish penetrates the tooth tissue for a few seconds before being air-dried. For the next two hours, the children were told to eat soft foods and beverages that were not sticky or firm and not to brush or floss for the rest of the day.

Follow-up examination

Lesions on permanent anterior teeth were evaluated by ICDAS-II criteria for two groups at the T0, T1, and T2 time periods. The collected information was analyzed statistically.

Statistical analysis was performed using the statistical software package SPSS version 26.0 (SPSS Inc, Armonk, NY: IBM Corp). Baseline characteristics were summarized as frequencies and percentages for categorical variables and mean ± standard deviation (SD) for continuous variables. Inter-group comparisons were performed using Student's t-test. A probability value of $P<0.05$ was considered statistically significant.

Results

A total of 173 teeth from 60 participants were included in our study. In Group 1, there were 16 females and 14 males; in Group 2, there were 18 females and 12 males. The number of teeth in Groups 1 and 2 was 85 and 88, respectively. The mean age of patients in Group 1 and Group 2 was 11.37±3.02 and 11.50±2.46 years, respectively (Table 1). Group 1 showed a significant decrease in ICDAS-II scores throughout time intervals T0-T1 (P=0.001), T0-T2 (P=0.001), and T1-T2 (P=0.041). In Group 2, there was no visible difference between T0-T1 (P=1.00) but a significant decrease between T0-T2 (P=0.001) and T1-T2 (P=0.001) (Table 2). After six months of follow-up, ICDAS-II scores decreased in two groups (Figure 1).

Table 1.

Distribution of study groups by gender.

	Group 1 n (%)	Group 2 n (%)	Total n (%)
Gender			
Female	16 (53.3)	18 (60.0)	34 (56.7)
Male	14 (46.7)	12 (40.0)	26 (43.3)
Total participants	30	30	60 (100)
Total teeth	85	88	173 (100)
Age (mean ± SD), years	11.37 ± 3.02	11.50 ± 2.46	

Table 2.

ICDAS-II scores throughout time intervals in two groups.

Groups	Time	ICDAS II scores (mean ± SD)	Comparison between different time intervals		
			Mean difference	Comparison	P-value
RI	T0	1.67 ± 0.488	1.133	T0-T1	0.001
	T1	0.53 ± 0.515	1.400	T0-T2	0.001
	T2	0.27 ± 0.458	0.267	T1-T2	0.041
BFV	T0	1.76 ± 0.437	0	T0-T1	1.00
	T1	1.76 ± 0.437	0.882	T0-T2	0.001
	T2	0.88 ± 0.600	0.882	T1-T2	0.001

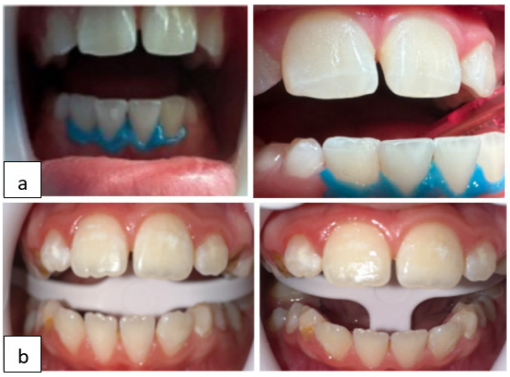

Fig. 1. *Photos of the subjects before and 6 months after the treatment.*

a) Group 1: WSLs + RI; b) Group 2: WSLs +BFV.

Comparisons between the two groups in relation to T0, T1, and T2 were analyzed using the independent samples t-test. Significant differences have been presented in two cases at T1 (P=0.001) and T2 (P=0.003) (Table 3). Figure 2 shows the changes in ICDAS-II scores with time. ICDAS-II scores decreased significantly in Group 1 after participants were treated with RI. Figure 3 shows a comparison between RI and BFV groups in three-time intervals.

Table 3.

Comparison between the two groups in different time intervals.

Group	Time	ICDAS II scores (mean ± SD)	Comparison between different time intervals		
			Mean difference	Comparison	P-value
RI	T0	1.67 ± 0.488	0.098	T0 (RI) – T0 (BFV)	0.556
BFV		1.76 ± 0.437			
RI	T1	0.53 ± 0.515	1.231	T1 (RI) – T1 (BFV)	0.001
BFV		1.76 ± 0.437			
RI	T2	0.27 ± 0.458	0.616	T2 (RI) – T2 (BFV)	0.003
BFV		0.88 ± 0.600			

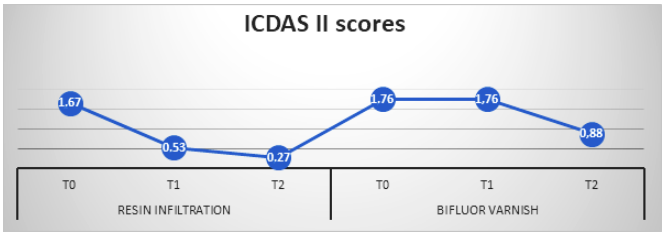

Fig. 2. *The changes in ICDAS II scores with time.*

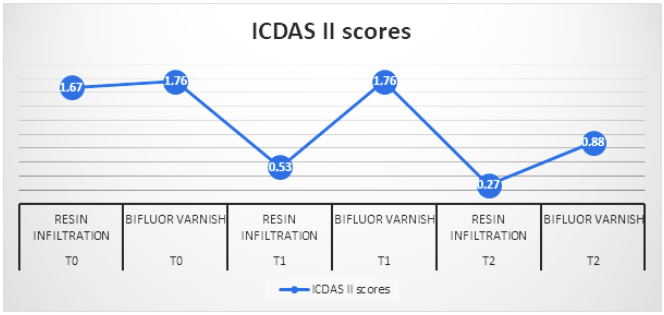

Fig. 3. *Comparison between RI and BFV groups in three-time intervals.*

Discussion

The present study was performed to determine the efficacy of the RI and BFV application on non-cavitated active WSLs in 8-15-year-old children. In this randomized controlled clinical trial, changes in lesions were evaluated before and after application, and at a 6-month application of RI and BFD on WSLs. The vestibular surface of teeth with WSLs was evaluated according to the ICDAS-II criteria.

White spot lesions are described as surface and subsurface enamel demineralization without cavitation. First, there is mineral loss, which generates microporosity. If mineral loss continues, these WSLs will progress to cavitation lesions.[4-7] White spot lesions often appear in patients with orthodontic appliances, especially around dentures and in areas where brushing is difficult.[9,10]

While some studies contend that WSLs cannot fully disappear, others assert that progress may take place over the course of 5 to 12 years. As part of preventative dentistry, it is increasingly essential to use minimally invasive procedures to preserve as many healthy tooth tissues as possible to treat WSLs on teeth and improve their appearance.

Since these techniques are well accepted by patients, they are preferable over restorative therapy. After a one-year follow-up without therapy, Enaia et al.[26] found that 57.1% of WSLs improved, 26% stayed the same, and 16.7% worsened. Given that lesions might worsen and patients may refuse to participate, it is obvious that masking the opaque look during remineralization using spontaneous and low fluoride treatments would take a long time. One noninvasive treatment option for WSLs is fluoride. Higher fluoride concentrations result in deposits of a material that resembles calcium fluoride if the varnish is applied to the tooth surface for a prolonged period. The calcium fluoride material that is formed in the pores and cariogenic sites of enamel might eventually cause fluoride to penetrate the tooth plaque or the underlying enamel. Fluoride release can help early WSLs get remineralized and prevent demineralization.[27]

Several studies have demonstrated that topical fluoride therapy is beneficial for remineralizing WSLs, and using an FV is a simple and reliable procedure. FVs offer several advantages, including a regulated release of fluoride and shorter treatment durations, compared to traditional fluoride techniques like gels.[28,29] In our study, we focused on evaluating the effects of BFV on WSLs. Our results demonstrated a significant decrease in ICDAS-II scores after a 6-month follow-up, indicating that BFV effectively reduces WSLs, consistent with findings from previous studies. However, it's worth noting that some studies, such as those by Güçlü et al.[30] and Girish Babu et al.,[31] did not find a significant difference in the remineralizing potential between varnishes containing both CPP-ACP and fluoride, compared to those containing fluoride alone. These contrasting results highlight the need for further investigation into the specific mechanisms and formulations of FVs to optimize their efficacy in managing WSLs. Furthermore, Autio-Gold and Courts [32] found that FV treatment effectively reversed and stopped active enamel lesions, thereby reducing the necessity for restorative interventions. Consistent with prior research, the present study observed a significant reduction in ICDAS-II scores of WSLs in the BFV group from T0 to T2.

In the present study, BFV was only administered at the initial therapy session to represent the typical clinical use of FV in children, and it was not repeated until the 6-month follow-up. This application differs from previous studies, which used repeated FV treatments over a short period.[33] The goal of the RI concept is to stop the progression of enamel caries lesions and block the enamel's ability to absorb dissolved minerals and acids.[34] Consistent with this concept, our results demonstrate that RI significantly reduced the ICDAS-II score immediately after application and at the 6-month follow-up, compared to baseline values of WSLs, which is supported by other studies.[35,36] The mean ICDAS-II score before, just after application, and at 6 months was 1.67, 0.53, and 0.27, respectively, in the RI group, and 1.76, 1.76, and 0.88, respectively, in the BFV group. The findings demonstrated a significantly higher decrease in mean ICDAS-II score before and just after application, before and after 6 months in the RI group, as compared to the BFV group. On the other hand, a decline in the mean ICDAS-II score before and after 6 months was recorded in the BFV group.

Comparing the efficacy of RI and BFV treatments in WSLs, we found that the RI group exhibited a statistically significant decrease in lesion reduction immediately after treatment and at the 6-month follow-up, compared to the BFV group. This finding is consistent with a study conducted by Giray et al.,[37] indicating the superiority of RI over BFV in WSL managing. Our results support previous research demonstrating the effectiveness and minimally invasive nature of RI, highlighting its advantages over alternative treatment options for WSLs.

Additionally, our findings align with an in vitro study comparing the effects of RI and BFV on enamel surface properties. By permeating into the enamel, the resin effectively blocks acid-entrance channels by forming a diffusion barrier. BFV, on the other hand, might provide a comparatively thin coating layer. These results further emphasize the superior efficacy of RI in managing WSLs and suggest its potential as a preferred treatment modality for enamel demineralization.

Conclusion

The application of resin infiltration in white spot lesions was found to be more effective than the application of bifluoride varnish. While the effects of bifluoride varnish in white spot lesions persisted over time, the effect of resin infiltration was evident as soon as white spot lesions were treated. Moving forward, we recommend considering resin infiltration as a favorable option for white spot lesion treatment. Future studies with long-term follow-ups are necessary to corroborate these results.

Competing Interests

The authors declare that they have no competing interests.

References

1. Selwitz RH, Ismail AI, Pitts NB. Dental caries. Lancet. 2007 Jan 6;369(9555):51-9. doi: 10.1016/S0140-6736(07)60031-2. PMID: 17208642.

2. Pitts NB, Zero DT, Marsh PD, Ekstrand K, Weintraub JA, Ramos-Gomez F, Tagami J, Twetman S, Tsakos G, Ismail A.

Dental caries. Nat Rev Dis Primers. 2017 May 25;3:17030. doi: 10.1038/nrdp.2017.30. PMID: 28540937.
3. Mathur VP, Dhillon JK. Dental Caries: A Disease Which Needs Attention. Indian J Pediatr. 2018 Mar;85(3):202-206. doi: 10.1007/s12098-017-2381-6. Epub 2017 Jun 23. PMID: 28643162.
4. Ferreira MA, Mendes NS. Factors associated with active white enamel lesions. Int J Paediatr Dent. 2005 Sep;15(5):327-34. doi: 10.1111/j.1365-263X.2005.00641.x. PMID: 16128996.
5. Cazzolla AP, De Franco AR, Lacaita M, Lacarbonara V. Efficacy of 4-year treatment of icon infiltration resin on postorthodontic white spot lesions. BMJ Case Rep. 2018 Jul 18;2018:bcr2018225639. doi: 10.1136/bcr-2018-225639. PMID: 30021744; PMCID: PMC6058148.
6. Dhamija M, Tyagi R, Kalra N, Khatri A. Efficacy of resin infiltration and fluoride casein phosphopeptide amorphous calcium phosphate varnish on non-cavitated active white spot lesions in children: a randomized clinical trial. Pesqui Bras Odontopediatria Clín Integr. 2022; 22:e210094. doi: 10.1590/pboci.2022.059.
7. Temel SS, Kaya B. Diagnosis, Prevention and Treatment of White Spot Lesions Related to Orthodontics. Int J Oral Dent Health.2019;5:085. doi: 10.23937/2469-5734/1510085.
8. Bishara SE, Ostby AW. White spot lesions: Formation, prevention, and treatment. Semin Orthod.2008;14:174-182.
9. Abbas BA, Marzouk ES, Zaher AR. Treatment of various degrees of white spot lesions using resin infiltration-in vitro study. Prog Orthod. 2018 Aug 6;19(1):27. doi: 10.1186/s40510-018-0223-3. PMID: 30079435; PMCID: PMC6081872.
10. Ogaard B, Rølla G, Arends J. Orthodontic appliances and enamel demineralization. Part 1. Lesion development. Am J Orthod Dentofacial Orthop. 1988 Jul;94(1):68-73. doi: 10.1016/0889-5406(88)90453-2. PMID: 3164585.
11. Borges BC, de Souza Borges J, de Araujo LS, Machado CT, Dos Santos AJ, de Assunçao Pinheiro IV. Update on nonsurgical, ultraconservative approaches to treat effectively non-cavitated caries lesions in permanent teeth. Eur J Dent. 2011 Apr;5(2):229-36. PMID: 21494394; PMCID: PMC3075999.
12. Sonesson M, Bergstrand F, Gizani S, Twetman S. Management of post-orthodontic white spot lesions: an updated systematic review. Eur J Orthod. 2017 Apr 1;39(2):116-121. doi: 10.1093/ejo/cjw023. PMID: 27030284.
13. Ferreira JM, Aragão AK, Rosa AD, Sampaio FC, Menezes VA. Therapeutic effect of two fluoride varnishes on white spot lesions: a randomized clinical trial. Braz Oral Res. 2009 Oct-Dec;23(4):446-51. doi: 10.1590/s1806-83242009000400015. PMID: 20027453.
14. Paris S, Hopfenmuller W, Meyer-Lueckel H. Resin infiltration of caries lesions: an efficacy randomized trial. J Dent Res. 2010 Aug;89(8):823-6. doi: 10.1177/0022034510369289. Epub 2010 May 26. PMID: 20505049.
15. Senestraro SV, Crowe JJ, Wang M, Vo A, Huang G, Ferracane J, Covell DA Jr. Minimally invasive resin infiltration of arrested white-spot lesions: a randomized clinical trial. J Am Dent Assoc. 2013 Sep;144(9):997-1005. doi: 10.14219/jada.archive.2013.0225. PMID: 23989837.
16. Bagher SM, Hegazi FM, Finkelman M, Ramesh A, Gowharji N, Swee G, Felemban O, Loo CY. Radiographic Effectiveness of Resin Infiltration in Arresting Incipient Proximal Enamel Lesions in Primary Molars. Pediatr Dent. 2018 May 15;40(3):195-200. PMID: 29793566.
17. Lee JH, Kim DG, Park CJ, Cho LR. Minimally invasive treatment for esthetic enhancement of white spot lesion in adjacent tooth. J Adv Prosthodont. 2013 Aug;5(3):359-63. doi: 10.4047/jap.2013.5.3.359. Epub 2013 Aug 31. PMID: 24049579; PMCID: PMC3774952.
18. Paris S, Meyer-Lueckel H, Cölfen H, Kielbassa AM. Resin infiltration of artificial enamel caries lesions with experimental light curing resins. Dent Mater J. 2007 Jul;26(4):582-8. doi: 10.4012/dmj.26.582. PMID: 17886464.
19. Paris S, Meyer-Lueckel H, Kielbassa AM. Resin infiltration of natural caries lesions. J Dent Res. 2007 Jul;86(7):662-6. doi: 10.1177/154405910708600715. PMID: 17586715.
20. Meyer-Lueckel H, Paris S. Improved resin infiltration of natural caries lesions. J Dent Res. 2008 Dec;87(12):1112-6. doi: 10.1177/154405910808701201. PMID: 19029077.
21. Taher NM, Alkhamis HA, Dowaidi SM. The influence of resin infiltration system on enamel microhardness and surface roughness: An in vitro study. Saudi Dent J. 2012 Apr;24(2):79-84. doi: 10.1016/j.sdentj.2011.10.003. Epub 2011 Nov 16. PMID: 23960533; PMCID: PMC3723288.
22. Paris S, Meyer-Lueckel H. Inhibition of caries progression by resin infiltration in situ. Caries Res. 2010;44(1):47-54. doi: 10.1159/000275917. Epub 2010 Jan 16. PMID: 20090328.
23. Paris S, Meyer-Lueckel H. Masking of labial enamel white spot lesions by resin infiltration--a clinical report. Quintessence Int. 2009 Oct;40(9):713-8. PMID: 19862396.
24. Kielbassa AM, Muller J, Gernhardt CR. Closing the gap between oral hygiene and minimally invasive dentistry: a review on the resin infiltration technique of incipient (proximal) enamel lesions. Quintessence Int. 2009 Sep;40(8):663-81. PMID: 19639091.
25. Hiremath SS. Textbook of Preventive and Community Dentistry. 2nd. ed. New Delhi: Elsevier India; 2011.
26. Enaia M, Bock N, Ruf S. White-spot lesions during multibracket appliance treatment: A challenge for clinical excellence. Am J Orthod Dentofacial Orthop. 2011 Jul;140(1):e17-24. doi: 10.1016/j.ajodo.2010.12.016. PMID: 21724067.
27. Petersson LG. Fluoride mouthrinses and fluoride varnishes. Caries Res. 1993;27 Suppl 1:35-42. doi: 10.1159/000261600. PMID: 8500123.
28. Tranaeus S, Al-Khateeb S, Björkman S, Twetman S, Angmar-Månsson B. Application of quantitative light-induced fluorescence to monitor incipient lesions in caries-active children. A comparative study of remineralisation by fluoride varnish and professional cleaning. Eur J Oral Sci. 2001 Apr;109(2):71-5. doi: 10.1034/j.1600-0722.2001.00997.x. PMID: 11347658.
29. Mohd Said SN, Ekambaram M, Yiu CK. Effect of different fluoride varnishes on remineralization of artificial enamel carious lesions. Int J Paediatr Dent. 2017 May;27(3):163-173. doi: 10.1111/ipd.12243. Epub 2016 Jun 27. PMID: 27348852.

30. Güçlü ZA, Alaçam A, Coleman NJ. Corrigendum to "A 12-Week Assessment of the Treatment of White Spot Lesions with CPP-ACP Paste and/or Fluoride Varnish". Biomed Res Int. 2018 Dec 24;2018:1816959. doi: 10.1155/2018/1816959. Erratum for: Biomed Res Int. 2016;2016:8357621. PMID: 30671446; PMCID: PMC6323475.
31. Girish Babu KL, Subramaniam P, Tele S. Remineralization potential of varnish containing casein phosphopeptides-amorphous calcium phosphate with fluoride and varnish containing only fluoride: comparative study. Saudi J Oral Sci 2018; 5(1):35-40. doi: 10.4103/sjos.SJOralSci_44_17.
32. Autio-Gold JT, Courts F. Assessing the effect of fluoride varnish on early enamel carious lesions in the primary dentition. J Am Dent Assoc. 2001 Sep;132(9):1247-53; quiz 1317-8. doi: 10.14219/jada.archive.2001.0367. PMID: 11665349.
33. Ciftci ZZ, Hanimeli S, Karayilmaz H, Gungor OE. The efficacy of resin infiltrate on the treatment of white spot lesions and developmental opacities. Niger J Clin Pract. 2018 Nov;21(11):1444-1449. doi: 10.4103/njcp.njcp_235_18. PMID: 30417842.
34. Meyer-Lueckel H, Paris S. Progression of artificial enamel caries lesions after infiltration with experimental light curing resins. Caries Res. 2008;42(2):117-24. doi: 10.1159/000118631. Epub 2008 Feb 28. PMID: 18305389.
35. Gözetici B, Öztürk-Bozkurt F, Toz-Akalın T. Comparative Evaluation of Resin Infiltration and Remineralisation of Noncavitated Smooth Surface Caries Lesions: 6-month Results. Oral Health Prev Dent. 2019;17(2):99-106. doi: 10.3290/j.ohpd.a42203. PMID: 30874252.
36. Dhamija M, Tyagi R, Kalra N, Khatri A. Efficacy of Resin Infiltration and Fluoride Casein Phosphopeptide Amorphous Calcium Phosphate Varnish on Non-cavitated Active White Spot Lesions in Children: A Randomized Clinical Trial. Pesqui Bras Odontopediatria Clín Integr [Internet]. 2022;22:e210094. Available from: https://doi.org/10.1590/pboci.2022.059
37. Giray FE, Durhan MA, Haznedaroglu E, Durmus B, Kalyoncu IO, Tanboga I. Resin infiltration technique and fluoride varnish on white spot lesions in children: Preliminary findings of a randomized clinical trial. Niger J Clin Pract. 2018 Dec;21(12):1564-1569. doi: 10.4103/njcp.njcp_209_18. PMID: 30560818.

***Corresponding author:** Teuta Kutllovci. Department of Pediatric and Preventive Dentistry, Alma Mater Europaea, Campus College "Rezonanca," Pristina, Kosovo. E-mail: teuta.kutllovci@rezonanca-rks.com*

International Journal of Biomedicine 14(2) (2024) 335-337
http://dx.doi.org/10.21103/Article14(2)_ShC

SHORT COMMUNICATION

INTERNATIONAL JOURNAL OF BIOMEDICINE

Dislocation of the Cervical Anastomosis toward the Mediastinum after McKeown Esophagectomy: A Single-Center Retrospective Study

E. A. Toneev[1,2*], A. L. Charyshkin[3*], A. A. Martynov[1], A. A. Firstov[2], L. A. Danilova[1,2], E. P. Anokhina[1], L. R. Zaripov[1]

[1]*Ulyanovsk Regional Oncology Center, Ulyanovsk, Russian Federation*
[2]*Ulyanovsk State University, Ulyanovsk, Russian Federation*
[3]*Almazov National Medical Research Centre, Saint-Petersburg, Russian Federation*

Abstract

Background: This study aimed to assess the frequency of cervical anastomosis dislocation toward the mediastinum after McKeown esophagectomy and the significance of this phenomenon for postoperative complications.

Methods and Results: The study included 82 patients with stage I-III esophageal cancer who underwent surgical intervention using McKeown esophagectomy in a completely open version (thoracotomy, laparotomy, cervicotomy) or hybrid esophagectomy (thoracoscopy on the right, laparotomy, cervicotomy).

After McKeown esophagectomy, dislocation of the cervical anastomosis (DCA) toward the posterior mediastinum was noted in 26.8% of cases. The overall incidence of anastomotic leakage was 18.3%. The groups of patients with and without DCA did not differ statistically in the incidence of anastomotic leakage (P=0.205). Mediastinal complications (mediastinitis, pleural empyema) were observed in 100% (6/6) of cases in the group with DCA and 33.3% (3/9) of cases in the group without DCA (P=0.013). Pulmonary complications (pneumonia, atelectasis) occurred in 5(22.7%) and 8(13.3%) of cases in groups with DCA and without DCA, respectively (P=0.304).

Conclusion: After McKeown esophagectomy, DCA toward the posterior mediastinum was noted in 26.8% of cases. Dislocation of the cervical anastomosis toward the posterior mediastinum does not significantly impact the anastomotic leakage. Mediastinal complications are more common in patients with DCA, but the incidence of pulmonary complications is not associated with this phenomenon.**(International Journal of Biomedicine. 2024;14(2):335-337.)**

Keywords: esophageal cancer • McKeown esophagectomy • anastomosis dislocation

For citation: Toneev EA, Charyshkin AL, Martynov AA, Firstov AA, Danilova LA, Anokhina EP, Zaripov LR. Dislocation of the Cervical Anastomosis toward the Mediastinum after McKeown Esophagectomy: A Single-Center Retrospective Study. International Journal of Biomedicine. 2024;14(2):335-337. doi:10.21103/Article14(2)_ShC

Introduction

Esophageal cancer is ranked as the seventh most common cancer worldwide.[1] In the Russian Federation, 6088 cases of esophageal cancer were registered in 2020, of which stage III-IV accounted for 65%.[2] The most studied and effective method for the treatment of stage I-III EC is multimodal therapy, which includes preoperative chemoradiotherapy followed by surgery.[3]

Esophagectomy is the most common radical treatment for esophageal cancer. Two types of surgical intervention are most often used in clinical practice. McKeown esophagectomy[4] is a well-described procedure with right thoracotomy, upper abdominal laparotomy, and cervical anastomosis by left cervicotomy. Ivor Lewis esophagectomy[5] is the classic transthoracic esophagectomy, which consists of laparotomy and right thoracotomy with intrathoracic anastomosis.

With cervical anastomosis formation, there is a risk of dislocation of the cervical anastomosis (DCA) toward the

Corresponding authors
Prof. Alexei L. Charyshkin, PhD, ScD. Almazov National Medical Research Centre, Saint-Petersburg, Russian Federation. E-mail: mail@charyshkin.ru
Evgeniy A. Toneev, PhD. Ulyanovsk Regional Oncology Center, Ulyanovsk, Russian Federation. E-mail: e.toneev@inbox.ru

mediastinum, which occurs in 10-20%. This phenomenon is an important cause of leakage into the mediastinum with the subsequent development of mediastinitis and an unfavorable operation outcome.[6]

This study aimed to assess the frequency of DCA toward the mediastinum after McKeown esophagectomy and the significance of this phenomenon for postoperative complications.

Materials and Methods

The study included 82 patients with stage I-III esophageal cancer who underwent surgical treatment at the Regional Clinical Oncology Center, Ulyanovsk, from January 1, 2016, to November 1, 2023. The patients underwent surgical intervention using McKeown esophagectomy in a completely open version (thoracotomy, laparotomy, cervicotomy) or hybrid esophagectomy (thoracoscopy on the right, laparotomy, cervicotomy).

Retrospective analysis was carried out according to the developed protocol. We used the TNM 8 classification system approved by the Union for International Cancer Control (UICC) for staging.

Technical features of the formation of anastomosis

In all cases, the anastomosis was performed manually. When forming an anastomosis on the neck, the end of the esophagus was anastomosed with the anterior wall of the gastric graft with a double-row suture, with the formation of the second row of sutures using a sled U-shaped suture according to E.L. Berezov on a 24 Fr gastric tube.

There were two criteria for the anastomosis migration toward the posterior mediastinum:

- The displacement of more than 2/3 of the width of the gastric graft to the right from the line at the edge of the sternum and the thoracic vertebral body.

- The location of the anastomosis below the first thoracic vertebra 5-6 days after surgery in X-ray with contrast.

All patients at the prehospital stage were examined according to a standard recommended by the Association of Oncologists of Russia to exclude the presence of distant metastases and assess the extent of the process.

Statistical analysis was carried out using the StatTech software v. 2.8.8 (StatTech LLC, Russia). Baseline characteristics were summarized as frequencies and percentages for categorical variables and mean±SD for continuous variables. For data with normal distribution, inter-group comparisons were performed using Student's t-test. Group comparisons with respect to categorical variables are performed using the chi-square test. A probability value of $P<0.05$ was considered statistically significant.

Results

Table 1 presents the main characteristics of the study patients. All patients were divided into 2 groups. Group 1 included 22(26.8%) patients with DCA toward the posterior mediastinum after McKeown esophagectomy, and Group 2 included 60(73.2%) patients without DCA. In our study, the overall incidence of anastomotic leakage was 18.3%). In Group 1, the incidence of anastomotic leakage was 1.82 times higher than in Group 2 without statistical significance. Mediastinal complications (mediastinitis, pleural empyema) were observed in 100% of cases in Group 1 and 33.3% of cases in Group 2 ($P=0.013$). Pulmonary complications (pneumonia, atelectasis) occurred in 5(22.7%) and 8(13.3%) of cases in Group 1 and Group 2, respectively ($P=0.304$) (Table 2).

Table 1.

Characteristics of study patients.

Variable		Group 1 n=22	Group 2 n=60	*P*-value
Gender	Male	16 (72.7%)	46 (76.7%)	0.713
	Female	6 (27.3 %)	14 (23.3%)	
Age (years)		57.6 ± 4.8	60.1 ± 5.4	0.060
Charlson index (points)		4.32 ± 0.87	3.17 ± 0.66	0.000
ICD-10	C15.4	10 (45.5%)	29 (48.3%)	0.818
	C15.5	12 (54.5%)	31 (51.7%)	
Stage	IIA	8 (36.5%)	22 (31.8%)	0.404
	IIB	9 (40.9%)	19 (36.6%)	
	IIIA	3 (13.5%)	17 (28.3%)	
	IIIB	2 (9.1%)	2 (3.3%)	
Histological type	Adenocarcinoma	4 (18.2%)	9 (15%)	1*
	Squamous	18 (81.8%)	51 (85%)	
Type of operation	Hybrid McKeown	4 (18.2%)	8 (13.3%)	0.843*
	Open McKeown	18 (81.8%)	52 (86.7%)	

*- *Yates' P-value*

Table 2.

Anastomotic complications in study groups.

Variable	Group 1 n=22	Group 2 n=60	*P*-value
Anastomotic leak	6 (27.3%)	9 (15%)	0.205
Mediastinal complications	6 (100)	3 (33.3%)	0.013
Pulmonary complications	5 (22.7%)	8(13.3%)	0.304

Discussion

Despite advances in multimodal treatment of esophageal cancer in recent years, radical surgery remains the standard of care. Currently, minimally invasive esophagectomies are being actively introduced into clinical practice with satisfactory short-term and long-term results. The classic version of esophagectomy involves two operations: the Lewis operation, which forms an intrathoracic anastomosis, and the McKeown operation, which forms an anastomosis on the neck.

In a study by Low et al.,[7] in 2704 esophagectomies, the overall complication rate was 59%, with the most common complications being pneumonia (14.6%) and arrhythmia (14.5%). Anastomotic leakage was 11.4%, and 30-day mortality was 2.4%.

A study by Nakajima M et al.[8] found dislocation of the gastric conduit in 38.3% of 149 patients who underwent transthoracic esophagectomy. Multivariate analysis revealed that dislocation of the gastric conduit was an independent risk factor for anastomotic leakage (OR=4.840, 95% CI: 1.770-13.30, P<0.001). Sakai et al.[9] examined 53 patients with thoracic esophageal cancer who underwent radical esophagectomy with gastric tube reconstruction and neck anastomosis. The displacement of anastomosis into the thoracic cavity was detected in approximately half of the patients with neck anastomosis.

In our study, out of 6 anastomotic leakages in the group with DCA, all 6 had mediastinal complications. In patients without DCA, the anastomotic leakage proceeded more smoothly, of which only 33.3% (3/9) experienced mediastinal complications.

In a study by Fumagalli et al.,[10] the proportion of leakage was 10.5% and 9% after open and hybrid esophagectomy, respectively, and doubled (20%) after totally minimally invasive esophagectomy (P=0.016). Chen et al.[11] recommended a high cervical anastomosis using a narrow gastric tube to reduce leakage-related complications for patients undergoing a McKeown esophagectomy effectively.

The studied mechanisms ensuring dislocation of the anastomosis to the mediastinum are increased tone of the esophagus and stomach after the cessation of anesthesia, the suction effect of the diaphragm, which stimulates the migration of the graft into the abdominal cavity and, therefore, provides traction of the anastomosis into the mediastinum, and gravity when filling the graft with food.[12] The fixation of cervical anastomosis on the neck may protect the anastomosis from distracting forces during the most vulnerable healing phase. Thus, esophagogastric anastomosis is subjected to several forces that create tension from the moment of recovery from anesthesia and act in the early postoperative period.

Conclusion

After McKeown esophagectomy, DCA toward the posterior mediastinum was noted in 26.8% of cases. Dislocation of the cervical anastomosis toward the posterior mediastinum does not significantly impact the anastomotic leakage. Mediastinal complications are more common in patients with DCA, but the incidence of pulmonary complications is not associated with this phenomenon.

Competing Interests

The authors declare that they have no competing interests.

References

1. Sung H, Ferlay J, Siegel RL, Laversanne M, Soerjomataram I, Jemal A, Bray F. Global Cancer Statistics 2020: GLOBOCAN Estimates of Incidence and Mortality Worldwide for 36 Cancers in 185 Countries. CA Cancer J Clin. 2021 May;71(3):209-249. doi: 10.3322/caac.21660. Epub 2021 Feb 4. PMID: 33538338.

2. Kaprin AD, Starinsky VV, Shakhzadova AO. The state of cancer care for the population of Russia in 2020. M.: MNIIOI named after P. A. Herzen. 2021; 252. (In Russian.)

3. Rogers JE, Sewastjanow-Silva M, Waters RE, Ajani JA. Esophageal cancer: emerging therapeutics. Expert Opin Ther Targets. 2022 Feb;26(2):107-117. doi: 10.1080/14728222.2022.2036718. Epub 2022 Feb 12. PMID: 35119973.

4. McKeown KC. Total three-stage oesophagectomy for cancer of the oesophagus. Br J Surg. 1976 Apr;63(4):259-62. doi: 10.1002/bjs.1800630403. PMID: 1276657.

5. LEWIS I. The surgical treatment of carcinoma of the oesophagus; with special reference to a new operation for growths of the middle third. Br J Surg. 1946 Jul;34:18-31. doi: 10.1002/bjs.18003413304. PMID: 20994128.

6. Verstegen MHP, Bouwense SAW, van Workum F, Ten Broek R, Siersema PD, Rovers M, Rosman C. Management of intrathoracic and cervical anastomotic leakage after esophagectomy for esophageal cancer: a systematic review. World J Emerg Surg. 2019 Apr 4;14:17. doi: 10.1186/s13017-019-0235-4. PMID: 30988695; PMCID: PMC6449949.

7. Low DE, Kuppusamy MK, Alderson D, Cecconello I, Chang AC, Darling G, et al. Benchmarking Complications Associated with Esophagectomy. Ann Surg. 2019 Feb;269(2):291-298. doi: 10.1097/SLA.0000000000002611. PMID: 29206677.

8. Nakajima M, Muroi H, Kikuchi M, Fujita J, Ihara K, Nakagawa M, Morita S, Nakamura T, Yamaguchi S, Kojima K. Dislocation of the gastric conduit reconstructed via the posterior mediastinal route is a significant risk factor for anastomotic disorder after McKeown esophagectomy. Ann Gastroenterol Surg. 2021 Aug 12;6(1):75-82. doi: 10.1002/ags3.12496. PMID: 35106417; PMCID: PMC8786694.

9. Sakai M, Sohda M, Miyazaki T, Yoshida T, Kumakura Y, Honjo H, Hara K, Yokobori T, Kuwano H. Impact of the Level of Anastomosis on Reflux Esophagitis Following Esophagectomy with Gastric Tube Reconstruction. World J Surg. 2017 Mar;41(3):804-809. doi: 10.1007/s00268-016-3786-5. PMID: 27798723.

10. Fumagalli U, Baiocchi GL, Celotti A, Parise P, Cossu A, Bonavina L, et al. Incidence and treatment of mediastinal leakage after esophagectomy: Insights from the multicenter study on mediastinal leaks. World J Gastroenterol. 2019 Jan 21;25(3):356-366. doi: 10.3748/wjg.v25.i3.356. PMID: 30686903; PMCID: PMC6343094.

11. Chen C, Ding C, He Y, Guo X. High cervical anastomosis reduces leakage-related complications after a McKeown esophagectomy. Eur J Cardiothorac Surg. 2024 Mar 1;65(3):ezae050. doi: 10.1093/ejcts/ezae050. PMID: 38341665.

12. Walsh TN. The Esophagogastric Anastomosis: The Importance of Anchoring Sutures in Reducing Anastomotic Leak Rates. Ann Surg Open. 2023 Feb 1;4(1):e231. doi: 10.1097/AS9.0000000000000231. PMID: 37600864; PMCID: PMC10431275.

International Journal of Biomedicine 14(2) (2024) 338-340
http://dx.doi.org/10.21103/Article14(2)_CR1

CASE REPORT

INTERNATIONAL JOURNAL OF BIOMEDICINE

Noninfective Endocarditis in a Young Patient with Systemic Lupus Erythematosus

Daniela Teferiçi[1], Arjan Shtylla[2], Alma Idrizi[3], Aldo Shpuza[4], Enver Roshi[4*], Alban Dibra[1]

[1]Department of Cardiology, Cardiac Surgery, University Hospital Center "Mother Theresa," Tirana, Albania
[2]Department of Obstetrics and Gynecology, University Hospital Center "K. Gliozheni," Tirana, Albania
[3]Department of Internal Medicine, Nephrology Service, University Hospital Center "Mother Theresa," Tirana, Albania
[4]Department of Public Health, University of Medicine, Tirana, Albania

Abstract

Noninfective endocarditis, particularly in association with systemic autoimmune diseases like systemic lupus erythematosus (SLE), presents a diagnostic challenge due to its nonspecific symptoms and the potential for severe cardiac complications. We describe a case of a 16-year-old female diagnosed with SLE who presented with fever, malaise, and a new heart murmur. Subsequent investigations revealed vegetations on the mitral valve consistent with noninfective endocarditis without any evidence of infectious etiology. This case underscores the importance of considering noninfective endocarditis in the differential diagnosis for patients with systemic autoimmune disorders presenting with fever and cardiac symptoms. Early recognition and management are crucial to prevent serious outcomes.**(International Journal of Biomedicine. 2024;14(2):338-340.)**

Keywords: systemic lupus erythematosus • noninfective endocarditis • Libman-Sacks endocarditis

For citation: Teferiçi D, Shtylla A, Idrizi A, Shpuza A, Roshi E, Dibra A. Noninfective Endocarditis in a Young Patient with Systemic Lupus Erythematosus. International Journal of Biomedicine. 2024;14(2):338-340. doi:10.21103/Article14(2)_CR1

Abbreviations

LSE, Libman-Sacks endocarditis; **LVH**, left ventricular hypertrophy; **SLE**, systemic lupus erythematosus; **CRP**, C-reactive protein.

Introduction

Libman-Sacks endocarditis (LSE), also known as verrucous, marantic, or nonbacterial thrombotic endocarditis, was first described by Emanuel Libman and Benjamin Sacks in 1924.[(1)] Heart valve abnormalities can be found in 1 of every 3 patients with systemic lupus erythematosus (SLE), while valvular vegetations, such as LSE, are present in 1 of every 10 SLE patients.[(2)] Libman-Sacks endocarditis is rare in children and adolescents, more so as a first manifestation of SLE. They are clinically silent in most cases. The presence of antiphospholipid antibodies in SLE is associated with a three times higher prevalence of mitral valve nodules and significant mitral regurgitation.[(3)] The diagnosis of LSE becomes challenging, especially in differentiating it from infective endocarditis, as both diseases may present similarly.

Case Presentation

A 16-year-old female was admitted with fatigue, fever, and shortness of breath. During the physical examination, she presented tachypnea, tachycardia (150 bpm), temperature of 38.8°C, blood pressure of 150/90 mmHg, increased central venous pressure, and a grade V/VI pan systolic mitral murmur. An electrocardiogram demonstrated sinus tachycardia without other associated anomalies. Three pairs of blood culture samples

were collected from different sites, and all had negative results. A cardiac ultrasound revealed a large pericardial effusion, and the decision to pericardiocentesis was made. The patient tolerated the procedure well, and 220 cc of serous fluid was aspirated and sent for laboratory studies. Blood test: WBC - $10.9\times10^3/\mu L$, RBC - $4.93\times10^6/\mu L$, Hb - 7.3 g/dL, platelets - $140\times10^3/\mu L$, lymphocytes -12%, urea – 123 mg/dL, creatinine - 3.1 mg/dL, CRP - 33.8 mg/L, AST - 25 U/L, ALT - 10 U/L, GGT - 72 U/L, LDH - 410 U/L, total protein - 7.3 g/dL. A urine analysis revealed proteinuria and hematuria. Workup showed positive antinuclear antibody, anti-dsDNA, anti-ENA screen, and slightly depressed serum complement levels. Chest X-ray revealed bilateral pleural effusion. During the hospital stay, the patient developed an episode of seizure. According to the diagnostic criteria, the diagnosis of SLE was made, and the patient started treatment with methylprednisolone and cyclophosphamide. The patient was sent for transthoracic echocardiography (2 days after pericardiocentesis), which revealed a diffuse infiltration of anterior mitral leaflet and a nodular thickening on it, sized 20×10 mm (Figures 1 and 2), with severe mitral regurgitation (Figure 3). Also, a nodular thickening was seen on the pulmonary valve, and there was mild regurgitation (Figure 4). A concentric left ventricular hypertrophy (LVH) was noticed with a mild dilatation of the left atrium; both ventricles' size and systolic function were preserved (Figure 5). A small amount of pericardial effusion was detected. Considering possible infective endocarditis and elevated CRP and WBC levels, the patient was placed on a regimen of ampicillin and gentamycin for 2 weeks. As the urea and creatinine levels rose and the patient became oliguric, she was transferred to the nephrology ward, where hemodialysis was started. Under the treatment with hemodialysis, methylprednisolone, cyclophosphamide, lercanidipine, carvedilol, ampicillin, gentamycin and levetiracetam, her symptoms improved. The patient remained afebrile, and her creatinine level, after reaching 7 mg/dl, went down to 3 mg/dl. Another transthoracic echocardiography was performed after 2 weeks, with the same results as the previous one, but without pericardial effusion. Echocardiographic studies have yet to be repeated as of writing this article.

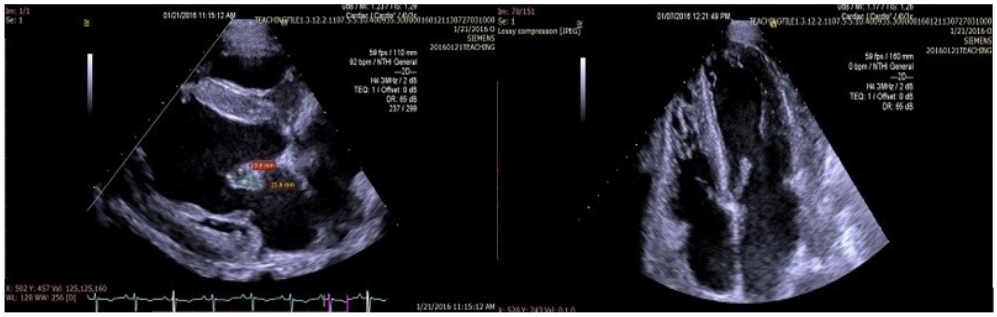

Fig. 1 and 2. *Diffuse infiltration of the anterior leaflet of the mitral valve with nodular thickening in the parasternal and apical 4-chamber view.*

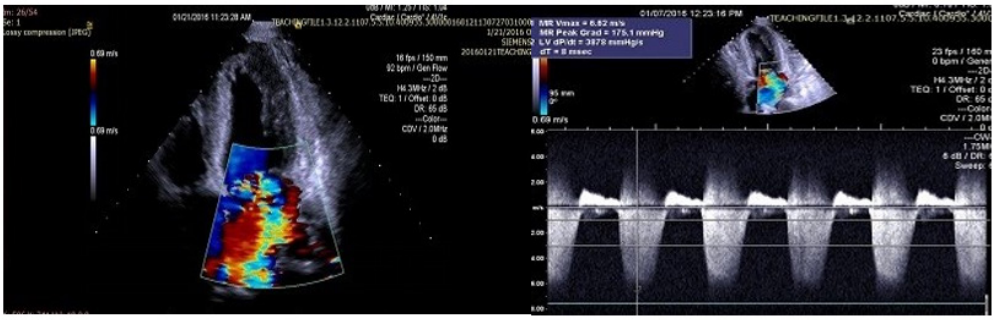

Fig. 3. *Severe mitral regurgitation.*

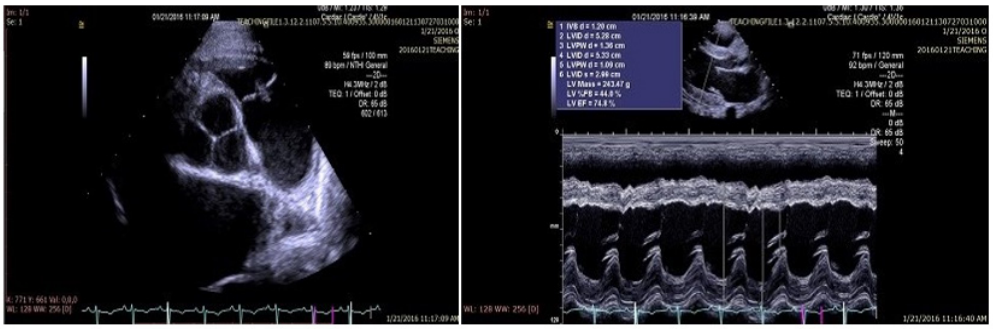

Fig. 4. *Nodular thickened on the pulmonary valve.* ***Fig. 5.*** *Concentric hypertrophy of LV with normal diameters and systolic function.*

Discussion

This case of a young patient with SLE presented with progressive dyspnea (which may have been caused by pericardial effusion) and fever was also characterized by the presence of aseptic vegetation on the mitral valve with severe mitral regurgitation. The lesions primarily consist of accumulations of immune complexes and mononuclear cells. These subendothelial deposits may eventually lead to deformed valves. The most involved valve is the mitral valve, followed by the aortic valve.[3] Characteristic valvular pathology can also distinguish infective endocarditis vegetations from Libman-Sacks endocarditis, but this may not always hold as vegetative lesions may evolve throughout the disease. Infective endocarditis is characterized by large, irregular masses on the valve cusps, which can extend onto the cords. Libman-Sacks endocarditis has small or medium-sized vegetation on either or both sides of the valve leaflets. The vegetation seen on the patient's echocardiogram was on the anterior mitral valve leaflet. Still, the exact size and extent of involvement in this leaflet could not be distinguished because of the infiltration of the entire leaflet.

Laboratory parameters such as WBC count, CRP, and blood cultures can also be useful in distinguishing infective endocarditis from Libman-Sacks endocarditis.[4] Leukocytes tend to decrease during lupus activity, and the opposite occurs in infectious endocarditis. Very high CRP levels suggest an infectious cause; blood cultures are more important for a definitive differential diagnosis.[5]

In our case, a diagnosis of Libman-Sacks endocarditis was more probable, as the leukocyte count was slightly elevated, the CRP was not highly elevated, and blood culture samples had negative results. SLE patients have an increased prevalence of left ventricular hypertrophy that is not exclusively a result of concomitant coronary artery or valvular heart disease, renal involvement, or other traditional stimuli, including hypertension. Our patient has an acute onset of renal failure and hypertension that doesn't explain the existing left ventricular hypertrophy. Results of studies suggest that inflammation-mediated arterial stiffening, a strong determinant of left ventricular hypertrophy, is likely the underlying mechanism for Libman-Sacks endocarditis in systemic lupus erythematosus.[6,7] Libman-Sacks endocarditis is known to lead to an increased risk of stroke, coronary artery disease, and sudden cardiac death in varied populations and, therefore, is likely to be a prognostic indicator of cardiac morbidity and mortality in SLE patients.[8,9] Our findings suggest that more aggressive and targeted therapy may be needed to control the inflammation-mediated effects on vascular stiffening that lead to left ventricular hypertrophy.

In conclusion, SLE patients will be more likely to develop cardiac manifestations, such as valvular regurgitation and possible Libman-Sacks endocarditis.

Competing Interests

The authors declare that they have no competing interests.

References

1. LIBMAN E, SACKS B. A HITHERTO UNDESCRIBED FORM OF VALVULAR AND MURAL ENDOCARDITIS. Arch Intern Med (Chic). 1924;33(6):701–737. doi:10.1001/archinte.1924.00110300044002

2. Ruiz-Irastorza, G. Khamashta M. Cardiopulmonary system in SLE. Dubois' Lupus Erythematosus and Related Syndromes.Wallace DJ et al., Eds. 8th ed. Elsevier, 2012: 352-362.

3. Moyssakis I, Tektonidou MG, Vasilliou VA, Samarkos M, Votteas V, Moutsopoulos HM. Libman-Sacks endocarditis in systemic lupus erythematosus: prevalence, associations, and evolution. Am J Med. 2007 Jul;120(7):636-42. doi: 10.1016/j.amjmed.2007.01.024. PMID: 17602939.

4. Hojnik M, et al. Hojnik M, George J, Ziporen L, Shoenfeld Y. Heart valve involvement (Libman-Sacks endocarditis) in the antiphospholipid syndrome. Circulation. 1996 Apr 15;93(8):1579-87. doi: 10.1161/01.cir.93.8.1579.

5. Barnes EV, Narain S, Naranjo A, Shuster J, Segal MS, Sobel ES, Armstrong AE, Santiago BE, Reeves WH, Richards HB. High sensitivity C-reactive protein in systemic lupus erythematosus: relation to disease activity, clinical presentation and implications for cardiovascular risk. Lupus. 2005;14(8):576-82. doi: 10.1191/0961203305lu2157oa.

6. Crozier IG, Li E, Milne MJ, Nicholls MG. Cardiac involvement in systemic lupus erythematosus detected by echocardiography. Am J Cardiol. 1990 May 1;65(16):1145-8. doi: 10.1016/0002-9149(90)90329-y. PMID: 2330902.

7. Fujimoto S, Kagoshima T, Nakajima T, Dohi K. Doppler echocardiographic assessment of left ventricular diastolic function in patients with systemic lupus erythematosus. Cardiology. 1994;85(3-4):267-72. doi: 10.1159/000176685. PMID: 7987885.

8. Manzi S, Meilahn EN, Rairie JE, Conte CG, Medsger TA Jr, Jansen-McWilliams L, D'Agostino RB, Kuller LH. Age-specific incidence rates of myocardial infarction and angina in women with systemic lupus erythematosus: comparison with the Framingham Study. Am J Epidemiol. 1997 Mar 1;145(5):408-15. doi: 10.1093/oxfordjournals.aje.a009122.

9. Roman MJ, Shanker BA, Davis A, Lockshin MD, Sammaritano L, Simantov R, Crow MK, Schwartz JE, Paget SA, Devereux RB, Salmon JE. Prevalence and correlates of accelerated atherosclerosis in systemic lupus erythematosus. N Engl J Med. 2003 Dec 18;349(25):2399-406. doi: 10.1056/NEJMoa035471. Erratum in: N Engl J Med. 2006 Oct 19;355(16):1746. PMID: 14681505.

***Corresponding author:** *Enver Roshi, Department of Public Health, University of Medicine, Tirana, Albania. E-mail: roshienvi@yahoo.com*

International Journal of Biomedicine 14(2) (2024) 341-344
http://dx.doi.org/10.21103/Article14(2)_CR2

CASE REPORT

INTERNATIONAL JOURNAL OF BIOMEDICINE

Overcoming Diagnostic and Management Hurdles: A Case Report on Superior Sagittal Sinus Thrombosis with Subarachnoid Hemorrhage

Kliti Pilika[1], Armand Shehu[2], Anita Pilika[3], Aldo Shpuza[4*], Xhesika Xhetani[5]

[1]*Neurosurgery Service, University Hospital Centre "Mother Teresa," Tirana, Albania*
[2]*Pediatric Service, University Hospital Centre "Mother Teresa," Tirana, Albania*
[3]*Psychiatric Service, University Hospital Centre "Mother Teresa," Tirana, Albania*
[4]*Department of Public Health, University of Medicine, Tirana, Albania*
[5]*Korca Region Hospital, Albania*

Abstract

Cerebral venous thrombosis is a rare but critical condition, presenting significant diagnostic challenges due to its varied clinical manifestations. This report underscores the complexity of the superior sagittal sinus thrombosis diagnosis and management, highlighting the need for heightened clinical awareness and prompt intervention.

We present a case of a 47-year-old male with a history of cerebral aneurysm, who arrived at the emergency department exhibiting acute neurological symptoms, including loss of consciousness, seizures, and muscular contractions, without any recent history of trauma or medication use. Neurological examination showed a Glasgow Coma Scale (GCS) of 15, with specific findings suggesting a significant neurological impact. Neuroimaging revealed subarachnoid hemorrhage in the left interhemispheric fissure and thrombosis of the superior sagittal sinus. Despite the complex presentation and rapid progression of symptoms, a multidisciplinary approach involving continuous monitoring, decompressive craniectomy, and subsequent rehabilitative measures led to a significant improvement in the patient's condition.

This case illustrates the critical nature of superior sagittal sinus thrombosis, and the challenges associated with its diagnosis and management. It emphasizes the importance of considering cerebral venous thrombosis in the differential diagnosis of acute neurological events and the effectiveness of a comprehensive, multidisciplinary approach in managing such complex cases. The positive outcome in this case contributes to the growing body of evidence supporting aggressive intervention strategies in managing cerebral venous thrombosis. **(International Journal of Biomedicine. 2024;14(2):341-344.)**

Keywords: cerebral venous thrombosis • superior sagittal sinus • subarachnoid hemorrhage • diagnosis

For citation: Pilika K, Shehu A, Pilika A, Shpuza A, Xhetani X. Overcoming Diagnostic and Management Hurdles: A Case Report on Superior Sagittal Sinus Thrombosis with Subarachnoid Hemorrhage. International Journal of Biomedicine. 2024;14(2):341-344. doi:10.21103/Article14(2)_CR2

Abbreviations

CVT, cerebral venous thrombosis; **CT**, computed tomography; **MRI**, magnetic resonance imaging **SSS**, superior sagittal sinus; **SSST**, SSS thrombosis; **SAH**, subarachnoid hemorrhage.

Introduction

Cerebral venous thrombosis (CVT) is a rare disorder with an estimated annual incidence of three to four cases per million, occurring slightly less frequently in peripartum and postpartum pregnant women (about 12 cases per 100,000 deliveries) compared to peripartum and postpartum arterial stroke, and it is three times more common in women than in men.[(1)] Initial presenting symptoms that resemble stroke in young patients, including focal neurological deficits like hemiparesis, signs of intracranial hypertension, seizures, and encephalopathy, should prompt consideration of thrombosis of the superior sagittal sinus (SSS), a major component of the superficial cerebral venous system, due to its variable

presentation.[2] Surgical thrombectomy is typically considered for severe neurological decline not improved by medical treatments, while decompressive surgery, despite being primarily supported by level C evidence, is deemed life-saving for large venous infarcts and hemorrhages with a risk of herniation, showing favorable outcomes in over 50% of patients and a mortality rate around 20%.[3] Given the intricate nature of CVT diagnosis and the broad spectrum of initial symptoms that may mimic those of a stroke, this case underscores the paramount importance of incorporating CVT, particularly superior sagittal sinus thrombosis (SSST), into the differential diagnosis of acute neurological events. It supports the utility of aggressive, multidisciplinary management strategies to optimize patient outcomes.

Case Presentation

A 47-year-old male patient presented to the Emergency Department of Internal Diseases at University Medical Center "Mother Teresa," with a history of a recent episode involving loss of consciousness, muscle spasms, and fixed gaze. The patient had been diagnosed with a cerebral aneurysm two years prior and had been monitored dynamically with MRI scans of the cranium. He reported no history of trauma and was not on any medications at the time.

Neurological examination revealed a Glasgow Coma Scale (GCS) score of 15 and a Hunt and Hess grade of 2. The patient was alert, conscious, and oriented in time, space, and person. Pupils were isochoric and photoreactive, with intact oculomotor function and no facial asymmetry. There were no evident deficits in other cranial nerves. The neck was rigid and painful on flexion. There were no sensory-motor deficits in the upper limbs, but a 3/5 deficit was noted in the lower right side.

Cranial CT and supra-aortic Angio CT scans showed subarachnoid hemorrhage (SAH), predominantly interhemispheric on the left side, with no evidence of an aneurysm in this examination. There was an absence of the A1 segment on the right side and lack of contrast in the anterior two-thirds of the SSS, suggesting thrombosis (Figure 1). Cranial MRI confirmed SAH mainly on the left interhemispheric side and the absence of contrast in two-thirds of the SSS, indicating sinus thrombosis.

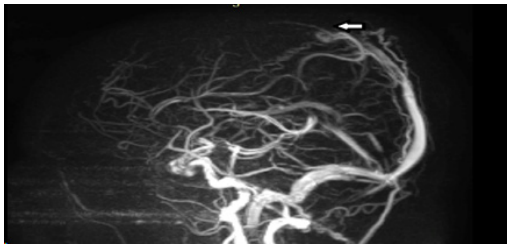

Fig. 1. *The superior sagittal sinus is not visualized in its anterior two-thirds, indicating extensive thrombosis.*

Initially, the patient was hospitalized in the Stroke Unit for continuous monitoring. After 10 hours, discreet right-sided prefrontal cortex symptoms and motor deficits on the right side were noted. Twelve hours later, the patient's condition worsened, showing closed eyes, unresponsive to verbal stimuli, right-sided hemiplegia, and spontaneous movement on the left side. After 16 hours, anisocoria began. Repeated cranial CT and MRI scans revealed an enlargement of the intraparenchymal hemorrhage with ventricular effusion (Figure 2). The patient was then transferred to the Neurosurgery ICU. On August 12, 2023, a decompressive right hemicraniectomy and evacuation of the hematoma were performed (Figure 3). A tracheostomy was performed on August 16. The skull was reconstructed without cortical damage on August 31 (Figure 4).

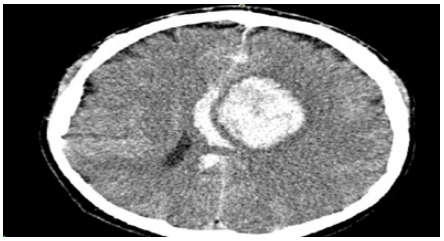

Fig. 2. *CT scan revealed an enlargement of the intraparenchymal hemorrhage with ventricular effusion.*

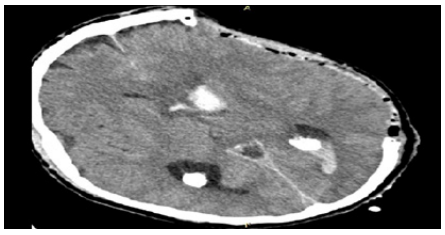

Fig. 3. *A decompressive right hemicraniectomy and evacuation of the hematoma were performed.*

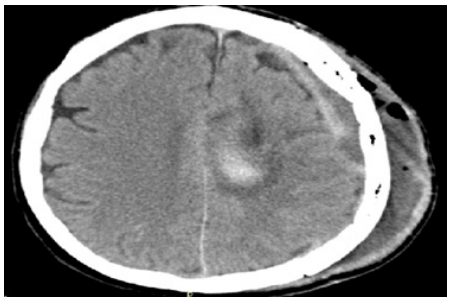

Fig. 4. *Skull reconstruction without cortical damage.*

During hospitalization, the patient was dynamically monitored with laboratory analyses and imaging examinations and received multidisciplinary consultations from neurology, infectious diseases, and hematology departments. The patient was discharged in an improved condition on September 19, 2023.

Discussion

In the intricate landscape of neurology, the diagnosis and management of SSST intertwined with SAH represent a formidable challenge, exemplified by the case of a 47-year-old male with a notable history of a cerebral aneurysm. This case encapsulates the critical nature of cerebral venous thrombosis and its potential to manifest in a spectrum of clinical presentations, underscoring the diagnostic hurdles and the imperative for prompt, multifaceted intervention strategies. The patient's acute neurological symptoms, devoid of any recent trauma or medication history, accentuate the unpredictable clinical course of cerebral venous thrombosis, aligning with the diagnostic complexities highlighted by other studies, which have advocated for cerebral venous thrombosis to be considered in the differential diagnosis of acute neurological events to mitigate the risk of rapid clinical deterioration.[4]

The use of sophisticated neuroimaging techniques, such as CT and MRI, has played an important role in establishing the SSST diagnosis and associated SAH. This echoes the sentiments of Ferro et al.[5] regarding the indispensable role of imaging in accurately identifying and characterizing cerebral venous thrombosis and its sequelae.

This case's pivotal decision to undertake decompressive craniectomy highlights the potential life-saving outcomes of aggressive surgical intervention in the face of large venous infarcts and hemorrhagic complications, reinforcing the critical need for timely and decisive action in the management of such complex clinical scenarios, also described in the literature.[6] The comprehensive, multidisciplinary approach to patient care, encompassing continuous monitoring and expert consultations from various specialties, mirrors the integrated care model proposed by Stam for optimizing patient outcomes in cerebral venous thrombosis, emphasizing the value of collaborative, cross-disciplinary strategies in navigating the complexities of this condition.[7]

This case not only showcases the multifaceted challenges in diagnosing and treating superior sagittal sinus thrombosis with subarachnoid hemorrhage but also illuminates the importance of maintaining a high index of suspicion, leveraging advanced neuroimaging techniques, and adopting a coordinated, aggressive management plan, as echoed in the broader literature.

Further, the literature underscores the variability in cerebral venous thrombosis clinical manifestations, which can range from headache to severe neurological deficits, emphasizing the heterogeneity of cerebral venous thrombosis presentations and the consequent challenges in achieving a timely diagnosis.[8]

This case's reliance on neuroimaging for CVT diagnosis and the subsequent surgical intervention aligns with the recommendations of other studies, which highlight the role of imaging in confirming cerebral venous thrombosis and guiding treatment decisions, particularly in cases where traditional treatment modalities are insufficient.

Many studies support the significance of a tailored therapeutic approach, considering both anticoagulation therapy and surgical options. Most patients with cerebral venous thrombosis have a good prognosis after anticoagulant therapy, and a minority of patients with malignant cerebral venous thrombosis may also benefit from endovascular treatment or decompressive surgery.[10] Anticoagulation is the current standard of care for cerebral venous thrombosis, but more aggressive therapies, such as mechanical thrombectomy with or without intrasinus thrombolysis, may be required in selected cases.[11] This nuanced approach to management, reflecting the complexities inherent in cerebral venous thrombosis cases, further highlights the need for a wide range of therapeutic strategies to address the varied presentations and complications associated with this condition.[12]

This case report not only exemplifies the diagnostic and management challenges associated with superior sagittal sinus thrombosis and subarachnoid hemorrhage but also contributes to the evolving discourse on the necessity for heightened clinical vigilance, the pivotal role of neuroimaging, and the efficacy of a comprehensive, aggressive treatment approach in improving patient outcomes. It reaffirms the consensus within the neurology community, as documented in the literature, on the imperative for an adaptive, multidisciplinary strategy in managing cerebral venous thrombosis, underscoring the continuous evolution of best practices in the face of such complex neurological conditions.

Conclusion

Our case report on a 47-year-old male with superior sagittal sinus thrombosis underscores the critical importance of recognizing and managing this rare but severe condition. Highlighting the necessity for high clinical suspicion, rapid multidisciplinary intervention, and the pivotal role of neuroimaging in diagnosis, the successful outcome of this case reinforces the potential for significant patient recovery. It emphasizes the value of a comprehensive approach, combining surgical, medical, and rehabilitative strategies to address the complex challenges posed by cerebral venous thrombosis, thereby improving patient prognosis and contributing valuable insights to the management of this intricate condition.

Competing Interests

The authors declare that they have no competing interests.

References

1. Tadi P, Behgam B, Baruffi S. Cerebral Venous Thrombosis. 2023 Jun 12. In: StatPearls [Internet]. Treasure Island (FL): StatPearls Publishing; 2024 Jan–. PMID: 29083599.
2. Zabalo San Juan G, Vázquez Míguez A, Zazpe Cenoz I, Casajús Ortega A, García Campos M, de Frutos Marcos

***Corresponding author**: Aldo Shpuza, Department of Public Health, University of Medicine, Tirana, Albania. E-mail:aldoshpuza@hotmail.com*

D, García Romero JC. Intracranial hypertension caused by superior sagittal sinus stenosis secondary to a depressed skull fracture: Case report and review of the literature. Neurocirugia (Astur: Engl Ed). 2019 Sep-Oct;30(5):243-249. English, Spanish. doi: 10.1016/j.neucir.2018.10.002. Epub 2018 Nov 16. PMID: 30449708.

3. Ulivi L, Squitieri M, Cohen H, Cowley P, Werring DJ. Cerebral venous thrombosis: a practical guide. Pract Neurol. 2020 Oct;20(5):356-367. doi: 10.1136/practneurol-2019-002415. PMID: 32958591.

4. Bousser MG, Ferro JM. Cerebral venous thrombosis: an update. Lancet Neurol. 2007 Feb;6(2):162-70. doi: 10.1016/S1474-4422(07)70029-7. PMID: 17239803.

5. Ferro JM, Canhão P, Stam J, Bousser MG, Barinagarrementeria F; ISCVT Investigators. Prognosis of cerebral vein and dural sinus thrombosis: results of the International Study on Cerebral Vein and Dural Sinus Thrombosis (ISCVT). Stroke. 2004 Mar;35(3):664-70. doi: 10.1161/01.STR.0000117571.76197.26. Epub 2004 Feb 19. PMID: 14976332.

6. Canhão P, Ferro JM, Lindgren AG, Bousser MG, Stam J, Barinagarrementeria F; ISCVT Investigators. Causes and predictors of death in cerebral venous thrombosis. Stroke. 2005 Aug;36(8):1720-5. doi: 10.1161/01.STR.0000173152.84438.1c. Epub 2005 Jul 7. PMID: 16002765.

7. Stam J. Thrombosis of the cerebral veins and sinuses. N Engl J Med. 2005 Apr 28;352(17):1791-8. doi: 10.1056/NEJMra042354. PMID: 15858188.

8. Einhäupl K, Stam J, Bousser MG, De Bruijn SF, Ferro JM, Martinelli I, Masuhr F; European Federation of Neurological Societies. EFNS guideline on the treatment of cerebral venous and sinus thrombosis in adult patients. Eur J Neurol. 2010 Oct;17(10):1229-35. doi: 10.1111/j.1468-1331.2010.03011.x. PMID: 20402748.

9. Stam J, Majoie CB, van Delden OM, van Lienden KP, Reekers JA. Endovascular thrombectomy and thrombolysis for severe cerebral sinus thrombosis: a prospective study. Stroke. 2008 May;39(5):1487-90. doi: 10.1161/STROKEAHA.107.502658. Epub 2008 Mar 13. PMID: 18340091.

10. Luo Y, Tian X, Wang X. Diagnosis and Treatment of Cerebral Venous Thrombosis: A Review. Front Aging Neurosci. 2018 Jan 30;10:2. doi: 10.3389/fnagi.2018.00002. PMID: 29441008; PMCID: PMC5797620.

11. Siddiqui FM, Dandapat S, Banerjee C, Zuurbier SM, Johnson M, Stam J, Coutinho JM. Mechanical thrombectomy in cerebral venous thrombosis: systematic review of 185 cases. Stroke. 2015 May;46(5):1263-8. doi: 10.1161/STROKEAHA.114.007465. Epub 2015 Apr 21. PMID: 25899238.

12. Coutinho JM, Zuurbier SM, Aramideh M, Stam J. The incidence of cerebral venous thrombosis: a cross-sectional study. Stroke. 2012 Dec;43(12):3375-7. doi: 10.1161/STROKEAHA.112.671453. Epub 2012 Sep 20. PMID: 22996960.

International Journal of Biomedicine 14(2) (2024) 345-347
http://dx.doi.org/10.21103/Article14(2)_CR3

CASE REPORT

INTERNATIONAL JOURNAL OF BIOMEDICINE

Extramedullary Hematopoiesis in a Patient with Beta Thalassemia: A Rare Case Report

Mohammed Saad Alqahtani*

Internal Medicine Department, College of Medicine, Prince Sattam bin Abdulaziz University, Al-Kharj 11942, KSA

Abstract

Extramedullary hematopoiesis (EMH) is a rare disorder, defined as the appearance of hematopoietic elements outside the bone marrow or peripheral blood due to ineffective erythropoiesis or inadequate bone marrow activity in a variety of hematological diseases. EMH often manifests as hemopoietic masses in a variety of normal and abnormal bodily sites. We present a 21-year-old man with a medical history of beta thalassemia since he was nine months old. The primary clinical symptom was mild abdominal pain. In this case, we describe a rare instance of small bowel obstruction due to EMH and portal hypertension. Surgery solved the clinical problems, and the patient was discharged home. **(International Journal of Biomedicine. 2024;14(2):345-347.)**

Keywords: thalassemia • small bowel obstruction • extramedullary hematopoiesis

For citation: Alqahtani MS. Extramedullary Hematopoiesis in a Patient with Beta Thalassemia: A Rare Case Report. International Journal of Biomedicine. 2024;14(2):345-347. doi:10.21103/Article14(2)_CR3

Introduction

Beta thalassemia is caused by an inherited mutation of the beta-globin gene and by the reduced or absent synthesis of the beta-globin chains of the hemoglobin tetramer. Three clinical and hematological conditions of increasing severity are recognized: the beta thalassemia carrier state, thalassemia intermedia, and thalassemia major.[1] Another classification of thalassemia defines it as two categories: transfusion-dependent thalassemia (TDT) and non-transfusion-dependent thalassemia (NTDT). TDT is defined as a condition where patients cannot produce adequate hemoglobin to survive without blood transfusion. NTDT is a descriptive term for patients who do not require regular lifelong transfusions. The majority of the complications of TDT are related to iron overload and bone-deforming marrow expansion with EMH.[2-8] EMH is a compensatory response to poor bone marrow function, which can result in the production of ectopic hematopoietic components outside of the bone marrow and peripheral circulation.[9]

Case Presentation

A 21-year-old man with a medical history of beta thalassemia since he was nine months old arrived at the Medical Services Center complaining of mild abdominal pain. His physical assessment was normal, and plain abdominal radiography showed incomplete small intestinal obstruction (Figure 1). After that, he was brought to the Department of Hematology for a computed tomography (CT) scan, which showed hepatomegaly and small paraspinal lobulated masses (Figure 2). The patient's abdominal pains subsided, and he was released after a five-day fast. The patient came back to the hospital complaining mainly of vomiting, distension, pain in the abdomen, and flatus for a week. His vital signs were normal upon physical examination, but there were small, palpable abdominal lumps, hyperactive bowel noises, and pallor. Hepatomegaly was also seen. After a repeat abdominal CT scan, the results showed hepatomegaly, massive ascites, and a thicker ileum wall with clear arterial phase enhancement that was obstructing flow. It was challenging to differentiate the nature of the intestinal lesion. The patient was given a nasogastric tube, blood transfusions, intravenous proton pump inhibitors, and antibiotics throughout the first ten days of hospitalization. After that, the patient was referred to the Department of Gastrointestinal Surgery, where a laparotomy and a partial enterectomy were carried out. Significant proliferation of vascular endothelial cells and blood vessel hyperplasia in the deep layers of the intestine were confirmed by a microscopic examination. Histopathological analysis

showed many myeloid and erythroid cells proliferating together with multiple megakaryocytes (Figure 3). Several inflammatory cells had invaded the intestinal wall, and there were also a lot of megakaryocytes around the serosal region, coupled with a buildup of immature myeloid and erythroid cells. Surgery solved the clinical problems, and the patient was discharged home.

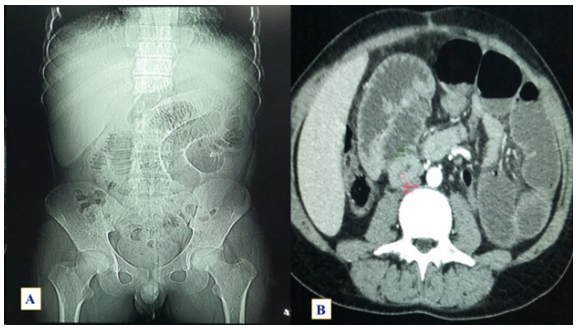

Fig. 1. *A) Abdominal radiography showing a dilated small bowel. B) CT scan: axial post IV contrasted abdominal study; a picture of the enhanced jejunal wall, with focal wall thickening and signs of pseudo intestinal obstruction.*

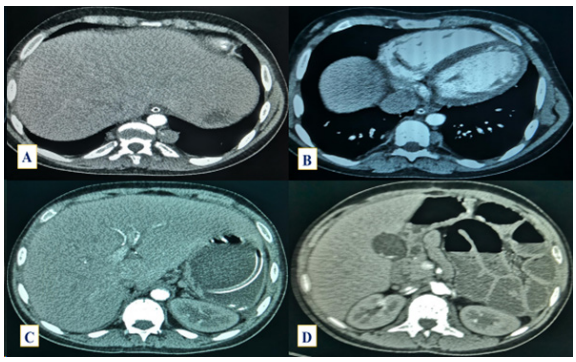

Fig. 2. *A) Axial CT abdomen shows huge hepatomegaly, left lobe focal low attenuation left paraspinal soft tissue masses.*
B) Axial contrast-enhanced lower chest mediastinal CT scan, arterial phase, nasogastric tube noted. No pericardial and pleural effusions; left paraspinal lobulated masses.
C) Abdomen CT: hepatomegaly, dilated stomach, and nasogastric tube. Normal enhanced left kidney and PV.
D) Axial contrast-enhanced CT scan, venous phase. Dilated bowel, pseudo-obstruction, GB stones, and nasogastric tube tip.

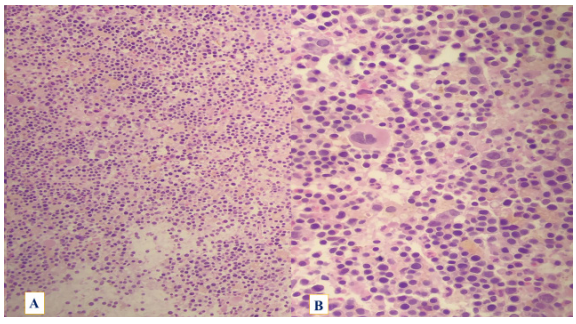

Fig. 3. *Histopathological study: the presence of EMH mass. A (X100), B (X200).*

Discussion

The clinical signs of EMH might vary widely because it can happen anywhere. There have been reports of EMH imitating acute appendicitis, intestinal obstruction, rectal stenosis, gastric outlet obstruction, and bladder outlet obstruction.[10] The reticuloendothelial system is the organ most frequently affected by EMH, but it can also affect the pleura, lungs, gastrointestinal tract, breast, skin, brain, kidneys, paraspinal tissue, and adrenal glands.[11] During the fetal stage, these areas are assumed to be involved in active hemopoiesis. Though this pathway ordinarily ends at birth, in cases of chronically inadequate erythropoiesis, the extramedullary hematopoietic vascular connective tissues continue to be able to synthesize red blood cells.[12]

The majority of EMHs are unintentionally found. The mass effect-related symptoms are specific to the afflicted spot.[13] There have been reports of EMH-related intestinal blockage, rectal stenosis, gastric outlet obstruction, and bladder outlet obstruction. The hematopoietic mass in our patient was adhered to nearby structures, which was a significant contributing factor to the symptoms. Due to an extramedullary hematopoietic mass adhering to the adjacent intestinal wall and intestinal stenosis, the patient experienced a closed-loop intestinal obstruction. Prior to surgery, the lesion was discovered via CT scanning. CT scanning can be a valuable technique for identifying gastrointestinal lesions, in addition to gastrointestinal endoscopic examinations. Masses with dense, soft sections that are typically homogeneous and have features comparable to those described by conventional radiologists can be observed on CT scans. These masses may or may not be highlighted after contrast material is administered.

The pathogenesis of this outside-bone marrow hematopoiesis is not clear. It may originate from the extension of hyperplastic marrow through the thin cortex of ribs and vertebral bodies; the capsule of the mass is formed by the periosteum.[14] Another explanation is that EMH results from transforming embryonal rests of osteogenic tissue into hematopoietic tissue under stress conditions to maintain sufficient red cell production.[15-17]

In conclusion, EMH in the small intestine is uncommon in patients with thalassemia. It is a sign of the severity of the disease and a poor prognostic factor because of small bowel obstruction. Surgery can solve the clinical problems that have arisen with EMH.

Acknowledgments

This publication was supported by the Deanship of Scientific Research at Prince Sattam bin Abdulaziz University, Al-Kharj, Saudi Arabia. We also thank all research participants.

Competing Interests

The authors declare that they have no competing interests.

References

1. Cao A, Galanello R. Beta-thalassemia. Genet Med. 2010 Feb;12(2):61-76. doi: 10.1097/GIM.0b013e3181cd68ed. PMID: 20098328.
2. Soliman A, Yassin M, Al Yafei F, Al-Naimi L, Almarri N, Sabt A, De Sanctis V. Longitudinal Study on Liver Functions in Patients with Thalassemia Major before and after Deferasirox (DFX) Therapy. Mediterr J Hematol Infect Dis. 2014 Apr 7;6(1):e2014025. doi: 10.4084/MJHID.2014.025. PMID: 24803998; PMCID: PMC4010606.
3. Yassin MA, Soliman AT, De Sanctis V, Abdelrahman MO, Aziz Bedair EM, AbdelGawad M. Effects of the anti-receptor activator of nuclear factor kappa B ligand denusomab on beta thalassemia major-induced osteoporosis. Indian J Endocrinol Metab. 2014 Jul;18(4):546-51. doi: 10.4103/2230-8210.137516. PMID: 25143915; PMCID: PMC4138914.
4. Soliman A, Yasin M, El-Awwa A, Osman M, de Sanctis V. Acute effects of blood transfusion on pituitary gonadal axis and sperm parameters in adolescents and young men with thalassemia major: a pilot study. Fertil Steril. 2012 Sep;98(3):638-43. doi: 10.1016/j.fertnstert.2012.05.047. Epub 2012 Jun 29. PMID: 22749224.
5. Soliman AT, Yassin M, Majuid NM, Sabt A, Abdulrahman MO, De Sanctis V. Cortisol response to low dose versus standard dose (back-to-back) adrenocorticotrophic stimulation tests in children and young adults with thalassemia major. Indian J Endocrinol Metab. 2013 Nov;17(6):1046-52. doi: 10.4103/2230-8210.122620. PMID: 24381882; PMCID: PMC3872683.
6. De Sanctis V, Soliman A, Candini G, Campisi S, Anastasi S, Iassin M. High prevalence of central hypothyroidism in adult patients with β-thalassemia major. Georgian Med News. 2013 Sep;(222):88-94. PMID: 24099820.
7. De Sanctis V, Elsedfy H, Soliman AT, Elhakim IZ, Pepe A, Kattamis C, Soliman NA, Elalaily R, El Kholy M, Yassin M. Acquired Hypogonadotropic Hypogonadism (AHH) in Thalassaemia Major Patients: An Underdiagnosed Condition? Mediterr J Hematol Infect Dis. 2016 Jan 1;8(1):e2016001. doi: 10.4084/MJHID.2016.001. PMID: 26740862; PMCID: PMC4696472.
8. Bukhari SS, Junaid M, Rashid MU. Thalassemia, extramedullary hematopoiesis, and spinal cord compression: A case report. Surg Neurol Int. 2016 Mar 2;7(Suppl 5):S148-52. doi: 10.4103/2152-7806.177891. PMID: 27069747; PMCID: PMC4802988.
9. Chiam QL, Lau KK. Extramedullary haematopoiesis in thalassaemia major causing spinal cord compression. Australas Radiol. 2007 Apr;51(2):168-71. doi: 10.1111/j.1440-1673.2007.01689.x. PMID: 17419864.
10. Elpek GO, Bozova S, Erdoğan G, Temizkan K, Oğüş M. Extramedullary hematopoiesis mimicking acute appendicitis: a rare complication of idiopathic myelofibrosis. Virchows Arch. 2006 Aug;449(2):258-61. doi: 10.1007/s00428-006-0230-5. PMID: 16738896.
11. Zhu G, Wu X, Zhang X, Wu M, Zeng Q, Li X. Clinical and imaging findings in thalassemia patients with extramedullary hematopoiesis. Clin Imaging. 2012 Sep-Oct;36(5):475-82. doi: 10.1016/j.clinimag.2011.11.019. Epub 2012 Jun 8. PMID: 22920349.
12. Haidar R, Mhaidli H, Taher AT. Paraspinal extramedullary hematopoiesis in patients with thalassemia intermedia. Eur Spine J. 2010 Jun;19(6):871-8. doi: 10.1007/s00586-010-1357-2. Epub 2010 Mar 5. PMID: 20204423; PMCID: PMC2899982.
13. Keikhaei B, Zandian K, Rahim F. Existence of cord compression in extramedullary hematopoiesis due to beta thalassemia intermedia. Hematology. 2008 Jun;13(3):183-6. doi: 10.1179/102453308X343347. PMID: 18702878.
14. Abdulla MAJ, Yassin MA, Abdelrazek M, Mudawi D, Ibrahim F, Soliman DS, ElOmri H, Nashwan AJ, Fernyhough LJ, De Sanctis V, Soliman AT. A persistent cough as atypical clinical presentation of intrathoracic extramedullary hematopoiesis (EMH) in a female with thalassemia intermedia. Acta Biomed. 2018 Feb 16;89(2-S):41-46. doi: 10.23750/abm.v89i2-S.7086. PMID: 29451228; PMCID: PMC6179037.
15. Bolaman Z, Polatli M, Cildag O, Kadiköylü G, Culhaci N. Intrathoracic extramedullary hematopoiesis resembling posterior mediastinal tumor. Am J Med. 2002 Jun 15;112(9):739-41. doi: 10.1016/s0002-9343(02)01128-2. PMID: 12079720.
16. Pornsuriyasak P, Suwatanapongched T, Wangsuppasawad N, Ngodngamthaweesuk M, Angchaisuksiri P. Massive hemothorax in a beta-thalassemic patient due to spontaneous rupture of extramedullary hematopoietic masses: diagnosis and successful treatment. Respir Care. 2006 Mar;51(3):272-6. PMID: 16533417.
17. Smith PR, Manjoney DL, Teitcher JB, Choi KN, Braverman AS. Massive hemothorax due to intrathoracic extramedullary hematopoiesis in a patient with thalassemia intermedia. Chest. 1988 Sep;94(3):658-60. doi: 10.1378/chest.94.3.658. PMID: 3409758.

***Correspondence**: Mohammed Saad Alqahtani. E-mail: Ms.alqahtani@psau.edu.sa*

International Journal of Biomedicine 14(2) (2024) 348-351
http://dx.doi.org/10.21103/Article14(2)_CR4

CASE REPORT

INTERNATIONAL JOURNAL OF BIOMEDICINE

The Role of MRI in Diagnosing Mayer-Rokitansky-Kuster-Hauser Syndrome: A Case Study

Diar Kabashi[1,3], Kreshnike Dedushi[2], Gojart Ferati[4], Argjira Juniku-Shkololli[3], Besiana Kabashi[5], Jeton Shatri[1,2*]

[1]*Institute of Anatomy, Faculty of Medicine, University of Prishtina, Prishtina, Kosovo*
[2]*Clinic of Radiology, University Clinical Centre of Kosovo, Prishtina, Kosovo*
[3]*Clinic of Gastroenterology, University Clinical Centre of Kosovo, Prishtina, Kosovo*
[4]*Clinic of Gynecology and Obstetrics, University Clinical Centre of Kosovo, Prishtina, Kosovo*
[5]*Clinic of Biochemistry, University Clinical Centre of Kosovo, Prishtina, Kosovo*

Abstract

The Mayer-Rokitansky-Kuster-Hauser (MRKH) syndrome is a rare condition that results from the disturbance of embryonic paramesonephric duct development, which gives rise to varying degrees of malformation of reproductive organs. It is characterized by uterovaginal aplasia with normal secondary sexual characteristics and 46,XX karyotype. We report a 15-year-old female patient with MRKH. Pelvic MRI revealed cervical and uterine agenesis with the absence of the vagina. The diagnosis was confirmed based on radiological findings. The correct clinical and radiological diagnosis of MRKH by MRI is crucial for long-term management. **(International Journal of Biomedicine. 2024;14(2):348-351.)**

Keywords: Müllerian anomaly • primary amenorrhea • magnetic resonance imaging

For citation: Kabashi D, Dedushi K, Ferati G, Juniku-Shkololli A, Kabashi B, Shatri J. The Role of MRI in Diagnosing Mayer-Rokitansky-Kuster-Hauser Syndrome: A Case Study. International Journal of Biomedicine. 2024;14(2):348-351. doi:10.21103/Article14(2)_CR4

Introduction

The Mayer-Rokitansky-Kuster-Hauser (MRKH) syndrome is a rare disorder characterized by congenital aplasia of the upper 2/3 of the vagina together with partial or total aplasia of the uterus in women with normal development of secondary sexual characteristics and a normal 46,XX karyotype. It is a rare congenital disorder with an incidence of 1 in 4,500 women.[1] Various assumptions exist for its etiology, which can be multi-factorial, such as genetic factors or the use of drugs such as diethylstilbestrol and thalidomide,[2] but to this day the etiology remains unknown. Triantafyllidi et al.[3] identified 76 studies describing multiple genetic defects that potentially contribute to the pathogenetic mechanism of MRKH syndrome. The most reported chromosomal regions and the possible genes implicated are: 1q21.1 (RBM8A gene), 1p31-1p35 (WNT4 gene), 7p15.3 (HOXA gene), 16p11 (TBX6 gene), 17q12 (LHX1 and HNF1B genes), 22q11.21, and Xp22. Usually, the first signs with which patients present to the doctor are primary amenorrhea, with well-developed secondary sexual characteristics. The associated abnormalities of this syndrome can include urological abnormalities (25%-50%), including renal agenesis, pelvic kidney or horseshoe kidney, other abnormalities of the collecting system as well as skeletal abnormalities (10-15%), including the spine, ribs, and extremities.[4]

MRI imaging of the uterus, cervix, and vagina offers in-depth insights into the anatomy of the uterovaginal region, with a specific focus on examining the external contours of the uterine fundus and the shape of the cavity, and it also allows tissue characterization of the possible septa, thus providing a complete classification of the specific anomaly.[5,6] At present, MRI boasts the utmost accuracy in diagnosing uterine anomalies, achieving a nearly perfect rate of nearly 100%, attributed to its outstanding resolution for soft tissue and its ability to visualize structures from multiple perspectives.[7,8] T1-weighted (T1W) and T2-weighted (T2W) MRI provide excellent zonal anatomy of the uterus, i.e., endometrium, junctional zone, and myometrial anatomy.[9,10]

***Corresponding author:** Prof. Ass. Dr. Jeton Shatri, University of Prishtina, University Clinical Centre of Kosovo, Prishtina, Kosovo. E-mail: jeton.shatri@uni-pr.edu*

Case Presentation

A 15-year-old female patient presented to the Radiology Clinic for an MRI of the abdomen and pelvis, ordered by her gynecologist, to whom she presented with primary amenorrhea and abdominal pain. Medical history showed only childhood diseases. Her mother was not a smoker, she rarely consumed alcohol, but she denies consuming alcohol during pregnancy. The woman also denied illness and exposure to medications during pregnancy. The patient's mother had menarche at the age of 12. Regarding the secondary sexual characteristics, the patient was normal for her chronological age. The hematological and biochemical laboratory examinations were all within the normal range (Table 1).

Table 1.

The hematological and biochemical tests.

Test name	Result	Range	Unit
Leukocytes	8.9	3.50-9.50	$\times 10^9$/L
Erythrocytes	4.8	3.80-5.80	$\times 10^{12}$/L
Platelets	250	125-350	$\times 10^9$/L
Hemoglobin	125	115-175	g/L
Hematocrit	38.2	35.0-50.0	%
Glucose	4.8	4.40-6.00	mmol/L
Urea	5.2	1.70-8.30	mmol/L
Creatinine	72	53-115	mmol/L
Ionized calcium	1.15	1.12-1.32	mmol/L
Potassium	140	132-146	mmol/L
Kalium	4.3	3.4-5.5	mmol/L
Progesterone	2.85	0.87-3.37	ng/mL
Testosterone	12.8	6.00-52.00	ng/dL
FSH	6.23	0.3-10	IU/L
LH	3.22	0.60-16.3	IU/L
Prolactin	15.20	4.04-23.30	ng/mL

The patient's weight and height at the time of the examination were 57kg and 155cm, respectively. A gynecological examination showed pubic hair, labia majora, labia minora, vagina opening, all these well-developed. The vagina was visible only at the entry, so only 1cm long with a blind end. Pelvic examination with MR examination technique included T2W pre-contrast images in axial/sagittal/coronal planes and axial T1FS images. DWI images for diffusion-weighted imaging were also obtained. Post-contrast images were obtained with fat suppression T1W axial, sagittal, and coronal planes (Figure 1). During the processing of the images acquired in a T2W sagittal plane, it was observed that there is a complete absence of the uterus and the upper 2/3 of the vagina (Figure 2). The small amount of free fluid in the pelvis can also be seen in these images. The images obtained in a T2W coronal plane clearly show that there is a lack of 2/3 of the upper part of the vagina; while in this view the vaginal remnant (distal part) can be evaluated, it was measured and found to be 1cm long. A T1W MRI scan in the axial plane showed normal, well-formed ovaries.

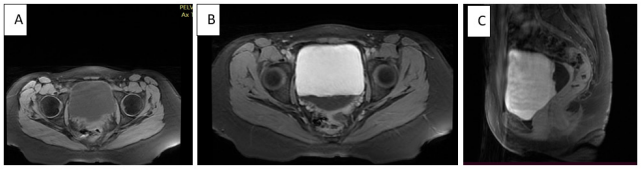

Fig. 1. *Magnetic resonance of pelvis. A) axial T1 (FS)-weighted images, B) axial and C) sagittal contrast-enhanced T1 (FS) - weighted images contrast-enhanced T1-weighted images.*

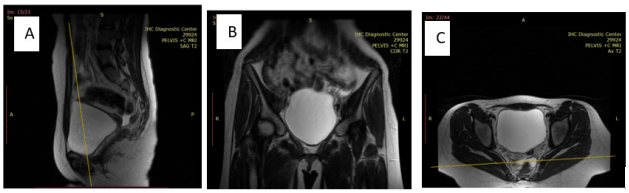

Fig. 2. *Magnetic resonance of pelvic. A) sagittal, B) coronal, and C) axial T2-weighted images show the absence of the uterus and vagina. Also, the presence of free fluid in the pelvis.*

Discussion

The MRKH syndrome manifests in two distinct forms. The typical form (Type 1) is defined by the congenital absence of the uterus and upper vagina, while the ovaries and fallopian tubes appear normal. The atypical form (Type 2) encompasses Müllerian anomalies in addition to non-gynecological anomalies affecting the urological, skeletal, vertebral, or cardiac systems.[11] In our case, it is presented as MRKH type 1. This syndrome was first described by Mayer in 1829, and later, in 1838, the description was completed by Rokitansky, who noted uterine and vaginal agenesis. Later, Kuster added renal abnormalities (renal agenesis, renal ectopy) and skeletal abnormalities. And finally, in 1961, Hauser separated MRKH from testicular feminization. Most cases appear to be sporadic.[11] A retrospective cohort study conducted from 1997 to 2011 at the University of Michigan in 2013 consisting of 48 MRKH patients found that 48% had a primordial uterus.[12] In a review in 2020,[13] it was estimated that 48%–84% of MRKH patients had a primordial uterus.

As for the clinical presentation, it was characterized by the normal development of secondary sexual characteristics and primary amenorrhea. The development of the ovaries and their function was normal. The levels of follicle-stimulating hormone (FSH) and luteinizing hormone (LH) were within normal ranges, and there were no indications of androgen excess, which helps differentiate it from androgen insensitivity syndrome.[14]

The diagnosis is usually made through clinical symptoms and clinical examination, also with imaging or laparoscopic confirmation, as a condition of the normal hormonal values and normal karyotype. It usually starts with

simple imaging procedures, such as 2D or 3D ultrasound, which are non-invasive methods and easy for the patient. As far as can be seen in ultrasound, it can be concluded from our study that there was a lack of development of the uterus. Usually, during the ultrasound examination, abnormalities such as renal ectopia, renal agenesis, or any other abnormality that is assumed to be related to MRKH syndrome are also looked for. Then, usually, patients are advised to undergo more detailed imaging procedures, such as CT or MRI. An MRI stands out for its superior efficacy, thanks to its multiplanar capacity and unparalleled soft tissue contrast. It surpasses all other imaging methods while avoiding the need for ionizing radiation.[15] By means of magnetic resonance, the abnormality of the relevant organs is assessed, through a higher sensitivity and specificity than other imaging methods. It provides accurate details regarding the anatomical positioning and any abnormalities within the uterus, potential tubal remnants, vestigial lamina, and ovaries.[16]

Usually, patients, after receiving the news that they have been diagnosed with MRKH, suffer from mental stress knowing that they do not have a uterus and vagina. This is exactly what the beginning of the treatment is, that is, the consultation with the patient before starting the treatment steps. The next steps include the creation of neovagina, which can be done after non-surgical treatment and surgical treatment. The non-surgical treatment includes the Frank's Method, which involves wearing vaginal dilators for at least 2 hours a day, which affects the increase in the width and length of the vagina. While the surgical treatment, of which there are different methods, consists in creating a channel that plays the role of the vagina. In a study by Motta and D'Alberton,[17] of 108 patients with MRKH syndrome from 1955 to 2003, 53 chose the option of creating neovagina with dilation (functional method), while 55 chose the surgical option. Of the patients who chose the non-surgical method, 83% expressed that they were satisfied with their treatment: 75% of the patients had an optimal result, 13% had an acceptable result, and 12% had a poor result. As for the group that chose the surgical option, 76% were satisfied with these methods, while 68% of the anatomical creation of the vagina were successful.[18,19]

Conclusion

The first point when there is suspicion of MRKH is the clinical presentation and gynecological examination. Imaging examinations, starting with ultrasound, are needed to verify the diagnosis. For a more detailed evaluation, an MRI is needed, which, in addition to showing genital abnormalities, can give us more information about whether it is Type 1 MRKH or Type 2 MRKH by showing other organs as well.

Competing Interests

The authors declare that they have no competing interests.

References

1. Hall-Craggs MA, Williams CE, Pattison SH, Kirkham AP, Creighton SM. Mayer-Rokitansky-Kuster-Hauser syndrome: diagnosis with MR imaging. Radiology. 2013 Dec;269(3):787-92. doi: 10.1148/radiol.13130211. Epub 2013 Oct 28. PMID: 23942608.
2. Bjørsum-Meyer T, Herlin M, Qvist N, Petersen MB. Vertebral defect, anal atresia, cardiac defect, tracheoesophageal fistula/esophageal atresia, renal defect, and limb defect association with Mayer-Rokitansky-Küster-Hauser syndrome in co-occurrence: two case reports and a review of the literature. J Med Case Rep. 2016 Dec 21;10(1):374. doi: 10.1186/s13256-016-1127-9. PMID: 28003020; PMCID: PMC5178070.
3. Triantafyllidi VE, Mavrogianni D, Kalampalikis A, Litos M, Roidi S, Michala L. Identification of Genetic Causes in Mayer-Rokitansky-Küster-Hauser (MRKH) Syndrome: A Systematic Review of the Literature. Children (Basel). 2022 Jun 27;9(7):961. doi: 10.3390/children9070961. PMID: 35883945; PMCID: PMC9322756.
4. Morcel K, Camborieux L; Programme de Recherches sur les Aplasies Müllériennes; Guerrier D. Mayer-Rokitansky-Küster-Hauser (MRKH) syndrome. Orphanet J Rare Dis. 2007 Mar 14;2:13. doi: 10.1186/1750-1172-2-13. PMID: 17359527; PMCID: PMC1832178.
5. Fukunaga T, Fujii S, Inoue C, Mukuda N, Murakami A, Tanabe Y, Harada T, Ogawa T. The spectrum of imaging appearances of müllerian duct anomalies: focus on MR imaging. Jpn J Radiol. 2017 Dec;35(12):697-706. doi: 10.1007/s11604-017-0681-4. Epub 2017 Sep 18. PMID: 28921452.
6. Troiano RN, McCarthy SM. Mullerian duct anomalies: imaging and clinical issues. Radiology. 2004 Oct;233(1):19-34. doi: 10.1148/radiol.2331020777. Epub 2004 Aug 18. PMID: 15317956.
7. Pan HX, Liu P, Duan H, Li PF, Chen RL, Tang L, Luo GN, Chen CL. Using 3D MRI can potentially enhance the ability of trained surgeons to more precisely diagnose Mullerian duct anomalies compared to MR alone. Eur J Obstet Gynecol Reprod Biol. 2018 Sep;228:313-318. doi: 10.1016/j.ejogrb.2018.07.007. Epub 2018 Jul 9. PMID: 30075412.
8. Console D, Tamburrini S, Barresi D, Notarangelo L, Bertucci B, Tamburrini O. Il valore della RM nella valutazione delle anomalie dei dotti di Müller [The value of the MR imaging in the evaluation of Müllerian duct anomalies]. Radiol Med. 2001 Oct;102(4):226-32. Italian. PMID: 11740449.
9. Boruah DK, Sanyal S, Gogoi BB, Mahanta K, Prakash A, Augustine A, Achar S, Baishya H. Spectrum of MRI Appearance of Mayer-Rokitansky-Kuster-Hauser (MRKH) Syndrome in Primary Amenorrhea Patients. J Clin Diagn Res. 2017 Jul;11(7):TC30-TC35. doi: 10.7860/JCDR/2017/29016.10317. Epub 2017 Jul 1. PMID: 28893003; PMCID: PMC5583891.
10. Shivalingappa SS, Shetty SB. Mayer-Rokitansky-Küster-Hauser (MRKH) syndrome with unilateral pulmonary agenesis-a rarity indeed: radiologic review. BJR Case Rep. 2016 Feb 3;2(2):20150157. doi: 10.1259/bjrcr.20150157. PMID: 30363603; PMCID: PMC6180887.

11. Carson SA, Simpson JL, Malinak LR, Elias S, Gerbie AB, Buttram VC Jr, Sarto GE. Heritable aspects of uterine anomalies. II. Genetic analysis of Müllerian aplasia. Fertil Steril. 1983 Jul;40(1):86-90. PMID: 6862043.
12. Marsh CA, Will MA, Smorgick N, Quint EH, Hussain H, Smith YR. Uterine remnants and pelvic pain in females with Mayer-Rokitansky-Küster-Hauser syndrome. J Pediatr Adolesc Gynecol. 2013 Jun;26(3):199-202. doi: 10.1016/j.jpag.2012.11.014. PMID: 23785713.
13. Committee on Adolescent Health Care. ACOG Committee Opinion No. 728: Müllerian Agenesis: Diagnosis, Management, And Treatment. Obstet Gynecol. 2018 Jan;131(1):e35-e42. doi: 10.1097/AOG.0000000000002458. PMID: 29266078.
14. Creighton S. Common congenital anomalies of the female genital tract. Rev Gynecol Pract. 2005;5:221–26
15. Siegel M. Pediatric applications. In: Computed body tomography with MRI correlation on CD-ROOM. Philadelphia: Lippincott-Raven; 1998.
16. Morcel K, Camborieux L; Programme de Recherches sur les Aplasies Müllériennes; Guerrier D. Mayer-Rokitansky-Küster-Hauser (MRKH) syndrome. Orphanet J Rare Dis. 2007 Mar 14;2:13. doi: 10.1186/1750-1172-2-13. PMID: 17359527; PMCID: PMC1832178.
17. D' Alberton A, Reschini E, Motta T. La sindrome di Rokitansky. Aggiornamento Del Medico. 1987;11.
18. Bianchi S, Von Wunster S, Marchini M, D' Alberton A, Motta T. Long-Term Satisfaction following Formation of a Neovagina By Regular Sexual Intercourses. Seattle, Wash, USA: The American Society For Reproductive Medicine; 1995
19. Motta T, Von Wunster S, De Giorgi O, D'Alberton A. The "functional method" as initial approach to the formation of a neovagina. In: Monduzzi, editor. Proceedings of the 6th European Congress on Pediatric and Adolescent Gynecology. Budapest, Hungary; 1993.

International Journal of Biomedicine 14(2) (2024) 352-356
http://dx.doi.org/10.21103/Article14(2)_CR5

CASE REPORT

INTERNATIONAL JOURNAL OF BIOMEDICINE

Unveiling a Novel *THOC2* Mutation's Role in X-linked Intellectual Disability

Mehdi Hashemipour[1*], Ayad Neissi[2], Mostafa Neissi[3,4,5*], Misagh Mohammadi-Asl[5], Motahareh Sheikh-Hosseini[5,6], Sasan Bavi[7], Mojdeh Roghani[5], Javad Mohammadi-Asl[5,8]

[1]*Department of Clinical Psychology, Andimeshk Branch, Islamic Azad University, Andimeshk, Iran*
[2]*Department of Arabic Language and Literature, Farhangian University, Tehran, Iran*
[3]*Department of Genetics, Khuzestan Science and Research Branch, Islamic Azad University, Ahvaz, Iran*
[4]*Department of Genetics, Ahvaz Branch, Islamic Azad University, Ahvaz, Iran*
[5]*Noor-Gene Genetic Laboratory, Ahvaz, Iran*
[6]*Pediatric Cell & Gene Therapy Research Center, Tehran University of Medical Sciences, Tehran, Iran*
[7]*Department of Psychology, Ahvaz Branch, Islamic Azad University, Ahvaz, Iran*
[8]*Department of Medical Genetics, School of Medicine, Ahvaz Jundishapur University of Medical Sciences, Ahvaz, Iran*

Abstract

Background: Intellectual disabilities encompass a spectrum of neurodevelopmental disorders profoundly impacting an individual's cognitive abilities, adaptive behaviors, and communication skills. This article delves into the complex challenges encountered by an individual with intellectual disability, particularly examining the interplay between cognitive limitations and speech difficulties, while presenting a case report detailing the experience of a son within a non-consanguineous family diagnosed with intellectual disability due to a new genetic defect in *THOC2*, thereby contributing significantly to our comprehension of *THOC2*-related pathogenic variants.

Case presentation: A 14-year-old boy from a non-consanguineous Iranian family presented with significant challenges in academics, communication, and adaptive skills, accompanied by speech problems and exhibiting distinctive physical characteristics. The exome-sequencing analysis revealed a novel hemizygous c.1559+5A>T mutation located in intron 14 (NM_001081550.2) within the *THOC2* gene in the proband. Sanger sequencing further confirmed the mother as a carrier of the mutation, although she remains in good health, while the father exhibits a normal genotype. This delineates an X-linked inheritance pattern, shedding light on the familial transmission of the identified genetic anomaly.

Conclusion: The precise identification of the c.1559+5A>T splicing mutation in the *THOC2* gene, achieved through exome-sequencing, conclusively diagnoses X-linked intellectual disability in our patient. This breakthrough not only unravels the molecular intricacies contributing to intellectual disability but also underscores the urgency for accurate and swift disease diagnosis. **(International Journal of Biomedicine. 2024;14(2):352-356.)**

Keywords: intellectual disability • *THOC2* gene • mutation • exome-sequencing

For citation: Hashemipour M, Neissi A, Neissi M, Mohammadi-Asl M, Sheikh-Hosseini M, Bavi S, Roghani M, Mohammadi-Asl J. Unveiling a Novel *THOC2* Mutation's Role in X-linked Intellectual Disability. International Journal of Biomedicine. 2024;14(2):352-356. doi:10.21103/Article14(2)_CR5

Published without substantive editing per OFAC Guidance.

Introduction

Intellectual disabilities (IDs) represent a multifaceted spectrum of neurodevelopmental disorders that significantly impact an individual's cognitive abilities, adaptive behaviors, communication skills, and daily living tasks.[1, 2] This diverse range of challenges emerges early in life, posing obstacles to various facets of a person's development. The term "IDs"

encompasses a variety of conditions, each contributing to unique struggles for those affected.

Within this intricate landscape, individuals with ID confront limitations in intellectual functioning, hindering their capacity to acquire and apply knowledge effectively.[1] These challenges extend beyond the cognitive realm, affecting adaptive behaviors that are crucial for navigating daily life and engaging in social interactions.[2] The profound impact of ID is not limited to isolated aspects but ripples through various dimensions of an individual's existence.

Moreover, a subset of individuals grappling with ID also contends with concurrent speech problems, adding an extra layer of complexity to their communication abilities.[1] This intersection of challenges can further impede their ability to articulate thoughts effectively, exacerbating the hurdles they face in interpersonal relationships, education, and societal integration.

Understanding ID necessitates delving into the intricate interplay of genetic, environmental, and neurological factors influencing development.[1] Recent research has spotlighted specific genetic mutations linked to ID, including mutations in the *THOC2* gene, identified as monogenic causes for neurodevelopmental disorders such as X-linked intellectual disability (OMIM: #300957).[3,4] The *THOC2* gene encodes a 183 kDa nuclear protein, an integral component of the highly conserved multimeric protein complex known as the TREX complex. This complex facilitates transcription elongation, mRNA export, and other critical processes.[4-6] Within the THO complex, comprising *THOC1*, *THOC2*, *THOC5*, *THOC6*, and *THOC7*, mutations in both *THOC2* and *THOC6* have been reported in patients with IDs, providing additional insights into the genetic underpinnings of neurodevelopmental disorders.[7, 8]

Exome-sequencing emerges as a vital tool for uncovering the roots of diseases, particularly those originating from rare gene mutations. This technique delves into the protein-coding regions of the genome, pinpointing mutations within genes that underlie the development of various disorders. By honing in on these functional segments, exome-sequencing significantly streamlines the process of identifying pathogenic variations, proving essential in deciphering the molecular basis of diseases. The method's focus on detecting rare gene mutations is instrumental in unveiling the genetic origins of diverse conditions, enabling more precise diagnostics and fostering the development of targeted treatments for improved patient outcomes.[9-12] Based on this evidence, we employed the exome-sequencing technique to discern the causative genetic defect in a non-consanguineous Iranian family affected by ID. The investigation involved an in-depth examination of the patient's genetic makeup through exome-sequencing, coupled with a meticulous segregation analysis. The compelling results obtained from this genetic scrutiny consistently point toward the likelihood that a novel mutation in the *THOC2* gene may serve as a potential candidate implicated in the causation of the observed ID in the patient.

Case Presentation

The patient, a 14-year-old boy from an Iranian family with a non-consanguineous parental relationship (Figure 1A), presented significant challenges in academics, communication, and adaptive skills. The parents reported a speech problem in the patient, further complicating effective communication. Challenges in school, including difficulties in grasping academic concepts and persistent speech issues, were noted by teachers, leading to a comprehensive evaluation and referral to a psychologist.

Upon assessment, a detailed examination revealed a moderate ID, affecting both intellectual functioning and adaptive behavior. To delve into the underlying causes of the observed impairments, standardized tests such as the Wechsler Intelligence Scale for Children (WISC) were administered. The results confirmed the presence of a moderate ID and identified a speech problem.

The general physical examination exposed additional features in the patient. Truncal obesity was observed, accompanied by dysmorphisms, including a broad and high forehead, a visibly large head with large ears, bushy eyebrows, synophrys, squint, and flat feet. The patient exhibited a reluctance to respond to commands, social anxiety with avoidance of eye contact, and his mother mentioned a hearing impairment. Further examination revealed a small penis and large testes. Notably, other systemic examinations showed no abnormalities (Table 1).

Table 1.

Physical examination findings.

Personal Particulars	
Sex	Male
Age	14
Perinatal Features	
Prematurity	-
Delivery	Term vaginal assisted
Low birth weight	-
Neurologic Features	
Intellectual disability	Moderate
Speech delay	+
Response to command	Slow
Power	4/5
Deep reflexes	N
Hyperkinesia	-
Tremor	-
Epilepsy	-
Gait disturbances	-
Behavior problems	+
Anxiety problems	-
Depression	-
Brain MRI and/or CT	ND
Growth Parameters	
Head circumference	56/5 cm
Macrocephaly	+
Short stature	-
Chest circumference	89 cm
Overweight	+
Truncal obesity	+
Dysmorphisms	
Broad high forehead	+
High palate	-
Large ears	+
Small penis	+
Macroorchidism	+
Other	
Flat feet	+
Medical conditions	-

N: normal, ND: no data

In light of the patient's maternal relatives, particularly the mother's male siblings (Figure 1A), displaying ID and speech issues, genetic testing was undertaken to elucidate potential hereditary factors influencing the condition. To pinpoint rare alleles associated with ID, we employed exome-sequencing for the patient under study. Macrogen Company conducted the library preparation using the SureSelect Human All Exon V6, followed by sequencing on the Illumina HiSeq 2000 genome analyzer platform.

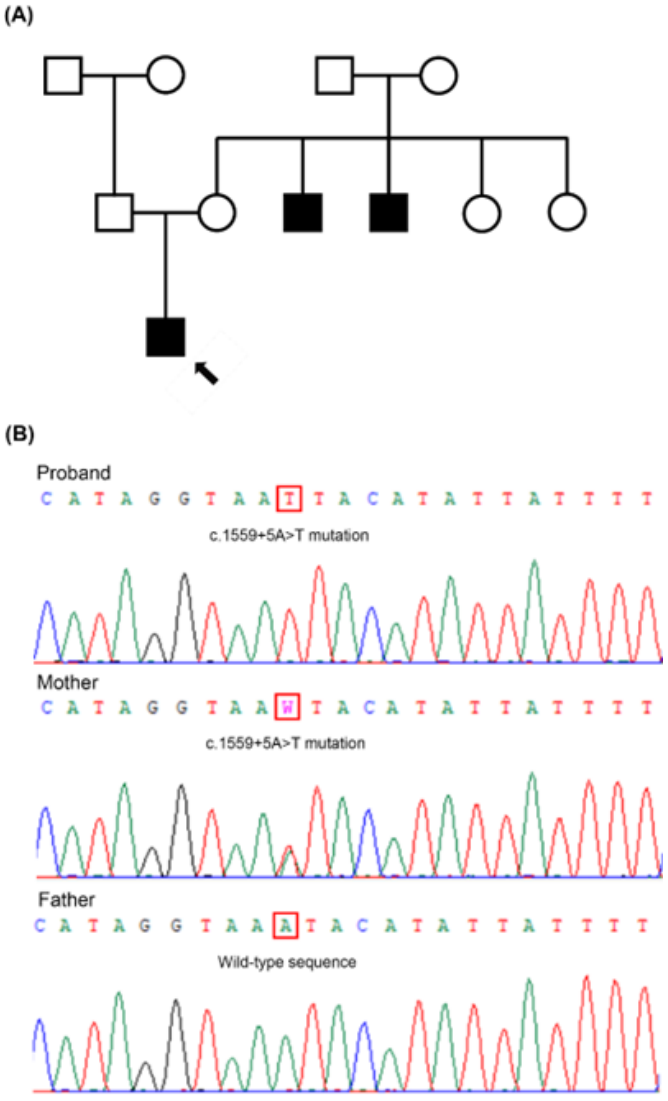

Figure 1. *(A) The pedigree of the studied family. Male individuals are represented by squares, while females are depicted by circles. Affected members are enclosed within symbols, with the proband highlighted by an arrow. (B) The sequence chromatograms depict a novel hemizygous mutation (c.1559+5A>T) in THOC2 within the proband, with his mother displaying a heterozygous state for the mutation. Conversely, the father's sequence analysis shows a normal genotype.*

The family history proved intricate, revealing a novel hemizygous c.1559+5A>T mutation in the *THOC2* gene (NM_001081550.2 - intron 14), in the 14-year-old male patient. The utilization of exome-sequencing brought forth a potential candidate variant within the gene, prompting an additional layer of confirmation through direct Sanger sequencing. This meticulous validation process, performed with an ABI3500 sequencer, conclusively confirmed the identification of the c.1559+5A>T mutation inherited from the heterozygous mother, but the father exhibited a normal genotype (Figure 1B). Notably, due to the involvement of the mother and her male siblings, the inheritance pattern was confirmed as X-linked. Interestingly, despite carrying the mutation, the mother remained unaffected.

The specific mutation (c.1559+5A>T) occurs at the splice donor site in the 14th intron of the *THOC2* gene, confirming its association with X-linked ID. This mutation has the potential to affect mRNA splicing during transcription. The alteration of the splice donor site could interfere with the recognition and cleavage of the intron during splicing, leading to the production of aberrant mRNA transcripts.

Discussion

We describe here the genetic and clinical findings of a patient with X-linked ID. The patient, hailing from an Iranian family with a non-consanguineous parental relationship, underscores the significance of both cultural and genetic backgrounds in shaping the clinical presentation. Notably, the absence of consanguinity within the family dispels any immediate attribution of the observed condition to familial relatedness. This case involves a 14-year-old boy, whose struggles extend across various facets of life, particularly in academics, communication, and adaptive skills. The patient exhibited moderate ID, truncal obesity, macrocephaly, a small penis, and distinctive dysmorphic features, including bushy eyebrows, synophrys, a broad and high forehead, large ears, flat feet, hearing impairment, and strabismus. Our patient displayed a complex array of symptoms resembling those reported in cases with *THOC2* mutations, such as ID, truncal obesity, genital abnormalities, hearing anomalies, ocular irregularities, and dysmorphic features.[13] Remarkably, approximately 82% of the previously reported patients experienced speech delay. However, our case presents the patient demonstrating problems in speech and frequently punctuated by a cheerful disposition. Nonetheless, during the clinical evaluation process, articulating coherent thoughts posed a significant challenge. Interestingly, the patient's mother attests to his proficiency in communication within the familial setting, indicating that the observed delay may be attributed to pragmatic language difficulties. Contrary to historical data, where 52% of patients exhibited short stature, our patient achieved normal growth milestones. While 34% of previous cases were microcephalic, our patient exhibited macrocephaly. Intriguingly, prior cases documented cryptorchidism and microorchidism, whereas our patient presented with macroorchidism. Our patient shared ocular and hearing impairments observed in prior cases. Moreover, genetic testing revealed a novel hemizygous mutation in the *THOC2* gene, specifically c.1559+5A>T, adding a crucial dimension to understanding the condition. However, additional reported features like hypotonia, gait disturbances, behavioral problems, epilepsy, and congenital anomalies in cardiorespiratory, skeletal, and gastroesophageal systems were conspicuously absent in our patient. The intricate

interplay between genetic and environmental factors becomes apparent in the challenges faced by the patient, prompting a thorough investigation into the underlying causes of the observed intellectual and speech impairments.

The Human Gene Mutation Database (HGMD, http://www.hgmd.cf.ac.uk/ac/index.php) has identified *THOC2* as a gene associated with IDs. Our study endeavors have extended this repertoire by uncovering an additional splicing mutation, namely c.1559+5A>T, within the *THOC2* gene. This novel mutation represents a noteworthy addition to the existing knowledge base.

This newfound splicing mutation holds significance in our understanding of *THOC2*-related pathogenic variants. We propose that the c.1559+5A>T mutation gives rise to an aberrant protein, potentially compromising its functionality or stability. The implications of this mutation are particularly pertinent to IDs, suggesting a possible link between THOC2 dysfunction and cognitive impairment.

Recent investigations have shed light on the role of *THOC2* gene mutations in IDs, providing a context for our novel findings. The *THOC2* gene encodes a subunit of the THO complex, crucial for mRNA processing and transport. In studies by Kumar et al.,[4,14] mutations within the *THOC2* gene were identified in individuals with IDs, reinforcing the gene's significance in cognitive function. Building upon this foundation, our investigation unveiled a distinct hemizygous mutation (c.1559+5A>T) in the 14th intron of the *THOC2* gene in a 14-year-old male patient. This mutation is anticipated to impact mRNA processing, potentially leading to abnormal protein expression. Consequently, the perturbation in protein production could disrupt essential cellular functions, contributing to IDs. Our findings align with Kumar R et al.'s studies, supporting the notion that variations in the *THOC2* gene contribute to IDs, thereby solidifying the understanding of the gene's implication in cognitive impairment.

Additionally, in a recent study conducted by Kumar et al.,[15] a comprehensive examination of *THOC2* revealed a total of 19 missense variants, one deletion, and two splice-altering mutations across three cohorts. This research significantly contributed to our understanding of the genetic landscape associated with neurodevelopmental disorders. In alignment with these findings, our case report identified a novel splicing mutation, c.1559+5A>T, in *THOC2*, which resulted in ID. This discovery not only underscores the diversity of mutations within the *THOC2* gene but also emphasizes its role in IDs. The inclusion of this unique splicing mutation in our case report adds a valuable piece to the puzzle of *THOC2*-related pathogenic variants, further highlighting the necessity for ongoing research in this domain.

The impact of the c.1559+5A>T mutation on ID underscores the critical need for advanced diagnostic approaches. Our study highlights the significance of utilizing exome-sequencing in parents, both prior to or after marriage, during pregnancy, and post-birth, as a pivotal tool for identifying potential or novel mutations associated with ID. This is particularly crucial for individuals with a familial history of mental retardation, offering a proactive means of diagnosis and intervention. By embracing such advanced techniques, we pave the way for early detection, comprehensive understanding, and targeted management of IDs, thereby contributing to improved outcomes for affected individuals and their families.

Conclusion

The conclusive diagnosis of intellectual disability in our patient, achieved through the precise identification of splicing c.1559+5A>T mutation mutations in the *THOC2* gene using exome-sequencing, represents a pivotal advancement in our understanding of the disorder's etiology. This study not only unravels the molecular intricacies contributing to intellectual disability but also emphasizes the urgent need for accurate and swift disease diagnosis. The implications of this research extend beyond the laboratory, offering a foundation for improved genetic counseling for affected families.

Competing Interests

The authors declare that they have no competing interests.

Ethical Considerations

All procedures performed in this study were in accordance with the ethical standards of the institutional research committee and with the 1964 Helsinki Declaration and its later amendments. Written informed consent was obtained from the family members for this publication.

Acknowledgments

We extend our heartfelt thanks to the family members for their invaluable cooperation.

References

1. Diagnostic and Statistical Manual of Mental Disorders, 5th Edition. (2013). American Psychiatric Publishing, Inc. https://doi.org/10.1176/appi.books.9780890425596
2. Felce D, Perry J. Quality of life: its definition and measurement. Res Dev Disabil. 1995 Jan-Feb;16(1):51-74. doi: 10.1016/0891-4222(94)00028-8. PMID: 7701092.
3. Deciphering Developmental Disorders Study. Prevalence and architecture of de novo mutations in developmental disorders. Nature. 2017 Feb 23;542(7642):433-438. doi: 10.1038/nature21062. Epub 2017 Jan 25. PMID: 28135719; PMCID: PMC6016744.

***Corresponding authors**

***Mostafa Neissi**: E-mail address: iammostafaneissi@gmail.com*
Department of Genetics, Khuzestan Science and Research Branch, Islamic Azad University, Ahvaz, Iran.

***Mehdi Hashemipour*: E-mail: Hasemimehdi@gmail.com**
Department of Clinical Psychology, Andimeshk Branch, Islamic Azad University, Andimeshk, Iran.

4. Kumar R, Corbett MA, van Bon BW, Woenig JA, Weir L, Douglas E et al. THOC2 Mutations Implicate mRNA-Export Pathway in X-Linked Intellectual Disability. Am J Hum Genet. 2015 Aug 6;97(2):302-10. doi: 10.1016/j.ajhg.2015.05.021. Epub 2015 Jul 9. PMID: 26166480; PMCID: PMC4573269.
5. Strässer K, Masuda S, Mason P, Pfannstiel J, Oppizzi M, Rodriguez-Navarro S et al. TREX is a conserved complex coupling transcription with messenger RNA export. Nature. 2002 May 16;417(6886):304-8. doi: 10.1038/nature746. Epub 2002 Apr 28. PMID: 11979277.
6. Yamazaki T, Fujiwara N, Yukinaga H, Ebisuya M, Shiki T, Kurihara T et al. The closely related RNA helicases, UAP56 and URH49, preferentially form distinct mRNA export machineries and coordinately regulate mitotic progression. Mol Biol Cell. 2010 Aug 15;21(16):2953-65. doi: 10.1091/mbc.E09-10-0913. Epub 2010 Jun 23. PMID: 20573985; PMCID: PMC2921121.
7. Accogli A, Scala M, Calcagno A, Castello R, Torella A, Musacchia F et al. Novel CNS malformations and skeletal anomalies in a patient with Beaulieu-boycott-Innes syndrome. Am J Med Genet A. 2018 Dec;176(12):2835-2840. doi: 10.1002/ajmg.a.40534. Epub 2018 Sep 20. PMID: 30238602.
8. Mattioli F, Isidor B, Abdul-Rahman O, Gunter A, Huang L, Kumar R et al. Clinical and functional characterization of recurrent missense variants implicated in THOC6-related intellectual disability. Hum Mol Genet. 2019 Mar 15;28(6):952-960. doi: 10.1093/hmg/ddy391. PMID: 30476144.
9. Neissi M, Mohammadi-Asl M, Roghani M, Al-Badran AI, Mohammadi-Asl J. Mutation Detection in MYO15A Gene in an Iranian Family with Non-Syndromic Hearing Loss. International Journal of Biomedicine. 2024;14(1):165-169. doi:10.21103/Article14(1)_CR3.
10. Hashemipour M, Sheikh-Hosseini M, Mabudi H. Association of Autism Spectrum Disorder in an Iranian Pedigree with a Novel Hereditary Mutation in SETD5. International Journal of Biomedicine. 2024;14(1):170-174. doi:10.21103/ Article14(1)_CR4.
11. Neissi M, Mabudi H, Mohammadi-Asl J. AHI1 gene mutation in a consanguineous Iranian family affected by Joubert syndrome: A case report. Clin Case Rep. 2021 Oct 23;9(10):e05002. doi: 10.1002/ccr3.5002. PMID: 34721863; PMCID: PMC8538011.
12. Neissi M, Al-Badran AI, Mohammadi-Asl J. A Novel Deleterious MYO15A Gene Mutation Causes Nonsyndromic Hearing Loss. Iran J Otorhinolaryngol. 2024 Jan;36(1):355-360. doi: 10.22038/IJORL.2023.69889.3372. PMID: 38259694; PMCID: PMC10800138.
13. Muthusamy B, Garapati K, Girimaji SC. Exome sequencing identifies a novel mutation in THO complex, subunit 2 in non-syndromic X-linked intellectual disability. Research Reports. 2021(5):e1-e10. doi:10.9777/rr.2021.10002.
14. Kumar R, Gardner A, Homan CC, Douglas E, Mefford H, Wieczorek D et al. Severe neurocognitive and growth disorders due to variation in THOC2, an essential component of nuclear mRNA export machinery. Hum Mutat. 2018 Aug;39(8):1126-1138. doi: 10.1002/humu.23557. Epub 2018 Jun 14. PMID: 29851191; PMCID: PMC6481655.
15. Kumar R, Palmer E, Gardner AE, Carroll R, Banka S, Abdelhadi O et al. Expanding Clinical Presentations Due to Variations in THOC2 mRNA Nuclear Export Factor. Front Mol Neurosci. 2020 Feb 11;13:12. doi: 10.3389/fnmol.2020.00012. PMID: 32116545; PMCID: PMC7026477.

International Journal of Biomedicine 14(2) (2024) 357-358
http://dx.doi.org/10.21103/Article14(2)_CR6

CASE REPORT

INTERNATIONAL JOURNAL OF BIOMEDICINE

Superficial Thrombophlebitis of Great Saphenous Vein Following Vaccine

Jose Maria Pereira de Godoy[1*], Ana Carolina Pereira de Godoy[2], Livia Maria Pereira de Godoy[3], Maria de Fatima Guerreiro Godoy[4]

[1]*Cardiology and Cardiovascular Surgery Department of the Medicine School in São José do Rio Preto (FAMERP), Clinica Godoy, CNPq (National Council for Research and Development), Sao Jose do Rio Preto, Brazil*
[2]*Intensive Care Hospital da Criança e Maternidade-HCM-Hospital de Base-Medicine School of Sao Jose do Rio Preto (FAMERP), Clinica Godoy, Sao Jose do Rio Preto, Brazil*
[3]*Instituto Lauro de Souza Lima-Bauru-Brazil, Clinica Godoy, Sao Jose do Rio Preto, Brazil*
[4]*Post-Graduate Stricto Sensu in Medicine School in São José do Rio Preto (FAMERP), Clinica Godoy, Sao Jose do Rio Preto, Brazil*

Abstract

This paper reports on the occurrence of thrombose of the left great saphenous vein (GSV) soon after being given the AstraZeneca vaccine and two recurrent events within three days after the suspension of the anticoagulant. A 53-year-old patient had superficial thrombophlebitis of the GSV in the left leg three days after taking the second dose of the AstraZeneca vaccine for COVID-19 and initiated treatment with rivaroxaban (Xarelto™) 15 mg twice a day, subsequently increasing to 20 mg. After 45 days, the patient contracted dengue and stopped taking the anticoagulant. Two days later, the patient had another thrombosis in the left GSV. The patient is currently in outpatient care with a prophylactic dose of 10mg/day of anticoagulant and undergoes evaluations at three-month intervals. The result of our study is a rare event. **(International Journal of Biomedicine. 2024;14(2):357-358.)**

Keywords: superficial thrombophlebitis • great saphenous vein • vaccine

For citation: Pereira de Godoy JM, Pereira de Godoy AC, Pereira de Godoy LM, Guerreiro Godoy MF. Superficial Thrombophlebitis of Great Saphenous Vein Following Vaccine. International Journal of Biomedicine. 2024;14(2):357-358. doi:10.21103/Article14(2)_CR6

Introduction

The vaccine, developed by Johnson and Johnson for SARS-CoV-2, has been related to more specific cases of thrombosis associated with low platelet levels similar to those found in heparin-induced thrombocytopenia.[1] A study by A. Mani and V. Ojha found that venous thrombosis was more frequent than arterial thrombosis and that a large portion of patients had thrombocytopenia (49%) and anti-platelet factor 4 antibodies (78.6%).[2]

Another study reported two cases of superficial venous thrombosis, suggesting that this may be another adverse effect to add to the list of events associated with the ChAdOx1 nCoV-19 vaccine.[3] Another report describes portal vein and right common iliac vein thrombosis in a 36-year-old woman two weeks after receiving the first dose of the AstraZeneca vaccine.[4] The cumulative incidence of any thrombotic event within 30 days after receiving the vaccine was 12 per 10,000 in the COVID-19 group and six per 10,000 in the influenza group (P=0.022).[5] Venous thrombosis has not been associated with COVID-19 vaccines in the literature. Therefore, the occurrence is rare.

This paper reports on the occurrence of thrombose of the left great saphenous vein (GSV) soon after being given the AstraZeneca vaccine and two recurrent events within three days after the suspension of the anticoagulant.

***Corresponding author**: Jose Maria Pereira de Godoy, MD, PhD. Cardiology and Cardiovascular Surgery Department of the Medicine School in São José do Rio Preto (FAMERP), Clinica Godoy, CNPq (National Council for Research and Development), Sao Jose do Rio Preto, Brazil E-mail: godoyjmp@gmail.com*

Case Presentation

A 53-year-old patient had superficial thrombophlebitis of the GSV in the left leg three days after taking the second dose of the AstraZeneca vaccine for COVID-19 and initiated treatment with rivaroxaban (Xarelto™) 15 mg twice a day, subsequently increasing to 20 mg. After 45 days, the patient contracted dengue and stopped taking the anticoagulant. Two days later, the patient had another thrombosis in the left GSV. The laboratory exams revealed normal platelets and coagulation, and the patient began taking the anticoagulant again. After 24 days, the patient stopped taking the anticoagulant because she was going to be submitted to surgery. Three days later, the third thrombotic event occurred in the GSV. Rivaroxaban was initiated again twice a day at a dose of 15 mg, which was subsequently increased to 20 mg. The patient had no family history of thrombotic events. Screening for neoplasm (chest x-ray, endoscopy, and ultrasound of the abdomen) was negative. Screening for antiphospholipid antibodies was negative. The patient is currently in outpatient care with a prophylactic dose of 10 mg/day of anticoagulant and undergoes evaluations at three-month intervals.

Discussion

The present study reports a case of GSV thrombosis three days after receiving the AstraZeneca vaccine, for which anticoagulant therapy was initiated with rivaroxaban. After 45 days, the anticoagulant was suspended because the patient contracted dengue. Two days later, thrombosis recurred in the same vein and the anticoagulant was reinitiated. After 25 days, the medication was suspended, and another episode of thrombosis occurred in the same vein. The literature reports cases of superficial venous thrombosis as a possible consequence of the ChAdOx1 nCoV-19 vaccine,[3] but no cases of recurrent thrombosis. Hence, the result of our study is a rare event. The patient had two episodes of recurrent thrombosis soon after going off the anticoagulant, suggesting the maintenance of a state of hypercoagulability. This raises the issue as to when anticoagulant therapy can be safely suspended. The decision was made to use a prophylactic dose of rivaroxaban to reduce the possibility of bleeding and ensure prophylactic protection. The patient did not have a family history of thrombotic events, did not present thrombocytopenia, and screening was negative for both antiphospholipid antibodies and neoplasm.

The literature reports atypical thrombotic events in patients with COVID-19,[6-8] but no cases of recurrent thrombosis. Venous thrombosis and thromboembolism are reported more often. Recurrent thrombosis almost immediately after suspending anticoagulant therapy is the most striking aspect in the present case.

In conclusion, this paper reports the occurrence of GSV thrombophlebitis, the possible cause of which was the AstraZeneca vaccine, and recurring thrombosis after the suspension of anticoagulant therapy.

Competing Interests

The authors declare that they have no competing interests.

References

1. Bangolo A, Cherian J, Ahmed M, Atoot A, Gupta B, Atoot A. A Case Report of DVT following the Johnson and Johnson Vaccine against the Novel SARS-CoV-2. Case Rep Infect Dis. 2022 May 17;2022:1292754. doi: 10.1155/2022/1292754. PMID: 35620132; PMCID: PMC9130020.
2. Mani A, Ojha V. Thromboembolism after COVID-19 Vaccination: A Systematic Review of Such Events in 286 Patients. Ann Vasc Surg. 2022 Aug;84:12-20.e1. doi: 10.1016/j.avsg.2022.05.001. Epub 2022 May 11. PMID: 35568325; PMCID: PMC9093198.
3. Sah MK, Singh BM, Sinha P, Devkota P, Yadav SK, Shrestha J, Shrestha A. Superficial venous thrombosisas a possible consequence of ChAdOx1 nCoV-19 vaccine: two case reports. J Med Case Rep. 2022 May 7;16(1):182. doi: 10.1186/s13256-022-03407-6. Erratum in: J Med Case Rep. 2022 Jun 27;16(1):266. PMID: 35524323; PMCID: PMC9076162.
4. Abbasi S, Alsermani A, Alsegayyir A, Altahan T, Alsermani M, Almustanyir S. Vaccine-Induced Thrombotic Thrombocytopenia: A Case of Splanchnic Veins Thrombosis. Cureus. 2022 Mar 26;14(3):e23507. doi: 10.7759/cureus.23507. PMID: 35494984; PMCID: PMC9038581.5.
5. Vallone MG, Falcón AL, Castro HM, Ferraris A, Cantarella RF, Staneloni MI, Aliperti VI, Ferloni A, Mezzarobba D, Vázquez FJ, Ratti MFG. Thrombotic events following Covid-19 vaccines compared to Influenza vaccines. Eur J Intern Med. 2022 May;99:82-88. doi: 10.1016/j.ejim.2022.03.002. Epub 2022 Mar 9. PMID: 35288031; PMCID: PMC8904150.
6. Hungaro Cunha C, Yuri Sato D, Pereira de Godoy JM, da Silva Russeff GJ, Franccini Del Frari Silva D, Pereira de Godoy HJ, Menezes da Silva MO, Amorim Santos H, Guerreiro Godoy MF. Mortality and Deep Vein Thrombosis in the Gamma Variant of Covid 19 and Lung Injury. Vasc Health Risk Manag. 2022 Nov 3;18:833-838. doi: 10.2147/VHRM.S367930. PMID: 36353368; PMCID: PMC9639391.
7. Pereira de Godoy JM, Russeff GJDS, Cunha CH, Sato DY, Silva DFDF, Godoy HJP, Silva MOMD, Amorim H, Soares MML, Godoy MFG. Increased prevalence of deep vein thrombosis and mortality in patients with Covid-19 at a referral center in Brazil. Phlebology. 2022 Feb;37(1):21-25. doi: 10.1177/02683555211041931. Epub 2021 Sep 8. PMID: 34494482; PMCID: PMC8829736.
8. Pereira de Godoy JM, Da Silva Russeff GJ, Hungaro Cunha C, Yuri Sato D, Franccini Del Frari Silva D, Guerreiro Godoy MF. Mortality and Change in the Prevalence of Deep Vein Thrombosis Associated With SARS-CoV-2 P.1 Variant. Cureus. 2022 Jul 8;14(7):e26668. doi: 10.7759/cureus.26668. PMID: 35949793; PMCID: PMC9357448.

IJBM

INTERNATIONAL JOURNAL OF BIOMEDICINE

Instructions for Authors

International Journal of Biomedicine (IJBM) publishes peer-reviewed articles on the topics of basic, applied, and translational research on biology and medicine. International Journal of Biomedicine welcomes submissions of the following types of paper: Original articles, Reviews, Perspectives, Viewpoints, and Case Reports.

All research studies involving animals must have been conducted following animal welfare guidelines such as *the National Institutes of Health (NIH) Guide for the Care and Use of Laboratory Animals*, or equivalent documents. Studies involving human subjects or tissues must adhere to the *Declaration of Helsinki and Title 45, US Code of Federal Regulations, Part 46, Protection of Human Subjects*, and must have received approval of the appropriate institutional committee charged with oversight of human studies. Informed consent must be obtained.

Pre-submissions

Authors are welcome to send an abstract or draft manuscript to obtain a view from the Editor about the suitability of their paper. Our Editors will do a quick review of your paper and advise if they believe it is appropriate for submission to our journal. It will not be a full review of your manuscript.

Manuscript Submission

Manuscript submissions should conform to the guidelines set forth in the Recommendations for the Conduct, Reporting, Editing and Publication of Scholarly Work in Medical Journals (ICMJE Recommendations), available from www.ICMJE.org.

Original works will be accepted with the understanding that they are contributed solely to the Journal, are not under review by another publication, and have not previously been published except in abstract form.

All manuscripts must be submitted through the International Journal of Biomedicine`s online submission system (www.ijbm.org/submission.php). Manuscripts must be typed, double-spaced using a 14-point font, including references, figure legends, and tables. Leave 1-inch margins on all sides. Assemble the manuscript in this order: Title Page, Abstract, Key Words, Text (Introduction, Methods, Results, and Discussion), Acknowledgments, Sources of Funding, Disclosures, References, Tables, Figures, and Figure Legends. References, figures, and tables should be cited in numerical order according to first mention in the text.

The preferred order for uploading files is as follows: Cover letter, Full Manuscript PDF (PDF containing all parts of the manuscript including references, legends, figures and tables), Manuscript Text File (MS Word), Figures (each figure and its corresponding legend should be presented together), and Tables. Files should be labeled with appropriate and descriptive file names (e.g., SmithText.doc, Fig1.eps, Table3.doc). Text, Tables, and Figures should be uploaded as separate files. (Multiple figure files can be compressed into a Zip file and uploaded in one step; the system will then unpack the files and prompt the naming of each figure. See www.WinZip.com for a free trial.)

Authors who are unable to provide an electronic version or have other circumstances that prevent online submission must contact the Editorial Office prior to submission to discuss alternate options (editor@ijbm.org).

Cover Letter

The cover letter should be saved as a separate file for upload. In it, the authors should (1) state that the manuscript, or parts of it, have not been and will not be submitted elsewhere for publication; (2) state that all authors have read and approved the manuscript; and (3) disclose any financial or other relations that could lead to a conflict of interest. If a potential conflict exists, its nature should be stated for each author. When there is a stated potential conflict of interest a footnote will be added indicating the author's equity interest in or other affiliation with the identified commercial firms.

The corresponding author should be specified in the cover letter. All editorial communications will be sent to this author. A short paragraph telling the editors why the authors think their paper merits publication priority may be included in the cover letter.

Types of articles

Original articles

Original articles present the results of original research. These manuscripts should present well-rounded studies reporting innovative advances that further knowledge about a topic of importance to the fields of biology or medicine. These can be submitted as either a full-length article (no more than 6,000 words, 4 figures, 4 tables) or a Short Communication (no more than 2,500 words, 2 figures, 2 tables). An original

article may be Randomized Control Trial, Controlled Clinical Trial, Experiment, Survey, and Case-control or Cohort study.

Case Reports

Case reports describe an unusual disease presentation, a new treatment, a new diagnostic method, or a difficult diagnosis. The author must make it clear what the case adds to the field of medicine and include an up-to-date review of all previous cases in the field. These articles should be no more than 5,000 words with no more than 6 figures and 3 tables. Case Reports should consist of the following headings: Abstract (no more than 100 words), Introduction, Case Presentation (clinical presentation, observations, test results, and accompanying figures), Discussion, and Conclusions.

Reviews

Reviews analyze the current state of understanding on a particular subject of research in biology or medicine, the limitations of current knowledge, future directions to be pursued in research, and the overall importance of the topic. Reviews could be non-systematic (narrative) or systematic. Reviews can be submitted as a Mini-Review (no more than 2,500 words, 3 figures, and 1 table) or a long review (no more than 6,000 words, 6 figures, and 3 tables). Reviews should contain four sections: Abstract, Introduction, Topics (with headings and subheadings, and Conclusions and Outlook.

Perspectives

Perspectives are brief, evidenced-based and formally structured essays covering a wide variety of timely topics of relevance to biomedicine. Perspective articles are limited to 2,500 words and usually include ≤10 references, one figure or table. Perspectives contain four sections: Abstract, Introduction, Topics (with headings and subheadings), Conclusions and Outlook.

Viewpoints

Viewpoint articles include academic papers, which address any important topic in biomedicine from a personal perspective than standard academic writing. Maximum length is 1,200 words, ≤70 references, and 1 small table or figure.

Manuscript Preparation

Title Page

The first page of the manuscript (title page) should include (1) a full title of the article, (2) a short title of less than 60 characters with spaces, (3) the authors' names, academic degrees, and affiliations, (4) the total word count of the manuscript (including Abstract, Text, References, Tables, Figure Legends), (5) the number of figures and tables, and (6) the name, email address, and complete address of corresponding author.

Disclaimers. An example of a disclaimer is an author's statement that the views expressed in the submitted article are his or her own and not an official position of the institution or funder.

Abstract

The article should include a brief abstract of no more than 200 words. Limit use of acronyms and abbreviations. Define at first use with acronym or abbreviation in parentheses. The abstract should be structured with the following headings: Background, Methods and Results, and Conclusions. The Background section should describe the rationale for the study. Methods and Results should briefly describe the methods and present the significant results. Conclusions should succinctly state the interpretation of the data. Authors should supply a list of up to four key words not appearing in the title, which will be used for indexing. The key words should be listed immediately after the Abstract. Use terms from the Medical Subject Headings (MeSH) list of Index Medicus when possible.

Main text in the IMRaD format

Introduction should describe the purpose of the study and its relation to previous work in the field; it should not include an extensive literature review.

Methods should be concise but sufficiently detailed to permit repetition by other investigators. Previously published methods and modifications should be cited by reference. A subsection on statistics should be included in the Methods section.

Results should present positive and relevant negative findings of the study, supported when necessary by reference to Tables and Figures.

Discussion should interpret the results of the study, with emphasis on their relation to the original hypotheses and to previous studies. The importance of the study and its limitations should also be discussed.

The IMRaD format does not include a separate Conclusion section. The conclusion is built into the Discussion. More information on the structure and content of these sections can be found in the Recommendations for the Conduct, Reporting, Editing and Publication of Scholarly Work in Medical Journals (ICMJE Recommendations), available from www.ICMJE.org.

Acknowledgments, Sources of Funding, and Disclosures

Acknowledgments : All contributors who do not meet the criteria for authorship should be listed in an acknowledgments section. Examples of those who might be acknowledged include a person who provided purely technical help, writing assistance, or a department chairperson who provided only general support. Authors should declare whether they had assistance with study design, data collection, data analysis, or manuscript preparation. If such assistance was available, the authors should disclose the identity of the individuals who provided this assistance and the entity that supported it in the published article.

Sources of Funding: All sources of financial support for the study should be cited on the title page, including federal or state agencies, nonprofit organizations, and pharmaceutical or other commercial sources.

Disclosure and conflicts of interest: All authors must disclose any financial or other relations that could lead to a conflict of interest. If a potential conflict exists, its nature should be stated for each author. All sources of financial support for the study should be cited, including federal or state agencies, nonprofit organizations, and pharmaceutical or other commercial sources. Please use ICMJE Form for Disclosure of Potential Conflicts of Interest (http://www.icmje.org/conflicts-of-interest/).

References

References should follow the standards summarized in the NLM's International Committee of Medical Journal Editors (ICMJE) Recommendations for the Conduct,

Reporting, Editing and Publication of Scholarly Work in Medical Journals: Sample References webpage (www.nlm.nih.gov/bsd/uniform_requirements.html) and detailed in the NLM's Citing Medicine, available from www.ncbi.nlm.nih.gov/books/NBK7256/. MEDLINE abbreviations for journal titles (www.ncbi.nlm.nih.gov/nlmcatalog/journals) should be used.

References should be presented in the Vancouver style. The first six authors should be listed in each reference citation (if there are more than six authors, "et al" should be used following the sixth). Periods are not used in authors' initials or journal abbreviations. Examples of journal reference style:

Journal Article: Serruys PW, Ormiston J, van Geuns RJ, de Bruyne B, Dudek D, Christiansen E, et al. A Polylactide Bioresorbable Scaffold Eluting Everolimus for Treatment of Coronary Stenosis: 5-Year Follow-Up. J Am Coll Cardiol. 2016;67(7):766-76. doi: 10.1016/j.jacc.2015.11.060.

Book: Murray PR, Rosenthal KS, Kobayashi GS, Pfaller MA. Medical Microbiology. 4th ed. St. Louis: Mosby; 2002.

Chapter in Edited Book: Meltzer PS, Kallioniemi A, Trent JM. Chromosome alterations in human solid tumors. In: Vogelstein B, Kinzler KW, editors. The Genetic Basis of Human Cancer. New York: McGraw-Hill; 2002:93–113.

References should be numbered consecutively in the order in which they are first mentioned in the text. Identify references in text, tables, and legends by Arabic numerals in parentheses and listed at the end of the article in citation order.

Tables

Tables should be comprehensible without reference to the text and should not be repetitive of descriptions in the text. Every table should consist of two or more columns; tables with only one column will be treated as lists and incorporated into the text. All tables must be cited in the text and numbered in order of appearance. Tables should include a short title. Place explanatory matter in footnotes, not in the heading. Explain all nonstandard abbreviations in footnotes, and use symbols to explain information if needed. Each table submitted should be double-spaced, each on its own page. Each table should be saved as its own file as a Word Document. Explanatory matter and source notations for borrowed tables should be placed in the table footnote.

Figures and Legends

All illustrations (line drawings and photographs) are classified as figures. All figures should be cited in the text and numbered in order of appearance. Figures should be provided in .tiff, .jpeg or .eps formats. Color images must be at least 300 dpi. Gray scale images should be at least 300 dpi. Line art (black and white or color) and combinations of gray scale images and line art should be at least 1,000 dpi. The optimal size of lettering is 12 points. Symbols should be of a similar size. Figures should be sized to fit within the column (86 mm) or the full text width (180 mm). Line figures must be sharp, black and white graphs or diagrams, drawn professionally or with a computer graphics package. Legends should be supplied for each figure and should be brief and not repetitive of the text. Any source notation for borrowed figures should appear at the end of the legend. Figures should be uploaded as individual files.

Units of Measurement

Measurements of length, height, weight, and volume should be reported in metric units (meter, kilogram, or liter) or their decimal multiples. Temperatures should be in degrees Celsius. Blood pressures should be in millimeters of mercury. All measurements must be given in SI or SI-derived units. Drug concentrations may be reported in either SI or mass units, but the alternative should be provided in parentheses where appropriate.

Style and Language

The journal accepts manuscripts written in English. Spelling should be US English only. The language of the manuscript must meet the requirements of academic publishing. Reviewers may advise rejection of a manuscript compromised by grammatical errors. Non-native speakers of English may choose to use a copyediting service.

Abbreviations and Symbols

Use only standard abbreviations; use of nonstandard abbreviations can be confusing to readers. Avoid abbreviations in the title of the manuscript. The spelled-out abbreviation followed by the abbreviation in parenthesis should be used on first mention unless the abbreviation is a standard unit of measurement.

Drugs should be referred to by their generic names. If proprietary drugs have been used in the study, refer to these by their generic name, mentioning the proprietary name, and the name and location of the manufacturer, in parentheses.

Permissions

To use tables or figures borrowed from another source, permission must be obtained from the copyright holder, usually the publisher. Authors are responsible for applying for permission for both print and electronic rights for all borrowed materials and are responsible for paying any fees related to the applications of these permissions. This is necessary even if you are an author of the borrowed material. It is essential to begin the process of obtaining permission early, as a delay may require removing the copyrighted material from the article. The source of a borrowed table should be noted in a footnote and of a borrowed figure in the legend. It is essential to use the exact wording required by the copyright holder. A copy of the letter granting permission, identified by table or figure number, should be sent along with the manuscript. A permission request form is provided for the authors use in requesting permission from copyright holders.

Page Proofs

Page proofs are sent from the Publisher electronically and must be returned within 72 hours to avoid delay of publication. Generally, peer review is completed within 4-5 weeks.

It is important to note that when citing an article from IJBM, the correct citation format is **International Journal of Biomedicine.**

IJBM

INTERNATIONAL JOURNAL OF BIOMEDICINE

International Journal of Biomedicine (IJBM) is an open access journal. IJBM publishes peer-reviewed articles on aspects of basic, applied, and translational research in biology and medicine. The main purpose of IJBM is to establish a scientific platform for targeted promotion of new scientific ideas and biomedical technologies focused on the applied aspects of biomedicine.

The journal publishes articles on:

Internal Medicine
Cardiology
Pulmonology
Endocrinology
Neurology
Hepatology
Gastroenterology
Nephrology
Ophthalmology
Otorhinolaryngology
Radiology
Surgery
Obstetrics and Gynecology
Pediatrics
Dermatology and STD
Clinical Immunology
Oncology
Genomics and Proteomics
Population Genetics
Epidemiology and Population Health
Reproductive Health
Adolescent Health
Cell Biology
Experimental Biology
Biotechnology
Dentistry
Infectious Diseases
Sports Medicine

Authors are invited to submit:

Original articles
Review articles
Case reports
Perspectives
Viewpoints